

UTILIZATION OF ACCELERATORS FOR TRANSMUTATION AND ENERGY PRODUCTION

R. L. Sheffield, LANL, Los Alamos, NM 87545, U.S.A.

Abstract

Given the increased concern over reliable, emission-free power, nuclear power has experienced a resurgence of interest. A sub-critical accelerator driven system (ADS) can drive systems that have either safety constraints (waste transmutation) or reduced fissile content (thorium reactor). The goals of ADS are some or all of the following: 1) to significantly reduce the generation or impacts due to the minor actinides on the packing density and long-term radiotoxicity in the repository design, 2) preserve/use the energy-rich component of used nuclear fuel, and 3) reduce proliferation risk.

ADS systems have been actively studied in Europe and Asia over the past two decades and renewed interest is occurring in the U.S. This talk will cover some of the history, possible applicable fuel cycle scenarios, and general issues to be considered in implementing ADS systems.

INTRODUCTION

A key roadblock to development of additional nuclear power capacity is the concern over management of nuclear waste. Nuclear waste is predominantly comprised of used fuel discharged from operating nuclear reactors. Worldwide, more than 250,000 tons of spent fuel from reactors currently operating will require disposal. The toxicity of the spent fuel, mainly due to ionizing radiation, will affect future generations for long into the future. The large quantity and its long-lived toxicity present significant challenges in waste management.

Nuclear fuel seems ideally suited for recycling. However, the low price for uranium ore over the last several decades has made the “once-through” cycle economical. Under any scenario, at some point in time a combination of short-term and long-term geologic repositories must be made available to receive the reactor waste.

Only a small fraction of the available energy in the fuel is extracted on a single pass and the majority of the “problem wastes” could be burned in fast reactors. Fast-reactors have a hard neutron spectrum relative to thermal reactors. Most of the remaining wastes have half-lives of a few hundred years and can be safely stored in man-made containment structures (casks or glass). The very small amount of remaining long-lived waste could be safely stored in a small geologic repository. The problem for the next 100 years is that a sufficient number of fast reactors will not be built by industry to burn their own waste and the LWR waste from existing and new reactors. So an interim solution is required to transition to a fast reactor economy.

One interim solution is to dispose spent fuel using a combination of approaches depending on the lifetime of

the radioactive isotope. The short-lived fission products can be stored in man-made containers until they safely decay to low radiotoxicity levels. Long-lived fissile isotopes like Pu-239 and U-235 can be stored with U-238 and Np-237 for fabrication into nuclear fuel at a future date. The long-lived fission products can be vitrified and buried.

Repository design is significantly impacted by the radioactive decay heat for at least 10,000 years. Long term storage is also limited by container failure and the potential spread of radiotoxic isotopes. Isotopic contributions to the decay heat are shown in Fig. 1. Note that Am-241 is the major source of decay heat at times longer than the lifetime of engineered barriers.

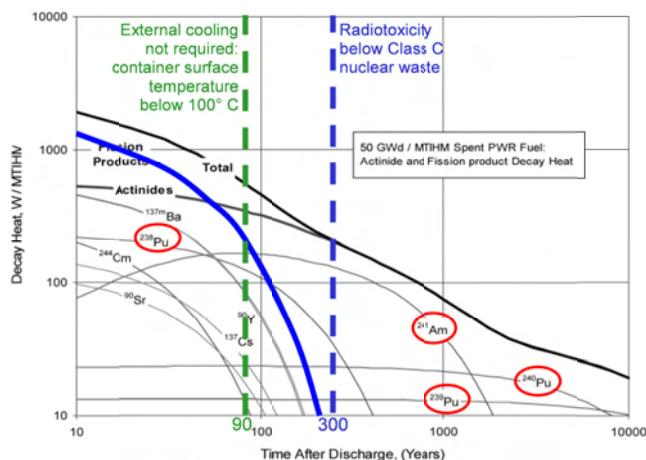


Figure 1: Dominant decay heat contributors in spent PWR fuel irradiated to 50 GWd/MTHM. [1] Goal is to eliminate components of the nuclear waste stream that account for the majority of the heat load and toxicity over the 300 to 10,000 year time frame. The isotopes circled in red are the major contributors to the decay heat in this time frame. If these isotopes are removed then: the solid blue line shows the decay heat of the remaining waste; the green dashed line shows the time at which the surface temperature of the waste container is below the boiling point of water; and the blue dashed line gives the time at which the waste radiotoxicity is below Class C nuclear waste.

ACCELERATOR DRIVEN SYSTEMS

Accelerator Driven Systems (ADS) operate in a sub-critical reactor mode. This mode offers two significant advantages over critical reactors: greater flexibility with respect to fuel composition, and potentially enhanced safety. Accelerator driven systems are ideally suited to burning fuels which are problematic from the standpoint of critical reactor operation, namely, fuels that would degrade neutronic characteristics of the critical core to

OVERVIEW OF HIGH INTENSITY ACCELERATOR PROJECTS

C.R. Prior, STFC Rutherford Appleton Laboratory, Chilton, Didcot, Oxon, U.K.

Abstract

This review covers high intensity hadron accelerator projects worldwide, ranging over spallation neutron sources, radioactive ion beams, accelerator driven systems and machines for particle physics, including both existing and proposed facilities. The aim is to compare requirements, explore parameter ranges, identify areas of commonality and highlight how experience in one project can be used to address challenges in others.

INTRODUCTION

The earlier series of ICFA mini-workshops were guided principally by studies of spallation neutron sources and high power proton accelerators. They led to the larger, more formal, HB workshops where the emphasis has considerably widened the spectrum of analysis and application. Different applications impose different requirements in terms of average power and beam energy. These are summarised in Table 1 and show how preferred parameters range from relatively low energy (MeV level), high power, irradiation and ADSR facilities to what might be termed intermediate energies (a few GeV) with slightly lower power (1-5 MW) for spallation sources, and the higher energies (perhaps as high as the 150 GeV of the Fermilab main injector) for particle physics purposes. Individual projects might be arranged into categories as follows:

- **Multi-purpose facilities:** LANSCE (US), J-PARC (Japan), PEFP (Korea), FAIR (GSI)
- **Spallation neutron sources:** SINQ@PSI (Switzerland), ISIS (UK), SNS (US), CSNS (China), ESS (Sweden)
- **Radioactive ion beams (RIB):** FRIB (US), EURISOL (Europe), RIKEN (Japan), SPIRAL2 (France), SPES (Italy), SARAF (Israel) .
- **Secondary beams (Neutrino/muon factories):** Linac4+SPL (CERN), Project-X (US), IDS-NF
- **Irradiation facilities:** IFMIF (Europe/US/Japan) + prototype EVEDA (CEA)
- **Accelerator Driven Systems (ADS):** EUROTRANS (Europe), TRASCO (Italy), ADS (China), MYRRHA (Belgium), ThorEA (UK)

These are plotted on a conventional “Energy Frontier” diagram, indicating how current and energy are balanced to achieve beam power, in Figure 1.

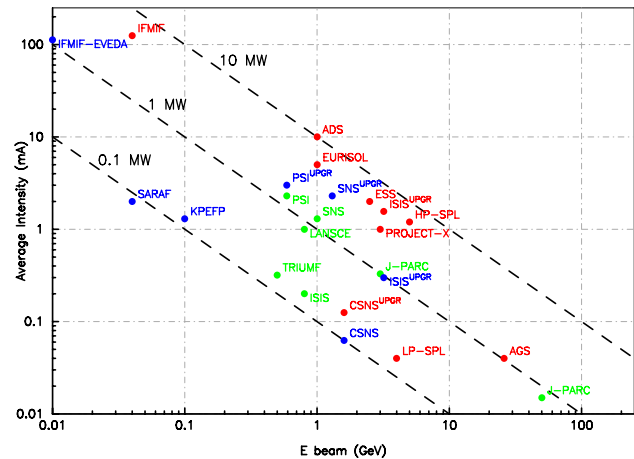


Figure 1: Beam Power Frontier: operating facilities in green, those under construction and upgrades in blue, and proposed new facilities in red.

SPALLATION NEUTRON SOURCES

The **SINQ spallation neutron source** at the Paul Scherrer Institute in Switzerland stands out not only because it is the current leader in terms of beam power but because it is the only spallation facility that operates CW and uses cyclotrons. An 870 keV Cockcroft Walton injector provides protons to a 72 MeV injector cyclotron which in turn feeds a main ring cyclotron taking the beam to 590 MeV. A separate beam line from the injector is used to send $\lesssim 100 \mu\text{A}$ to an isotope production facility. The ring cyclotron (Fig. 2) is optimised for high intensity and delivers 2.2 mA of current (1.3 MW) to a spallation neutron production target. Considerable efforts have been made in recent years to improve reliability to above 90% and reduce beam loss to the 10^{-4} level. A new beam intensity record was achieved in 2009 with stable operation at 2.3 mA for several hours [1]. An upgrade programme to 1.8 MW is being implemented with the installation of new resonators in the injector cyclotron and a new 10th harmonic buncher. Completion is planned for 2013. There is great confidence at PSI that the cyclotron concept now represents a viable option for generating high power beams for other applications, including accelerator driven systems (ADS), where very high reliability is in demand.

The new generation of spallation neutron facilities is led by SNS and J-PARC. In contrast to the CW operation of SINQ, **SNS at Oak Ridge, Tennessee**, is the world’s most powerful pulsed neutron facility [2]. Based on a 1 GeV

SNS OPERATIONL EXPERIENCE: EXPECTATIONS AND REALITIES*

J. Galambos, on behalf of the SNS team, SNS, Oak Ridge, TN, USA

Abstract

The Spallation Neutron Source (SNS) accelerator [1] has operated at 1 MW for about one year, as a driver for a pulsed neutron source. This represents the highest pulsed power operational level for a proton accelerator. This paper discusses the experiences encountered in the four year operational period, compared to expectations. The superconducting linac has shown some surprises, yet is capable of delivering the required beam to the storage Ring. On the other hand the Ring is operated close to expectations.

EXPECTATIONS

During the design period, challenges were recognized associated with increasing the existing pulsed beam power capability by nearly an order of magnitude. Inherent with high-pulsed beam power is high beam intensity. Space charge effects were a concern for both the linac and the ring. Charge exchange injection in the ring was recognized as a challenge, with foil survivability a major concern. In the end, beam loss was expected to be the final limit to the attainable operational power.

THE SNS POWER RAMPUP

A quite aggressive internal power ramp-up schedule was initially proposed [2]. While the attained power level did not completely meet this initial plan, sponsor commitments were met and 1 MW achieved within three years of initial operation. Figure 1a shows the realized beam power compared to the initial expectation (more detail on the power rampup history is given in Ref [3]). From the neutron user perspective, the beam availability is at least as important as beam power (see Fig. 1b). The availability goal for the last year was 85% (which was met), and approaches 90% over the next two years. SNS has approached the availability typical for mature high power accelerators for spallation sources. A more detailed history of the power ramp-up is shown in Fig. 2, with annotations indicating some periods where operational power was limited by equipment issues. Presently the operational power is limited by availability concerns. The beam pulse length is about 15% short of the design goal, beam energy is 7% low, and the average beam current is about 5% lower than the design. Increasing these parameters to their design goal will be done slowly, to mitigate any adverse impact on the availability of beam to the neutron scattering user program.

The aggressive initial power ramp-up schedule had an unanticipated benefit. In the early ramp-up years, more time was dedicated to accelerator studies, as the neutron user program was just evolving. Making fast progress in

the increase of accelerator beam power was crucial to reaching one MW within 3-4 years. Later, as more neutron user program matured, less time was available for accelerator development and importantly, fewer risks could be taken in beam operation.

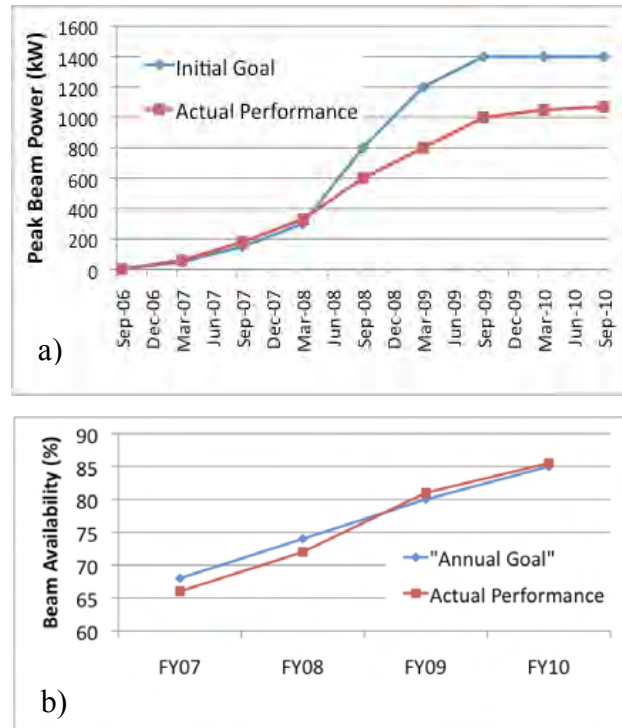


Figure 1: Expectations vs actual a) neutron production beam power, and b) neutron production availability.

THE LINAC

The SNS linac is comprised of a traditional copper accelerator structure to 186 MeV and a superconducting linac (SCL) RF structure to 1 GeV [1]. SNS is the first accelerator to employ superconducting RF for a pulsed beam, for a high-energy hadron beam, as well as for a high power hadron beam. A number of technical issues were encountered [4], but the implications on beam dynamics are emphasized here.

SCL Experience

A major unforeseen SCL linac experience was the high degree of variability in cavity-to-cavity performance. Figure 3 shows the present cavity performance relative to the expected design values (initial operational experience had even larger variations). Not only is the cavity gradient capability spread higher than the expected $\pm 10\%$ level; there are systematic differences in the average cavity family performance relative to expectations (the medium

* ORNL/SNS is managed by UT-Battelle, LLC, for the U.S. Department of Energy under contract DE-AC05-00OR22725.

HIGH INTENSITY ASPECTS OF THE J-PARC FACILITY

T. Koseki[#] and J-PARC Accelerator Group, J-PARC Center, KEK and JAEA, Tokai, Ibaraki, Japan

Abstract

Recent status of the high intensity operation of the J-PARC accelerators is presented. Improvements performed in the 2010 summer shutdown period and near future plan are also reported briefly.

INTRODUCTION

The J-PARC is a multi-purpose proton accelerator facility aiming at MW-class output beam power. The J-PARC accelerator comprises an H⁻ linac, a Rapid-Cycling Synchrotron (RCS), a slow-cycling Main Ring Synchrotron (MR) and related experimental facilities. The H⁻ beam from the linac is injected into the RCS by charge-exchange injection. The RCS provides a 3-GeV proton beam to neutron and muon targets in the Materials and Life Science Experimental Facility (MLF) at a repetition rate of 25 Hz. A part of the beam extracted from the RCS is injected into the MR. The MR accelerates the beam up to 30 GeV and delivers the beam to the hadron (HD) beam facility using a slow extraction (SX) system and to a neutrino (NU) beam line using a fast extraction (FX) system.

Figure 1 shows a panoramic view of the J-PARC site. Beam commissioning was initiated starting from the upstream accelerators, while the construction of the downstream accelerators and experimental facilities was still in progress. The components are colored in this figure to indicate the Japanese fiscal year (JFY) in which beam commissioning was initiated in the various parts of the facility.



Figure 1: Bird's eye view of the J-PARC site.

LINAC

The linac consists of an H⁻ ion source, RFQ, DTL and separated-type DTL. The beam energy is 181 MeV at present. The designed maximum peak current for the 181 MeV operation is 30 mA. The repetition is 25 Hz and

pulse width maximum is 0.5 msec. An energy upgrade project has already been approved by the government and the energy will be increased to 400 MeV by installing a new accelerating structure, the Annular Coupled Structure linac (ACS) in the 2012 summer shutdown.

The linac beam commissioning was initiated in November 2006, and a 181 MeV beam was successfully accelerated in January 2007. Since then, the linac has been delivering beams for commissioning of the linac itself, the downstream accelerators and experimental facilities. Trip rates for the RFQ, however, unexpectedly increased in September 2008. This problem has limited the RCS beam power available for the MLF users to below 20 kW.

In March 2009, we added two ion pumps to the RFQ, one turbo molecular pump in the Low Energy Beam Transport (LEBT, the beam transport between the ion source and the RFQ), and an orifice was installed in the LEBT to reduce the gas flow from the ion source. We also performed further vacuum system improvements during the 2009 summer shutdown. The oil rotary pumps were replaced with oil-free scroll pumps. In addition, we replaced the old LEBT chamber with a new clean chamber containing a divider plate with an orifice for differential pumping. One cryopump was installed on the RFQ side and one 1500 L/s turbo molecular pump on the ion source side. In July, we performed in-situ baking for 10 days to accelerate degassing [1].

The vacuum system improvements reduced base pressure in the RFQ section to several $\times 10^{-7}$ Pa, a quarter of the pressure before the improvements. In addition, hydro-carbon components gradually decreased during rf conditioning.

In November 2009, based on the stable operation of the RFQ at 20 kW in October, we tried to increase the beam power for the MLF user operation by increasing the beam pulse length from 0.1 to 0.2 msec and peak beam current from 5 to 15 mA, thus obtaining a 6-fold increase from 20 up to 120 kW. We were able to deliver beam to MLF users without any incident. Since December 2009, the linac and the RFQ delivered the beam with a maximum pulse width of 0.5 msec, which is in accordance with the full design specifications. The results verified the restoration of the RFQ performance.

RCS

The RCS has three-fold symmetry and a circumference of 348 m. Each super-period consists of two 3-DOFO arc modules and a 3-DOFO dispersion-free straight section. The arc module has a missing bend cell, which makes a very high transition energy of 9 GeV, far beyond the extraction beam energy.

[#] tadashi.koseki@kek.jp

COLLIMATION FOR THE LHC HIGH INTENSITY BEAMS

R. Assmann for the LHC Collimation Team^{*}, CERN, Geneva, Switzerland

Abstract

The unprecedented design intensities of the LHC require several important advances in beam collimation. With its more than 100 collimators, acting on various planes and beams, the LHC collimation system is the biggest and most performing such system ever designed and constructed. The solution for LHC collimation is explained, the technical components are introduced and the initial performance is presented. Residual beam leakage from the system is analysed. Measurements and simulations are presented which show that collimation efficiencies of better than 99.97 % have been measured with the 3.5 TeV proton beams of the LHC, in excellent agreement with expectations.

INTRODUCTION

The Large Hadron Collider LHC [1,2] at CERN is the new frontier collider for Particle Physics. Its discovery reach depends critically on the beam energy and the luminosity (event rate) reached. The beam energy is presently limited to 3.5 TeV [3] from non-conformities in the magnet and powering system. Maximizing the stored beam intensity increases the achievable luminosity. A powerful collimation system is required to handle the ultra-intense LHC beams in a super-conducting environment [4,5,6,7]. Only with highly efficient collimation can the LHC targets be reached.

The important beam parameters of the proton beam operation in LHC are compared in Table 1 with the nominal design values, with E being the beam energy, D_z the bunch spacing, $\gamma\epsilon_{h/v}$ the normalized transverse emittances, N_p the number of protons per bunch, N_b the number of bunches, E_{stored} the stored beam energy, L_{peak} the peak instantaneous luminosity and N_{tot} the total beam intensity. It is seen that the energy stored in the LHC beams passed already much beyond the 2 MJ values achieved in HERA and Tevatron. Milestones of the LHC collimation project

^{*}The reported work on the LHC collimation system was performed from 2003 to 2010 and relied on the work of the following persons at CERN and at outside collaborating institutes: O. Aberle, R. Assmann, J.P. Bacher, V. Baglin, G. Bellodi, A. Bertarelli, P. Bestmann, R. Billen, V. Boccone, A.P. Bouzoud, C. Bracco, H. Braun, R. Bruce, M. Brugger, S. Calatroni, F. Caspers, M. Cauchi, F. Cerruti, R. Chamizo, A. Cherif, E. Chiaveri, A. Dallochio, D. Deboy, B. Dehning, M. Donze, N. Hilleret, E.B. Holzer, D. Jacquet, J.B. Jeanneret, J.M. Jimenez, M. Jonker, Y. Kadi, K. Kershaw, G. Kruk, M. Lamont, L. Lari, J. Lendaro, J. Lettry, R. Losito, M. Magistris, A. Masi, M. Mayer, E. Métral, C. Mitifiot, N. Mounet, R. Perret, S. Perrolaz, V. Previtali, C. Rathjen, S. Redaelli, G. Robert-Demolaize, C. Roderick, S. Roesler, A. Rossi, F. Ruggiero, M. Santana, R. Schmidt, P. Sievers, M. Sobczak, K. Tsoulou, G. Valentino, E. Veyrunes, H. Vincke, V. Vlachoudis, T. Weiler, J. Wenninger, D. Wollmann, CERN, Geneva, Switzerland. D. Kaltchev et al, TRIUMF, Canada. I. Bayshev, IHEP, Russia. T. Markiewicz et al, SLAC, USA. N. Mokhov et al, FNAL, USA. A. Ryazanov et al, Kurchatov, Russia. N. Sammut et al, University Malta, Malta. N. Simos et al, BNL, USA.

are listed in Table 2. It is seen that the work on the LHC collimation system was performed under strong time pressure, as this was the last major LHC system to be designed and produced.

Table 1: Important parameters of LHC operation with proton beams as achieved in 2010 and compared to the nominal design values.

Parameter	Unit	2010	Design
E	TeV	3.5	7.0
Δ_z	ns	150	25
$\gamma\epsilon_{h/v}$	μm	1.8	3.75
N_p	p	1.2×10^{11}	1.15×10^{11}
Luminosity production			
N_b		368	2808
N_{tot}	p	4.4×10^{13}	3×10^{14}
E_{stored}	MJ	24.8	362
L_{peak}	$\text{cm}^{-2} \text{s}^{-1}$	2×10^{32}	1×10^{34}
Peak intensity at 3.5 TeV			
N_b		424	2808
N_{tot}	p	5.1×10^{13}	3×10^{14}
E_{stored}	MJ	28.5	362

Table 2: Major milestones of the LHC collimation project.

Time	Milestone
01/2003	Start of the LHC collimation project. System and hardware design.
06/2004	System solution approved
10/2004	Verification of collimator prototypes with 450 GeV beam
06/2005	Signature of production contract with industry
09/2008	Minimal system installed in LHC and used for first beam
06/2009	Full initial system installed
10/2010	LHC reaches 28 MJ stored energy in first year of full operation without quench from stored beam

REQUIREMENTS FOR COLLIMATION

Storage rings like the LHC would ideally store charged particles with infinite beam lifetime. In this case there would be no particles and no power lost. However, there are a number of processes that will always lead to beam losses [5]. It would go beyond the scope of this paper to list and discuss them in detail. It is just noted that the collision process for luminosity production itself creates beam diffusion and losses at the aperture restrictions of the ring. Beam losses are therefore unavoidable and become usually stronger as intensity and luminosity is increased.

TOWARDS THE HIGH INTENSITY LIMIT IN THE FAIR PROJECT – PRESENT STATUS AND FUTURE CHALLENGES

P. Spiller, GSI, Darmstadt, Germany

INTRODUCTION

In order to reach the desired intensities of heavy ion beams for the experiments of FAIR [1, 2], SIS18 and SIS100 have to be operated with intermediate charge states [3, 4]. Operation with intermediate charge state heavy ions at the intensity level of about 10^{11} ions per cycle has never been demonstrated elsewhere and requires a dedicated upgrade program for SIS18 and a dedicated machine design for SIS100. The specific problems coming along with the intermediate charge state operation in terms of charge exchange processes at collisions with residual gas atoms, pressure bumps by ion induced desorption and corresponding beam loss appears far below the typical space charge limits. Thus, new design concepts and new technical equipment addressing these issues are developed and realized with highest priority.

The upgrade program of SIS18 addressing the goal of minimum ionization beam loss [5] and stable residual gas pressure conditions has been defined in 2005. A major part of this upgrade program has been successfully realized, with the result of a world record in accelerated number of intermediate charge state heavy ions.

INTERMEDIATE CHARGE STATE HEAVY ION OPERATION

In order to minimize the required magnetic and electrical field strengths, so far heavy ion accelerators made use of highly charged ions where ever possible. For the generation of highly charged ions, stripper stages made of supersonic gas jets or foils have been installed at suitable positions (energies) along the accelerator. Even the major intensity loss resulting from the selection of one charge state out of the generated charge state distribution has been accepted.

Table 1: Existing and proposed heavy ions synchrotrons operated with intermediate charge state heavy ions.

AGS Booster	BNL	Au ³²⁺
LEIR	CERN	Pb ⁵⁴⁺
NICA Booster	JINR	Au ³²⁺
SIS18	GSI	U ²⁸⁺
SIS100	FAIR	U ²⁸⁺

With the aim for higher intensities and consequently increasing space charge effects and intensity restrictions, the charge state of heavy ions must be reduced. However, there are only a small number of heavy ion synchrotrons world-wide operating or designed with such intermediate charge state heavy ions. Table 1 shows the presently running and planned synchrotrons using intermediate charge state heavy ions.

The strength of the charge exchange processes in a machine cycle depends on the cross sections for ionization and electron capture as a function of the beam energy. The atomic physics models used for the calculation of these cross sections have been improved in the last ten years significantly and extended to relativistic energies [6]. Various experiments have been conducted, e.g. with the internal gas target of the ESR at GSI, to benchmark the predicted cross sections [7].

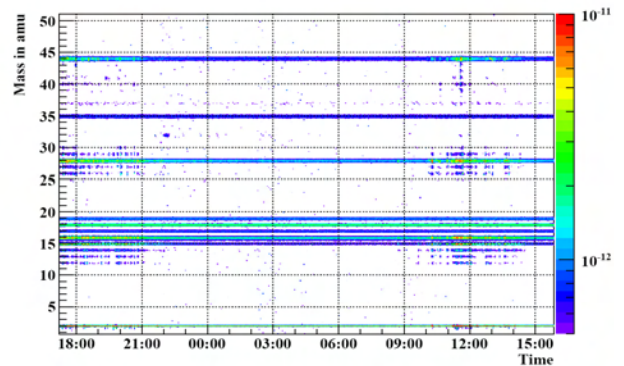


Figure 1: The residual gas spectrum in a synchrotron is changed by desorbed gases. During high current operation (left and right), additional components appear with a density comparable with the background components. The gap in between indicates the time of low intensity operation.

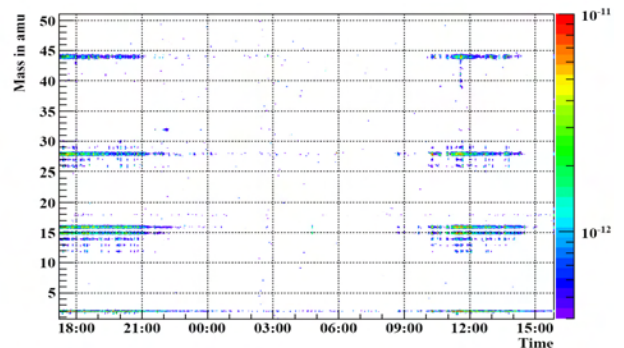


Figure 2: After subtracting the background spectrum (static case) the spectrum of the desorbed gases is obtained.

The cross sections depend significantly on the target ion, or in other words the residual gas composition of the accelerator. Here, it must be considered that the mass spectrum differs significantly in the dynamic case (with beam in the machine) from the static situation (without beam). The mass spectrum is strongly influenced by the gases which are desorbed from the walls by the impact of ions. Figures 1 and 2 show the mass spectrum measured in SIS18 in phases with and without beam. Figure 2 shows the spectrum of the desorbed gases which is

HIGH INTENSITY ASPECTS OF THE CSNS ACCELERATORS

Jing-Yu Tang, Shi-Nian Fu, Li Ma, IHEP/CSNS

Abstract

China Spallation Neutron Source is a multi-disciplinary research platform under detailed technical design, which is based on a high power proton accelerator complex. Beam loss control is key in designing and operating the accelerator complex of high beam power. Major high intensity aspects of the accelerators that may result in beam losses are discussed in the paper. The emittance growth due to space charge effects in the linac and the rapid cycling synchrotron (RCS), the RF trapping and the injection/extraction in the RCS are the major loss sources. The measures to reduce the loss rate and the collimation methods in the accelerators are presented. Some beam loading effects to the RF systems in the linac and in the RCS, and the uniformization of the beam spot at the spallation target by non-linear magnets are also mentioned.

INTRODUCTION

CSNS (China Spallation Neutron Source) is a project under construction, which will be a unique facility in China for multi-disciplinary research using neutron scattering techniques. The CSNS accelerator complex, which consists of a medium-energy linac and a Rapid Cycling Synchrotron (RCS), is to deliver proton beams of 100 kW at Phase One, and progressively upgraded to 200 kW at Phase Two and 500 kW at Phase Three. The upgrading path in beam power is via the increase in linac energy and more accumulated particles in the RCS. The main parameters of the accelerators are shown in Table 1.

Table 1: Main Parameters of the CSNS Accelerators

	CSNS-I	CSNS-II	CSNS-III
Beam power (kW)	100	200	500
Repetition rate (Hz)	25	25	25
Average current (μA)	62.5	125	312.5
Proton energy (GeV)	1.6	1.6	1.6
Linac beam energy (MeV)	80	132	250
Linac peak current (mA)	15	30	40
Linac duty factor (%)	1.05	1.05	1.7
Linac cavities	4 DTL	+3 DTL	+SCL
RCS circumference (m)	228	228	228
RCS accumulated particles	1.6×10^{13}	3.1×10^{13}	7.8×10^{13}
RCS RF cavities (~ 20 kV/cavity)	8 (H=2)	+3 (H=4)	-

Note: “+” means added equipments from the previous phase.

SPACE CHARGE EFFECTS

Space charge effects play important roles in both the linac and the RCS, even in the beam transport line LRBT (Linac to RCS Beam Transport). They are the main causes of the emittance growth and beam loss.

Linac

Strong space charge effects have been found in high intensity linac including the CSNS linac (see Figure 1). They are the major causes for the emittance growth from the ion source to the DTL end.

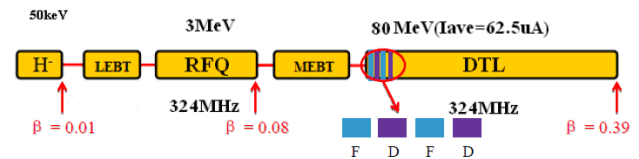


Figure 1: Schematic layout of CSNS-I linac.

In the LEBT, magnetic focusing by solenoids has been used to neutralize the space charge effect. A fast electrical chopper is placed just before the RFQ. The three solenoids can also produce symmetric emittance at the RFQ entrance for a non-symmetric beam from the Penning H^- ion source by using coupling effect [1]. However, quadrupoles are needed for a good matching when space charge is included even with a neutralization of 90% [2].

In RFQ, based on the experience of the ADS RFQ [3], the CSNS RFQ is expected to carry out high intensity beam up to 50 mA with good transmission efficiency.

In MEFT, a shorter MEFT without choppers has been designed following the successful test of the LEFT chopper. The transverse matching and longitudinal bunching are critical to control emittance growth during the structure transition from the RFQ to the DTL, since this is the most space charge dominant section in the linac. The matching should be adaptable to different peak currents in the CSNS phases.

On the one hand, linear space charge effect can be compensated by adjusting the transverse focusing and synchronous phase. The zero-current phase advance changes smoothly with beam energy to follow the tune depression change, as shown in Figure 2. On the other hand, non-linear space charge effect is difficult to be compensated and will result in betatron mismatch and

BRIEF REPORT OF THE FIRST WORKSHOP OF THE JOINT ICFA-ICUIL TASKFORCE ON HIGH AVERAGE POWER LASERS FOR FUTURE ACCELERATORS

W.P. Leemans, Lawrence Berkeley National Laboratory, Berkeley, USA

Abstract

A new taskforce has been formed in 2009, jointly with the International Committee for Future Accelerators (ICFA) and the International Committee for Ultra-Intense Lasers (ICUIL). This Joint Taskforce (JTF) has as goal to understand the needs imposed by future accelerators on laser technology. A preliminary summary, from a personal perspective, is presented of the activities at the first workshop held at GSI (Darmstadt) from April 8-10, 2010.

INTRODUCTION

Accelerators, x-ray light sources and lasers have been essential tools for advancement of science and technology, and have provided the basis for a vast number of industrial activities and societal benefits in the 20th century. As we enter the second decade of the 21st century, key challenges in science and technology will require next generation accelerators, light sources and lasers that far exceed today's capabilities.

Modern accelerators have become increasingly dependent on laser technology ranging from the production and manipulation of electron beams, to novel acceleration techniques and advanced light sources. The high average power demands imposed by today's accelerators on lasers is rapidly exceeding their state-of-the-art capabilities. Future accelerators that may rely entirely on lasers to power them far exceed today's capabilities. In order to bridge the gap between what exists today and what will be needed in the future, a Joint Taskforce (JTF) was formed with endorsement by both ICFA and ICUIL, to develop a roadmap for laser technology for future accelerators.

JTF ORGANIZATION

The 2009-2011 membership of the JTF consists of members of the ICFA Beam Dynamics Panel (Ralph Assman, Weiren Chou -- Chair ICFA BD, Ingo Hofmann, Kaoru Yokoya), the ICFA Advanced and Novel Accelerator Panel (Bruce Carlsten, Dino Jaroszynski, WL, Akiro Noda, James Rosenzweig, Siegfried Schreiber and Mitsuru Uesaka -- Chair ICFA ANA) and ICUIL (Chris Barty, Paul Bolton, Robert Byer, Almantas Galvanauskas, WL and Wolfgang Sandner). The JTF is chaired by WL.

WORKSHOP ORGANIZATION

A first workshop was organized at GSI (Darmstadt) from April 8-10, 2010 by the JTF to discuss the needs of accelerators that drive collider facilities, light source facilities and medical applications as well as an overview of the state-of-the-art in laser technology. The Chair of

the local organizing committee was Ingo Hofmann. Experts on high power laser technology as well as accelerator technology and their applications were invited to this first meeting. The 47 participants came from China (1), France (4), Germany (18), Japan (4), Switzerland (2), the UK (4) and the US (14).

The goals of the workshop were the following:

- Establish a comprehensive survey of requirements for laser-based light and particle sources with emphasis on sources that can advance light and particle driven science, and that require lasers beyond the state-of-the-art or state-of-current use. The emphasis was placed on the fact that the workshop was not intended to carry out a down selection of specific designs or technology choices but instead have an inclusive approach that represent a community consensus.
- Identify future laser system requirements and key technological bottlenecks.
- From projected system requirements, provide visions for technology paths forward to reach the survey goals and outline the required laser technology R&D steps that must be undertaken.
- Write a technical report.

Four work packages were identified:

- Colliders -- effort led by Weiren Chou
- Light sources -- effort led by WL
- Medical applications -- effort led by Mitsuru Uesaka
- Lasers -- effort led by Chris Barty and Wolfgang Sandner.

The first day of the workshop was devoted to plenary talks covering the different workpackages and discussions of the material presented. The second day was devoted to working group discussions and material development and gathering. On the third and final day, final discussions were held followed by a summary and assignment of follow-up tasks for manuscript preparation.

COLLIDER WORK PACKAGE

The largest challenge for laser technology is a laser-plasma e-e collider up to the 10 TeV goal. The consensus in the world high energy physics community is that the next large collider after the LHC would be a TeV-scale lepton collider. Options currently under study include the ILC (0.5-1 TeV), CLIC (up to 3 TeV) and the muon collider (up to 4 TeV), all using RF technology. The very high gradients (~10 GeV/m) possible with laser plasma acceleration, on the other hand, open up new avenues to

DYNAMIC APERTURE AND SPACE CHARGE EFFECT STUDIES FOR THE RECYCLER RING FOR PROJECT-X*

M. Xiao[#], L.G. Vorobiev and D.E. Johnson, Fermilab, Batavia, IL 605010, U.S.A.

Abstract

A simplified Recycler lattice was created to fine tune injection straight, ring tune, and phase trombone. In this paper, we will present detailed modifications for further optimization of Recycler lattice which requires the investigation of tune footprint and dynamic aperture based on higher order momentum components of the magnetic fields, together with the space charge effects.

INTRODUCTION

Project X [1] is a multi-MW intense proton source that provides beam for various physics programs. The Recycler ring will be used as a proton accumulator where H^- would be injected and converted to protons. Protons are provided to the Main Injector and accelerated to desired energy. The injection system for converting H^- to protons in Recycler is a multi turn stripping system, see Fig. 1. A simplified toy lattice was created to fine tune the injection insertion, ring tunes and phase trombone for the Recycler ring [2]. In this paper, a realistic lattice was created by using the measured magnetic field for all the magnets and further optimization of this lattice was completed. Based on this lattice, the tune footprint and dynamic apertures in the present of higher order multipole components of the magnetic fields have been investigated and are presented. Space charge effect is another issue for this lattice since the beam intensity at the end of injection reach $1.6E14$, which is 2 order of magnitude larger than the existing beam intensity in the Recycler ring. The preliminary results of the space charge effect study is also presented in this paper.

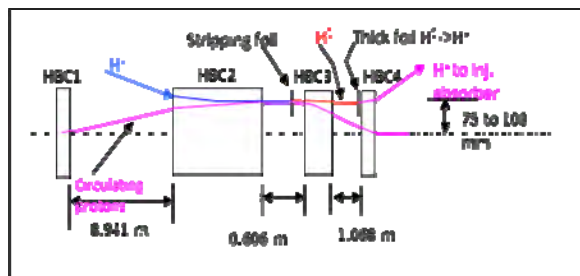


Figure 1: Injection insertion.

REAL RECYCLER LATTICE FOR PROJECT X

To accommodate the injection system in the Recycler ring, a 21.5 m long drift space is designed by converting the existing FODO lattice in RR10 straight section into a doublet, shown in Fig. 2. Instead of the standard ideal magnetic field used in the toy lattice, the measured magnetic fields, up to 8th order multipole components, have been implemented in the real lattice for Project X. In addition, the RR30 straight section was converted to a FODO lattice with standard permanent quads, and the trim quads in RR60 phase trombone straight section are set to zero. To get nominal tunes (25.425, 24.415),

- the end-shim field of each gradient magnet in the arc cell were adjusted, so that the phase advances of the arc cell changed from $\mu_x = 83.624^\circ$, $\mu_y = 78.290^\circ$ to $\mu_x = 85.236^\circ$, $\mu_y = 79.007^\circ$
- added additional trim quads in the dispersion suppressor sections on either side of the RR10 to match the two ends of the RR10 injection insertion to the whole ring

The lattice was shown in Fig. 3. The chromaticities in the Recycler ring were designed to be corrected by body sextupole components and the sextupole components of the end-shims of each dipole gradient magnets. The chromaticities are now (-1,-1) with the measured magnetic field. For additional chromaticity corrections, there are 8 and 16 sextupoles in horizontal plane and vertical plane respectively. They are set to 0 for this lattice.

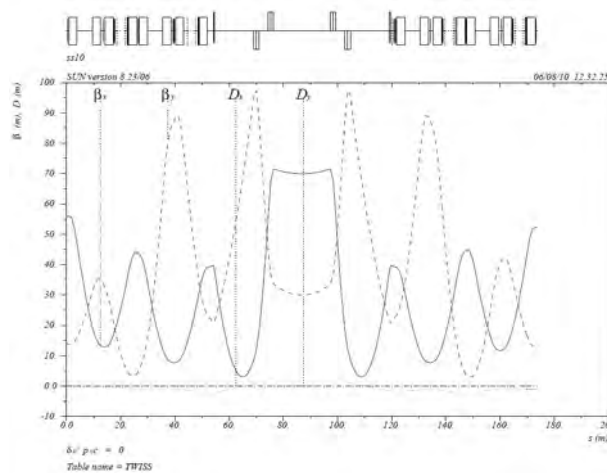


Figure 2: The lattice in RR10 with symmetric structure for injection.

*Work supported by U.S.Department of Energy under the contract No. DE-AC02-76CH03000.

[#]meiqin@fnal.gov

ACHIEVING HIGH LUMINOSITY IN AN ELECTRON-ION COLLIDER*

Yaroslav Derbenev, Geoffrey Krafft, Byung Yunn and Yuhong Zhang[#],
Thomas Jefferson National Accelerator Facility, Newport News, VA 23693, U.S.A.

Abstract

A future electron-ion collider is required to deliver a high luminosity exceeding $10^{33} \text{ cm}^{-2}\text{s}^{-1}$ per detector for probing the hadronic structure of matter. At JLab, a medium energy ring-ring collider (MEIC), based on the CEBAF SRF linac as a full-energy electron injector and a green-field design of an ion complex, is one of several proposals to meet this science need. The present MEIC design relies on high bunch repetition and high average-current colliding electron and ion beams with short bunch length and small transverse emittance for reaching the high luminosity goal. This is an approach significantly different from traditional hadron colliders. In this paper, we present a review of this luminosity concept and its impact on the accelerator design, particularly design of the ion complex for delivering required ion beams. We will also discuss some new ideas towards the realization of this high collider luminosity concept.

INTRODUCTION

As articulated in the latest Long Range Plan [1] issued by US DOE-NSF Nuclear Science Advisory (NSAC) Committee, a new electron-ion collider (EIC) is critically needed as a gluon microscope for the emerging QCD frontier. While the EIC science programs are under active development, a set of basic machine requirements has been gradually converging. Among them is a minimum luminosity of $10^{33} \text{ cm}^{-2}\text{s}^{-1}$, roughly 100 times higher than the final achieved luminosity of HERA, the world's only and highly successful high energy electron-proton collider at DESY recently decommissioned.

JLab has been engaged in feasibility studies and conceptual design of a polarized electron-ion collider for over a decade. The present baseline is a medium energy ring-ring collider (MEIC) with a CM energy up to 52 GeV [2] while a future energy upgrade (ELIC) will extend the CM energy to or beyond 100 GeV [3]. Since the very beginning, the focus of the JLab EIC studies has centered on achieving ultra-high luminosity over multiple (3 or 4) collision points, an order of 20 to 100 times higher than the desired luminosity requested by the Long Range Plan. Such unprecedented high luminosity is achievable in principle due to MEIC or ELIC employing a special luminosity concept which has already been proved in several lepton-lepton colliders but is still new to colliders involving hadron beams. JLab possesses a unique opportunity to adopt this luminosity concept for its MEIC design due to the following two facts: the 12 GeV upgraded CEBAF SRF linac will serve as a full energy injector into the MEIC electron ring; and being a green

field, the MEIC ion complex can be specially designed to produce ion beams with optimized time and spatial bunch structures. Therefore, MEIC and its energy upgraded version ELIC hold a very attractive promise of an ultra-high luminosity in a range from a few 10^{34} to above $10^{35} \text{ cm}^{-2}\text{s}^{-1}$, depending on acceptance of the detectors and arrangement of interaction regions.

Though the JLab EIC designs and their luminosity concept were proposed nearly a decade ago and reported in various conference proceedings [3,4] and a design report [5], we will present a comprehensive review in the next section with emphasis on the luminosity concept itself rather than machine design details. In the third section we will discuss ideas and accelerator design for forming the required ion beams to support high luminosity.

MEIC LUMINOSITY CONCEPT

Briefly, the key to the MEIC high luminosity concept is that both colliding electron and ion beams have short bunch lengths and small transverse emittance such that a strong final focusing can be adopted to reduce beam spot sizes to a few μm at collision points, hence, combined with a high bunch repetition rate and high averaged current, greatly boosting the collider luminosities. To illustrate this concept, let us first examine how ultra high luminosities had been achieved in several lepton-lepton colliders.

Lessons Learned from Lepton-Lepton Colliders

The present world records of the highest achieved luminosity are held by e+e- colliders at the KEK-B and PEP-II B-factories, with sustained peak values of 2.11 and 1.21 times $10^{34} \text{ cm}^{-2}\text{s}^{-1}$ respectively [6,7]. These high luminosities can be attributed to the following machine design features and key beam parameters (see Table 1): (1) high bunch repetitions, up to 508.6 MHz for KEK-B and 476 MHz for PEP-II; (2) high average beam current, up to 3 A; (3) short bunches, with RMS bunch lengths shorter than 1 cm; (4) small transverse emittance, of the order of a few mm-mrad (normalized) on vertical direction and very high aspect ratio; (5) extremely small (less than one cm) vertical beta-star (betatron function at collision points). It is clear that (1) and (2) lead to modest bunch charges, about several 10^{10} electrons or positrons per bunch, hence lesser effects of single bunch instabilities. (5) is possible since (3) ensures the hour-glass effect is still relatively small even under a very strong final focusing (beta-star), combined with (4), leading to micrometer beam spot sizes at collisions points. In addition, (4) reduces the beam spot size inside the final focusing quads, and thus requires smaller apertures in

* Authored by Jefferson Science Associates, LLC under U.S. DOE Contract No. DE-AC05-06OR23177.

[#] yzhang@jlab.org

NEW, HIGH POWER, SCALING, FFAG DRIVER RING DESIGNS

G. H. Rees, D. J. Kelliher, ASTeC Division, Rutherford Appleton Laboratory, STFC,
Chilton, Didcot, Oxon OX11 0QX, U.K.

Abstract

High power driver rings are examined, using new FFAG designs, based on cells of five, symmetrical, scaling pumplet magnets. Apertures are minimized by using large, betatron phase shifts per cell, typically $\mu_h \sim 280^\circ$ and $\mu_v \sim 130^\circ$. Key aspects are the lengths of the long straight sections, particularly if H^- charge exchange injection is required. Rings are considered for ISIS upgrades and Neutrino Factory proton and muon drivers, both with and without insertions.

INTRODUCTION

FFAG rings of pumplet cells have previously been thought better in a non-scaling than a scaling form [1]. However, scaling pumplets may be simpler and have smaller apertures if operation is in a higher stability region of Hill's equation [2], at betatron phase shifts per cell of $\mu_h \sim 280^\circ$ and $\mu_v \sim 130^\circ$. Scaling triplet cells, in such a mode, using similar non-linear magnet field profiles, are found to have *beta*-functions which are significantly larger than those of the pumplet cells.

The cell forms are: O f(+) o D(-) o F(+) o D(-) o f(+) O (when scaling) and : O d(-) o F(\pm) o D(+) o F(\pm) o d(-) O (when non-scaling), where the \pm refer to bend directions. Long (OO) and short (o) straight sections interleave with vertical focusing (D) and defocusing (f, F) units. Scaling cells have the same normalized field gradients and bend radius in all magnets, whereas isochronous and non-isochronous, non-scaling cells do not, having more complex, non-linear magnet field profiles.

Field gradients and unit spacings may be varied to adjust the cell tunes. To minimize misalignment and field error effects, the scaling cells are set with the tunes above the fourth-order betatron resonances, $4q_v = 1$ and $4q_h = 3$ ($\mu_h = 270^\circ$) but below the fifth-order, $5q_h = 4$. The stable area is wide, but the vertical *beta*-values, β_v , need optimization, as the clearances required for extraction set the acceptances for injection above the typical values used in synchrotrons.

Fields are modified from traditional scaling forms, as discussed later in the report. Also described are the ways in which various sequences of long and short straight sections may be realized in rings of pumplet cells. More non-linear cell resonances may be excited than in a typical high current linac focussing structure.

SCALING PUMPLET CELLS

A scaling pumplet cell has the sequence of combined-function magnets: O f(+) o D(-) o F(+) o D(-) o f(+) O, where (+) and (-) represent normal and reverse bending and (OO) and (o) are the long and short straight sections. The cell has mirror symmetry about the centre of the F(+).

The traditional magnet field profile for a scaling cell and its local, normalized field gradient are described by: $B_{y=0} = B = B_o (1 + x/r_o)^K$, and $B'/B\rho_o \approx K/\rho_o(r_o + x)$, where x defines a radial offset from a B_o reference orbit, at distance r_o from the centre of the FFAG ring, and the common values of the parameter K define the magnetic field gradients.

Parallel edged magnets are used, offset relative to one another. Vertical guide fields are then modified, from the traditional scaling form given above, to an exponential form, to produce a smaller variation of $B'/B\rho_o$ values over the poles of the high k/ρ_o ($=K/r_o$), parallel edged magnets: $B_{y=0} = B = B_o \exp(kx/\rho_o)$ and $B'/B\rho_o \approx k/\rho_o^2$.

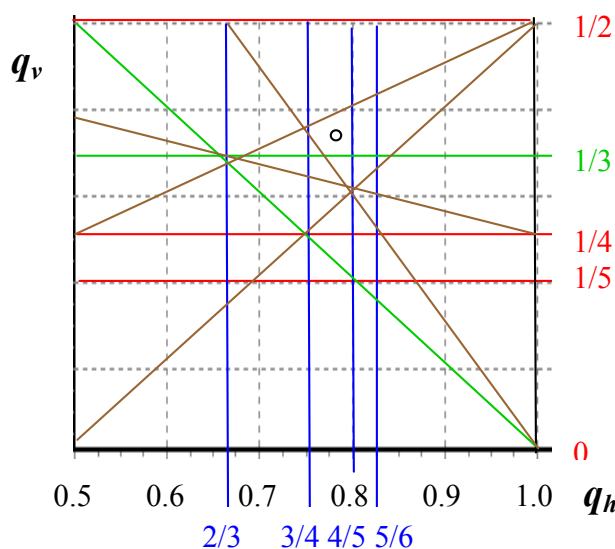


Figure 1: Pumplet cell, q_h, q_v resonance diagram.

Cell tunes for Figure 1 are at $q_h = 11/14$ and $q_v = 5/14$. The adjacent resonances are shown in blue (horizontal), red (vertical), brown (for coupled, sextupole ($q_h - 2q_v = 0$) or octupole ($2q_h - 2q_v = 1$) or for decapole ($q_h + 4q_v = 2, 3q_h + 2q_v = 3$)) and in green ($q_h + q_v = 1, 3q_v = 1$). The two cell resonances in green are due to the combined effect of vertical orbit errors and the sextupole or octupole field components in the pumplet magnets.

Tunes are set to optimize lattice parameters, avoid as many of the cell and ring resonances as possible, and also provide straights, approximately two cell lengths apart, for the 3π -horizontal and π -vertical, orbit bump units. Typical choices that are provided for the cell tunes are: ($q_h = 11/14, q_v = 5/14$) or ($q_h = 10/13, q_v = 5/13$). These have the form of a ratio of two integers, as this is often found advantageous in the lowering of cell resonance excitations.

BEAM BASED ALIGNMENT OF SYNCHROTRON UNDER COUPLED QUADRUPOLE MAGNET ENVIRONMENT

N. Hayashi*, S. Hatakeyama, H. Harada, H. Hotchi, JAEA/J-PARC, Tokai, Ibaraki, Japan
 J. Takano, M. Tejima, T. Toyama, KEK/J-PARC, Tsukuba, Ibaraki, Japan

Abstract

The Beam Based Alignment (BBA) of the BPM is inevitable for precise and absolute beam position measurements. Even though careful fabrication and installation of the BPM detector, it has to be calibrated by using the beam. Usually, it requires that the individual quadrupole magnet is able to be controlled. However, it is not always that case. In addition, scanning over the all BPM is time consuming procedure. The BBA method under coupled QM environment would help to reduce time for calibration. It presents general formula and experiences at J-PARC RCS and parts of results are compared with the ordinal method at J-PARC MR.

INTRODUCTION

The Japan Proton Accelerator Research Complex (J-PARC) comprises three accelerators [1] and three experimental facilities by using various intensive secondary particles for a variety of scientific programs. Its construction phase has been completed and started user operation[2, 3]. The RCS (3-GeV rapid-cycling synchrotron) is a 25Hz cycle machine and designed to provide 1 MW beam power for the MLF (Material and Life science experimental facility) and the MR (Main Ring). The RCS beam power has been regularly 120kW (intensity of $1 \times 10^{13}ppp$) since November 2009. One hour 300kW operation, which intensity is about $2.6 \times 10^{13}ppp$, was also performed as a demonstration. This intensity is provided to the MR every 3.52s, if the MR beam power is set to 100kW. The MR has been beam commissioned in May 2008, started from very low intensity, $4 \times 10^{11}ppp$. Before a summer shut down of 2010, it gives maximum beam power of 100kW (several 10kW in regularly) for Fast Extraction (FX) to the neutrino beam line.

The BPM (Beam Position Monitor) system of the RCS [4, 5] and that of the MR [6, 7] is one of the important devices. These BPM detectors have a good linear response due to its diagonal cut electrode and a resolution of 20~30 μ m. However, its offset with respect to the nearest QM (quadrupole magnet) remains as uncertainties, in spite of careful and precise fabrication and installation. Those uncertainties have to be measured using the beam experimentally, namely by beam based alignment (BBA).

If an individual QM is controllable, it is rather simple and there are some examples of such analysis [8, 9, 10, 11]. However, in the RCS, it is more complicated, since several

QMs are coupled together and only a group of QM can be controlled as family. For such a case, by extending the single QM sweep method to the multiple QM sweeping, and multiple BPM offset can be determined simultaneously and its preliminary results are presented [12].

In the MR, only some selected BPMs, which are in the slow or the fast extraction section, are corrected. Although determination of the offset and its correction is important, BBA is time consuming measurements. So far, it is not able to find such measurements during the limited accelerator machine study time. If the multiple BPM offsets are determined at once, it may help.

In this paper, in order to show this multiple QM sweeping method works generally, two analysis methods were applied to the MR for comparison. It is also presents further analysis, including higher order effect, on the RCS are presented.

REVIEW OF BEAM BASED ALIGNMENT METHOD AND ITS EXTENSION

The principle of BBA is that the orbit is not affected when one QM focusing is changed (ΔK), if the beam passes through the center of that QM. Otherwise, the beam is displaced by $x_1 \neq 0$ at that QM and the orbit is modified due to the dipole kick of $\Delta K x_1$.

BPM COD data for different initial orbits are taken with varying the QM field strength for BBA. An original orbit, $x_1(s)$, is described by following Hill's equation using a focusing function $K(s)$ of QM, and any field error $-\Delta B/B\rho$.

$$x_1''(s) + K(s)x_1(s) = -\frac{\Delta B}{B\rho} \quad (1)$$

Then, one of QM at $s = s_n$, has a changed field gradient by the amount ΔK , and the orbit is modified from $x_1(s)$ to $x_1(s) + x_2(s)$. This is expressed as,

$$(x_1(s) + x_2(s))'' + (K(s) + \Delta K)(x_1(s) + x_2(s)) = -\frac{\Delta B}{B\rho} \quad (2)$$

By taking the difference between eq.(2) and (1), it becomes

$$x_2''(s) + K(s)x_2(s) = -\Delta K \times [x_{1n} + x_{2n}] \simeq -\Delta K x_{1n} \quad (3)$$

by ignoring the term $\Delta K x_{2n}$. Here, $x_1(s_n) \equiv x_{1n}$, and $x_2(s_n) \equiv x_{2n}$. Since $\Delta K(s)$ is none-zero only at $s = s_n$, eq.(3) could be rewritten using this constant ΔK as,

$$x_2''(s) + K(s)x_2(s) = -\Delta K \delta(s - s_n)x_1(s) \quad (4)$$

* naoki.hayashi@j-parc.jp

IBS FOR NON-GAUSSIAN DISTRIBUTIONS*

A.V. Fedotov[#], BNL, Upton, NY 11973, USA
A. O. Sidoren, A. V. Smirnov, JINR, Dubna, Russia

Abstract

In many situations distribution can significantly deviate from Gaussian which requires accurate treatment of IBS. Our original interest in this problem was motivated by the need to have an accurate description of beam evolution due to IBS while distribution is strongly affected by the external electron cooling force [1]. A variety of models with various degrees of approximation were developed and implemented in BETACOOOL in the past to address this topic [2]. A more complete treatment based on the friction coefficient and full 3-D diffusion tensor was introduced in BETACOOOL at the end of 2007 under the name “local IBS model” [3]. Such a model allowed us calculation of IBS for an arbitrary beam distribution. The numerical benchmarking of this local IBS algorithm and its comparison with other models was reported before. In this paper, after briefly describing the model and its limitations, we present its comparison with available experimental data.

INTRODUCTION

Typically, in the absence of beam loss and external amplitude-dependent force, time evolution of beam profiles due to the Intrabeam Scattering (IBS) can be described by Gaussian distribution. Thus, analytic models of IBS developed for Gaussian distribution are very useful and provide good agreement with experimental measurements (see Ref. [4], for example). When longitudinal distribution starts to deviate from Gaussian for example due to the losses from the RF bucket, assumption of Gaussian distribution may already result in inaccurate prediction of intensity loss. To address this issue 1-D Fokker-Planck approach was effectively used before [5-6]. A more dramatic situation occurs when there is an externally applied force, like electron cooling. Since electron cooling force depends on the amplitudes of individual particles, the distribution under such force very quickly deviates from Gaussian. This effect is especially magnified when electron cooling is “magnetized” [7]. The problem of how to accurately account for IBS for such distributions became of special interest with a proposal to use electron cooling directly in a collider. For realistic prediction of luminosity gain from electron cooling an accurate treatment of IBS is required. Several approximate models were developed in the past to address this issue [1, 8-9]. However, a more general description requires full treatment of kinetic problem. Such a treatment was introduced in the BETACOOOL code under the name “local IBS model” [3].

*Work supported by the U.S. Department of Energy

[#]fedotov@bnl.gov

LOCAL IBS MODEL

The process of change of distribution function as a result of many small-angle scatterings can be described by Fokker-Planck equation, which offers self-consistent description of the system in diffusion approximation. The diffusion approximation reduces the problem of determining the effect of the fluctuations in the interaction force to the calculation of the dynamical friction F and diffusion coefficient D , which are related to the first and second velocity jump moments, respectively. For the case of Coulomb interaction, expressions for the friction force and diffusion tensor are well known from plasma physics and are given by:

$$\vec{F} = \frac{\langle \Delta \vec{p} \rangle}{\Delta t} = - \frac{4\pi n e^4 Z_t^2 Z_f^2}{\left(\frac{m_f m_t}{m_f + m_t} \right)} \int \ln \left(\frac{\rho_{\max}}{\rho_{\min}} \right) \frac{\vec{U}}{U^3} f(\vec{v}) d^3 v \quad (1)$$

$$D_{\alpha, \beta} = \frac{\langle \Delta p_\alpha \Delta p_\beta \rangle}{\Delta t} = 4\pi n e^4 Z_t^2 Z_f^2 \int \ln \left(\frac{\rho_{\max}}{\rho_{\min}} \right) \frac{U^2 \delta_{\alpha, \beta} - U_\alpha U_\beta}{U^3} f(\vec{v}) d^3 v \quad (2)$$

Here $\alpha, \beta = x, y, z$, the angular brackets indicate averaging over the field particles, Z_t, Z_f are the charge numbers of the test and field particle, $\vec{U} = \vec{V} - \vec{v}$ is the relative velocity of the test and field particle, n is the mean density and $f(v)$ is the distribution function in the velocity space of field particles, respectively. The logarithm under the integrals is also called Coulomb logarithm, and is a measure of the relative contribution of (weak) remote interactions compared to (strong) near interactions. A validity of the diffusion approximation requires Coulomb logarithm $\gg 1$, which is valid for IBS.

In standard treatment of IBS one usually assumes Gaussian distribution function and also averages over beam distribution to produce expressions for the growth rate of beam emittances. For present problem we need to keep dependence of the friction and diffusion coefficients on particle amplitudes. The beam distribution is represented by an array of particles. For each of the particles a smaller array of local particles is chosen, and local density and rms parameters of the particle distribution in each local array are calculated. The local parameters are used for calculation of the friction and diffusion coefficients. Since evaluation of the friction and diffusion coefficients is done numerically, the algorithm

LINEAR AND NON-LINEAR OPTIMIZATION OF THE PS2 NEGATIVE MOMENTUM COMPACTION LATTICE

H. Bartosik, Y. Papaphilippou, CERN, Geneva, Switzerland

Abstract

PS2 is a design study of a conventional magnet synchrotron considered to replace the existing PS at CERN. In this paper, studies on different aspect of single particle dynamics in the nominal PS2 Negative Momentum Compaction lattice are described. The global tuning flexibility of the ring and the geometric acceptance is demonstrated by a systematic scan of quadrupole settings. Frequency map analysis and dynamic aperture plots for two different chromaticity correction schemes are presented. The impact of magnet misalignments on the dynamic aperture is studied for one of them. A first study of the beam dynamics with magnetic multipole errors using frequency maps and the corresponding analytical tune-spread footprints is reported. It is thus demonstrated that multipole errors determine to a large extend the beam dynamics in PS2.

INTRODUCTION

A possible upgrade scenario of the CERN injector complex considers the aging PS to be replaced by a separated function synchrotron called PS2. As the PS2 lattice is designed with negative momentum compaction (NMC), the transition energy γ_t is imaginary, thus allowing operational flexibility and reducing beam losses during acceleration. The PS2 should provide the same flexibility for handling different kind of beams as the PS but with higher intensity. Since the intensity of the proton beam will be roughly doubled with respect to the PS, the injection energy is increased from 1.4 GeV to 4 GeV for obtaining similar space charge induced incoherent tune shift. The extraction energy is increased to 50 GeV, which would allow a further reduction of beam instabilities due to collective effects in the subsequent SPS. In order to achieve an optimized filling pattern of the SPS for delivering LHC bunch trains, the circumference of the PS2 is fixed to 1346.4 m, i.e. 15/77 of the circumference of the SPS. A summary of the main lattice design constraints is given in Table 1.

Table 1: PS2 Lattice Design Constraints

Parameter	Value
Injection energy, kinetic	4 GeV
Extraction energy, kinetic	50 GeV
Circumference	1346.4 m
Transition energy	imaginary
Maximum bending field	1.7 T
Maximum quadrupole gradient	16 T/m
Minimum drift space, dipoles / quads	0.8 / 1.3 m

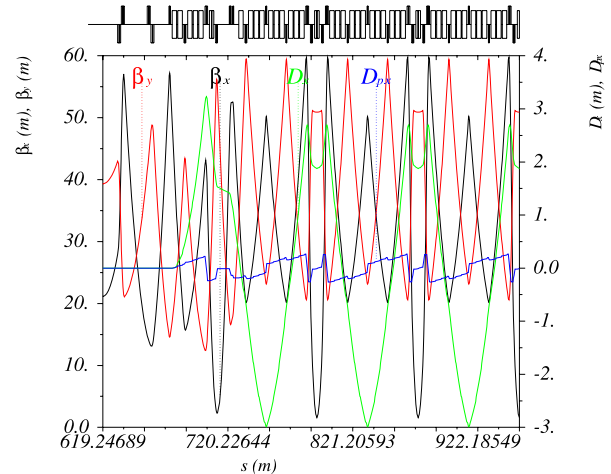


Figure 1: Optics functions for a quarter of the PS2 lattice, with $(Q_x, Q_y) = (11.81, 6.71)$ and $\gamma_t = 25.3i$.

The baseline lattice for the PS2 [1] has a twofold symmetry with tunable arcs and two zero dispersion long straight sections (LSS). Each of the arcs consists of five NMC cells and two dispersion suppressor modules. The working point of the machine is tuned by adjusting the phase advances in the NMC cells and matching the dispersion suppressors to the optics of the LSSs. The mirror symmetric LSSs are based on two pairs of quadrupole doublets [2] formed by wide aperture magnets with a length of 2.4 m. As required by the general layout of the LHC injector complex, all beam transfer systems are installed at the same LSS. The layout of the NMC cell is based on two FODO cells, linked by a central insertion of quadrupole doublets. Imposing negative dispersion at the entrance of the module leads to negative momentum compaction [3]. Optimizing to maximum gradients of 16 T/m yields 3 types of quadrupoles for the 4 families with lengths of 0.8 m, 1.6 m and 2.2 m. The dispersion suppressor modules on either side of the NMC arc share their first and last quadrupole with the adjacent LSS and NMC cell, respectively. Ten dipole magnets and 6 independent quadrupole families based on the same types of magnets as used in the arc cells are needed to achieve the matching constraints. The PS2 lattice contains 170 dipoles with a length of 3.7 m and a maximum field of 1.7 T at top energy. The 116 quadrupole magnets are grouped to 15 families. They are based on 4 different types, 3 for the arcs and the wide aperture magnets for the LSSs.

Figure 1 shows the optics functions for the working point $(Q_x, Q_y) = (11.81, 6.70)$ with $\gamma_t = 25.3i$. The natural chromaticities of $(\xi_x, \xi_y) = (-21.5, -11.0)$ are compensated by relatively weak sextupoles, as they are located at high-dispersion areas.

SPACE CHARGE EFFECTS DURING MULTITURN INJECTION INTO SIS-18

Stefan Paret, Oliver Boine-Frankenheim, GSI, Darmstadt, Germany

Abstract

For the FAIR [1] project, the intensity of heavy-ion beams in SIS-18 has to be increased by an order of magnitude. In order to achieve the design intensities, the efficiency of the multiturn injection from the UNILAC has to be optimized for high beam currents. This is especially important for the operation with intermediate charge state heavy-ions, where beam loss during injection will lead to pressure bumps and to a reduced lifetime of the beam. An analytic model exploring the limits of lossless injection without collective effects is discussed. The multiturn injection into SIS-18 is studied by virtue of 2D particle tracking simulations using an extended version of the computer code PATRIC. The impact of space charge and image currents on the efficiency of the injection process is analyzed.

INTRODUCTION

GSI's UNILAC and SIS18 are being upgraded in order to increase the beam intensity to the ambitious design parameters for the booster operation for FAIR [2]. For U^{28+} the goal is to accumulate effectively a current of 15 mA for 15 turns in SIS18, corresponding to 2.3×10^{11} particles. For these beam parameters, collective effects are expected to affect the multiturn injection (MTI). The impact of space charge and image currents on the injection efficiency and the particle distribution needs therefore to be investigated.

Furthermore, endeavors are being made to reduce the horizontal emittance in UNILAC [3], which is a key quantity for the MTI. However, investigations are needed to specify the maximal acceptable emittance. For this reason, the injection efficiency and effective particle accumulation are studied as a function of the beam emittance and the particle distribution. The results of the numerical studies shall serve as reference for planned experiments in SIS18.

The particle tracking code PATRIC was modified enabling it to simulate the MTI. In the first section the implementation of the MTI is described. Then an analytic model helping to find good injection parameters is discussed. Finally simulation results without and with space charge are shown. The phase-space distribution, losses and particle accumulation are discussed. An outlook on planned experiments and numerical studies is given.

MTI IN PATRIC

Over the years, PATRIC has been developed at GSI for numerical studies of various kinds of collective effects (see e.g. [4]). So far it was applied to accumulated beams in a ring in storage mode only. In order to investigate the MTI,

the sources of the code were modified.

The most important aspect is the introduction of a time dependent local orbit bump to adjust the orbit to the incoming beam. PATRIC is able to read the sector-maps produced by a MAD-X [5] script which provide the transport matrices around the synchrotron. At the position of the 4 bumpers generating the local orbit bump, markers were inserted as place holders into the file providing the SIS18 beam optics. Hence MAD-X is used to calculate the sector map without injection bump. The bump is added by PATRIC by virtue of horizontal kicks at the markers representing the bumpers. The corresponding elements of the kick vector (K), provided by the sector-map file, are changed to deflect the particles. The deflection angles are adapted turn by turn, until the bump disappeared.

Another change concerns the generation of the particle distribution. Instead of initializing the beam once at the beginning of a simulation, this procedure is repeated at the beginning of the loop until the injection finished. The particles are transported using the transport matrices from MAD-X and the modified kick vectors. If space-charge effects are to be included, Poisson's equation is solved on a 2D transverse grid and momentum kicks corresponding to the local field strength are applied. The boundary conditions can be set to represent the (perfectly conducting) beam pipe or empty space. Thus the impact of image currents can be separated from that of direct space charge.

The modified version of PATRIC can be employed to study losses, particle accumulation, emittance growth and the phase-space distribution for varying tune, bump settings, injection duration and initial particle distribution, emittance and intensity.

LOSSLESS INJECTION

An injection scheme without losses allowing the longest injection is looked for as first step. The beam lattice functions at the end of the injector are assumed to be matched to the synchrotron. The beam cross section is presumably elliptical. The bumper ramp is linear and the ramp rate constant. The position of the septum and the injection angle are taken from SIS18. What remains to be optimized for a given emittance and working point are the height of the orbit bump and the angle of the bumped orbit with respect to the incoming beam, as well as the ramp rate of the orbit bump.

First the phase space after a single turn injection is considered. The position of the incoming beam in the horizontal phase space is parameterized as depicted in Fig. 1. The horizontal coordinate x of the beam's barycenter is decomposed into the bump height x_{r0} and the offset \tilde{x} . Due to

REDUCING LOSSES AND EMITTANCE IN HIGH INTENSITY LINAC AT BNL *

D. Raparia[#], J. Alessi, B. Briscoe, J. Fite, O. Gould, V. Lo Destro, M. Okamura, J. Ritter,
A. Zelenski, C-AD Dept., BNL, Upton, NY, USA

Abstract

BNL 200 MeV linac has been under operation since 1970 and gone through several changes during its 40 year lifetime. The latest (2009-10) reconfiguration in low and medium energy (35 and 750 keV) beam transport lines resulted in about a factor of 2 reduction in the transverse emittance for the accelerated polarized proton beam, and a several fold reduction in the radiation levels due to beam losses throughout the linac and isotope production facility complex with 30% more beam current for the unpolarized H⁺ beam for BLIP.

INTRODUCTION

The Brookhaven National Laboratory (BNL) 200 MeV drift tube linac (DTL) has been operating since November 1970 and was designed for 100 mA of peak current with 200 μs of pulse length at 10 Hz. During last 40 years of operation, linac has gone through many changes to accommodate changing requirements of the BNL accelerator complex for higher average beam current, better beam quality, or higher reliability. To satisfy present requirements, linac now provides H⁺ beam at 6.67 Hz, 200 MeV for the polarized proton program at Relativistic Heavy Ion Collider (RHIC) and 66-200 MeV for Brookhaven Linac Isotope Production (BLIP) [1]. The requirements for these programs are quite different and are the following. (1) RHIC: 200 MeV, 200 μA beam current, 400 μs pulse length, polarization as high as possible and emittance as low as possible, (2) BLIP: 66-200 MeV, 450 μs pulse length, current as high as possible (~40 mA), uniform beam distribution at the target, and losses as low as possible. In this article, we will discuss only the high intensity aspects of the linac.

BNL 200 MEV LINAC HISTORY

Table 1 summarizes changes of the last 40 years. There are several points worth noting. In 1982 switching to H⁺ operation increased the intensity in the AGS, while decreasing the linac output. In 1989 switching to RFQ preinjector provided high reliability and lower cost of operations. The changes in 1996 included shorting 35 keV line by removing diagnostics and adding PMQ in the flange of the RFQ at the high energy end to better match the beam line. These changes resulted in a 50% higher peak beam current and about 45% lower emittance. In 2009, the medium energy beam line length was reduced to 70 cm from 7 meters, resulting in an emittance reduction for high current by a factor of 4 and for the polarized H⁺ by a factor of 2. The reduction in emittance for polarized

H⁺ was translated into emittance reduction in RHIC by 25% at the collision energies. But due to longer 35 keV line, the beam current for BLIP was not increased as expected. In 2010, the beam current for BLIP was increased by 30 % by reducing the length of 35 keV line to two meters. Now linac is delivering the highest average current to BLIP while maintaining minimum losses since it was built in 1970.

Table 1: BNL 200 MeV Linac History

Year	Rep Rate Hz	Pulse Length μs	Peak Current mA	Avg. Curret μA
Design	10	200	100	200
1972	10	80	55	44
1975	10	100	60	60
1976	Switch to 5 Hz operation			
1979	5	220	70	77
1982	Switch to H- acceleration			
1984	5	200	25	25
1984	Add polarized H- operation			
1986	5	470	30	71
1989	Switch to RFQ pre-injector			
1990	5	500	25	63
1996	Switch to 6.67 HZ and changes in LEBT/MEBT			
1996	6.67	400	38	90
2000	Add Polarized source OPPIS			
2009	LEBT/MEBT reconfiguration (short MEBT)			
2009	6.67	430	32	80
2010	Shorten LEBT			
2010	6.67	430	38	110
2011	New Buncher and einzel-lens solenoid combo			

The linac was designed for 100 mA and smaller emittance since it was designed for protons. Particle simulations showed that transverse and longitudinal matching and the quadrupole focusing laws are essential for controlling the emittance growth in transverse as well as longitudinal planes. All the emittance growth occurs within the 1st tank (10MeV).The beam was pre accelerated with Cockcroft-Walton (C-W) to 750 keV than followed by an 8.5 meter long line consisting with eight triplets and two bunchers. To minimize the emittance growth in the 750 keV line, the beam size was kept small and the emittance growth in the line was about 50%. The beam was matched to DTL in all three planes. The capture efficiencies in the DTL were about 65-70%. It was recognized that longitudinal beam size was the key contributor in the transverse emittance growth, and the

*Work supported by US. Department of Energy
[#]raparia@bnl.gov

THE EMMA ACCELERATOR AND IMPLICATIONS FOR HADRON NON-SCALING FFAGS

S. L. Sheehy*, John Adams Institute, Oxford, UK

Abstract

EMMA (Electron Model for Many Applications) is the worlds first non-scaling FFAG constructed at the Daresbury Laboratory, UK. Commissioning activities have recently been undertaken and beam dynamics results relevant to hadron non-scaling FFAGs are presented. The impact of these results on the future design of non-scaling FFAGs for high intensity hadron beam applications is discussed.

THE EMMA NS-FFAG

The EMMA accelerator has been built as a proof-of-principle demonstrator for ns-FFAG technology [1, 2, 3, 4]. The project aims to demonstrate feasibility of ns-FFAGs and to study the novel beam dynamics of these machines in detail. The availability of the partial EMMA ring in the initial stages of commissioning in August 2010 allowed a few basic measurements to be made including the betatron tune and dispersion. These measurements are relevant to the design of proton ns-FFAGs as they are a crucial test of the ZGOUBI simulation code, used both for the EMMA design and in existing work towards proton ns-FFAGs for low intensity [5] and high intensity [6] beams.

The ALICE 35 MeV electron energy recovery linac prototype [7] is used to inject appropriate beams into EMMA. During EMMA operation the two linac sections of ALICE (the booster linac and main linac) are used to provide beams in the 10 to 20 MeV energy range of EMMA. The electron beam is diverted out of ALICE to the EMMA injection line and so ALICE does not run in energy recovery mode during EMMA operation. Details of ALICE and its setup for EMMA can be found in Ref. [8].

The main parameters of EMMA are given in Table 1. EMMA consists of 42 cells which are physically organised into seven sectors, with six cells in each sector. For some of the experimental work outlined here, only four of the seven sectors of EMMA were used.

Table 1: Lattice Parameters of the EMMA Accelerator

Parameter	Value
Radius	2.637 m
Circumference	16.57 m
No. of cells	42
Cell type	DF doublet
Cell length	394.481 mm
RF	19 cavities; 1.3 GHz
Energy range	10 to 20 MeV

*s.sheehy1@physics.ox.ac.uk

EXPERIMENTAL METHOD

In planning the experimental commissioning work the decision was made to keep the beam energy of the ALICE injector constant and to represent different relative momenta by changing the EMMA quadrupole strengths while maintaining the ratio between the D and F quadrupoles (the D/F ratio). This means that to reproduce the dynamics of a relative momentum of +5% the main quadrupole magnet strengths have to be changed by -5% ¹.

The EMMA ring is heavily instrumented with diagnostic devices as it is an experimental machine with novel beam dynamics that need to be studied in detail. The full EMMA Beam Position Monitor (BPM) system consists of 81 button BPMs. Each BPM includes a button electrode pickup and a pair of front-end modules connected via a single low loss cable 40 m in length to a VME module², where the pickup signals are measured using analog to digital converters (ADCs) [9].

During the initial commissioning process the electronic BPM readout system was not yet available. To read positions from the installed BPMs, seven coaxial cables were available which were connected directly from the BPMs to the control room where the analog signals were monitored using a Tektronix TDS6124C oscilloscope. For each BPM, the left-right signals are multiplexed onto the same cable with a set time delay, which is one of the main functions of the front-end module. This means that the horizontal position can be read from a single cable, and similarly for the top-bottom signals for the vertical position. The oscilloscope was used to read out the raw voltage signals from the BPMs and beam positions were calculated from these raw values using a pre-measured calibration algorithm [10].

With a total of just seven coaxial cables the amount of data taken was limited during this period, as each cable can only supply either a horizontal or vertical position. A machine shut down is required in order to change which BPMs are connected, so this is minimised during the commissioning shifts.

During the measurements only horizontal BPMs were connected to give the maximum of 7 horizontal positions simultaneously. The vertical offset prior to the injection septum was minimised using the vertical correctors in the injection line, though only to within a few mm.

¹This change is not immediately obvious. As $B\rho \propto pc$, usually for constant B (in a fixed field accelerator) pc is increased and the bending radius ρ increases proportionally. In this case we keep pc constant but want to mimic the increase in ρ , hence B is reduced.

²Versa Module Europa (VME)

CONTROLLED LONGITUDINAL EMITTANCE BLOW-UP IN A DOUBLE HARMONIC RF SYSTEM AT CERN SPS

T. Argyropoulos, T. Bohl, T. Linnecar, E. Shaposhnikova, J. Tückmantel, CERN, Geneva, Switzerland

Abstract

Controlled longitudinal emittance blow-up together with a fourth harmonic RF system are two techniques that are being used in the SPS in order to stabilize the beam before injecting into the LHC. The emittance blow-up has been achieved by introducing a band-limited phase noise during acceleration. Measured variations of the final emittance along the batch can be explained by the modification of the synchrotron frequency distribution due to the effect of beam loading in a double harmonic RF system.

INTRODUCTION

The nominal LHC beam in the SPS consists of four batches separated by 3 gaps of 225 ns. Each batch contains 72 bunches spaced by 25 ns with 1.15×10^{11} protons per bunch. This beam is accelerated by four 200 MHz travelling wave cavities, equipped with feed-forward and feed-back systems. However, a longitudinal coupled bunch instability observed at high energies appeared to be a limiting factor because of its low threshold at 2×10^{10} p/b. This beam is finally stabilised by increased synchrotron frequency spread using a fourth harmonic RF system [1] and controlled longitudinal emittance blow-up which is applied during the ramp by introducing band limited noise through the phase loop of the main RF system [2].

Although the controlled emittance blow-up is necessary to stabilize the nominal intensity beam at flat top, the final bunch length and therefore emittance is limited due to the injection into the 400 MHz buckets of LHC. For that reason, bunch to bunch emittance variations along the batch can lead to particle losses in the LHC. Non-uniform emittance blow-up of high intensity beam in SPS had been observed at the end of 2004 and previous studies [3, 4] suggested that this effect can be attributed to the bunch to bunch variation of the incoherent synchrotron frequency due to the residual beam loading. This analysis showed that for the bunches at the edges of the batch the zero amplitude synchrotron frequency is lower than for those in the middle. Therefore, for a constant noise band along the batch for all bunches we would expect the blow-up to be more effective for those in the middle of the batch (optimum phasing). However, the experimental results show that bunches at the edges of the batch are blown-up more than those in the middle.

The present work extends the previous analysis by considering how the whole synchrotron frequency distribution is modified for the different bunches in the batch, defined mainly by the residual beam loading in the 200 MHz RF system. It will be shown that for the bunches at the edges

of the batch, where the bigger synchronous phase variations due to beam loading occur, a significant change in the synchrotron frequency distribution appears, making larger blow-up possible.

OBSERVATION OF NON-UNIFORM EMITTANCE BLOW-UP

With the controlled emittance blow-up a stable beam of emittance up to ~ 0.6 eVs can be delivered to the LHC. However, the measurements that are presented here were done for a single batch with nominal intensity, with the aim to obtain maximum emittance (~ 0.9 eVs) for transfer to LHC which might be requested. Particle momentum and applied RF voltages (200 MHz and 800 MHz) for the SPS cycle are shown in Fig. 1. The band limited noise [2] was introduced through the phase loop of the 200 MHz RF system at 185 GeV (14.8 s along the cycle) and lasted for 3 s. Figure 2 depicts the noise band and the synchrotron frequency spread (calculated for low intensity) during the cycle where the noise is applied. For nominal intensity beam the low intensity settings should be shifted down by ~ 10 Hz due to an incoherent frequency shift produced by the SPS inductive impedance $\text{Im}Z/n \approx 7$ Ohm.

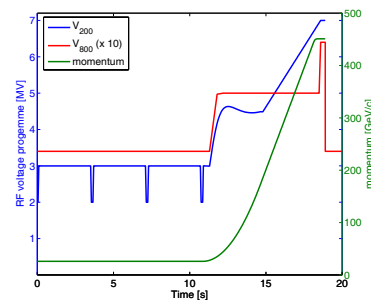


Figure 1: Particle momentum (green), the 200 MHz voltage (blue) and 800 MHz voltage (red, $\times 10$) programme along the cycle.

The bunch lengths were deduced from the acquired bunch profiles after correcting for the pick-up and cable transfer function [5]. Figure 3 shows the results for two cycles where different noise bands were applied. The plots present the bunch lengths at different moments in the cycle. Both cases correspond to a successful blow-up in the sense that at the flat top the bunches were stable. However, it is apparent that bigger blow-up occurs for the bunches at the beginning and the end of the batch. Furthermore, we can clearly see from the bottom plot where the noise band was lifted up 10 Hz compared to the top one, that the relative

SIMULATION OF THE LONG TERM BEAM INTENSITY PERFORMANCE OF THE NEG-COATED SIS18*

P. Puppel, GSI, Darmstadt, Germany and Goethe-Universität Frankfurt, Germany
P. Spiller, GSI, Darmstadt, Germany
U. Ratzinger, Goethe-Universität Frankfurt, Germany

Abstract

The StrahlSim code has been developed to simulate dynamic vacuum effects and charge exchange beam loss in the GSI and FAIR heavy ion accelerators. The code accounts for charge exchange cross sections at the actual beam energy, it determines the loss positions of charge exchanged ions, and the pressure rise caused by desorption due to the impact of these ions onto the vacuum chamber. Recently, the modeling of time dependent longitudinal pressure profiles has been implemented in StrahlSim. Thereby, localized pressure bumps during a cycle and the lifetime of NEG-coated surfaces depending on their distance from the local pressure bumps, and the corresponding influence on the beam performance resulting from the saturation process can be simulated. The new code was applied to SIS18 considering two scenarios: 1) the currently available U^{28+} intensity of 2×10^{10} extracted particles per cycle, and 2) the proposed FAIR booster operation with 1.5×10^{11} extracted particles per cycle. The simulations show, that the beam scrubbing effect, which is also accounted by the code, is crucial for a stable booster operation of SIS18, as it stabilizes the dynamic vacuum over long term operation. Already for the currently available beam intensity, the beam scrubbing effect is important, as it prevents an exceeding saturation of the NEG near the injection septum.

INTRODUCTION

In order to provide high intensity heavy ion beams, the FAIR project [1] relies on the use of intermediate charge state heavy ions. SIS100, the main synchrotron of the FAIR accelerator complex, is supposed to accumulate 5×10^{11} U^{28+} ions per cycle. The existing SIS18 will work as booster for SIS100 and is supposed to accelerate 1.5×10^{11} U^{28+} ions per cycle. Four SIS18 cycles will be accumulated in SIS100. A major upgrade program, which is still ongoing, is performed to increase the beam intensities of SIS18 [2].

The use of intermediate charge state heavy ions is necessary to avoid intensity losses in stripping stages, and to increase the space charge limit. However, the operation with such intermediate charge state ions may suffer from significant beam loss due to charge exchange processes. Beam ions are ionized by collisions with residual gas particles and deflected differently with respect to the reference ion in

dispersive elements. At collisions with the vacuum chamber or other inserts, a high-energy desorption process takes place, which leads to a local pressure rise in the machine. This effect can be self amplifying and is referred to as dynamic vacuum. In order to minimize the amount of desorbed gas, a dedicated ion catcher system has been installed in SIS18 [3]. The catcher system is able to catch about 68 % of the charge exchanged uranium ions¹ and has a very low desorption yield, three orders of magnitude lower than that of a standard stainless steel vacuum chamber.

In order to minimize the static residual gas pressure and to remove the desorbed gases as fast as possible, all dipole and quadrupole chambers of the SIS18 were coated with the non-evaporable getter (NEG) material TiZrV. The NEG-coating provides a high pumping speed of approximately $71/s\cdot cm^2$ for heavy gases like carbon monoxide and carbon dioxide [4]. Unfortunately, the NEG-coated surfaces saturate over time, depending on the amount of absorbed particles. The maximum capacity was measured to be about 10^{15} particles per cm^2 . Since the hydrogen molecules diffuse into the getter material, it has to be noted that hydrogen does not contribute to the saturation. Chemically inert gases like argon and methane are not pumped at all.

A natural effect which counteracts the desorption problem is beam scrubbing. Measurements by Mahner et al. [5] show that the desorption yield decreases with an increasing number of heavy ions bombarding the surface of a vacuum chamber. After a bombardment of 10^{12} ions per cm^2 , the desorption yield from a stainless steel vacuum chamber drops by two orders of magnitude, and is finally comparable with the low desorption yield from the ion catchers.

The StrahlSim code has been developed to simulate beam loss due to charge exchange processes and the corresponding pressure evolution in a synchrotron. The new code version has been extended for the simulation of longitudinal time dependent pressure profiles [6]. The real distance and vacuum conductance from the locations of the desorption to the pumps is considered. The locations of beam loss and desorption are determined by tracking simulations of the charge exchanged ions. The intensity of the charge exchange processes depends on the pressure profile and the energy of the beam ions at a given time in the machine cycle. The number of lost ions hitting the vacuum chamber and the number of particles absorbed by the

¹This number is valid for the main charge exchange process $U^{28+} \rightarrow U^{29+}$.

* This work is supported by HIC for FAIR.

VERTICAL ORBIT EXCURSION FFAGs

S.J. Brooks*, RAL, Chilton, OX11 0QX, UK

Abstract

Fixed-field strong focussing accelerators (FFAGs), in which the beam orbit moves with increasing momentum into higher field regions, have been widely studied. Less well-known is that the central orbit does not need to move outwards with energy: it can move in any direction including the vertically-moving orbit discussed in this paper. This allows for a magnet design with a smaller magnetised volume for a larger total energy range. A vertical analogue to the scaling FFAG is defined and its dynamic aperture studied for the case of an energy booster to the 800 MeV ISIS synchrotron [1] at RAL with various possible lattices.

MAGNETIC FIELD FOR VERTICAL ORBIT EXCURSION

Many magnetic fields permit vertical orbit excursion: if a dipole field (B_y) exists at $y = 0$, the central orbit will move to paths where $B_y \ell$ is larger as momentum increases in order to close the orbit. Thus if the magnetic field for $x = 0$ and $y > 0$ is a pure B_y component that increases with increasing y , then closed orbits for higher momenta will exist moving up the y axis. It is a misconception to think that ‘centrifugal force’ moves the orbit outwards as momentum increases: in fact the beam adiabatically tracks the closed orbit provided it has stable optics. In the vertical excursion case, any initial outward movement from centrifugal force moves particles horizontally into regions where the vertical gradient implies there is a B_x component, which then pushes the particles upwards as required.

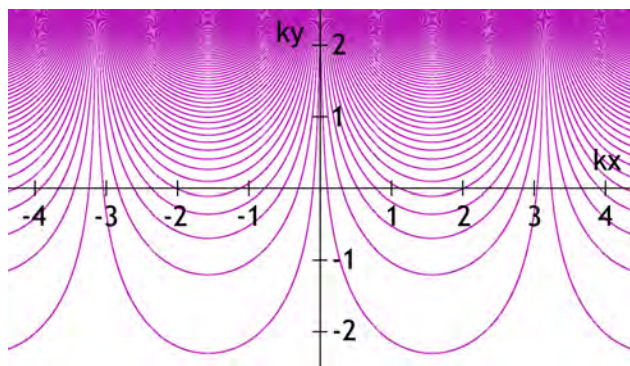


Figure 1: General form of a two-dimensional magnetic field that varies exponentially with y .

This paper concentrates on what could be termed the *scaling* vertical-orbit-excursion field by analogy with (horizontal) scaling FFAGs. The magnetic fields in scaling ma-

chines are derived from a symmetry principle. If a closed orbit is scaled by a factor a in size (and possibly translated or rotated) while magnetic fields on that orbit are scaled by b , then the beam momentum $p \propto B\rho$ must scale by ab . Scaling FFAGs use a group of transformations that scale about the ring centre with $b = a^k$ [2] for some *field index* k . Vertically scaling FFAGs as defined here use a group of translations for which $a = 1$ but $b = e^{k\Delta y}$ for vertical orbit offset Δy .

The field in a long magnet (with no field variation in z) that satisfies the vertical scaling condition can always be written, after a possible shift of x origin, as

$$B_y = B_0 e^{ky} \cos kx \quad B_x = -B_0 e^{ky} \sin kx.$$

This field is plotted in Figure 1: its strength increases exponentially with y and Maxwell’s equations ensure that the field vector rotates with x . This stems from the one-to-one correspondence between 2D magnetic fields and complex functions, in this case e^{-ikz} .

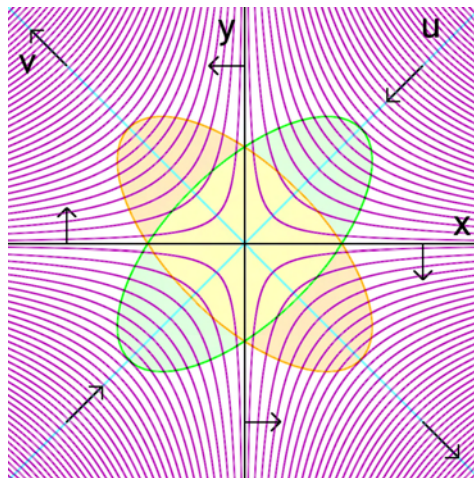


Figure 2: Skew focussing in the vertically-scaling FFAG field. The purple field lines cause the focussing forces (black arrows) along the u and v axes, giving beam cross sections that vary between the two elliptical shapes shown.

As in scaling FFAGs, this magnetic field is combined function, with a dipole and gradient (and all higher multipoles) superimposed. For small distances from the origin, the field is to first order

$$\begin{aligned} B_y &= B_0 + B_0 ky + \dots \\ B_x &= -B_0 kx + \dots, \end{aligned}$$

which produces skew focussing optics as shown in Figure 2. Is it useful to define new transverse axes

$$u = (x + y)/\sqrt{2} \quad v = (y - x)/\sqrt{2},$$

* stephen.brooks@stfc.ac.uk

TRANSVERSE DECOHERENCE IN BUNCHES WITH SPACE CHARGE

Vladimir Kornilov and Oliver Boine-Frankenheim,
 GSI, Planckstr. 1, 64291 Darmstadt, Germany

Abstract

Transverse bunch offsets typically occur after bunch-to-bucket transfer between synchrotrons. Decoherence of the oscillations can cause emittance growth and beam loss, which should be avoided in high-intensity synchrotrons, like the projected SIS-100 synchrotron of the FAIR project. In this contribution we investigate how space charge modifies the bunch decoherence and associated diagnostics methods as turn-by-turn chromaticity measurements.

DECOHERENCE DUE TO CHROMATICITY

As a result of an initial transverse displacement A_0 , a bunch oscillates in the corresponding plane (here x). In the case of the Gaussian momentum distribution, the amplitude of the bunch offset evolves with the turn number N as [1]

$$A(N) = A_0 \exp \left\{ -2 \left(\frac{\xi Q_0 \delta_p}{Q_s} \sin(\pi Q_s N) \right)^2 \right\}, \quad (1)$$

here Q_0 is the bare betatron tune, ξ is the chromaticity: $\Delta Q_\xi / Q = \xi \Delta p / p$, $\delta_p = \sigma_p / p$ is the normalized rms momentum spread and Q_s is the synchrotron tune. Here, the linear synchrotron motion is assumed, the only source of the tune spread is the chromaticity with the momentum spread. Figure 1 shows an example for bunch decoherence after the kick $\bar{x} = \sigma_{x0}$, where σ_{x0} is the horizontal rms beam width, ε_0 is the initial transverse rms emittance. The effect of the chromaticity is usually quantified by the betatron phase shift over the bunch length,

$$\chi_b = \frac{Q_0 \xi}{\eta} \tau_b, \quad (2)$$

where η is the slip factor and τ_b is the bunch length in radian, calculated accordingly to the longitudinal truncation at 2σ , which was taken for simulations. Figure 1 demonstrates that a higher chromaticity provides a faster decoherence, and that after the synchrotron period $N_s = 1/Q_s$ the initial offset amplitude appears again, which is called re-coherence.

The usual rms emittance, to which we refer here as the ‘‘global’’ rms emittance, is given by

$$\varepsilon = \left[\langle (x - \bar{x}_b)^2 \rangle \langle (x' - \bar{x}'_b)^2 \rangle - \langle (x - \bar{x}_b)(x' - \bar{x}'_b) \rangle^2 \right]^{1/2}, \quad (3)$$

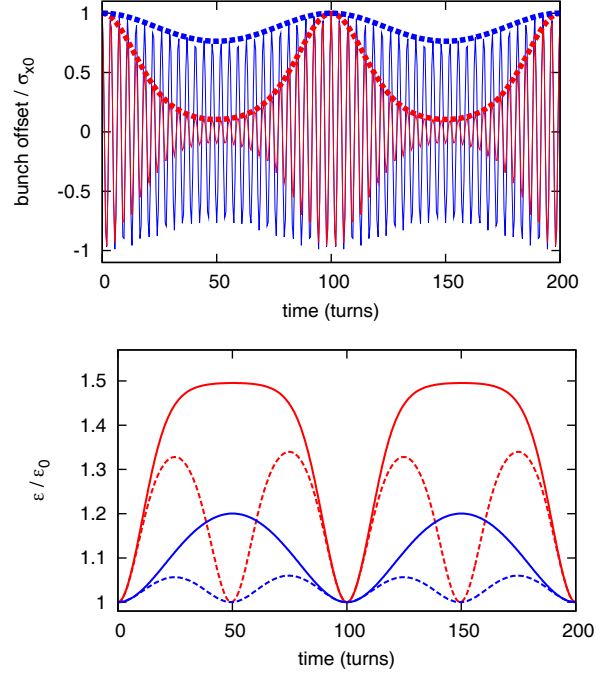


Figure 1: A particle tracking simulation for a Gaussian bunch after an offset kick $\bar{x}(\tau) = \text{const}$. Top plot: time evolution of the bunch offset for the head-tail phase shift $\chi_b = 1.5$ (blue) and $\chi_b = 4.3$ (red), the dashed lines are given by Eq. (1). Bottom plot: time evolution of the global rms emittance [full lines, Eq. (3)] and of the local rms emittance [dashed lines, Eq. (4)]. Line colors correspond to the top plot. The synchrotron period is $N_s = 100$ turns.

where $\langle \dots \rangle$ denotes averaging over bunch particles; \bar{x}_b and \bar{x}'_b are the coordinate offset and the momentum offset of the whole bunch. Additionally, the so-called ‘‘local’’ rms emittance can be defined,

$$\varepsilon_{\text{local}} = \left\{ \langle [x - \overline{x(\tau)}]^2 \rangle \langle [x' - \overline{x'(\tau)}]^2 \rangle - \langle (x - \overline{x(\tau)})(x' - \overline{x'(\tau)}) \rangle^2 \right\}^{1/2}, \quad (4)$$

where $\overline{x(\tau)}$ and $\overline{x'(\tau)}$ are the bunch offsets at the longitudinal particle position τ in the bunch. Figure 1 (bottom) demonstrates the difference between these two values for the bunch decoherence and re-coherence due to the chromaticity.

For the decoherence due to the chromaticity, all the bunch parameters behave periodically. The opposite case

SLOW EXTRACTION FROM SIS-100 AT HIGH BEAM INTENSITY

S. Sorge*, GSI, Darmstadt, Germany

INTRODUCTION

The heavy ion synchrotron SIS-100 will play a key role within the future FAIR project underway at GSI. Although this synchrotron is optimised for fast extraction, also slow extraction will be used.

A major requirement to provide high-intensity beams, particularly, of the reference heavy ion U^{28+} . Uncontrolled beam loss within high-intensity operation can lead to irradiation of the device and degradation of the vacuum resulting in a reduction of the beam life time. During slow extraction, particles can become lost due to collisions with the blade of the electro-static (ES) septum, where they are scattered out of the beam. Furthermore, the particle collisions can damage or destroy the ES septum blade.

Slow extraction from SIS-100 is based on the excitation of the 3rd order resonance given by $52 = 3\nu_x$ by means of 11 resonant sextupoles. During slow extraction, the particles leave the phase space area occupied by the beam along separatrices. The spread in the particle momenta generating a tune spread causes an effective broadening of the separatrices resulting in an increase of the cross section for particle collisions with the ES septum. A reduction of this tune spread will be achieved by the correction of the horizontal chromaticity ξ .

The extraction process can be influenced by additional, undesired non-linearities in the lattice arising from errors in magnets and space charge fields. In the present study, systematic errors in bending magnets and quadrupoles as well as the space charge of the ion beam have been included in a particle tracking model based on the MAD-X code. The space charge has been introduced as frozen space charge. Although the maximum number of U^{28+} ions is $5.0 \cdot 10^{11}$, simulations with space charge according to an ion number up to $N_{ion} = 5.0 \cdot 10^{12}$ have been performed in order to investigate the effect of very large space charge fields. Furthermore, the lowest extraction energy $E = 400$ MeV has been used.

First results are presented in this work, where, up to now, the simulations were restricted to a few thousand turns and test particles. Calculations concerning longer time intervals and using larger test particle ensembles will be done later.

SETTINGS AND PARAMETERS

Chromatic Sextupoles

A reduction of the dependence of the separatrices to reduce beam loss due to particle collisions with the ES septum blade can be achieved by a correction for the chromaticity [2].

Table 1: SIS-100 Parameters as Proposed in the Technical Design Report [1]. The horizontal position of the ES septum blade are negative although it is located at the outer side of the ring because the direction of beam motion in SIS-100 is counterclockwise so that the x axis points to the centre of the ring.

Circumference, C	1083.6 m
Reference ion	U^{28+}
Maximum ion number, $N_{ion,max}$	$5.0 \cdot 10^{11}$
Working point, ν_x, ν_y	17.31, 17.8
Harmonic number of the resonance, n	52
Hor. Twiss functions at ES septum start: β_x α_x	16.126 m 1.23
Number of sextupoles for resonance excitation, M_{rsext} chromaticity correction, M_{csext}	11 48
Sextupole amplitude, $k_{2,a}L$, Equation (1) Standard settings Modified settings Chromatic sextupoles' strength, $k_{2,c}L$ Harmonic number h , Equation (1)	0.15 m^{-2} 0.7 m^{-2} -0.41 m^{-2} 4
Hor. ES septum blade position, x_{sep} Tilt angle of ES septum blade, x'_{sep}	-41 mm 1.3 mrad
RMS momentum spread, δ_{rms}	$5 \cdot 10^{-4}$

For that purpose, 48 chromatic sextupole will be installed in SIS-100. It turned out that the vertical dynamic aperture is strongly decreased if the chromaticity is corrected to a degree that the Hardt condition is totally fulfilled [3]. Therefore, in the present scheme only a partial correction of the chromaticity is foreseen. The natural chromaticity is $(\xi_{nat,x}, \xi_{nat,y}) = (-1.17, -1.16)$, after correction it is $(\xi_{corr,x}, \xi_{corr,y}) = (-0.29, -2.23)$. That will be performed using a scheme where all 48 chromatic sextupoles have the focussing strength $k_{2,c}L = -0.408 \text{ m}^{-2}$ [4], see Figure 2.8-19 in in [1]. In doing so, a large maximum strength is avoided which could drive additional resonances.

Resonant Sextupoles

Slow extraction from SIS-100 will be done using the 3rd order resonance given by $52 = 3\nu_x$ excited by 11 resonant sextupoles. They are symmetrically located in the ring, where there are two sextupoles in each section except for the section used for beam transfer from SIS-100 to the next synchrotron SIS-300. The focussing strengths of the

*S.Sorge@gsi.de

USING ELECTRON COOLING FOR OBTAINING ION BEAM WITH HIGH INTENSITY AND BRIGHTNESS

V.V. Parkhomchuk, V.B. Reva, BINP, Novosibirsk, Russia
X. D. Yang, IMP, Lanzhou, China

Abstract

Electron cooling is used for damping both transverse and longitudinal oscillations of heavy particle. This effect is widely used in the existing and is being designed storage rings. This article describes the last experiments with electron cooling carried out on the cooler EC-300 produced by BINP. The ultimate sizes of the ion beam are discussed. The accumulated experience may be used for the project of electron cooler on 2 MeV (COSY) for obtaining high intensity proton beam with internal target. Using electron beam enables to have physics experiment with high quality of the ion beams at despite of the target interaction.

INTRODUCTION

One way to increase or keep constant by compensation scattering the luminosity in hadron storage ring is using electron cooling. In this method hadron and electron beams with equal velocity are brought together in an interaction section. Because of Coulomb interactions the hadrons transfer own thermal energy to the electron beam. In presence time the main goal of the electron cooling devices is operation at the injection energy with purpose to storage a maximum storage current. The main reason of such using the electron coolers is insufficient electron energy of the typical medium energy coolers device (30 kV). However, there is permanently desire of the electron technique for high energy [1-2] that can provide luminosity upgrade of the physics experiment. The electron cooler is considered as essential part for the PANDA experiment at the planned HESR storage ring for antiprotons at the new GSI facility [3-4]. The 2 MeV cooler for COSY storage ring is under construction now will be used with the internal target.

The operation with internal target imposes the requirement on the cooling rate. This value should be large enough for the suppression of the target effects that can be categorized into longitudinal (energy loss due to ionization) and transverse effects (due to Rutherford scattering on target nuclei). So, the cooling rate should be enough high. The HESR facility requires the cooling rate about a few sec [4].

The strong cooling can only be achieved by the so-called magnetized cooling requiring a strong longitudinal magnetic field ($B \geq 0.5$ T) that guides the electron beam along the entire interaction region. The requirements on the parallelism of the magnetic field are very strong ($B_r/B_z \leq 1 \times 10^{-5}$) and it is necessary for fast electron cooling.

The 4.34 MeV cooler is used for cooling antiproton beam at RECYCLER [5] and preparing the antiproton bunch for TEVATRON. Conclusion about efficiency the electron cooler made in [6]: "Without the Recycler and electron cooling, we estimate that the yearly integrated luminosity would be half of its current level". But FNAL project is not focused to achieve the considerably higher cooling rates with magnetized cooling. The system electron cooling for experiments with inner target need few order magnitude faster cooling- instead hour cooling time it should be few seconds.

New generation of the electron coolers designed and produced at BINP has made with classical scheme and has purposed to obtain the maximum friction force. The coolers were commissioned with ion beams during last years at storage rings CSRm, LEIR and CSRe. These coolers have a few specifics features:

a. The electron guns of these coolers have possibility for the easy variation of the electron beam profile from the parabolic shape with maximum at center to the hollow electron beam with deep minimum at the center of the beam. Such type of profile can be used for optimizations of accumulation, when accumulated beam interacts with low density electron beam. As results we can control the recombination rate and prevent the overcooling storage ion beam.

b. For bending electron beam at toroid the electrostatic field is used. This bending doesn't depend from the direction of the electron velocity and helps to return main part of the reflected from collector electrons again at collector. In this case the resulting efficiency of the electron capture of collector becomes better then 10^{-6} . The low losses of the electron beam at cooling section lead to good vacuum condition and high life-time of high charge ions.

c. The design of the cooling section magnet system from moveable pancake coils lets to have very good straightness magnet lines at cooling sections. Increasing the cooling rate for the low ions amplitude play key roles for obtain high luminosity with internal target.

COOLING FORCE MEASURING

First cooling of a carbon beam with energy 400 MeV/u was made in CSRe coolers at May 2009. The ion beam was accumulated with electron cooling at CSRm ring (energy 7 MeV/u), was injected at CSRe after acceleration and was cooled down as it is shown in Fig 1 and Fig. 2. The typical life-time at the cooling process was about 500-1000 sec.

THE FAIR PROTON LINAC: THE FIRST LINAC BASED ON A ROOM TEMPERATURE CH-DTL

G. Clemente, W. Barth, L. Groening, S. Yaramishev, GSI, Darmstadt, Germany
 R. Brodhage, U. Ratzinger[#], R. Tiede, J.W. Goethe University, Frankfurt a.M., Germany

Abstract

The antiproton program at FAIR requires a dedicated proton linac to be used as injector for the SIS 100 synchrotron. This 325 MHz linac will accelerate up to 70 mA proton beam to the injection energy of 70 MeV. This linac will be the first machine based on CH-DTL's, the novel cavity developed at the Frankfurt University. This new cavity is characterized by slim drift tubes without internal focusing elements which allow the construction of very compact cavities resulting in higher shunt impedance when compared to conventional RF structures. The proton linac is based on 3 coupled CH-cavities followed by three standard CH's for a total length of around 22 meters. A complete description of the beam dynamics together with the general status of the project is presented and discussed.

INTRODUCTION

The FAIR Project [1] (Facility for Antiprotons and Ions Research) requires a massive upgrade of the existing GSI accelerator facilities in terms of beam intensities and quality.

In particular a considerable increase of ion beam intensities up to a factor of 5 at the end of the UNILAC is required from the heavy ion physics program while a new proton injector [2] will start the accelerator chain for the production of cooled antiprotons.

The final goal is to provide primary proton fluxes of $2 \cdot 10^{16}$ protons/h by the accelerator chain shown in Fig. 1. Taking into account the pbar production and cooling rate this primary beam will lead to a secondary beam of $7 \cdot 10^{10}$ cooled antiprotons/h.

The dedicated proton linac will deliver a proton beam of 70 MeV which will be then injected into the SIS 18. At this energy in fact the saturation of *p-bar* production [2] is reached. The injection into the synchrotron is planned by a multiturn injection scheme. The horizontal acceptance of the SIS 18 will be filled by a 35 mA within a normalized brilliance of $16.5 \text{ mA}/\mu\text{m}$, while a momentum spread of less than 1 ‰ is required. The maximum repetition rate is fixed at 4 Hz.

Concerning the RF frequency, a multiple of the basic resonance frequency of the UNILAC HSI (36.136 MHz) has been considered as the best option. The value of 325.224 MHz meets this criterion and allows the use of the 3 MW klystrons developed for the JPARC facility at 324 MHz. The adaption to the small difference in frequency has been straightforward.

The general parameters of the proton linac are listed in Table 1.

Table 1: The Main Parameters of the FAIR Proton Linac

Source	H ⁺ , 95 keV, max. 100 mA
LEBT	95 keV, 100 mA, $\epsilon_{\text{norm.}}=1.8 \mu\text{m}$
RFQ	3 MeV, 90 mA, $\epsilon_{\text{norm.}}=2 \mu\text{m}$
DTL	3 CCH+ 3 CH-DTL, 70 MeV
Frequency [MHz]	325.224
Current [mA]	70 (design), ≥ 35 (operation)
Emittance (μm)	≤ 2.8
Mom. Spread [%]	≤ 1
RF Pulse [μs]	70
Max Beam Pulse [μs]	36
Repetition Rate [Hz]	4
Duty Factor [%]	0.1
Total Length [m]	~ 30

LINAC GENERAL DESIGN

The general layout of the proton injector is presented in Fig.2: an ECR ion source developed at CEA, Saclay, will provide a proton beam extracted at 95 kV. The first stage of acceleration to 3 MeV is provided by a four-rod RFQ [3] investigated at the University of Frankfurt. After a compact matching section which includes a quadrupole triplet, an RF buncher, a doublet and the required diagnostics, the beam enters the first section of the main linac. Three coupled cavities [4] provide the acceleration to the intermediate energy of 37 MeV where a 1.6 meter long dedicated diagnostic section is foreseen.

This section will include the main diagnostic devices such as an emittance scanner, phase probes, current transformers and transverse scrapers to get rid of particles with larger emittances with respect to the beam

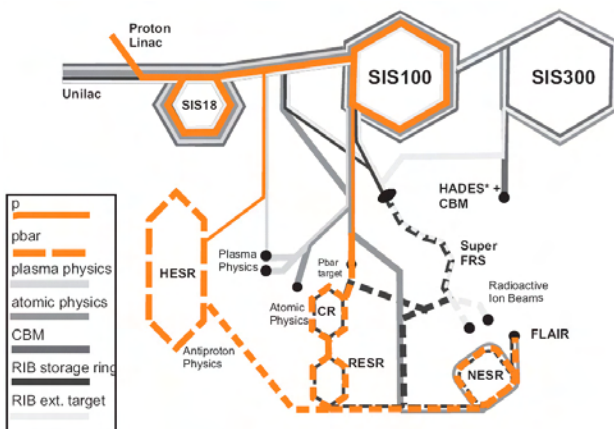


Figure1: The schematic view of FAIR showing in the detail the accelerator chain for the production of antiprotons.

ION BEAM INTENSITY INCREASING IN UNDULATOR LINEAR ACCELERATORS

E.S. Masunov, S.M. Polozov, A.V. Voronkov,
National Research Nuclear University “MEPhI”, Moscow, Russia

Abstract

The undulator linear accelerator (UNDULAC) was suggested as an initial part of high intensity ion linac [1, 2]. Ion beam is accelerated by the combined field of two non-synchronous space harmonics in UNDULAC. The space charge force is the main factor limiting beam intensity. There exist two ways to increase ion beam intensity: (i) to enlarge the beam cross section and (ii) to use the space charge neutralization. The high intensity ribbon ion beam can be accelerated in UNDULAC [3]. Accelerating force value in UNDULAC is proportional to squared particle charge and oppositely charged ions can be accelerated simultaneously within the same bunch and the beam space charge neutralization can be realized.

INTRODUCTION

As it is well known, the space charge is the main factor limiting the beam intensity in ion bunchers and low energy accelerators. We can say that the limit low energy beam current is achieved or close now. But it must be enlarged up to 300-1000 mA for same facilities as neutron generators, accelerating driven systems or medical isotopes breeders. It is provide to discussion about new acceleration and focusing methods which can to be used for this facilities. There are two ways to increase ion beam intensity: to enlarge the beam's cross section and to use the space charge neutralization. The aperture of accelerator and the necessary RF potential on electrodes should be enlarged in first case. The ribbon ion beam acceleration can be used as an alternative method of beam current enlarging [1-3].

The second way of the limit beam current enlargement is more discussable. It is known three (or more?) ideas for beam space charge neutralization: (i) neutralization using plasmas, ionized residual gas or electron cloud; (ii) so-called “funneling” method; (iii) simultaneous acceleration of positive and negative ions in the same bunch.

The idea of beam space charge neutralization by means of electron cloud was proposed and analytically studied in [4, 5]. It was shown that electron cloud can really provide to the proton or heavy ion partially neutralization.

The neutralization of Coulomb field influence by means of plasma lenses is widely used in beam transport lines (see for an example [6]). More interest results were analytically shown and experimentally verified by number of research groups [7-10] for bunched and continuous proton and ion beams. The ionized residual gas influence was studied in the all noted experiments. It was shown that the influence of ionized gas can provide to beam emittance decreasing.

The term “funneling” we can find in 30 years old reports [11, 12]. The LAMPF DTL linac long time works in LANL uses funneling (but not use this term) [13, 14]. The previously accelerated to 300 MeV H^+ and H^- were injecting in last section of LAMPF linac and simultaneously accelerated up to 800 MeV. The acceleration was provided in different (opposite) reference phases and bunches of H^+ and H^- ions were spatially separated.

The systems for beam bunching and low energy acceleration were proposed later in LANL [15] and Frankfurt University [16] using RFQ or magnetic quadrupole lenses [17]. A number of RFQ linacs using funneling was studied and constructed in Frankfurt University [18-20]. The funneling is used to increase the total beam current in these linacs. The four stage funneling scheme was presented in [18]. As it is clear the funneling method can be used for positive (or negative) ion beam acceleration only using frequency multiplying. The linac with very high current can be used for fusion technologies facilities or spallation neutron sources (see for example [21]).

Other bunching and acceleration mechanism can be realized in case when the positive and negative ions were accelerated in RFQ simultaneously. It was shown by numerical simulation [22] that the total beam flux is lower and beam transverse emittance decreases in case of simultaneously acceleration of H^+ and H^- ions. The decreasing of output beam flux seems very strange and can be caused by specific model used for simulation. The space-charge forces in this model was calculated by assuming that the charge distribution is periodic and treating by following a separate group of particles for each beam. In case when the two beams have equal input parameters the problem was simplified by following only the positive ions.

The results of experiential study of simultaneously acceleration of O^+ and O^- ions were represented in [23]. It was shown that the total beam flux can be sufficiently (approximately 1.8 times) increased using funneling method. The analysis of beam dynamics shows that in RFQ or DTL the intensity of the ion beam can be made twice as higher by simultaneous acceleration of ions with opposite charge signs. The accelerating force in these linacs is proportional to the charge of the ion. Oppositely charged ions are bunched and accelerated in the different phases of the accelerating wave. Two bunches (one with a positive and another one with a negative ions) become separated and weakly interact with each other after the initial part of the buncher and full space charge neutralization can't be achieved. The intensity of the ion beam can be made twice as higher therefore. These results

BEAM LOADING EFFECT SIMULATION IN LINACS

E.S. Masunov, S.M. Polozov, V.I. Rashchikov, A.V. Voronkov, T.V. Bondarenko,
National Research Nuclear University MEPhI, Moscow, Russia

Abstract

The accurate treatment both self beam space charge and RF field is the main problem for all beam dynamics codes. Traditionally only the Coulomb field is taken into account for low energy beams and the RF part is account for high energy beams. But now the current of accelerated beam enlarges and some radiation effects should be discussed for low energy beam also. The beam loading is being more important. This effect should be studied now not only in electron linacs but for proton one too.

INTRODUCTION

The high-current accelerators has the great perspectives for solving the problems of thermonuclear fusion, safe nuclear reactors, transmutation of radioactive waste and free electron lasers. A large number of low energy particle accelerators are applied in micro- and nanoelectronics, material science, including the study of new construction materials for nuclear industry, in medical physics, in particular for cancer by using the accelerators of protons and light ions, in radiation technology over the past three decades.

The accurate treatments of the beam self field and its influence on the beam dynamics is one of the main problems for developers of high-current RF accelerators. Coulomb field, radiation and beam loading effect are the main factors of the own space charge. Typically, only one of the components is taken into account for different types of accelerators. It is Coulomb field for low energy linacs and radiation and beam loading for higher energies. But both factors should be treated in modern low and high energy high intensity linacs. The mathematical model should be developed for self consistent beam dynamics study taking into account both Coulomb field together with beam loading influence. That is why three-dimensional self-consistent computer simulation of high current beam bunching with transverse and longitudinal motion coupling is very actual.

Let us describe the beam loading effect briefly. The beam dynamics in an accelerator depends not only on the amplitude of the external field but on the beam self field. The RF field induced by the beam in the accelerating structure depends on the beam velocity as well as the current pulse shape and duration in general. The influence of the beam loading can provide irradiation in the wide eigen frequency mode and decrease the external field amplitude. Therefore we should solve the motion equations simultaneously with Maxwell's equations for accurate simulation of beam dynamic.

The most useful methods for self-consistent problem solving are the method of kinetic equation and the method of large particles.

Solving the Maxwell equation can be replaced by solving the Poisson equation if we take into account only the Coulomb part of the own beam field. This equation can be solved by means of the well-known large particles methods as particle in cell (PIC) or cloud in cell (CIC). There is no easy method for dynamics simulation that takes into account the beam loading effect.

Currently there are a large number of commercial programs for electron and ion beam dynamics study. The most famous of them are MAFIA, PARMELA. Unfortunately they are not considering the important aspect associated with the beam loading in the beam bunching for the different cases.

The mathematical model for beam dynamics simulation taking into account the beam loading effect has been developed in MEPhI; the results are described in [1-2]. Now beam intensity in ion and electron linacs has considerably increased and the accounting of beam loading became necessary. New code development has led to necessity for modern computers. The new mathematical model for three-dimensional computer simulation in the Cartesian coordinates system has been developed.

The purpose of the present work is self-consistent high current beam dynamics investigation in uniform and non-uniform traveling wave accelerating structures by means of three-dimensional program BEAMDULAC-BL. The BEAMDULAC code is developing in MEPhI since 1999 [3-4] for high current beam dynamics simulation in linear accelerators and transport channels. Runge-Kutta 4th order method is using for the integration of differential equations of motions. The algorithm of BEAMDULAC-BL code uses any previously defined initial particles distribution in 6D phase space to calculate the Coulomb field distribution and radiation in harmonic form. As a result, the new coordinates, velocities and phases of large particles are determined, and the new values of the self-consistent field is defined. The traditional CIC method is used for Coulomb field calculation.

THE EQUATION OF MOTION IN SELF CONSISTENT FIELD AND SIMULATION METHODS

Let us discuss the methods of beam loading effect simulation used in BEAMDULAC-BL. Usually a longitudinal movement of charged particles is considered only for high current beam dynamics calculation in self-consistent fields. Thus, it is assumed, that the beam is in strong enough focusing field and transverse motion can be neglected. In traditional linear resonant accelerators where longitudinal components of current density $j_z \gg j_\perp$ this approach is quite reasonable as the integral of current density and field interaction is defined by an amplitude

TRANSVERSE MATCHING PROGRESS OF THE SNS SUPERCONDUCTING LINAC*

Y. Zhang, S. Cousineau, Y. Liu,
Spallation Neutron Source, ORNL, Oak Ridge, TN 37831, USA

Abstract

Experience using laser-wire beam profile measurement to perform transverse beam matching in the SNS superconducting linac is discussed. As the SNS beam power is ramped up to 1 MW, transverse beam matching becomes a concern to control beam loss and residual activation in the linac. In our experiments, however, beam loss is not very sensitive to the matching condition. In addition, we have encountered difficulties in performing a satisfactory transverse matching with the envelope model currently available in the XAL software framework. Offline data analysis from multi-particle tracking simulation shows that the accuracy of the current online model may not be sufficient for modeling the SC linac.

INTRODUCTION

The Spallation Neutron Source (SNS) is a short-pulse neutron facility. Its accelerator complex consists of a 2.5-MeV H^- injector, a 1-GeV linac, an accumulator ring and associated beam transport lines. The SNS linac has a normal conducting front end approximately 100-m long that includes a medium energy beam transport (MEBT) line, six drift tube linac (DTL) cavities and four coupled cavity linac (CCL) tanks for beam energy of up to 186 MeV, and a superconducting linac (SCL) 160-m long that consists of 81 independently powered 6-cell niobium cavities installed in 23 cryomodules, with a design output beam power of 1.56 MW [1].

Because of the high beam intensity and the SRF technology, no beam intercepting diagnostic device is allowed in the SCL. Laser wire (LW) beam profile monitors are used for transverse profile measurements and for performing beam matching. For more details about the nine LW monitors installed in the SCL see reference [2]. The usual matching process include LW measurements first, and then fits to the measured beam size with an envelope model in the XAL [3], which is applied online in the control room. For offline analysis, we use the multi-particle tracking code IMPACT [4]. Currently, the later is still not appropriate for online application because of lengthy computational times, but it has been proved to be a very helpful tool to analyze the SNS linac [5].

Beam matching in the SNS linac with the online model has not been a success thus far. Fortunately, beam loss in the linac system is not very sensitive to the beam matching condition: even without a good transverse match, we are able to control the SCL beam loss to a tolerably low level (10^{-5} to 10^{-4}) for 1 MW neutron

production, thanks to a very robust linac design. A lot of efforts have been taken to address potential problems with laser wire measurements since it is a relatively new diagnostic device. However, offline analysis with multi-particle tracking simulation shows that a major issue is the model itself. We previously attributed all the problems of the model to nonlinear issues such as emittance growth, chromatic aberrations, etc, but ignored errors associated with basic linear optics, which are more important.

FIRST MATCHING ATTEMPT

Based on the linear envelop model, we performed beam transverse matching with laser wire measurements in 2008. The effort failed: instead of reducing the beam size beating in the SCL, it actually made both the horizontal and vertical planes worse. Figure 1 shows the laser wire measurements and the beam model obtained by a fitting those measurements, before any matching was done. Figure 2 shows the same plot after the matching.

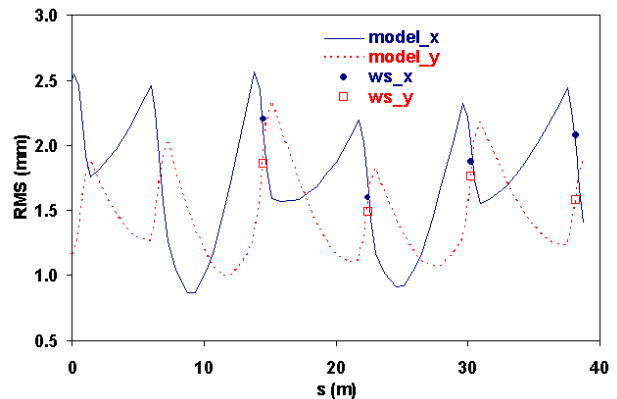


Figure 1: LW measurements (markers) and envelope model (lines) before a transverse matching in the SCL.

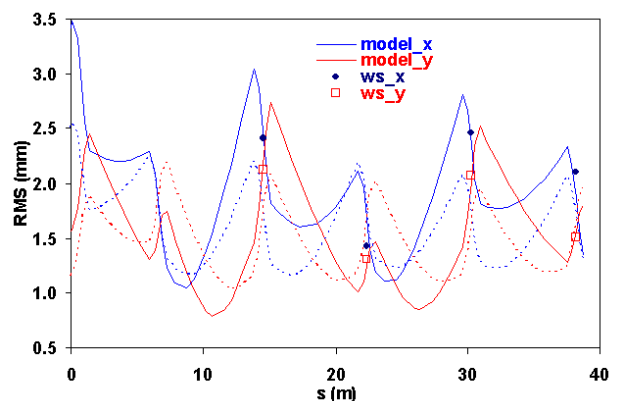


Figure 2: After transverse matching, the beam size beating in both horizontal and vertical planes is worse (solid lines) than the model predicted (dashed lines).

* SNS is managed by UT-Battelle, LLC, under contract DE-AC05-00OR22725 for the U.S. Department of Energy.

BEAM DYNAMICS SIMULATIONS FOR THE LASER PROTON INJECTOR TRANSPORT LINE*

A. Orzhekhovskaya, W. Barth, I. Hofmann, S. Yaramyshev, GSI, Darmstadt, Germany

Abstract

The DYNAMION code was implemented to perform beam dynamics simulations for different possible transport lines for a proton beam with an energy of 10 MeV, coming from a high intensity laser ion source. It was intended to check the chromaticity and space charge effects taking into account high order aberrations. The investigations were performed for a solenoidal focusing and alternatively for a quadrupole channel applying different beam parameters (energy spread, transverse divergence, beam current) as well as different layouts of the transport line. The beam evolution along the transport line, the emittance growth and the beam transmission were analyzed and compared. Finally, the influence of an rf - buncher, required to match the proton beam to the following accelerating structure, was investigated.

INTRODUCTION

The recent development in the field of "laser acceleration of protons and ions" has initiated several investigations of this concept of a innovative and compact accelerator. The currently known beam parameters do not allow for a realistic detailed study. But a simulation of proton collimation and transport, based on output data from the PHELIX experiment [1], already give a useful hint, especially chromatic and geometric aberrations of the first collimator as an interface between the production target and the adjacent accelerator structure are of particular importance [2].

The advanced multiparticle code DYNAMION [3], dedicated to the beam dynamics simulations in linacs, was created in 1992 in the Institute of Theoretical and Experimental Physics (ITEP, Moscow) and developed in a long-term collaboration of GSI Helmholtzzentrum fuer Schwerionenforschung (Darmstadt) and ITEP. Due to the most common form of 3D particle motion equation and detailed description of the external electromagnetic field, the non-linear effects and high order aberrations are included in this code automatically. The space charge calculations in the DYNAMION code are based on the particle-particle interactions, including a dedicated routine to avoid artificial collisions of particles. Numerous comparisons of the calculated results with measured data have proved the reliability of DYNAMION simulations for convenient linacs [4-8]. For this reason the DYNAMION code is used to perform beam dynamics investigations for the laser proton injector beam transport line. For special tasks, as the very early expansion phase of the proton cloud, simulations with a recent DYNAMION version were carried out introducing

estimated beam parameters, based on numerical and experimental data. The simulations for the zero current case attract a particular interest as the most optimistic case. Addition of any diversifications of the input beam parameters leads to emittance growth.

BEAM LINE LAYOUT

Calculations were done for quadrupole (Q-line) and solenoidal (S-lines) channels varying the input beam parameters (Fig. 1).

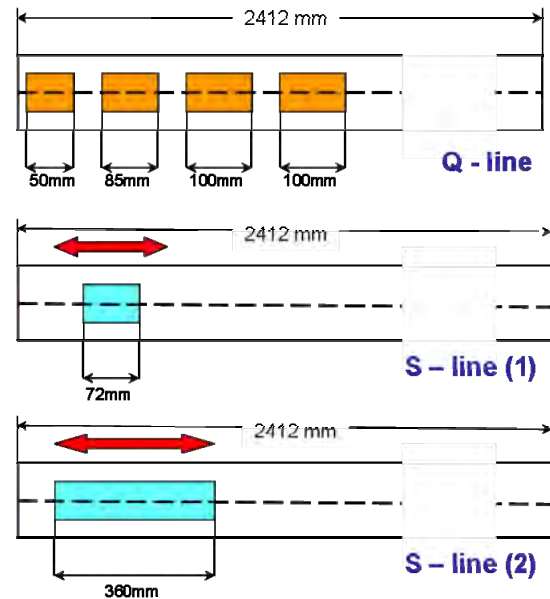


Figure 1: Layout of the beam transport line with quadrupole or solenoidal focusing.

For this set of simulations the following beam parameters were fixed:

- energy 10 MeV;
- transverse size ± 0.03 mm;
- transverse divergence ± 43 mrad, ± 86 mrad;
- total unnormalized emittance $\epsilon_x = \epsilon_y = 1.25$ mm·mrad, 2.5 mm·mrad;
- phase spread $\Delta\phi = \pm 0.75^\circ$ (related to 108 MHz);
- energy spread $0\% \leq \Delta W/W \leq 6\%$;
- current $0 \text{ mA} \leq I \leq 50 \text{ mA}$;
- Gaussian particle distribution, truncated at 2σ .

Q-line Layout

The position of the 4 quadrupoles and their gradients (optimized by TRACE 3D code) are fixed; maximum magnetic field in quadrupoles is 1.2 T; «open» aperture of the quadrupoles in order to study high order aberrations and space charge effects without particle losses. The total length of the line is 2412 mm.

* Work supported by EURATOM (IFK KiT Program) and Helmholtz International Center for FAIR

RELAXATION, EMITTANCE GROWTH, AND HALO FORMATION IN THE TRANSPORT OF INITIALLY MISMATCHED BEAMS*

T. N. Teles, R. Pakter[†], Y. Levin

Instituto de Física, Universidade Federal do Rio Grande do Sul, Brazil

Abstract

In this paper, a simplified theoretical model that allows to predict the final stationary state attained by an initially mismatched beam is presented. The proposed stationary state has a core-halo distribution. Based on the incompressibility of the Vlasov phase-space dynamics, the core behaves as a completely degenerate Fermi gas, where the particles occupy the lowest possible energy states accessible to them. On the other hand, the halo is given by a tenuous uniform distribution that extends up to a maximum energy determined by the core-particle resonance. This leads to a self-consistent model in which the beam density and self-fields can be determined analytically. The theory allows to estimate the emittance growth and the fraction of particles that evaporate to the halo in the relaxation process. Self-consistent N -particle simulations results are also presented and are used to verify the theory.

INTRODUCTION

In experiments that require the transport of intense beams, space charge forces make it virtually impossible to launch a beam with a distribution that corresponds to an exact equilibrium state. As a consequence, as the particles are transported the beam will tend to relax towards a stationary state [1, 2]. Along this process, effects such as emittance growth and halo formation are expected to occur. These effects are very detrimental because they limit beam efficiency and may be responsible for particle losses which can cause wall damage and activation. Therefore, a quantification of the amount of emittance growth and halo formation that can be expected becomes an important issue in the design of such systems. In order to estimate these, a good knowledge of the mechanisms that lead to beam relaxation and, especially, of the *final* stationary state reached by the beam is necessary.

In general, injected beams may deviate from the equilibrium state because of various effects, such as envelope mismatches [3, 4, 5, 6, 7, 8, 9], off-axis motion [10, 11, 12, 8, 13], nonuniformities in the beam distribution [14, 15, 16, 17, 18, 19, 20], and forces due to the surrounding conductors [21, 22, 23]. Among all these effects, the one that has attracted most of attention is the envelope mismatch because it is believed to be a major cause of emittance growth and halo formation. For mismatched beams, an unbalance between the focusing force due to the external

applied field and the defocusing forces due to space charge and thermal effects, causes the whole beam to oscillate in a coherent breathing mode. Some single beam particle trajectories resonate with this mode, gaining a lot of energy to form the halo. Based on a low dimensional particle-core model it is possible to observe this resonance process and to determine the maximum range of halo particles [3, 4, 5]. Due to conservation of energy, as the halo is being formed the particles that remain in the core loose energy and the amplitude of the breathing mode decreases. Eventually, halo formation ceases and the stationary state is reached. The whole scenario is analogous to an evaporative cooling process where the core particles cool down via evaporation of hot, energetic halo particles. The thermodynamic equilibrium that corresponds to the Maxwell-Boltzmann distribution [24, 25] is not expected to be attained in this process because the beam dynamics is collisionless [26, 27, 28, 29]. In fact, in the particular case of an initially mismatched high-intensity cold beam, it has been shown that the final stationary state can be very well modeled by a completely cold dense core surrounded by a cloud of energetic particles that carry all the beam emittance [8, 9]. From this model one can successfully determine the total emittance growth and the fraction of particles that form the halo in the stationary state.

In the case of beams with a finite initial emittance, however, the assumption of a completely cold core for the relaxed state is no longer correct. The existence of emittance in the initial distribution indicates that the beam occupies a finite volume in the phase-space. Because the Vlasov dynamics that governs beam evolution is incompressible, this volume has to be preserved. Hence, the occupation of low-energy regions of the phase-space by the particles as the core progressively cools down is limited by the finite density of the initial distribution in phase-space, which is not compatible with a completely cold core. In other words, although we are dealing with purely classical particles, the conservation of volume in the phase space imposed by the Vlasov equation, leads to a Pauli-like exclusion principle for the beam particles. Taking this into account, here we propose that the stationary state for the core corresponds to a completely degenerate Fermi gas, where the particles occupy the lowest possible energy states accessible to them. This leads to a self-contained model where the beam density and self-fields can be determined analytically as a function of two parameters – the core size and the halo density. This parameters are, in turn, readily obtained by numerically solving two algebraic equations that correspond to the conservation of the total number of particles and the

* This work was supported by CNPq and FAPERGS, Brazil, and by the US-AFOSR under Grant No. FA9550-09-1-0283.

[†] pakter@if.ufrgs.br

SELF-CONSISTENT BEAM DYNAMICS IN RF LINACS WITH NON-SYNCHRONOUS HARMONICS FOCUSING*

V. S. Dyubkov[#], S. M. Polozov,

National Research Nuclear University “MEPhI”, Moscow, Russian Federation

Abstract

It was done the studies on high intensity ion beam dynamics in axisymmetric rf linacs both analytically, in terms of the so-called smooth approximation, and numerically in [1-3] rather carefully. For all that, effects of beam self-space-charge field were not taken into consideration under analytical investigations of the focusing by means of non-synchronous harmonics up to date. These effects are said to affect a focusing parameters choice deeply. A “beam-wave” Hamiltonian is derived under assumption that a bunch has an ellipsoidal form. Analytical results specify that given in [4] and it is verified numerically.

INTRODUCTION

Linac design is of interest to many fields of science, industry and medicine (e.g. nuclear physics, surface hardening, ion implantation, hadron therapy). The number of linacs is increased steadily. The most significant problem for low-energy high-current beams of charged particles is the question of its stability because of the influence of Coulomb’s repelling forces. Beam motion stability can be realized by means of the following focusing types: alternating phase focusing, radio frequency quadrupoles, focusing by means of the nonsynchronous wave field as well as the undulator one.

However, system with alternating phase focusing is not suitable for low-energy high-current beam acceleration, because it requires small values of synchronous phase. Radio frequency quadrupoles showed itself as initial linac sections well, but careful beam dynamics study gives, that considerable part of input rf power is spent on transverse focusing. Due to such rf power disproportion between degrees of freedom radio frequency quadrupoles have a small acceleration rate usually. Acceleration and focusing can be realized by means of the electromagnetic waves which are nonsynchronous with a beam (the so-called undulator focusing). Unfortunately, systems without the synchronous wave are effective only for light-ion beams. For low-energy heavy-ion beams to be accelerated it is necessary to have the synchronous wave with particles.

Linac sections with rf focusing by the nonsynchronous harmonics can be adequate alternative to that with alternating phase focusing and radio frequency quadrupoles, joining its advantages. Zero-intensity beam dynamics analysis in linac sections with rf focusing by the nonsynchronous harmonics was done previously [1-3]. For intense, high-brightness beams from rf linacs, it is important to have analytical results together with

numerical ones which help do a linac parameters choice to ensure total beam stability. In this paper analytical results specify that given in [4] and it is verified numerically.

BASIC RELATIONS

Self-consistent beam dynamics is described by the 2nd Newton’s law together with Poisson’s equation as

$$\begin{cases} \frac{d}{dt} \left(m \frac{d\mathbf{R}}{dt} \right) = q(\mathbf{E} - \nabla_{\mathbf{R}}\Phi_c); \\ \nabla_{\mathbf{R}}^2 \Phi_c = -\rho/\epsilon_0, \end{cases} \quad (1)$$

where m is a beam mass, \mathbf{R} is a beam radius-vector, q is a beam charge, \mathbf{E} is an external rf field, Φ_c is the self-space-charge field potential, ρ is a beam charge density, ϵ_0 is the free space permittivity.

Let us express rf field in axisymmetric periodic resonant structure as an expansion by the standing wave spatial harmonics assuming that a structure period is a slowly varying function of the longitudinal co-ordinate z

$$\begin{cases} E_z = \sum E_n I_0(k_n r) \cos(\int k_n dz) \cos \omega t; \\ E_r = \sum_n E_n I_1(k_n r) \sin(\int k_n dz) \cos \omega t, \end{cases} \quad (2)$$

where E_n is the n th harmonic amplitude of RF fields the axis; $k_n = (\theta + 2\pi n)/D$ is the propagation wave number for the n th RF field spatial harmonic; D is the geometric periods of the resonant structure; θ is the phase advances per period D ; ω is the circular frequency; I_0, I_1 are modified Bessel functions of the 1st kind of orders 0 & 1.

One assumes the beam velocity does not equal one of the spatial harmonic phase-velocities except the synchronous harmonic of rf field, the geometric period of rf structure being defined as $D = \beta_s \lambda (s + \theta/2\pi)$, where s is the synchronous harmonic number, β_s is the relative velocity of the synchronous particle, λ denotes rf wavelength.

The analytical investigation of the beam dynamics in a polyharmonic field (2) is a difficult problem. Rapid longitudinal and transverse oscillations as well as a strong dependence of field components on transverse coordinates does not allow us to use the linear approximation in the paraxial region for a field series. Nevertheless the self-consistent analytical beam dynamics investigation can be carried out by means of the so-called smooth approximation [5].

*Work supported by Research Project Grant of Russian Federal Education Agency under Contract Number P546.

[#]VSDyubkov@mephi.ru

MODELLING OF ELECTRON AND ION DYNAMICS IN THE ELECTRON CYCLOTRON RESONANCE ION SOURCE BY MEANS OF PIC-SELF CONSISTENT NUMERICAL SIMULATIONS*

L. Celona[#], S. Gammino and G. Ciavola, INFN-LNS, Via S. Sofia 62, 95123, Catania, Italy
D. Mascali, CSFNSM, Viale A. Doria 6, 95125 Catania, Italy

Abstract

The properties of Electron Cyclotron Resonance Ion Sources (ECRIS) plasmas, up to now, have been largely studied on the basis of a global approach. However the design of new generation sources, able to provide high intensity beams of multiply charged ions, requires a more accurate investigation of both electron and ion dynamics.

Recent experiments have demonstrated that even slight frequency's changes (of the order of MHz) considerably influence the output current, and what's more important, even the extracted beam properties (beam shape, brightness and emittance) are affected [1,2].

The paper will briefly describe the approach used to simulate the phenomena observed by referring to some recent papers for further details.

INTRODUCTION

According to the model that has driven the development of ECRIS in the last years, a large variation of the pumping microwave frequency (order of GHz) along with the proportional increase of the magnetic field boosts the extracted current for each charge state because of a larger plasma density.

However the improvement of ECRIS performances, based on the simultaneous increase of the above mentioned parameters, is now close to saturation, limited mainly by the reliability of the magnets and by the costs.

Therefore to overcome such limitations several alternative heating schemes were proposed, by different teams spread over the world. The most successful, named Two Frequency Heating (TFH) [3], consists in the use of two waves at different frequency instead of one, both carrying a total amount of power that is approximately the same of a single wave. Even if a clear improvement has been observed, these experiments have not given an explanation or a methodology to better understand the coupling mechanism between feeding waveguide and cavity filled with plasma and the energy transfer between the electromagnetic field in the source plasma chamber and the plasma therein confined.

From a couple of years, the INFN-LNS ion source group, on the basis of different experiments carried out from 2001 [4,5] has proposed a model [6,7], now accepted from the scientific community, to explain the observed results, based on the hypothesis that standing waves are formed inside the ECRIS plasma chamber.

Such hypothesis has been verified experimentally on different 2nd generation ECRIS by slightly changing the frequency around the operating one [1,8,9]. Remarkable changes in the beam intensity and in its distribution have been observed confirming that a frequency dependent electromagnetic distribution is preserved even in the presence of plasma inside the source (the so called "Frequency Tuning Effect").

In order to investigate how this fine tuning affects the plasma heating, a set-up for the injection of variable microwave frequency into the ECRIS cavity has been prepared. The microwave power was fed by means of a Klystron-based generator [1,8] or a by means of a Travelling Wave Tube amplifier with a broad operating frequency range [9]. The frequency has been systematically changed and the beam output was recorded either in terms of charge state distributions and beam emittance. Since the microwave frequency was the only parameter changed in each measurement, the variation observed in terms of reflection coefficient, extracted current and beam emittance, clearly reveal the role of the electromagnetic distribution inside the plasma chamber cavity which changes with the frequency and affects the final structure of the extracted beam.

In recent experiments we recorded also the bremsstrahlung X-rays emission in order to achieve some insights about the electron energy distribution function (EEDF) [10]. The ECRIS have a broad EEDF, not ideal for the safe operation of the sources, especially when superconducting magnets are used. X-rays measurements reveal a large amount of MeV electrons, that locally heat the cryostat and make the aging of the insulator faster. Conditions for the suppression of high energy particles must be understood in order to fully exploit the ECRIS ability to produce high brightness beams, and the plasma heating modelling permits a better insight.

In order to take into account all the above mentioned phenomena a numerical code has been developed at INFN-LNS with MATLAB in order to follow the electron and ion dynamics by means of a Monte Carlo collisional approach. More details are available in [6,7]. We are able to perform fully 3D collisional simulations of ECRIS plasma, splitting the electron and ion dynamics, and looking separately to their time evolution.

The collision probability is calculated according to a well known Monte Carlo technique, once known the characteristic time of Spitzer collisions. Finally, the Monte Carlo hybrid code solves the relativistic Landau equation for electrons and a non-relativistic equation for ions:

*Work supported by the Fifth INFN National Committee through the HELIOS experiment.

[#]celona@lns.infn.it

ELECTRODE DESIGN OF THE ESS-BILBAO ACCELERATOR PROTON EXTRACTION SYSTEM*

D. Fernández-Cañoto[†], I. Bustinduy, D. de Cos, J. L. Muñoz, J. Feuchtwanger, F. J. Bermejo,
ESS-Bilbao, Leioa, Bizkaia, Spain

Abstract

The goal of extracting high proton currents from the ECR source of the ESS-Bilbao Accelerator has required comprehensive and systematic studies to find the appropriate geometric parameters for the electrode extraction system. Electrostatic and beam dynamics simulations are used to achieve a complete optimization of the accelerating electrode shapes, gap distances, and extraction electrode apertures, in order to ensure the extraction of a 70 mA proton beam from a 3.75 mm aperture radius. For the accelerating electrode shapes two different designs were mainly analyzed; the first is based on a Pierce geometry; and the second on a spherically convergent layout. Both designs consist of a tetrode system comprising a plasma electrode fed at 75 kV, followed by a puller system formed by a grounded extraction electrode separated to a certain distance from the plasma chamber, an electron repeller electrode fed at -3 kV; and finally, a fourth electrode at ground potential.

INTRODUCTION

The ESS-Bilbao project aims to build an accelerator able to produce high current proton beams [1]. The extraction system, which intrinsically determines the current of the beam and its quality, is a critical part of the ECR source where strong magnetic solenoidal field traps the plasma such that it is further ionized by means of a 2.7 GHz and 1.2 kW klystron [1]. In fact, an optimal electrode shaping is fundamental to extract a well focalized beam with high current and low emittance. An extraction system with four electrodes in a tetrode configuration seems very suitable for extracting high current proton beams in good conditions. The performance of this kind of extractors in similar ECR sources was already demonstrated numerically and experimentally by the Sherman [2] investigations which are used as a reference in this analysis. To design the shapes of the accelerating electrodes two different approaches are taken; firstly, the analytic derivation of Pierce [3]; and secondly, by considering the space charge dominated beam flowing between a concentrically spheric electrode geometry [4]. The Pierce geometry is often used by space charge dominated extraction systems where undesired forces, specially coming from radial electrostatic fields and from the longitudinal component of the magnetic field produced on the ECR solenoids can be more easily minimized [5]. On the other hand, using spherically shaped electrodes could con-

tribute to improve even further the charged particle flow and to extract higher currents than the Pierce layout.

It is expected that the new ESS-Bilbao ECR ion source will deliver a current density at the injection plane around 2500 A/m^2 . In fact, similar sources like SILHI [6] and LEDA [2] have already provided plasma densities of 2470 A/m^2 and 2590 A/m^2 , respectively. Higher currents could be extracted by increasing the aperture; however, it would also deteriorate the emittance and the probability of charge transfer in the extraction system because of higher residual gas pressure. Moreover, the maximum field strength is also reduced if the aperture is increased [5].

The well-known POISSON-SUPERFISH [7] software from LANL is used to calculate the electrostatic fields by solving the Laplace equation for well defined boundary conditions. The GPT [8] code is used to solve the equation of motion with a 5th order embedded Runge-Kutta solver.

The aim of these simulations is to obtain an electrode system capable of extracting, accelerating, and delivering a high quality proton beam from the plasma chamber to the LEBT system. Moreover, the normalized rms emittance at the LEBT position must be kept about $0.2 \pi\text{-mm-mrad}$ in order to get an acceptable matching to the elements downstream the accelerator, in particular the RFQ [9]. The extraction system geometry that delivers the best beam parameters calculated at 530 mm from the source (LEBT first solenoid position) is selected.

ELECTRODE SYSTEM GEOMETRY ANALYSIS

The extraction system is principally composed of a 75 kV plasma electrode and an extraction grounded electrode placed downstream at a certain accelerating gap distance, so that the electric field strength \mathbf{E} is mainly given by the voltage applied to the plasma electrode and the distance d_{gap} between the plasma and the extraction electrode. The extraction electrode is followed by another electrode fed at -3 kV to be used as a repeller for the low energy electrons that could be attracted to the plasma potential. The tetrode system is completed with a ground electrode placed next to the electrode repeller to limit the -3 kV potential. The repeller and its associated grounded electrode delimits a maximum radius and a certain longitudinal distance where the beam has to go through without hitting the electrodes.

The extracted ion beam current can be either limited by emission or by space-charge. For space-charge limitations and considering an infinite and planar emission area of ions with zero initial longitudinal velocity, the maximum ex-

* Work supported by ESS-Bilbao

[†] davidfer@essbilbao.com

CONSIDERATIONS ON A NEW FAST EXTRACTION KICKER CONCEPT FOR THE CERN SPS

M.J. Barnes, W. Bartmann, B. Goddard[#], CERN, Geneva, Switzerland

Abstract

A new 450 GeV/c extraction kicker concept has been investigated for the SPS, based on open C-type kickers and a fast-bumper system. The beam is moved into the kicker gap only a few ms before extraction. The concept is illustrated in detail with the LSS4 extraction in the SPS – very similar parameters and considerations apply to the other fast extraction system in LSS6. A similar concept could also be conceived for injection but is more difficult due to the larger beam size. The technical issues are presented and the potential impact on the machine impedance is discussed.

INTRODUCTION

The present SPS fast extraction is in the horizontal plane. The kickers are ferrite C-core with a return conductor closing the gap, Fig. 1, which provide enough aperture for the injected beam at 14 GeV. An alternative extraction kicker concept, Fig. 2, is investigated with the idea to build an open C-type kicker and fast-bumper system, such that the beam is moved into the kicker gap shortly before extraction. In this note the concept is illustrated with the SPS LSS4 extraction [1] from the SPS – very similar parameters and considerations apply to LSS6 [2]. A similar concept could also be used for injection, with a fast bump to move the beam out of the kicker aperture; however, this is much more difficult due to the larger beam size, and is not investigated here in any detail.

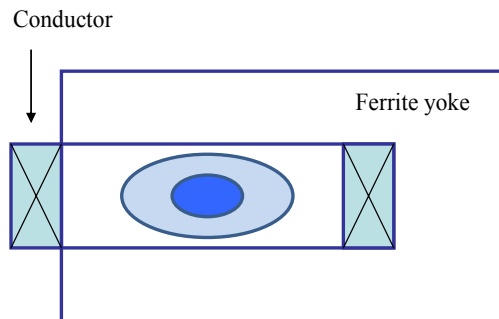


Figure 1. Schematic of present MKE kicker. The vertical gap height is determined by the injected beam size.

For a given magnet current, the kicker field is defined by the vertical gap; a smaller gap will be an advantage since more kick strength is available for a given Pulse Forming Network (PFN) voltage and system impedance. Kicker beam coupling impedance is an issue for beam stability, and having the beams present in the kicker gap for a short time only, and at high energy, could be a big advantage. Similarly, kicker heating from the real part of

the beam coupling impedance will be less of an issue if the coupling impedance seen by the beam is much less for most of the accelerating cycle. In addition, since a smaller vertical gap is required (for a given current), less installed kicker length will be required, which helps reduce the overall beam coupling impedance [3]. The smaller vertical gap and single conductor of the new kickers mean that the impedance per metre will, however, be higher.

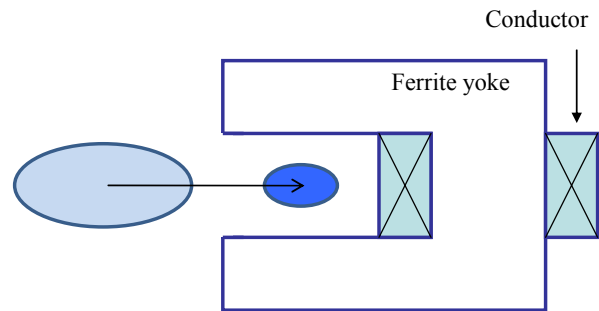


Figure 2. Schematic of alternative MKE kicker, where a fast bump moves beam into the gap. The vertical gap height is determined by the extracted beam size.

CONSTRAINTS AND ASSUMPTIONS

The constraints and assumptions used in investigating the feasibility of such a concept are listed. These are initial estimates and clearly have scope for optimisation.

- Extraction angle from kicker should be 0.5 mrad;
- Kicker vertical and horizontal gap should provide enough aperture for extracting CNGS beam at 300 GeV, and a sufficiently good field quality for this beam;
- The aperture of the kicker for the injected beam should not be less than at present;
- The flat-top ripple of the kick less than $\pm 1\%$;
- The kicker rise- and fall-time should be 1 μ s for the CNGS (this can be longer for LHC, to a maximum of 6 μ s);
- The pulse-length should be enough for CNGS, i.e. 10.8 μ s;
- One design is used for LSS6 and LSS4 (the vertical aperture could be smaller for LSS6);
- Optics and beam size at kicker locations:
 - Maximum beta functions assumed are 100 m X, 35 m Y;
 - $12/8 \pi$.mm.mrad normalised emittance for CNGS beam;
 - Dispersion at kicker location: 0.5 m
 - $\delta p/p$: 0.1 %;
 - Orbit allowance: ± 4 mm;

[#]brennan.goddard@cern.ch

THIRD INTEGER RESONANCE SLOW EXTRACTION SCHEME FOR A MU->E EXPERIMENT AT FERMILAB*

V.Nagaslaev[#], J. Amundson, J. Johnstone, L. Michelotti, C.S. Park, S. Werkema,
 FNAL, Batavia, IL 60510, U.S.A.
 M. Syphers, MSU, East Lansing, MI 48825, U.S.A.

Abstract

The current design of beam preparation for a proposed mu->e conversion experiment at Fermilab is based on slow resonant extraction of protons from the Debuncher. The Debuncher ring will have to operate with beam intensities of 3×10^{12} particles, approximately four orders of magnitude larger than its current value. The most challenging requirements on the beam quality are the spill uniformity and low losses in the presence of large space charge and momentum spread. We present results from simulations of third integer resonance extraction assisted by RF knock-out (RFKO), a technique developed for medical accelerators. Tune spreads up to 0.05 have been considered.

INTRODUCTION

The Mu2e experiment, proposed at FNAL is aimed to search for rare neutrinoless decays of a muon to electron in the Coulomb field of the atomic nucleus [1]. This experiment is designed to be sensitive to muon conversion at the level of 6×10^{-17} , which improves existing experimental limits by 4 orders of magnitude. This requires a large suppression of the background. A pulsed structure of the proton beam suits this purpose. A veto gate allows prompt beam background to die down during 750ns, after which the detector is activated to look for mu-atom decays. The search time is limited by the muon lifetime in the atom (864ns), therefore, the time structure defined by the revolution time in the Debuncher, 1.69 μ s, is almost ideal for this scheme. A single bunch of 20-40ns width is formed in the Debuncher and resonantly extracted towards the mu2e production target. This bunch structure provides a substantial natural initial background suppression. Additional suppression is provided by external extinction system at level of 10^{-10} . There are currently two alternative schemes of the resonant extraction under consideration: the half-integer and the third-integer resonance. Here we consider the latter one.

DEBUNCHER

The 8 GeV proton beam from the FNAL Booster is sent to the Accumulator via the Recycler. Three batches of 53MHz Booster beam are momentum stacked and then rebunched into an h=4, 2.5MHz rf. Beam bunches then are sequentially transferred one at a time to the Debuncher and slowly extracted during 160ms.

The Debuncher ring has 3-fold symmetry, 3 arcs and 3

straight sections. In addition, each arc and each straight are mirror symmetric, giving the machine an overall dihedral symmetry. Presently the machine optics is not quite symmetric, in order to accommodate stochastic cooling and maximize the machine acceptance. After completion of Run-II, stochastic cooling equipment will be removed and the lattice symmetry will be restored to allow high intensity proton operation.

SPACE CHARGE

Main requirements to the resonant extraction are the spill uniformity and minimal beam losses in the presence of substantial space charge tune shift. Slow spill from the Debuncher is done with a single bunch with rms length of 40ns and initial intensity of 3×10^{12} protons. Space charge tune shift is therefore significant. Due to high dispersion in the arcs ($D_x=2$ m) and finite momentum spread ($\sigma_p/p=0.004$), however, this tune shift is reduced to about 0.015. It is very important for the experiment to keep the bunch length as low as possible. However, reduction of rms length down from 40ns requires a considerable increase of the rf power in the Debuncher, and therefore its cost. If the trade-off between cost and performance is made in favour of the latter, the bunch length will be reduced to 20-30ns, therefore increasing the space charge tune shift to 0.025-0.03. This kind of a tune spread with a strong asymmetry of the tune distribution represents difficulties for the resonant extraction, in particular when a good uniformity of the spill shape is required.

TRACKING SIMULATIONS

Computer simulations of third-integer resonance extraction has been performed using the ORBIT code developed at ORNL [2]. Horizontal resonance tune was chosen at 29/3, the closest point to the current machine tune. Transfer matrices based on the improved symmetric lattice were used in this simulation. The sextupole field was formed by 2 orthogonal groups of 3 sextupoles, located in two straight sections. A quad circuit for tune ramping comprised 3 trim quads in the middle of each straight section. An extraction septum and lambertson magnet are located in the third straight. The septum width is assumed to be 100 μ , as that used in other applications around the lab.

For calculating the space charge (SC) effects we used a so-called 2.5D-mode of ORBIT, where the particle density in longitudinal bins is calculated according to the actual longitudinal distribution, and the transverse distribution is assumed to be the same along the bunch.

*Work supported by DOE under contract No. DE-AC02-07CH11359
[#]vnagasla@fnal.gov

IMPACT OF UNCAUGHT FOIL-STRIPPED ELECTRONS IN THE SPALLATION NEUTRON SOURCE RING

S. Cousineau, M. Plum, J. A. Holmes, W. Lu,
Oak Ridge National Laboratory*, Oak Ridge, TN, USA

Abstract

Evidence of hardware damage in the Spallation Neutron Source ring suggests that a non-negligible fraction of the foil stripped electrons are reflected back into the vacuum chamber. This paper summarizes the results of a 3D computational study that explores the dynamics of the foil-stripped, uncaught electrons.

INTRODUCTION

In high beam power accelerators which utilize H-charge exchange injection, the stripped electron beam must be carefully controlled to minimize the probability of electrons intercepting local hardware. In the 1 GeV, 1.4 MW Spallation neutron source ring [1], an electron catcher was installed for this purpose. The catcher was designed to catch the stripped electrons with very high efficiency [2]. However, due to relocations of the injected beam spot after the start of beam operations, as well as improper positioning of the catcher itself inside the chamber, the catcher is unlikely to have ever achieved the design efficiency. Multiple observations of hardware damage in the injection region suggest that a non-negligible fraction of the electrons are being reflected back into the chamber where they pose a significant threat to the local hardware.

This project was initiated to explore the dynamics of uncaught electrons in the SNS injection region. Only electrons which strike the top surface of the catcher are considered, e.g. those which constitute “catcher inefficiency”. The computational model employed includes electron tracking in the 3D field of the magnet, a surface interaction model for the electrons intercepting the catcher surface, and absorbing apertures to map out the final impact distribution of electrons.

The SNS injection configuration has evolved over time [3]. Two specific operational configurations were simulated in detail in this study, and results were compared with experimental observations. This paper presents only a brief overview the project. A full description can be found in reference [4].

EVIDENCE OF REFLECTED ELECTRONS

Three experimental observations indicate the presence of uncaught, reflected electrons in the SNS injection region. First, black marks have been observed on the top surface of the catcher surface. In the design electron catcher scheme, electrons should intercept the underside of one of five undercut wedges. The fact that there are black marks on the top surface of the catcher indicates that a substantial fraction of the electrons either are not now, or were not at some point during operations, being properly caught.

Second, a ring-shaped black mark has been observed on the top of the vacuum chamber above the stripper foil mechanism. This mark is thought to be caused by reflected electrons impacting the top of the beam pipe.

Third and last, melted metal was observed on the bracket and arm of a 3rd generation foil assembly [3]. The suspected cause was reflected electrons, and modifications were made to the geometry and material of the next generation assembly to alleviate the problem.

ORBIT 3D COMPUTATIONAL MODEL

The ORBIT code is a PIC-style, open-source code developed for simulating high intensity beams [5]. The code contains a module for particle tracking in a 3D magnetic field. This feature was combined with a Monte-Carlo style surface interaction model to simulate the stripped electrons in the SNS injection chamber. The surface model is based on scattering probability distributions generated by MCNPX for 545 keV electrons impinging on carbon at various incident angles. Only one scattering event is allowed for each electron, and for typical SNS electron incident angles, the MCNPX results indicate that the probability of absorption vs. reflection at the catcher surface is 60/40, respectively. Furthermore, the scattering is primarily elastic and within the plane of incidence, and the in-plane scattering angle is peaked near mirror-reflection.

Finally, hardware in the injection region, such as the top of the vacuum chamber and the foil assembly, were modelled as absorbing apertures.

* SNS is managed by UT-Battelle, LLC, under contract DE-AC05-00OR22725 for the U.S. Department of Energy.

COMPACT SOLID STATE DIRECT DRIVE RF LINAC EXPERIMENTAL PROGRAM

O. Heid, T. Hughes, Siemens AG, Erlangen, Germany

Abstract

We introduce a **solid state direct drive**TM linear induction particle accelerator concept, which integrates a modular solid state RF power source and a resonant RF accelerator cavity [1,4]. Individual RF drive of each cell in multi-cavity accelerators obviates RF power distribution issues between cavities as in conventional LINACs and allows arbitrary RF phases and amplitudes in each cell.

Key enabling technologies are novel Silicon Carbide (SiC) JFET RF transistors and a power combining RF wall current injection scheme including EMV suppressor cavity.

An experimental direct drive $\lambda/4$ cavity with a power rating of 1MW at 150MHz has been constructed. The integrated RF power source consists of one to 64 RF modules with eight SiC JFETs each, which are connected to a radial power combiner and surrounded by a toroidal EMV suppressor cavity. Initial trials with four power modules succeeded in delivering 200 μ s bursts with 10kW RF power, which corresponds to 16MV/m electrical field strength at the accelerating gap.

INTRODUCTION

In its current implementation the solid state direct driveTM concept [1] includes a $\lambda/4$ cavity and up to 64 RF modules (Fig. 1).

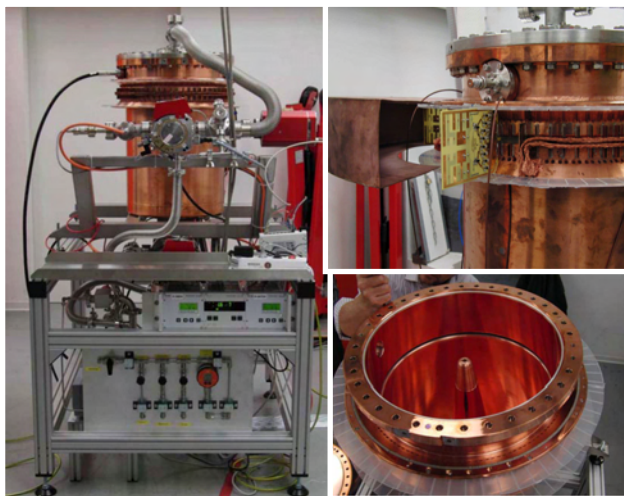


Figure 1: The experimental cavity and support equipment (left). Module mounted on current injection slot (right top). Interior cavity electrode (right bottom).

Each RF module contains eight SiC JFETs in class F push pull parallel (PPP, circlotron) arrangement [2], and currently provides 80A peak output current and 500V peak output voltage (20kW RMS) at negligible internal source impedance and with high efficiency. Figure 2 shows the module PCB layout.



Figure 2: 20kW RF module with SiC devices (red arrows).

EXPERIMENTAL

The first implementation of a solid state direct driveTM accelerator is based on a $\lambda/4$ cavity (Fig. 3). The tank material is copper plated stainless steel conditioned by Argon RF processing. Two ports accommodating calibrated RF pickup antennae serve as Argon processing power feeds and RF pickups. The cavity was characterised with shorted RF injection slit using standard RF techniques: Resonance frequency 150.043 MHz, unloaded Q 13200, loaded Q with Ar processing antenna 7666. The effective load impedance for each module was $(90/N^2) \Omega$ with N active modules.

The resonator cavity has been designed to operate at up to 1 MW RF power and >100 MV/m E field over 200 μ s RF burst duration when driven by by 64 RF modules. So far the tests used a maximum of four modules. Shorting the unused slots enabled the majority of the wall current to flow unimpeded across the slit to preserve the fundamental resonance mode.

The modular RF power stage operates in class F parallel push-pull topology (PPP, Circlotron, see Fig. 4), which allows very high power conversion efficiencies $> 85\%$ oblivious of load matching. The ultrafast SiC JFET body diodes allow bidirectional power flow, e.g. for

PROJECT X H- INJECTION DESIGN HISTORY AND CHALLENGES*

D.E. Johnson, A.I. Drozhdin, I. Rakhno, L.G. Vorobiev, Fermilab, Batavia, Illinois, U.S.A.
T. Gorlov, ORNL, Oak Ridge, Tennessee, U.S.A.; D. Raparia, BNL, Upton, New York, U.S.A.

Abstract

One of the initial motivations for replacing the aging Fermilab Proton Source was to support the 120 GeV Neutrino program at the 2 MW level while supporting a broad 8 GeV Physics program. Over the years the design parameters of the new Proton Source have evolved from the 2005 Proton Driver configuration of a 2MW 8 GeV pulsed H- linac injecting directly into the Main Injector or Recycler; to a 2MW 2 GeV CW linac supporting a 2 GeV Experimental Program while injecting into a new 2 to 8 GeV Rapid Cycling Synchrotron which would then supply protons to the Recycler. The current design parameters of the project include a 3 GeV CW linac accelerating up to 1 mA (average) H- and a 3 GeV Experimental Area with the connection to the Main Injector Complex as an upgrade. Whether the upgrade path includes a new 6(or 8) GeV CW or pulsed linac, or 3 to 8 GeV RCS and the ultimate linac current, remains to be determined. The basic issues of injection insertion design, foil and laser stripping options, foil survivability and loss issues will be analysed in context of the present options. Both analytical estimates and simulation results will be discussed.

INTRODUCTION

Current Configuration

The current accelerator configuration [1], as documented in the Reference Design Report [2], consists of

- a 3 GeV CW superconducting linac accelerating 1 mA of H⁻ in a 325 MHz bunch structure,
- a 3 GeV H⁻ transport line to simultaneously deliver MW range beam power to at least three experiments with variable bunch configurations,
- a 3 to 8 GeV Rapid Cycling Synchrotron (RCS) running at 10 Hz with H⁻ multi-turn injection,
- a 8 GeV proton transport line from the RCS to the Recycler where 6 batches are accumulated for single turn injection into the MI for the LBNE program.

Path Forward

It is recognized that the RCS configuration does not lead to an upgrade path toward muon source for a possible Muon Collider and/or Neutrino Factory at the 4 MW power level. Therefore, an R&D program to establish a self-consistent design of a 3 to 8 GeV superconducting linac, based upon 1.3 GHz SCRF cavity technology, injecting into the Recycler (RR) or directly

into the Main Injector (MI), is being developed. Implicitly included in this plan is the development of a self-consistent design for H- injection into the Recycler or Main Injector.

High Energy Linac Design

Two design options for a high energy (HE) linac fed from the 3 GeV CW linac are being investigated: 1) a pulsed linac operating at ~ 10 Hz with a range of macro beam pulse lengths between 1 and 4 ms and average beam currents between 4 and 1 mA, and 2) a low current CW linac with a beam current ~ 1 mA and macro beam pulse of ~26ms.

Design Challenges

This report will utilize the injection system design previously reported [3-7] and focus on potential options for the development of two techniques for implementing H-injection. Carbon foil stripping has been the main stay of multi-turn H- injection for the last several decades. It is currently the default technique. Recently, the technique of laser assisted stripping has gained much attention as a technique for H- injection without the use of physical stripping foils. We will discuss the status of each in relation to their impact on the choice of HE linac type.

CARBON FOIL INJECTION

The basic issues related to carbon stripping foils are: foil lifetime, losses associated with single coulomb scattering and nuclear interactions, and emittance growth due to multiple coulomb scattering.

The interaction of the injected H- and circulating beam impact the foil life time through heating due to energy deposition and radiation damage of the carbon crystalline structure [8] and create particle losses through scattering and nuclear interactions. The key is to minimize the number (and density) of foil traversals through the choice of injection lattice, ring lattice, painting algorithm, and foil size and geometry.

We report on the current status of optimization of H-injection into the RR/MI. Here, we look at the foil traversal rate and density for a range of linac currents from 1mA to 4 mA and pulse lengths from 1 to 4 ms for two coil configurations.

The short linac pulse lengths require six injections to accumulate the required charge (26 mA-ms). The circulating beam is removed from the foil between injections so the foil cools down between injections. Additionally, the instantaneous intensity from the injected beam is a factor of 6 less than that from a high current short pulse single injection, as in the Proton Driver [4].

For both the RR and MI, each 1 ms of injection requires ~90 turns with the complete injection time for six

*Work supported by U.S. Department of Energy under the contract No. DE-AC02-76CH03000.

#dej@fnal.gov

BEAM EXTRACTION IN PAMELA NS-FFAG*

Takeichiro Yokoi[†], Ken Peach, Holger Witte
John Adams Institute, Oxford University, Oxford, UK

Abstract

PAMELA (Particle Accelerator for MEDical Application) is a design study of particle therapy facility using NS-FFAG. PAMELA lattice realizes stable betatron tune with relatively small orbit excursion for a field accelerator with the help of newly developed combined function magnet. The combined function magnet provide an ability to flexibly change the operating point. The challenge of the beam extraction in PAMELA is the variability of extraction energy. The small orbit excursion of PAMELA helps to realize it. To tackle the problem, PAMELA employed vertical extraction with large gap kicker magnet. In addition to the fast extraction, PAMELA has a possibility of resonant extraction with a help of its ability to change the tune footprint. This feature opens up wide range of applications for PAMELA lattice such as ADSR.

OVERVIEW OF PAMELA

PAMELA is a design study of particle therapy facility using NS-FFAG(Non-Scaling Fixed Field Alternating Gradient)[1]. Employing fixed field accelerator enables rapid change of particles from proton to carbon ions and provide a high repetition rate operation. The pulsed beam of FFAG is considered to be fit well to the spot scanning treatment, which is the next generation treatment scheme for particle therapy.

The small but finite orbit excursion requires a large aperture, strong field magnet for the main magnet. Unlike a scaling FFAG, PAMELA employs truncated multipole field as Eq.1

$$\left(\frac{B}{B_0}\right) = \left(\frac{R}{R_0}\right)^k \rightarrow 1 + \sum_{n=1} \alpha(k, n) \left(\frac{\Delta r}{R_0}\right)^n \quad (1)$$

where Δr , $\alpha(k, n)$ are the deviation from magnet centre, $r - R_0$, expansion factor of the , respectively.

A new type of superconducting combined function magnet realises such field[3]. The magnet has an ability to change the multipole field component individually. The truncated multipole field configuration and the variability of multipole field configuration provide operational flexibility which makes it possible to change not only the average tune but overall tune footprint. One application of such tune footprint trimming is presented in the later section of the paper. In addition, thanks to the small orbit excursion (~ 17 cm for proton lattice, ~ 21 cm for carbon) for a fixed

field accelerator[1, 2], PAMELA has a possibility to extract beam with arbitrary energy over the entire energy range for treatment. The variable energy extraction and flexible tunability of operation point are unique features for a fixed field accelerator and are expected to improve beam quality in the treatment. The ring parameters of PAMELA are summarised in Table 1.

Table 1: Main Parameters of PAMELA Ring

particle	proton	carbon
Energy(inj)	31(MeV)	68(MeV/u)
Energy(ext)	70~250(MeV)	140~400(MeV/u)
Mean radius	6.251m	9.2m
Maximum field	3.6T	3.5T
Straight section	1.3m	1.2m
Orbit excursion	0.17m	0.21m
No. of cells	12	12
Magnet	FDF triplet SC	FDF triplet SC

EXTRACTION SYSTEM REQUIREMENT

For a fixed field accelerator, energy variable beam extraction is one of the key challenges of PAMELA. Ordinary fixed field accelerators including FFAG and cyclotron have considerably large orbit excursion . Horizontal extraction, which is employed in existing FFAGs and cyclotron, has three difficulties in changing the extraction energy. Those are

1. large inductance and strong field of kicker magnet,
2. beam distortion caused by nonlinear detuning, and
3. matching with extraction channel.

In PAMELA proton ring, the entire orbit excursion is about 17cm. To cover the excursion with a kicker, it needs aperture of more than 20cm. In horizontal extraction in PAMELA, an orbit separation of more than 10cm needs to be generated in maximum to cover the entire treatment energy range, 70MeV~250MeV. Such a large aperture and orbit separation result in huge inductance and huge pulse voltage of the kicker. Analytically, inductance of dipole magnet is expressed as $L = w \cdot l/g$, where w , l , g mean width, length and gap height of kicker. The formula tells that for a fixed magnet volume, a kicker with larger width and smaller gap height has larger inductance compared to one with smaller width and larger gap height. In addition, the non-linear field of FFAG has intrinsic nonlinear detuning of betatron motion, and the detuning sets the upper limit of

*Work supported by the COMFORM collaboration under EPSRC grant number EP/E033286/1

[†]t.yokoi1@physics.ox.ac.uk

PREDICTED PERFORMANCE OF COMBINED CLEANING WITH DS-COLLIMATORS IN THE LHC

D. Wollmann, A. Rossi, R.W. Assmann, R. Bruce and S. Redaelli,
CERN, Geneva, Switzerland

Abstract

The LHC has two dedicated cleaning insertions: IR3 for momentum cleaning and IR7 for betatron cleaning. During the first months of beam experience the presently installed Phase-I system performed as predicted earlier in detailed studies with tracking simulations. As the current system is not sufficient to allow LHC operation with nominal or ultimate intensity at 7 TeV/c, simulations with an upgraded system are ongoing to overcome these limitations. In this contribution a collimation scheme with combined momentum and betatron cleaning in the interaction region 3 (IR3) with additional collimators in the IR3 dispersion suppressor is presented. The predicted improvements compared to the Phase-I system and the limitations of this scheme are discussed.

INTRODUCTION

At nominal momentum (7 TeV/c) and intensity ($\sim 3 \cdot 10^{14}$ protons) the LHC will have a stored energy of 362 MJ per beam. The uncontrolled loss of only a small fraction of beam in the superconductive magnets of the LHC can cause the loss of their superconducting state (quench limit at 450 GeV/c: $R_q = 7 \cdot 10^8 \text{ ps}^{-1} \text{ m}^{-1}$; at 7 TeV/c: $R_q = 7.6 \cdot 10^6 \text{ ps}^{-1} \text{ m}^{-1}$) [1, 2]. Therefore, a powerful collimation system is needed to intercept these unavoidable beam losses. In addition the collimators shall provide a passive machine protection [3, 4, 5]. The measure for the performance of a collimation system is the local cleaning inefficiency

$$\eta_c = \frac{N_{local}}{N_{total} \cdot \Delta s}, \quad (1)$$

with N_{local} the number of protons lost within an aperture bin Δs and N_{total} the total number of lost particles.

To achieve these goals a phased approach was taken. The present Phase-I system consists of 44 collimators per beam, which are mainly installed in two dedicated cleaning insertions. IR3 collimators are used for the cleaning of off-momentum particles and IR7 to intercept particles with too large betatron amplitudes. A sketch of the layout of the Phase-I collimation system is shown in Figure 1. The calculated local cleaning inefficiency of this system with imperfections ($\eta_c = 5 \times 10^{-4} \text{ m}^{-1}$) is expected to limit the maximal possible beam intensity stored in the LHC to 4% of the nominal [6, 7].

In addition to the installed collimators empty slots in the cleaning insertions for future Phase-II collimators were prepared. The main intensity limit due to cleaning was

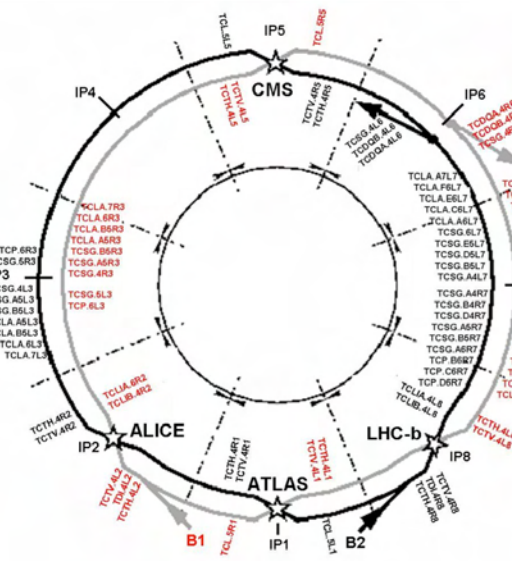


Figure 1: Sketch of the layout of the present phase-I collimation system. Beam 1 (beam 2) collimators are shown in red (black). [7].

identified to losses in the cold dispersion suppressor (DS) region at the end of the cleaning insertions. Simulations with an improved system using collimators in the prepared Phase-II slots and two collimators in the dispersion suppressor of the betatron cleaning insertion (IR7) in addition to Phase-I showed that a gain in cleaning efficiency of a factor 30 could be achieved [8].

Another future limitation for the LHC intensity could be collimation related radiation to electronics. Therefore a combined betatron and momentum cleaning in IR3 was studied. Compared to the present Phase-I system this would reduce the performance by a factor of two [9].

These two results lead to the idea to combine the two proposals and study a system with combined betatron and momentum cleaning in IR3 with additional collimators in the superconductive dispersion suppressor of IR3 without using the collimators in IR7. The cleaning performance of such a system is discussed and presented below. This system was proposed and approved for installation in the long shutdown of the LHC in 2012.

MULTISTAGE CLEANING

Figure 2 shows a simplified sketch of the gap opening arrangement of the different classes of collimators normalized by beam size for the multistage cleaning in the

LEAKAGE FROM LHC DUMP PROTECTION SYSTEM

Chiara Bracco, Ralph Assmann, Wolfgang Bartmann, Christophe Boucly, Roderik Bruce, Etienne Carlier, Bernd Dehning, Brennan Goddard, Eva Barbara Holzer, Malika Meddahi, Annika Nordt, Stefano Redaelli, Adriana Rossi, Mariusz Sapinski, Jan Uythoven, Daniel Wollmann, CERN, Geneva, Switzerland

Abstract

A single-sided mobile diluter (TCDQ) and a horizontal secondary collimator (TCSG) are installed in the extraction region of the LHC to protect the downstream elements from damage in case of asynchronous beam dump. These collimators have to be precisely set up to shield the arc aperture at 450 GeV, the triplet apertures and the tungsten tertiary collimators (TCT) at the low beta collision points. During the LHC beam commissioning, several machine protection tests were carried out to validate collimator setup and hierarchy at different beam energies and intensities. The outcomes of these measurements are presented in this paper together with the results of particle tracking simulations for asynchronous beam dump. These studies allowed to quantify the leakage expected from dump protection collimators to the downstream elements and to validate the system performance towards higher beam intensity.

INTRODUCTION

The LHC beam dump system is formed by 15 extraction kicker magnets (MKD) which deflect horizontally the beam towards a set of 15 steel septum magnets (MSD). The beam is then painted, by means of dilution kickers, onto special graphite absorber blocks (TED) [1].

The filling pattern in the LHC is constituted by batches of 72 consecutive bunches, which are separated by 25 ns. The unfilled space between the first and the last injected batch defines the abort gap and corresponds to 3 μ s (120 bunches). This larger gap, between bunches, allows for the rise time of the MKD which must be triggered simultaneously and with the correct phase with respect to the beam abort gap to achieve a loss-free extraction. If the RF system, which defines the correct bunched structure of the beam, loses the synchronization with respect to the MKDs or if it breaks down, the beam populates the abort gap and enters in the extraction region when the kicker voltage is still rising and part of it is swept across the machine aperture. Two protection elements, per each beam, are installed downstream of the MSD and have to absorb the beam swept during an asynchronous beam dump in order to avoid damage of the downstream elements. The first protection element is a horizontal mobile diluter (TCDQ) made up by one single 6 m long CFC (Carbon Fiber Compound) jaw which is located at the extraction side of the machine. A standard horizontal secondary collimator (TCSG), with two 1m long CFC jaws, is installed immediately after the TCDQ and allows to precisely define the horizontal beam position at

this location providing further collimation of the secondary halo.

TCDQ AND TCSG SETUP

The extraction protection collimators have to be precisely set up respecting a well established hierarchy valid for the full LHC collimation system [2]. They do not have to intercept the primary halo since this could increase the loss load on the downstream superconducting magnets and potentially induce a quench [3]. On the other hand they have to be closed enough to shield and minimize the energy deposition on the tungsten tertiary collimators (TCT: horizontal TCTH, vertical TCTV) which protect the triplet apertures at the experiments. At injection the TCDQ has to be set up at 8σ , where σ is the beam size, and the TCSG at 7σ while, at the low beta collision points, the retraction between these two elements has to be reduced to 0.5σ (TCSG at 7.5σ for 7TeV and $0.55\text{ m } \beta^*$).

Several manual setups of the full collimation system, including the extraction protection elements, have been performed during the first year of the LHC beam commissioning and, in particular, for any significative change in optics and beam conditions. The TCDQ and the TCSG have been set at the nominal aperture at injection and, due to the low energy (3.5 TeV) and bigger β^* (3.5 m), at 9.8σ and 9.3σ at collision. An accuracy of about 1σ has been defined for the positioning of the TCDQ with 0.1 mm resolution. The protection level provided by the these collimators depends strongly on the relative settings of the TCT with respect to the TCDQ. A 5σ retraction (TCTs set up at 15σ), which takes into account triplet protection, collimator setup errors, dynamic orbit change and dynamic beta-beat, has been used up to now. This retraction has to be reduced by a factor of 10 for nominal LHC operation. An upgrade of the TCDQ motor system and a better control of the machine stability are necessary to reach this target.

ASYNCHRONOUS BEAM DUMP TESTS

Loss map studies have been periodically carried out to validate the hierarchy of the collimation system and, in particular, asynchronous beam dump tests have been performed to quantify the leakage from the TCDQ towards the downstream elements. These tests consisted in switching off the RF cavities and leaving the beam particles populating the abort gap for about 90 s (0.01% energy loss). A beam dump was then triggered by means of the emergency switches located in the CERN Control Centre (CCC)

PROTECTION OF LHC AGAINST FAST FAILURES DURING INJECTION AND BEAM DUMP

C. Bracco, R. Assmann, W. Bartmann, E. Carlier, B. Goddard, V. Kain, M. Meddahi, A. Nordt, S. Redaelli, J. Uythoven, J. Wenninger, CERN, Geneva, Switzerland

Abstract

The LHC transfer lines, injection and beam dump systems are equipped with a series of active and passive protection systems. These are designed to prevent as many failures as possible, for example through surveillance and interlocking, or to absorb any beam which is mis-kicked or mis-steered on passive absorbers. The commissioning, validation tests and performance of the different systems are described, and the implications for the protection of the LHC against different failures during beam transfer are discussed.

PROTECTION AGAINST FAST FAILURES

Transfer Lines

Each transfer line is equipped near the LHC injection with a series of six two-sided collimators TCDI with adjustable jaws, to limit the maximum beam excursion. The collimators are arranged in both planes at 60 degree phase advance, to provide optimum phase space coverage for the single pass [1-2]. The nominal setting of the TCDI jaws is ± 4.5 betatron sigma.

Injection System

The injection kicker MKI can fire erratically or a switch can also fail to fire when required. Also a synchronisation failure could lead to the beam not being deflected, or to the circulating beam being kicked by mistake. Finally, the kickers can also fail with high voltage breakdown (flashover), which can in theory give a kick of any amplitude up to 125% of the nominal one.

To protect against these fast failures each injection is equipped with a primary protection device TDI, which is a 4m long two-sided collimator, nominally placed at 6.8 sigma from the beam. The TDI is 90 degrees in phase downstream of the MKI kicker, and therefore intercepts any miskicked injected beam with an amplitude greater than the jaw setting. A fixed 1 m long mask TCDD is placed in front of the superconducting dipole D1, to reduce the beam load on the coils of this magnet. The TDI is supplemented with two auxiliary collimators at phase advances of $n \times 180 \pm 20$ deg, which improve the system performance in the event of phase advance errors between MKI and TDI. The TDI and TCLIs are interlocked such that injection is only possible if the jaws are in position around the beam. After injection the jaws are retracted.

Beam Dump Failures

To protect the downstream elements against a beam sweep from an erratic kicker firing, protection devices are installed. A 6 m long composite fixed absorber (TCDS) is located in front of the extraction septum, and must dilute

the impacting ~ 30 bunches to a level where the septum is not damaged. Another 6 m long single-sided absorber is located in front of Q4, to protect Q4 and also to limit the amplitude of beam escaping into the LHC. For this latter purpose this absorber is movable, and is placed at around 8-10 sigma from the beam. The TCDQ is supplemented by a short 1.2 m long two-sided graphite collimator TCSG which allows an accurate definition of the beam position, and also can be positioned more accurately than the long TCDQ. A fixed 2.4 m long steel mask protects the Q4 magnet coils from the showers from these elements.

The TCSG and TCDQ are closed during the ramp to maintain the correct position with respect to the beam. The jaw positions are ensured by HW interlocks, and an additional interlock is present on the maximum TCSG gap and TCDQ position which depends only on the LHC energy. The beam position at the TCDQ is maintained by the orbit feedback system and interlocked by the SW interlock system SIS. This is presently set at ± 1.7 sigma at 3.5 TeV, corresponding to about ± 1.2 mm.

INJECTION PROTECTION SYSTEM COMMISSIONING

TCDI System

The TCDI alignment was made during a dedicated LHC filling sequence, where a minimum number of nominal bunches (to date 1 or 4) was repeatedly injected into the LHC, while the jaw positions were scanned. To avoid the potential danger of opening the jaws, the method used was to scan the jaws only towards the beam. Sample scans are shown in Figure 1, for locations with low dispersion and for large normalised dispersion ($D/\sqrt{\beta}$). The locations with large dispersion have less room for alignment errors, and these collimators are the ones which need to be most frequently adjusted.

Validation checks of the TCDI collimators were made by sending free betatron oscillations with different phases through the system, using correctors upstream in the line, to measure the system opening as a function of phase. A small emittance low intensity 'pilot' beam of about $1 \mu\text{m}$ normalised in both planes was used, with small bunch length, to accurately probe the acceptance of the system. The position in sigma of the edge of the jaws was then estimated from the fraction of beam lost, scaling the offset by the ratio of the actual to nominal emittances to derive a setting in nominal sigma.

OPERATIONS OF THE TEVATRON ELECTRON LENSES*

X.L. Zhang[#], V. Shiltsev, A. Valishev, G. Stancari, G. Kuznetsov, G. Saewert,
 FNAL, Batavia, IL 60510, U.S.A.
 V. Kamerdzhev, FZ-Jülich, IKP, Germany

Abstract

The two Tevatron Electron Lenses (TEL1 and TEL2) are installed in Tevatron in 2001 and 2006 respectively. TEL1 is operated as the vital parts of the Tevatron for abort gap beam clearing, while TEL2 is functioning as the backup as well as the test device for beam-beam compensation, space charge compensator and soft beam collimator. Both of them are working exceptionally reliable after a few initial kinks being worked out. Their operations in Tevatron are summarized in this report.

INTRODUCTION

The Electron Lenses have been installed in the Tevatron with the objective to compensate the beam-beam effects on antiproton beams which may limit the collider performance [1, 2]. The electron-beam current can be adjusted bunch-by-bunch to optimize the performance of all bunches in a multi-bunch collider by using fast high voltage modulator [6]. In addition, the electron transverse current profile (and thus the radial dependence of electromagnetic (EM) forces due to electron space-charge) can also be changed for different applications using different electron guns.

However for the present Tevatron operations, the antiproton beam lifetimes are dominated by luminosity consumptions [2], which leave the TEL a primary vital function as abort gap beam cleaner.

TEVATRON ELECTRON LENSES

Both Tevatron Electron Lenses (TELS) direct their beam against the antiproton flow. Figure 1 shows the layout of the TEL2.

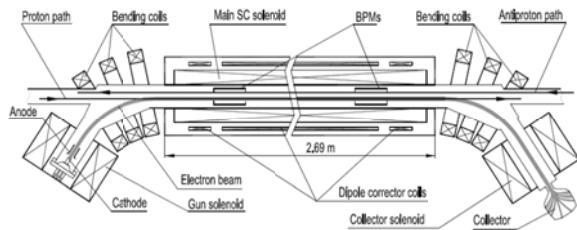


Figure 1: TEL2 layout.

Extensive studies have been carried out with electron beam profiles of flattop, smooth edge flattop (SEFT) and Gaussian in the Tevatron. The SEFT gun has been designed and built in order to generate much less nonlinearity than the flattop gun at the transit edges so that it causes much less proton loss when electron beam is not perfectly aligned with proton beam it acted on. The Gaussian gun was installed to study the nonlinear beam-

beam compensation effects. Recently we have installed the hollow electron gun to study the electron beam collimations.

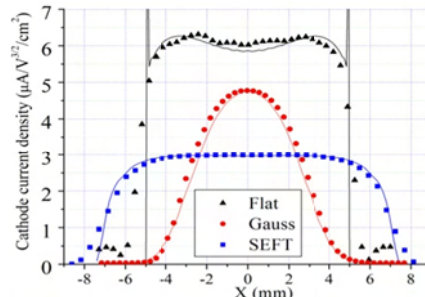


Figure 2: Three profiles of the electron current density at the electron gun cathode: black, flattop profile; red, Gaussian profile; blue, SEFT profile. Symbols represent the measured data and the solid lines are simulation results. All data are scaled to refer to an anode-cathode voltage of 10 kV.

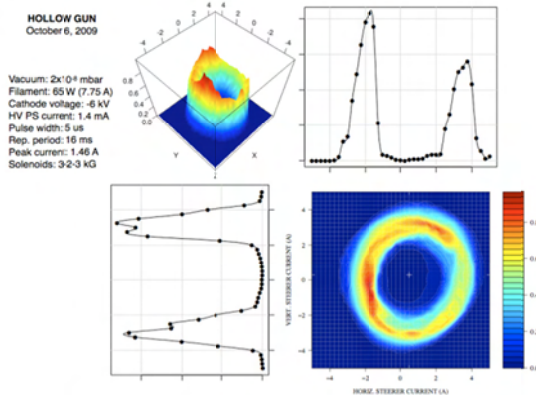


Figure 3: Current profiles of the hollow electron gun.

One example of the hollow electron beam profile was measured with a 0.2 mm pinhole and reconstructed as in Figure 3. To make this hollow cathode, a 0.6 inch spare SEFT gun cathode was bored out about 3/8 inch hole in the center. And about 2.5 A peak electron current achieved at 9 KV anode to cathode voltage.

REMOVING UNCAPTURED BEAM

In Tevatron, uncaptured protons are generated by various mechanisms such as coalescing in the MI, intra-beam scattering (IBS), phase and amplitude noise of the RF voltage. The longitudinal instabilities or trips of the RF power amplifiers can contribute large spills of particles to the uncaptured beam. Uncaptured beam particles are outside of the RF buckets, and therefore, move longitudinally relative to the main bunches to fill the beam abort gap. If the number of particles in the

*Work supported by the Fermi Research Alliance, under contract DE-AC02-76CH03000 with the U.S. Dept. of Energy.

[#]zhangxl@fnal.gov

EMITTANCE PRESERVATION AT INJECTION INTO LHC

V. Kain, W. Bartmann, C. Bracco, B. Goddard, W. Hofle, D. Karadeniz, M. Meddahi,
D. Valuch, J. Wenninger, CERN, Geneva, Switzerland

Abstract

The very demanding LHC beam parameters put very strict requirements on the beam quality along the SPS-to-LHC transfer. In particular, the budget for the emittance increase is very tight. During the LHC commissioning, the emittances have been measured in the SPS, the two SPS-to-LHC transfer lines and in the LHC. Preliminary results show the importance of a very well controlled beam steering in the transfer lines together with the need of a robust trajectory correction strategy and transverse damping in order to guarantee long-term reproducibility. Another source comes from the tilt mismatch between the LHC and its transfer lines which generates coupling at injection into the LHC and in turn will contribute to emittance increase. Preliminary results are also discussed.

INTRODUCTION

The preservation of the transverse emittance from injection to collisions is crucial for the LHC luminosity performance. The transfer and injection process is particularly critical in this respect. The LHC is filled from the SPS via two transfer lines, each about 3 km long. For nominal performance the total emittance increase budget between SPS extraction and LHC collision energy is only $\varepsilon/\varepsilon_0 < 1.07$. This places stringent requirements on the various mismatch factors at injection. In total an emittance increase of 5 % should not be exceeded. The nominal emittance of nominal intensity bunches (1.15×10^{11} p⁺ per bunch) is 3.5 μm : the allowed increase is therefore only about 0.08 μm .

SOURCES FOR EMITTANCE GROWTH

Beam stability, kicker ripple, betatron, dispersion and coupling mismatch at the LHC injection point all lead to emittance increase. How the different effects impact the emittance increase is summarised in [1]. For example, the emittance increase from steering errors at the injection point is given by

$$\frac{\varepsilon}{\varepsilon_0} = 1 + \frac{1}{2} \cdot \Delta e^2 \quad (1)$$

with Δe being the steering error in betatron sigma. There is also a rotation angle between the reference frame of the transfer lines and the LHC. This ‘tilt mismatch’ leads to a phase dependant coupling, see [2], and emittance increase following

$$\frac{\varepsilon_x}{\varepsilon_{0x}} = 1 + \frac{1}{2} \cdot (\beta_x \gamma_y + \beta_y \gamma_x - 2\alpha_x \alpha_y - 2) \cdot \sin^2 \theta \quad (2)$$

The emittance increase due to this effect is 1.3 % for TI 8 (tilt angle of 54 mrad) and 0.3 % (tilt angle of 20 mrad) and is presently uncorrectable, although

correction schemes using skew quadrupoles are under study.

2010 OBSERVATIONS

Emittance Delivered to LHC

A series of BTV screens was used in the transfer lines for the emittance measurement. In the LHC wire scanners measured the beam sizes for circulating beam.

The optics in the line is very well under control, see Fig.1, after several years of measurements and corrections, see e.g. [4]. A big effort also went into understanding the dispersion matching into the LHC [4]. As a result, the transverse emittance is conserved (within the accuracy of the measurement) between SPS extraction and LHC injection – and this even for emittances below nominal. Table 1 shows the results for a comparative measurement done in beginning of July 2010 in the vertical plane.

Table 1: Vertical Emittance with Transverse Blow-up in the SPS, Measurement from 7th of July 2010

	ε_{yn} [μm]
SPS	3.3 ± 0.5
TI 2	3.2 ± 0.3
TI 8	3.4 ± 0.4
LHC B1	3 ± 0.3
LHC B2	3 ± 0.3

The emittance increase from SPS to LHC is clearly below the resolution of the measurement. The emittance measurement in the SPS and LHC is in fact a beam size measurement, using the nominal optics functions to estimate emittance – the estimate in the LHC could possibly be improved by using the measured (or interpolated) β function at the wirescanner, and by cross-checking with emittance measurement in the beam dump lines, each of which is equipped with three screens.

Fig. 2 shows the evolution of the emittance in the vertical plane for beam 1 during filling beginning of July.

LONGITUDINAL PERFORMANCE WITH HIGH-DENSITY BEAMS FOR THE LHC IN THE CERN PS

H. Damerou*, S. Hancock, M. Schokker, CERN, Geneva, Switzerland

Abstract

As one of the pre-injectors for the Large Hadron Collider, the CERN Proton Synchrotron must reliably deliver beams in a wide range of parameters. The large variety of bunch spacings from 25 to 150 ns at extraction requires the acceleration of small, high-density bunches as well as highly intense ones. Above a threshold bunch density, longitudinal coupled-bunch instabilities are observed after transition crossing and the main accelerating cavities have been identified as part of the impedance driving them. Transient beam loading causes asymmetries of the various bunch splittings used to establish the required bunch spacing, compromising beam quality at the head of the bunch train delivered. Recent measurements of longitudinal limitations of beams for the LHC are presented, together with possible cures and options for future hardware improvements.

INTRODUCTION

The optimum bunch spacing in the Large Hadron Collider (LHC), especially during the commissioning phase, is determined by a large set of constraints from the machine itself, as well as from the experiments. Hence, the accelerators in the injector chain of the LHC must be flexible to provide bunches spaced by 25, 50, 75 or 150 ns. The 150 ns variant had originally not been foreseen. Following a request by the LHC experiments, it has been set-up in 2010 for the first time. It is important that the bunch parameters at injection into the LHC are independent from bunch spacing.

The major part of the preparation of the different variants of LHC-type beams is performed by radio frequency (RF) manipulations already in the Proton Synchrotron (PS). In all cases, up to six bunches from the PS Booster (PSB) are injected into RF buckets at the 7th harmonic ($h = 7$) of the revolution frequency, f_{rev} . One bucket remains empty to provide a gap for the PS extraction kicker. The up to $\tau_{\text{batch}} = 1.8 \mu\text{s}$ long batch sent to the Super Proton Synchrotron (SPS) may thus be filled with $\tau_{\text{batch}}/\tau_{\text{bs}}$ bunches spaced by τ_{bs} . The different variants of the LHC-type beams are produced by combinations of triple and double bunch splittings on both injection and extraction plateaus (Table 1). For these manipulations the PS is equipped with sets of cavities covering frequencies of 2.8–10 MHz (ferrite-loaded, tunable), 13.3 MHz, 20 MHz, 40 MHz and 80 MHz. Additional cavities at 200 MHz are used for controlled blow-up of the longitudinal emittance. The labels LHC25ns, LHC50ns, etc. are used throughout

Table 1: Longitudinal Manipulations for the Different Variants of Nominal LHC-type Beams [1, 2]. Each bunch (b) is split in two (2-split) or three (3-split) parts.

LHC25ns	LHC50ns	LHC75ns	LHC150ns
Inject 6 bunches on harmonic $h = 7$			
Flat-bottom RF manipulation			
Controlled emittance blow-up to match splitting			
3-split	3-split	2-split	2-split
$h = 7, 14, 21$		$h = 7, 14$	
Blow-up for transition			
Acceleration			
18b, $h = 21$		12b, $h = 14$	
Blow-up			
Intensity and longitudinal emittance per bunch:			
$5.2 \cdot 10^{11}$	$2.6 \cdot 10^{11}$	$2.6 \cdot 10^{11}$	$1.3 \cdot 10^{11}$
1.3 eVs	0.65 eVs	0.65 eVs	0.33 eVs
Total intensity for $N_b = 1.3 \cdot 10^{11}$ ppb at extraction:			
$9.4 \cdot 10^{12}$	$4.7 \cdot 10^{12}$	$3.1 \cdot 10^{12}$	$1.6 \cdot 10^{12}$
1 st RF manipulation on flat-top			
2-split	2-split	2-split	
$h = 21, 42$		$h = 14, 28$	
2 nd RF manipulation on flat-top			
2-split	Rebucket	Rebucket	Rebucket
$h = 42, 84$	$h = 28, 84$	$h = 28, 84$	$h = 14, 84$
Bunch shortening on $h = 84$, final bunch pattern:			
72b, 25 ns	36b, 50 ns	24b, 75 ns	12b, 150 ns

this paper to indicate the beam type according to its bunch spacing at extraction, which differs from the bunch spacing during acceleration in most cases.

As each bunch at extraction to the SPS should nominally contain $N_b = 1.3 \cdot 10^{11}$ ppb within a longitudinal emittance of $\varepsilon_l = 0.35 \text{ eVs}$ (2σ), the total intensity of the beam accelerated in the PS varies from $1.6 \cdot 10^{12}$ ppp (150 ns bunch spacing) to $9.4 \cdot 10^{12}$ ppp (25 ns). The average longitudinal density, $N_b/\varepsilon_l = 3.7 \cdot 10^{11}$ p/eVs, during the last part of acceleration and on the flat-top is however identical for all different species. Since the harmonic number during acceleration is the same for LHC25ns/LHC50ns ($h = 21$) and LHC75ns/LHC150ns ($h = 14$), this allows direct comparison of beams with the same longitudinal density but very different total intensity. In the PS, the maximum intensity with LHC-type beams remains well below the intensity of beams accelerated for fixed-target experiments ($> 3 \cdot 10^{13}$ ppp), but the latter beams are much less dense.

* heiko.damerou@cern.ch

QUENCH PROTECTION WITH LHC BEAM LOSS MONITORS

M. Sapinski*, B. Dehning, E. Effinger, J. Emery, E.B. Holzer, C. Kurfuerst, A. Priebe, C. Zamantzas, CERN, Geneva, Switzerland

Abstract

To prevent from beam-induced quenches of the superconducting magnets a system of about 4000 beam loss detectors is installed on the magnets cryostat. These detectors, being ionisation chambers, measure the particle shower starting inside the magnet. Examples of simulations linking the heat deposited in the superconducting coils with signals in the ionisation chambers are presented. A comparison of the simulations to the data is done. Limits of the present system are discussed.

INTRODUCTION

The Beam Loss Monitor (BLM) system uses mainly cylindrical ionisation chambers, installed in various locations on the LHC, as radiation detectors. Most of the chambers are installed on the cryostat of the superconducting magnets. Their main goal is to detect if the energy deposition in the superconducting coil due to beam losses is high enough to provoke a transition of the coil to a normal-conducting state (quench). If the BLM system detects such a loss it sends a signal to the beam dump and the beam is removed from the LHC ring within 4 revolutions.

The beam-abort thresholds set up in BLM electronics [1] are a function of beam energy and signal integration time. Because the temporal and spatial distribution of the loss have a large impact on threshold, usually the most conservative values are chosen.

Various aspects of quench-protecting threshold estimations, which authors found especially interesting, are discussed in this paper.

METHOD

The ingredients needed to estimate the beam-abort thresholds are:

- beam loss distribution,
- quench margin of the magnet,
- energy deposited in the coil,
- signal in the BLM.

In the following, the four ingredients are discussed in detail.

* mariusz.sapinski@cern.ch

Beam Loss Distribution

The distribution of the beam losses depend on the trajectories of the particles and on the aperture of the vacuum chamber. An example of the loss pattern, obtained from SixTrack [2] simulation of beam halo particles, is shown in Figure 1, where the beam goes from left to right. To obtain this plot losses over all arcs were superimposed according to MB-MQ interconnection geometry. The red line shows the shape of the vacuum chamber. A loss peak is observed after the interconnection, at the beginning of the MQ beam screen.

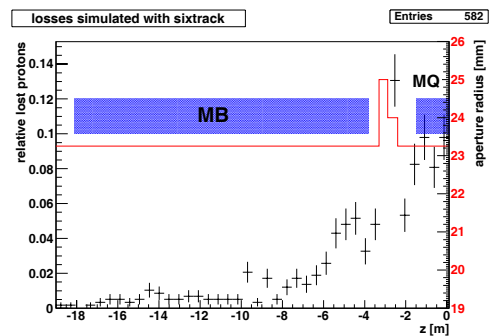


Figure 1: Loss pattern at interconnection between arc magnets simulated using SixTrack code. This loss is generated by halo particles.

The loss pattern to large extent follows the lattice β – function. Therefore, almost independent of the mechanism which causes the loss, the highest loss probability is in vicinity of quadrupole magnets where the β – function reaches its maximum. In transverse plane the losses are usually concentrated in horizontal or in vertical direction, depending on the onset of the loss phenomena.

The BLM locations have been chosen to minimise the impact of the spatial loss distribution on the BLM thresholds. In case of MB and MQ magnets the impact of the loss distribution on the BLM signal is discussed in [3] and [4].

The temporal distribution of losses has a critical influence on the quench margin of the magnet but also on the signal observed in the BLM due to temporal effects in the analog and digital part of the acquisition system. The ongoing investigations show weak influence of the loss temporal distribution on the quench margin [5]. Losses with a very short rise time are seen in the BLM system with a delay which might in some cases be too large and therefore the beam-abort thresholds needs to be lowered in order to compensate for it.

COMMISSIONING OF RAMP AND SQUEEZE AT THE LHC

S. Redaelli*, M. Lamont, G. Müller, R. Steinhausen, J. Wenninger,
CERN, Geneva, Switzerland
X. Buffat, EPFL, Lausanne, Switzerland

Abstract

The energy ramp and the betatron squeeze at the CERN Large Hadron Collider (LHC) are particularly critical operational phases that involve the manipulation of beams well above the safe limit for damage of accelerator components. In particular, the squeeze is carried out at top energy with reduced quench limit of superconducting magnets and reduced aperture in the triplet quadrupoles. In 2010, the commissioning of the ramp from 450 GeV to 3.5 TeV and the squeeze to 2 m in all the LHC experiments have been achieved and smoothly became operational. In this paper, the operational challenges associated to these phases are discussed, the commissioning experience with single- and multi-bunch operation is reviewed and the overall performance is discussed

INTRODUCTION

The Large Hadron Collider (LHC) has seen an exciting initial operation at 3.5 TeV, with stored energies up to 9 MJ per beam at the time of this workshop. The energy ramp and the betatron squeeze are particularly critical operational phases that involve delicate handling of beams above the safe limits (assumed limit is 3.1×10^{10} protons at 3.5 TeV). Presently, the nominal parameters have been achieved in terms of bunch intensity, ramp rate, transverse and longitudinal beam emittance. The commissioning is now focused on increasing the stored beam energy to reach by the end of the 2010 run the luminosity goal of $10^{32} \text{cm}^{-2} \text{s}^{-1}$ and up to 30 MJ stored energy [1].

In order to achieve a good collider performance and minimize the risk of quench and damage, it is clearly important to keep under control losses during ramp and squeeze. Machine protection constraints also impose tight tolerances on the orbit and optics stability. In this paper, we present the performance of ramp and squeeze at the LHC under various conditions. After a brief introduction on the run configurations and on the commissioning strategy, the tools developed to perform ramp and squeeze are presented and the performance in term of beam transmission, orbit stability and tune and chromaticity stability are presented.

2010 RUN CONFIGURATIONS

The main beam and machine parameters for the 2010 LHC run configurations are given in Table 1. After an initial pilot run at a reduced energy of 1.18 TeV (I), limited by

Table 1: LHC 2010 proton run configurations and achieved performance at the time of this workshop. The goal for 2010 is to achieve a luminosity of $10^{32} \text{cm}^{-2} \text{s}^{-1}$ by the end of October, with stored energies up to 30 MJ per beam.

Parameter	Value		
	I	II	III
Colliding beam energy [TeV]	1.18	3.5	3.5
Peak luminosity [$10^{32} \text{cm}^{-2} \text{s}^{-1}$]	–	0.11	0.5
Maximum stored energy [MJ]	<0.01	2.7	9 #
Single bunch intensity [10^{10} p]	3	11	11
Norm. transv. emittance [μm]	3.5	2.0	2.0
Bunch length at flat-top [ns]	1.	1.4	1.2
β^* in IP1/IP5 [m]	11	2.0/3.5	3.5
β^* in IP2/IP8 [m]	10	2.0/3.5	3.5
Crossing angle IP1/IP5 [μrad]	0	0/100	100
Crossing angle IP2 [μrad]	0	0	110
Crossing angle IP8 [μrad]	0	0	100
Parallel beam separation [mm]	± 2.0	± 2.0	± 2.0
Main dipole ramp rate [A/s]	2.0	2.0	10.0

Achieved on Sep. 29th at time of Workshop

the maximum current of the main dipoles, the commissioning of the 3.5 TeV ramp was achieved in March, with ramp rate of 2 A/s (II). The nominal rate of 10 A/s was commissioned with beam in August in preparation for a third run configuration for operation with multi-bunch trains (III). The first operation at 3.5 TeV was limited to about 2.7 MJ stored energy to collect operational experience on the machine protection systems over a period of 4 weeks in summer. Since the month of September, the LHC has entered a new operational phase compatible with up to 400 bunches (which requires crossing angles in all interaction points) with the goal of achieving a luminosity of $10^{32} \text{cm}^{-2} \text{s}^{-1}$ by the end of October. The proton run will be followed by 4 weeks of ion run with the configuration III. Presently, the LHC has seen fills with up to 9 MJ stored at top energy, for a peak luminosity up to $5 \times 10^{31} \text{cm}^{-2} \text{s}^{-1}$.

The squeeze to 2 m in all IPs was achieved on April 7th for the configuration II with zero crossing angle. The commissioning took profit from preliminary tests carried out at the end of the 2009 run [2], whose operational experience was feed back into procedures and software implementation. On the other hand, for the operation with 100 μm crossing angle in the multi MJ regime, it was decided to step back and run at 3.5 m in all IPs in order to ensure sufficient aperture margin at the superconducting triplets.

* Stefano.Reddaelli@cern.ch

A FIELD EMISSION AND SECONDARY EMISSION MODEL IN OPAL

C. Wang*, A. Adelman, Y. Ineichen, PSI, Villigen, Switzerland

Abstract

Dark current and multipacting phenomena, as observed in accelerator structures, are usually harmful to the equipment and the beam quality. These effects need to be suppressed to guarantee stable operation. Large scale simulations can be used to understand the cause and develop solutions for these phenomena. We extend OPAL [1], a parallel framework for charged particle optics in accelerator structures and beam lines, with the necessary physics models to simulate multipacting phenomena. This is achieved by adding a Fowler-Nordheim field emission model and a secondary emission model, as well as 3D boundary geometry handling capabilities to OPAL. With these capabilities we can evaluate dark current and multipacting in high-gradient linac structures and in RF cavities of high intensity Cyclotrons. In state of the art accelerator structures the electric fields are strong, therefore space charge effects in the Fowler-Nordheim model cannot be neglect. In a first step we add the Child-Langmuir model to phenomenologically model space a charge limited field emission. In the near future a multigrid preconditioned iterative space charge solver capable of handling complicated boundary geometries will be used to make our field emission model more self-consistent.

INTRODUCTION

Dark current and multipacting phenomena have been observed in various RF structures of accelerators, e.g. [2] [3]. These phenomena are usually harmful to the equipment and beam quality, as they will cause galvanic etching on the surface of the cavity and thus cause RF breakdown. In this paper we will discuss our efforts to extend OPAL in order to get a feasible tool for performing large scale dark current and multipacting simulations. This would allow more thorough analysis and a deeper understanding of these phenomena. Accurate simulations could lead to methods how these situations can be prevented or diminished. To achieve these goals, first we introduce a particle-boundary collision test model into OPAL to facilitate the particle searching during tracking process. In a subsequent step we add surface physics models including an analytic Fowler-Nordheim field emission model and a phenomenological secondary emission model to OPAL.

The Child-Langmuir space charge model for emitted electrons is discussed here. A multigrid preconditioned iterative space charge solver able to treat complicated boundaries with higher accuracy is still work in progress and will be incorporated in the near future.

*C.Wang is on leave from China Institute of Atomic Energy.

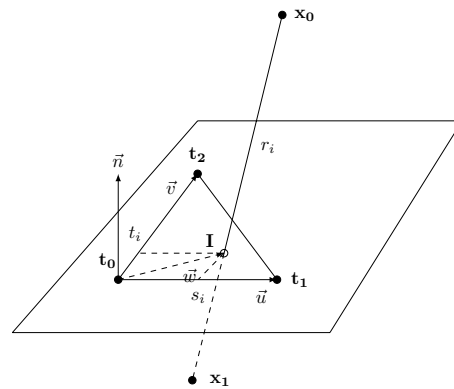


Figure 1: Line segment-triangle intersection.

A code benchmark of the implemented secondary emission model and visualization results are given in the last section of the paper.

PARTICLE-BOUNDARY COLLISION TEST MODEL IN OPAL

Testing particle-boundary collisions is crucial to both dark current and multipacting simulations. We need an efficient way to distinguish between dark current particles potentially reaching the beam diagnostic equipment (e.g. a screen) and those hitting the surface of beam line elements causing multiplication.

The particle-boundary collision test in a 3D geometry is complicated and computational expensive. Our complex 3D geometries are hard to parameterized by simple functions. Instead we represent geometries as triangulated surface meshes. Subsequently we can make use of efficient 3D line segment-triangle intersection (LSTI) tests to find particle-boundary collisions. In the following we will describe how we implemented this collision tests while still retaining code efficiency.

The Line Segment-Triangle Intersection (LSTI) Test

An efficient LSTI test algorithm is described in [4]. Since we need to precompute all triangle normals for triangle orientation anyway we can make use of a faster algorithm relying on having triangle normals available [5]. In order to compute a LSTI we need the starting and end point of the line segment under consideration, triangle vertices and normal. A schematic view is sketched in Figure 1. Vectors are denoted with arrows (i.e. \vec{n}), points (here in \mathcal{R}^3) are bold (i.e. \mathbf{x}_0) and the remaining symbols de-

SIMULATIONS FOR THE SNS LINAC

A. Shishlo[#] on behalf of SNS Accelerator Group, ORNL, Oak Ridge, TN 37831, U.S.A.

Abstract

Review of the simulations tools used for the Spallation Neutron Source (SNS) linac tuning and beam dynamics studies is presented. The usage and comparison of the different approaches like single-particle, envelope, particle-in-cell and codes for particular tasks is discussed. The codes considered include Parmila, Impact, Track, and XAL online model. Future code development for the SNS linac is suggested.

INTRODUCTION

Usually there are varieties of computer simulation codes that are used during different stages of a machine history: design, commissioning, tuning, production etc. Different codes can be used to analyze different aspects of beam physics or to verify results from other codes. The SNS linac is not an exception. This paper discusses computer codes that were used for the SNS during its more than 10 years of transformation from design to operational machine.

SNS LINAC

The SNS linac consists of two structures which are a normal temperature and super-conducting (SCL) linac. The normal-conducting section (accelerating the beam up to 185 MeV) includes a Low-Energy Beam Transfer (LEBT) line downstream of the H⁻ ion source leading to a 2.5 MeV RFQ, a Medium-Energy Beam Transfer (MEBT) line, a 402.5-MHz drift tube linac (DTL), followed by a 805-MHz coupled cavity linac (CCL). The SRF structure accelerates the beam from a nominal energy of 185 MeV to 1000 MeV. The SCL section consists of two sections: a low beta ($\beta_g = 0.61$) and a high beta ($\beta_g = 0.81$).

The two parts (room temperature and super-conducting) of the linac are quite different from the beam dynamics point of view. The RF gap phases and longitudinal beam dynamics in the normal conducting sections were defined at the design stage. The purpose of the tuning process is to reproduce the design settings in the real structures. In contrast, the amplitudes and phases of the SCL cavities can be changed in a wide range, and the performance of SCL should not suffer from this [1]. As a result the tuning procedures should be different for these parts of the SNS linac.

In the design of the SNS linac measures were taken to avoid halo generation and, therefore, to minimize beam losses [2]. The measures include: the zero-current phase advances (transverse and longitudinal) per period never exceed 90° ; transverse and longitudinal phase advances do not cross to avoid the second order parametric resonance, except in DTL tank 1 and CCL module 4

where matching considerations prevail; transverse and longitudinal phase advances per meter are smooth functions along the linac to provide a current independent design.

The nominal peak current in the SNS linac is 38 mA, and space charge effects are expected to be significant for the beam dynamics [2].

COMPUTER CODES

The following computer simulation codes were and are being used at SNS

- XAL online model (OM) [3] is a part of the XAL application programming framework developed at SNS [4]. The online model has both envelope and single particle tracking capabilities. The tracking algorithms were borrowed from TRACE 3-D (space charge) and PARMILA (RF gaps). The online model was thoroughly benchmarked against both these codes. The XAL OM is a base for dozens of XAL applications used for SNS linac tune up and offline analysis.

- TRACE 3-D is a beam-dynamics program that tracks the envelopes of a bunched beam through a user-defined transport system [5]. The space charge calculations are included as linear forces. It was used for fast beam dynamics calculations during the early stages of the SNS project.

- PARMILA (Phase and Radial Motion in Ion Linear Accelerators) is a computer code used for the design and simulation of proton and heavy ion linear accelerators [6]. The SNS linac was designed on the basis of PARMILA simulations. PARMILA's algorithm for calculating a RF gap transition was adopted by the XAL online model. Now at SNS, PARMILA is occasionally used as an online tool for matching the beam into the DTL and CCL (under MATLAB GUI script) and for offline analysis.

- IMPACT (Integrated Map and Particle Accelerator Tracking) is a parallel computer PIC accelerator code which includes realistic 3D space charge calculations [7]. At SNS it is used for offline analysis.

- TRACK is a ray-tracing general beam dynamics code. This code is capable of tracking a multi-component beam with realistic space charge, full 3-D time-dependent field maps for RF cavities and magnets, and it includes a module to simulate the beam interaction with material media. At SNS it was mostly used for benchmarking with other codes.

SINGLE PARTICLE DYNAMICS

A simulation of single particle motion (as the center of the bunch) is a relatively simple task. All of the codes mentioned above can do this except IMPACT and PARMILA which do not have dipole corrector elements, and therefore cannot be used for orbit analysis and

[#]shishlo@ornl.gov

A SCINTILLATION-SOLID STATE DETECTOR FOR NON-DESTROYING SYNCHROTRON DIAGNOSTICS FOR HIGH ENERGY PROTON BEAMS

A. Maltsev, JINR, Dubna, Russia
M. Maltseva, TENZOR, Dubna, Russia

Abstract

The opportunity of application of a method not destroying infra-red (IR) synchrotron diagnostics for measuring intensity and a structure of a proton beam in synchrotron using scintillation-solid state detector (SSSD) is considered.

INTRODUCTION

Synchrotron radiation (SR) is generated by relativistic protons at their passage through area of sharp change of intensity of a magnetic field at edges dipole magnets of the accelerator. In proton ring accelerators of SR it was experimentally observed and used for diagnostics of a beam with energy above 250 ГэВ [1]. In experiments for registration of radiation were used photoelectronic multiplier and semi-conductor gauges.

However for the decision of similar tasks application of photoelectronic multiplier is limited for the following reasons: big size of photoelectronic multiplier, a high working voltage, low noise immunity from electromagnetic fields, and use semi-conductor gauges not always probably because of their signal-noise owing to absence of the appreciable internal amplification similar to amplification SSSD ($10^5 \dots 10^6$). SSSD has not above listed lacks. This technology of SSSD creation develops actively last years in Russia [2] and abroad.

SOLID STATE SCINTILLATOR DETECTORS

A typical solid-state photomultiplier receiver contains [3] a matrix (an ordered array) of pn -junctions (pixels) with dimensions of the order of $(30 \times 30) \cdot 10^{-3}$ mm, mounted on a common substrate. All the pixels are joined by aluminum buses, and the same bias voltage is applied to them. This bias voltage exceeds the breakdown voltage (20–60 V), which means that the device operates in the Geiger mode. The outputs of the all the pixels are connected to the common output of the device through load resistors. Each pn -junction operates in the Geiger mode with a multiplication factor of 10^6 , but the whole matrix acts as an analog detector, since the output signal is equal to the sum of the signals of the pn -junctions, generated by the photons absorbed by them. A light quantum incident on the active part of the pixel generates a primary electron, which produces a discharge in the pixel, which is extinguished when the voltage on the pixel falls below the breakdown voltage. Quenching, i.e., cessation of the discharge, occurs when the voltage on the pn -junction falls below the breakdown voltage due to the presence in each pixel of a current-limiting load resistor. The current signals from the operating pixels are added in

the common load. The particular features of operation in the Geiger mode is the linear dependence of the pixel gain on the bias voltage and the low requirements imposed on the temperature and supply-voltage stability compared, for example, with avalanche light-emitting diodes.

Because of its advantages, solid-state photomultipliers can successfully replace vacuum photomultipliers in the measuring system [4]. For this purpose, using solid-state photomultipliers, we developed a combined ionizing radiation detector for detecting x-rays, gamma rays and neutrons, together with a solid-state scintillation detection (SSSD) unit [5, 6]. It consists of a scintillator, a solid-state photomultiplier, a preamplifier, a casing and an electrical connector. In Fig. 1, we show a diagram of one version of this system – the BDST-10P, which has the following basic characteristics: volume of the CsI (Tl) scintillator 16 mm³, counting efficiency ~ 10 pulses/ μ R (137Cs), measured energy range 10–3000 keV, temperature range from -60°C to $+60^\circ\text{C}$, energy resolution with respect to the 662 keV not more than 10%, permissible load not less than 105 pulses/sec, dosage power measurement range not less than $5 \cdot 10^{-8}$ –0.3 Gy/h, power supply 5 V, 5 mA and 24 V, 100 μ A, diameter 13 mm, and length 80 mm.

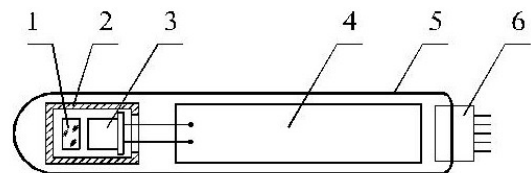


Figure 1: Sketch of the BDST-10P.

1) scintillator; 2) body; 3) solid-state photomultiplier; 4) electron preamplifier; 5) body of the detection unit; 6) plug.

Table 1 lists the merits and advantages of the solid-state photomultiplier, where we compare the characteristics of the solid-state scintillation detector (SSSD) and other combined CsI(Tl)-scintillator-photoreceiver detectors, such as the vacuum photomultiplier and pin and avalanche light-emitting diodes. It follows from the table that the SSSD is superior in a number of parameters to traditional detectors, employed in nuclear and accelerator techniques. The built-in preamplifier enables the SSSD to be employed directly with a standard spectrometer. The experimental equipment contains the object being investigated (the source of ionizing radiation), a combined detector and preamplifier, an amplifier-shaper, a spectrum analyzer and a computer.

TRANSVERSE PHASE-SPACE BEAM TOMOGRAPHY AT PSI AND SNS PROTON ACCELERATORS*

D. Reggiani[#], M. Seidel, PSI, 5232 Villigen, Switzerland
C.K. Allen, ORNL, Oak Ridge, TN 37831, U.S.A.

Abstract

Operation and upgrade of very intense proton beam accelerators like the PSI facility and the neutron spallation source (SNS) at ORNL is typically constrained by potentially large machine activation. Besides the standard beam diagnostics, beam tomography techniques provide a reconstruction of the beam transverse phase space distribution, giving insights to potential loss sources like irregular tails or halos. Unlike more conventional measurement approaches (pepper pot, slits) beam tomography is a non destructive method that can be performed at high energies and, virtually, at any beam location. Results from the application of the Maximum Entropy Tomography (MENT) algorithm [1] to different beam sections at PSI and SNS are shown. In these reconstructions the effect of non-linear forces is made visible in a way not otherwise available through wire scanners alone. These measurements represent a first step towards the design of a beam tomography implementation that can be smoothly employed as a reliable diagnostic tool.

The principle of beam tomography is depicted in Fig. 1. The plot on the left side represents the unknown beam transverse phase-space distribution at the reference position $z = z_0$. Beam profile monitors acquire projections of the phase-space onto the x coordinate at different locations (middle plots). These projections are related to the beam distribution at $z = z_0$ through linear transport matrices accounting for drift space and/or quadrupole magnets. In beam tomography the profile data are employed by a mathematical algorithm in order to reconstruct the two-dimensional beam density distribution (right plot).

Contrary to the case of medical imaging, in beam tomography, due to the very limited number of available projections, the solution of the problem can only be made unique by requiring additional conditions. For the reconstructions presented here the well established MENT approach was employed. Of all possible distribution functions, this algorithm chooses the most probable one, namely the distribution having the maximum entropy. A detailed description of MENT is given in [1] while its first application to beam tomography is described in [2].

INTRODUCTION

The goal of phase-space beam tomography is to reconstruct the phase-space beam density distribution starting from projection data acquired by means of profile monitors. Due to its capability of unveiling the structure of beam tails and halo, the tomography technique can be a very powerful tool for all those accelerator facilities where it is mandatory to keep even tiny beam losses under control.

BEAM TOMOGRAPHY AT PSI

The PSI proton accelerator [3] is a facility generating a continuous wave 590 MeV kinetic energy and, presently, 1.3 MW average power beam and furnished with two graphite meson production targets as well as a neutron spallation target. An overview of the complex is given in Fig. 2.

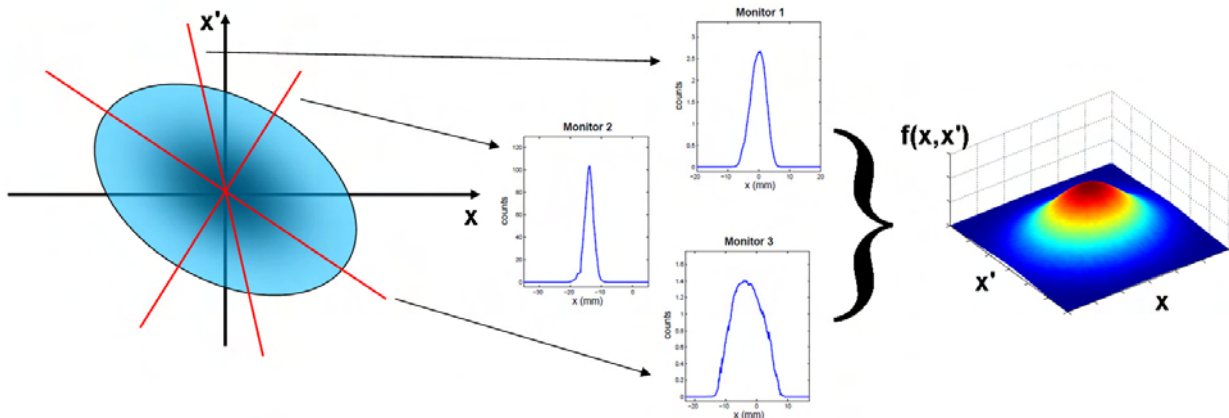


Figure 1: Schematic visualization of the principle of phase-space beam tomography. The coordinates (x, x') refer to the horizontal plane while (y, y') are used for the vertical one.

*SNS is managed by UT-Battelle, LLC, under contract DE-AC05-00OR22725 for the U.S. Department of Energy

[#]Corresponding author (davide.reggiani@psi.ch)

THE STUDY ON BEAM LOSS CONTROL BASED ON A HIGH INTENSITY RFQ*

T.G. Xu[#], C. Chen, S.N. Fu, L.X. Han, T. Hang, W. Kang, F. Li, P. Li, H.C. Liu, H.F. Ouyang, J. Peng, Y.F. Ruan, J.L. Sun, J.M. Tian, A.X. Wang, B. Wang, S. Xiao, M.H. Xu, Y.S. Zhu, IHEP, Beijing, China

Abstract

A high intensity RFQ has been built with output energy of 3.5 MeV and average current of 3 mA. Based on this RFQ, we plan on performing a number of experimental tests on beam loss control. A series of beam diagnostic devices such as BPM, BLM, WS and so on have thus been developed. Our work can also be easily applied to the CSNS project.

The beam diagnostics will be discussed in the following sections.

RFQ STATUS

As mentioned above, the end plate and coupling plate can't work on CW mode. The reason is that the stabilized rod is not cooling by water. Just the plate is cooling. When the duty factor of RFQ is increased to 15%, the signal of the RFQ field pickup is little changed. So the RFQ health is cared. The new end plate and coupling plate is manufactured. The plate is made of stainless steel coated by copper and the dipole mode stabilized rod is made of Cr-Cu alloy. And both the plate and rod have the cooling channel.

INTRODUCTION

A four-vane RFQ has been built in IHEP. Its output energy is 3.5MeV, and pulse peak current is 46mA. The RFQ cavity that is designed can work in CW mode. Limited by the infrastructure, now the RFQ's maximum duty factor is limited to 20%. The power coupler and end plates of RFQ can't work in CW mode because of its structure. Now the end plate and coupling plate is replaced by water-cooling type.

When the RFQ cavity is opened, what we see exceeded what we imagine (see Fig. 2). There are many little metal flakes around the dipole mode stabilized rod on the inner surface of RFQ. And the copper electroplated coating on the rod is disappeared. So the rod colour is changed from copper colour to stainless steel colour. We think the RF heat evaporation is the main reason.

Based on this RFQ, a plan is carried on beam halo and beam loss controlling research [1]. A new beam line will be built. There are 28 Quadrupole magnets, 14 Wire Scanners (WS) having scraper, 6 Beam Position Monitors (BPM), 6 Steering magnets, 2 Fast Current Transformers (FCT) in the beam line (see Fig. 1).

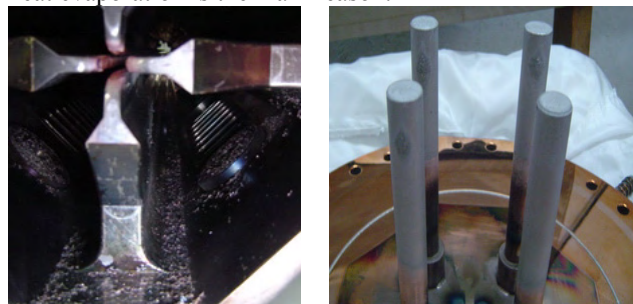


Figure 2: The picture of inner RFQ and end plate.

The total length of the new beam line is about 5.5m. According to the result of beam dynamic, the distance between two Q magnets is 190mm. Thought about the length of magnet itself, it is just left about 63mm for other device. The diameter of the vacuum tube is 36mm.

The first 4 Q magnets are used as matched magnet. The other 24 Q magnets can form FD or FFDD lattice. If the matched magnet working current is adjusted, the beam emittance will be changed.

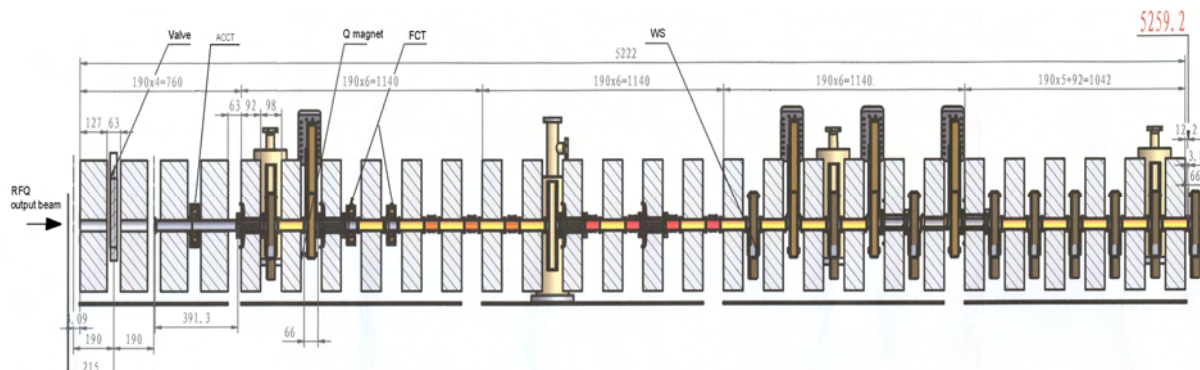


Figure 1: The layout of new beam line after RFQ.

*Work supported by 973 Project (2007CB209904)...

[#]xutg@ihep.ac.cn

OBSERVATION OF SPACE CHARGE EFFECTS ON TUNE AT SIS-18 WITH NEW DIGITAL BASE BAND TUNE MEASUREMENT SYSTEM*

R. Singh, GSI, Darmstadt, Germany and TEMF, Technische Universität Darmstadt, Germany
 P. Forck, P. Kowina, U. Springer, P. Moritz, GSI, Darmstadt, Germany
 T. Weiland, TEMF, Technische Universität Darmstadt, Germany

Abstract

To achieve a high current operation close to the space charge limit, a precise tune measurement during a full accelerating cycle is required. A tune measurement system was recently commissioned at GSI synchrotron SIS-18, which allows evaluation of tune using digital position data. Using this system, the space charge effects were observed by correlating the current levels to tune shifts in the GSI SIS-18. The experiment was conducted at injection energy of 11.4 MeV/nucleon using a ${}^{238}_{92}\text{U}^{73+}$ ion beam with stored number of particles from $2.5 \cdot 10^7$ to $2.5 \cdot 10^9$. A significant broadening of the tune spectrum in dependence of the stored number of particles was detected. This proves the reliability of this measurement method for bunched beams and opens the possibility of detailed beam physics investigations.

INTRODUCTION

High current operations at injection energies in hadron accelerators lead to large tune shifts which can result in emittance blow up or loss of particles. Emittance blow up is not desirable for storage rings or accelerators, thus it is very important to station frozen tune at appropriate point in resonance diagram.

A new system has been commissioned at GSI for position and tune measurements. It consists of three distinct parts; A band-limited exciter which provides power to excite coherent betatron oscillations in the bunched beam. Fast ADCs digitize the BPM signals at 125 MSa/s and the post processing electronics integrate the data bunchwise to acquire one position value per bunch. Subsequently the baseband tune is determined by Fourier transformation of the position data. One tune value can be calculated typically from 256 turns to 4096 turns based on the investigation needs.

The first objective of this work is to observe the space charge effects on the tune at SIS-18 injection energies. By space charge effects we mean both the effects of self fields and image charges often termed as incoherent and coherent tune shift respectively. Incoherent tune shift is caused by the interaction of individual charged particles in the beam. Since incoherent tune shift causes a spread in the tune spectrum, the term “tune spread” has been interchangeably used for refer this effect throughout this report. Coherent tune

shift stems from the boundary conditions, e.g. the beam pipe and all other devices in the beam pipe surrounding the charged ion beam [1]. The second objective is to see the influence of noise excitation on various beam parameters like tune spectrum, emittance and life time.

METHODS

This section highlights the working of the tune measurement system as a whole, and then explains the working principle of tunable noise generator in further detail.

TOPOS: Tune Orbit Position Measurement System

TOPOS is the tune, orbit and position measurement system established in SIS-18 at GSI [2]. Figure 1 gives an overview of the fragment of TOPOS used for tune measurement.

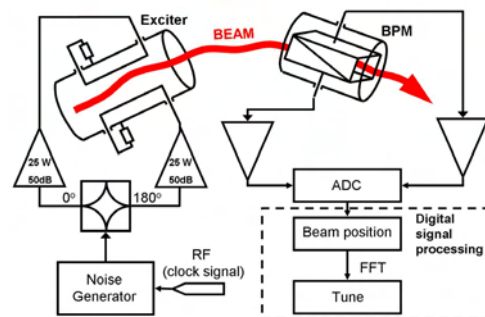


Figure 1: TOPOS: Tune measurement system.

Particles revolve in an accelerator with unrelated phases due to finite injection time and momentum spread, and thus the barycentre of a bunch of particles does not provide any information on the transverse movement of the individual particles. Thus beam excitation is needed to make the motion of particles coherent, and capture the transverse movements for tune measurement. A band limited noise exciter is employed to give this excitation. The advantages of this exciter are: lower continuous power is transferred to the beam causing minimal disturbance to the beam parameters; It can be used throughout the ramp for continuous monitoring of the tune [3, 4]. A tunable noise generator synthesizes a frequency centered at the baseband tune frequency and twice the span of maximal expected tune spread (Eq. 1). It is modulated by the revolution frequency f_0 and fed to

*This work is supported by DITANET (novel Diagnostic Techniques for future particle Accelerators: A Marie Curie Initial Training NETWORK), Project Number ITN-2008-215080

CARBON FIBER DAMAGE IN PARTICLE BEAM

M. Sapinski*, B. Dehning, A. Guerrero, M. Meyer, T. Kroyer
CERN, Geneva, Switzerland

Abstract

Carbon fibers are commonly used as moving targets in beam wire scanners. The heating of the fiber due to energy loss of the particles travelling through is simulated with Geant4. The heating induced by the beam electromagnetic field is estimated with ANSYS. The heat transfer and sublimation processes are modelled. Due to the model non-linearity, a numerical approach based on discretization of the wire movement is used to solve it for particular beams. Radiation damage to the fiber is estimated with SRIM. The model is tested with available SPS and LEP data and a dedicated damage test on the SPS beam is performed followed by a post-mortem analysis of the wire remnants. Predictions for the LHC beams are made.

INTRODUCTION

A thermodynamic model of a carbon fiber scanning a particle beam has been developed [1]. To validate this model and determine the breakage mechanism of the fiber, a damage test has been performed on the SPS beam at CERN in November 2008. The main purpose of the test was to verify the predictions of the limits for the wire damage in LHC proton and ion beams and to conclude about the specifications of the future wire scanner. In addition, recommendations about a type of carbon fiber to be used are given.

In frame of this study a radiation damage to a fiber is also investigated, as a possible long-term damage mechanism.

DAMAGE MECHANISMS

The carbon fibers are known to break after a few thousand scans. The possible mechanisms responsible for this breakage are radiation damage, low-cycle thermal and mechanical fatigue or a slow sublimation of the wire material. The LHC wire scanners are equipped with an acquisition system which allows the estimation of the total dose absorbed by the wire as well as the thermal cycle history.

The wire can also break during a single scan of high intensity beam. In this case the possible breakage mechanisms are thermal stress or a sublimation of the wire material. The estimation of the maximum beam intensities which can still be scanned without damaging the wire are particularly important for the intense LHC beams.

* mariusz.sapinski@cern.ch

RADIATION DAMAGE

The estimation of the radiation damage has been made using SRIM code [2] using a PS beam as an example because of their high intensity and heavy use. It has been found that a single scan of a proton beam will introduce about $3.5 \cdot 10^{-7}$ displacements per atom (dpa) and for the ion beam the results are similar [3]. The measurable effects of radiation damage on mechanical properties of the fiber start to present themselves at about 1 dpa level. One can therefore conclude that the wire properties are not affected by radiation during a few thousand scans. The mechanism of the wire breakage is therefore a slow sublimation of the wire material or thermal and mechanical fatigue.

WIRE BREAKAGE EXPERIMENT

An experiment at the CERN SPS accelerator has been performed to validate the thermodynamic model of carbon fiber in the accelerator beam and to determine LHC beam intensity limits for the wire scanner.

Experimental Conditions

A rotational wire scanner equipped with electronics which allows the measurement of wire resistivity and thermionic emission during the scan has been used in the experiment. The scanner contains two wires which scan the beam in horizontal and vertical directions. The maximum scan speed is 6 m/s and each time two scans called IN and OUT are performed. The speed of each scan and the interval between them is set independently. This interval has been set to at least 1 second to allow the wire to cool down. In this test the scan IN has always been performed with maximum speed and the speed of scan OUT has gradually slowed from scan to scan in the following sequence: 6, 3, 1.5, 1, 0.8, 0.7, 0.6, 0.5 m/s. Two other wire scanners have been used during the test to measure independently the beam sizes.

A special beam cycle on the SPS has been prepared for this test. Beam intensity has been maximized and reached about $2.4 \cdot 10^{13}$ circulating protons. In order to diminish the effect from RF-coupling [4] the beam has been debunched. It has been estimated, using Ansoft HFSS code, that RF-coupling of the debunched beam has negligible effect on the results of the experiment. A 12-second long flat-top plateau has been kept, providing enough time to perform measurements in stable beam conditions. The beam momentum has been 400 GeV/c and the beam transverse profiles have been close to Gaussian in both directions.

BUNCH SHAPE MEASUREMENTS AT INJECTOR 2 AND RING CYCLOTRON

R. Dölling, Paul Scherrer Institut, Villigen, Switzerland

Abstract

The longitudinal-horizontal 2-dimensional (2D) density distribution of a bunched 2.2 mA beam of ~ 72 MeV protons has been measured at the last turns of the Injector 2 cyclotron, in the middle of the transfer line to and at the first turns of the Ring cyclotron. Protons scattered by a thin carbon-fibre target are stopped in a scintillator-photomultiplier detector. The longitudinal bunch shape is given by the distribution of arrival times measured with respect to the 50 MHz reference signal from the acceleration cavities. More probes are foreseen at 72 and 590 MeV which will use additional fibres to also determine the longitudinal-vertical and two longitudinal-diagonal 2D density distributions. These measurements together with more detailed beam transport calculations will support the matching of beam core and halo and the quest for a reduction of beam losses. The achievable dynamic range in the given environment of the cyclotrons and the connecting beam line is discussed.

INTRODUCTION

The Injector 2 cyclotron delivers a 72 MeV 2.2 mA CW proton beam via a ~ 50 m long injection line to the Ring cyclotron, where it is accelerated to 590 MeV [1]. Beam loss is one of the main factors limiting the attainable beam current since hands-on maintenance is required for nearly all machine components. At this high current beam, already a thin beam halo contributes significantly to the beam losses. The transport of the whole distribution is strongly influenced by the beam space charge and the creation of new halo by scattering at collimators. Hence, already small changes at any location along the beam path can alter the total losses strongly. This makes setup and tuning difficult and leads to a tuning method mainly determined by examining the losses of the beam along its path and "turning all available knobs" to minimize losses at a given beam current level [2, 3]. Although this empirical concept is useful for finding the optimum operation for a *given* machine configuration, well-directed *changes* of the machine configuration, leading to significant improvement, cannot be initialized by it. Also it is very difficult to find hidden causes in the case of a persistently bad beam quality. To overcome this, detailed numerical simulations [4] of the beam transport and matching including the beam halo are required *together* with *detailed* measurements of the 6D phase space distribution. This should result in an improved beam cleaning at low energies by additional slits, a matched beam core *and* halo, lower losses at higher energies, the ability to setup the whole machine in one pass and the ability to find sources of deteriorated beam by examining the beam in detail.

The time-structure, i. e. the longitudinal bunch shape, is given by the distribution of arrival times of beam particles measured with respect to the 50 MHz reference signal from the acceleration cavities. In our case, protons are scattered by a thin carbon-fibre target towards a scintillator-photomultiplier detector [5, 6]. (This type of measurement is known since long and alternative methods are available [7-9].)

From the wire position also a transversal coordinate is determined. By moving the wire horizontally, a 2D profile of the bunch density "as seen from above" can be measured. This has been done at the last two turns of Injector 2, in the middle of the connecting line to the Ring cyclotron (approximately at the superbuncher position) and at the first two turns of the Ring cyclotron (Fig. 1).

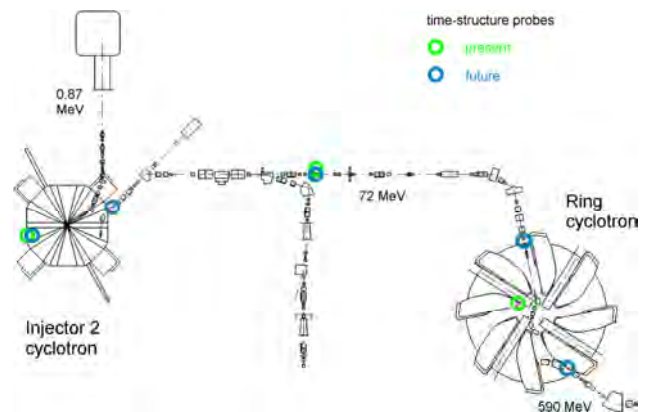


Figure 1: Locations of time-structure probes.

Repeating this with several wire orientations, does not yield the full 3D spatial charge density distribution, but rather several 2D projections. Hence, e.g. all 9 parameters describing size and orientation of an ellipsoid representing the bunch in real space can be determined and used in beam transport simulations on the matching of the beam core. More detailed information is available for detailed simulations including the beam halo. This type of measurement is under preparation for the last two turns of Injector 2, three locations in the connecting line and one behind the Ring cyclotron (Fig. 1).

The wire target precisely defines the location of measurement and hence the time-structure even of short bunches can be determined with good accuracy. Although the pulse width from scintillator and photomultiplier tube (PMT) is quite large (~ 3 ns fwhm), the time-resolution can be of the order of 30 ps due to the statistics from the many created photo-electrons [5]. However, the level of radiation background from beam losses strongly determines the achievable temporal and spatial resolution and the dynamic range.

DEVELOPMENT, CHARACTERIZATION AND PERFORMANCE OF THE LHC BEAM LOSS MONITORING SYSTEM

A. Nordt, B. Dehning, E. Effinger, J. Emery, E.B. Holzer, E. Lebbos, D. Kramer, M.G. Sapinski, M. Stockner, C. Zamantzas, CERN, Geneva, Switzerland

Abstract

The LHC Beam Loss Monitoring (BLM) system should prevent the superconducting magnets from quenching and protect the machines elements from damage. The main monitor types are an Ionization Chamber (IC) and a Secondary Emission Monitor (SEM) (about 4000 monitors in total). Lost beam particles initiate hadronic showers in the machines components which are then measured by the monitors installed on the outside of the equipment. For the calibration of the BLM system the signal response of the IC and the SEM was simulated using GEANT4, GEANT3 and FLUKA for all relevant particle types and energies (keV to TeV range). For validation, the simulations were compared to measurements using protons, neutrons, photons and mixed field radiation fields at various energies and intensities.

INTRODUCTION

An unprecedented amount of energy will be stored in the circulating LHC beams (up to 360MJ per beam) and in the magnet system (10GJ). The loss of even a small fraction of this beam may induce a quench of the superconducting magnets. Therefore a fast signal detection and robustness against aging were the main design criteria for the BLM monitors. Depending on the loss location the monitors are exposed to different radiation fields and in order to ensure stable operation within a high dynamic range, an ionization chamber and a secondary emission monitor were chosen. The system detects and quantifies the amount of lost particles and triggers a beam abort when the losses exceed predetermined threshold values. The start up calibration of the BLM system was required to be initially within a factor of five in accuracy and finally within a factor of two in accuracy. For the calibration and threshold determination a number of simulations were combined: beam particles were tracked to find the most probable loss locations. At these locations hadronic showers in the machines components were simulated to get the particle spectra at the detectors locations. A further simulation was done to determine the detector response. The quench levels of the superconducting magnets, according to loss duration and beam energy were simulated separately. Whenever possible, crosschecks with measurements have been performed before the start up of the LHC.

IONIZATION CHAMBER (IC) RESPONSE

The main detector type is an ionization chamber (~3700 ICs). It consists of 61 aluminium electrodes that are

arranged in parallel and equally spaced with 0.5 cm. The IC is ~50 cm long (diameter 9 cm) with a sensitive volume of 1.5 litres. The chambers are filled with N₂ at 100 mbar overpressure and operated at 1.5 kV. The collection time of the electrons and ions is of the order of 300 ns and 120 µsec (simulated: 40 -80 µsec, measured 80 -120 µsec, depending on signal cable length).

GEANT4 Simulations

GEANT4 simulations of the ionization chamber have been performed to determine the signal response for different particle types at various kinetic energies in the range from 10 keV to 10 TeV (see Fig. 1). Also the effects of longitudinal and transverse impacting directions with respect to the detector axis were simulated. The longer path for a longitudinal direction increases the response approximately by a factor of two. Less wall material has to be passed in the transverse direction leading to a lower energy cut-off. The deposited energy in the sensitive volume was converted with the so called W-value to the number of produced charges. The W-value for N₂ is 35 eV per electron-ion pair. Different parameters were varied in order to identify the contributions to the systematic error of the simulation. The detector response is different for different impacting angles: at high energies up to a factor of 100 for protons. Changing the production range cut from 1 mm (standard value in GEANT4) to 10 µm increased the response by 12%. The sensitive volume was determined by simulation of the electric field configuration. It is 4% bigger than the volume covered by the electrodes (2 mm larger diameter). NIST data were used to cross check the simulation: The energy cut-off for protons, electrons and gamma rays was estimated. Protons of about 65 MeV start producing a signal, electrons at 9 MeV and gammas at 150 keV. The energy deposition for a positive muon was calculated with the Bethe-Bloch formula and compared to the simulation (agreement at 1 GeV: 95% and at 35 MeV: 75%) [1].

Verification Measurements

Mixed Radiation Field Measurements:

A mixed radiation field experiment at the CERF target area (CERN-EU High Energy Reference Field Facility) was compared to the simulations results. A copper target (length 50 cm, diameter 7 cm) was placed in a secondary beam of 120 GeV/c hadrons. The main beam particles were pions (60.7%), protons (34.8%) and kaons (4.5%) with intensities up to $9.5 \cdot 10^7$ hadrons per 4.8 seconds. Five ionization chambers were positioned around the copper target so that they were exposed to different radiation fields, (varying in particle composition and energy). The

VISUAL INSPECTION OF A COPPER COLLIMATOR IRRADIATED BY 590 MeV PROTONS AT PSI

Å Strinning*, P. Baumann, M. Gandel, D. Kiselev, Y.J. Lee, S. Adam,
Paul Scherrer Institut, 5232 Villigen PSI, Switzerland

Abstract

In March 2010 one of the most exposed collimators of the 590 MeV proton beam line at the Paul Scherrer Institut, was visually inspected after 20 years of operation without failure and a total beam charge of 120 Ah. Two samples of pieces peeling off the surface were taken and analyzed with a HPGe detector. The (relative) activity was compared to calculations (MCNPX and Cinder'90). Due to the high dose rate of the collimator, radiological precautions had to be taken when removing it from the beam line.

INTRODUCTION

The High Intensity Proton Accelerator (HIPA) facility at the Paul Scherrer Institut (PSI) uses a 4 cm thick graphite wheel, called Target E, to produce mesons. When the 590 MeV protons pass Target E, the beam diverges mainly due to multiple scattering by about 6 mrad. To protect the magnets and to reduce the beam losses along the beam line, collimator KHE2 is used to shape the defocused proton beam after Target E. It is located 4.7 m behind Target E. With a current of 2 mA on Target E, ~150 kW is deposited as heat in the collimator. KHE2 is made out of copper and actively cooled by water tubes placed on the outer surface of the collimator.

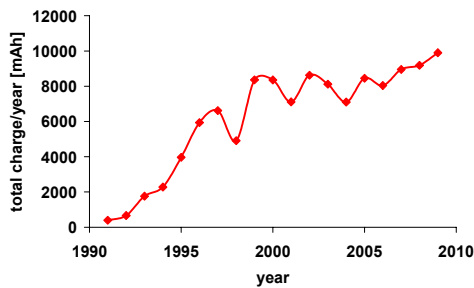


Figure 1: Charge per year in mAh on KHE2 during the last 20 years. The integrated charge today is ~120Ah.

The total beam charge today is 120 Ah after 20 years of operation. At the time the collimator was designed, the total charge per year was much smaller than today (Figure 1) and it was not expected that KHE2 would be exposed to such high thermal stress and accumulated charge. It is known that this can cause defects in the lattice, which can lead to a change of material properties, like its strength or the thermal conductivity. For thermal neutrons, considerable swelling of the material (change of geometry) would already have occurred. For high energetic protons much less is known about their effect on radiation damage. In general, the amount of damage is not

really quantifiable and many factors play a role like e.g. the operating temperature.

Therefore, to keep the reliability of the facility, also in view of the upgrade plans to 3 mA, which require a new design of the collimator, it was decided to perform a visual inspection of the collimator and to remove KHE2 from the beam line for the first time after 20 years of operation.

Design and Temperature Distribution

The design of the collimator is not only driven by the needs of the beam shape but also by cooling demands. The 30 cm long collimator is segmented into six parts, each having an inner conical “teeth”-design for better thermal power distribution (Figure 2). The copper collimator is cooled by water flowing with 8 m/s in tubes of 9 mm inner diameter. The steel tubes are brazed to the outer surface of the copper body.

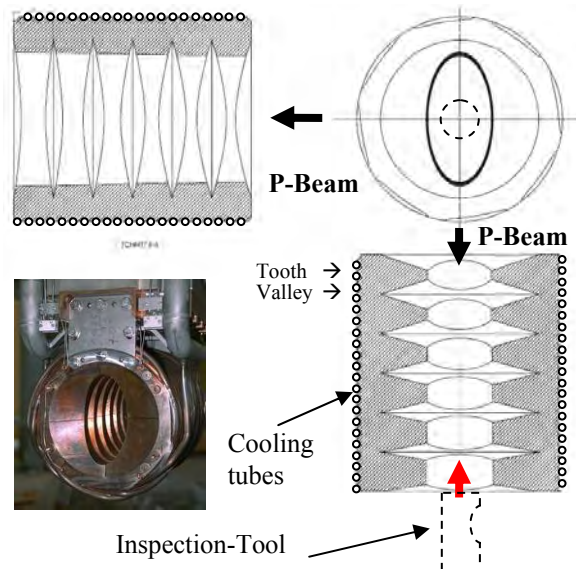


Figure 2: Photo and sketch of collimator KHE2. The insertion of the inspection tool is shown at the bottom (dashed line).

The temperature distribution inside the collimator (Figure 3) was calculated with the CFD-ACE+ [4] code for 2 mA on Target E. Due to its elliptical aperture, the collimator cuts the beam symmetrically at one and two standard deviations, respectively. The resulting temperature is much higher on the sides than at the top or bottom. The maximum temperature inside the collimator for a 2 mA beam current is about 380 °C (Figure 3).

*ake.strinning@psi.ch

ACTIVATION OF ALUMINIUM BY URANIUM*

V. Chetvertkova[#], U. Ratzinger, I. Strasik, IAP, Goethe-University, Frankfurt am Main, Germany
 E. Mustafin, GSI, Darmstadt, Germany
 C L. Latysheva, N. Sobolevskiy, INR RAS, Moscow, Russia

Abstract

The research into the activation of materials used for accelerator components is performed at GSI as a part of studies selecting appropriate materials for FAIR. The project "Verification of Monte Carlo transport codes: FLUKA, MARS and SHIELD" was started in the frame of these studies. Series of irradiations were completed already. This paper presents the results of irradiation of aluminium targets with uranium. Experimentally achieved depth profiles of nuclides' production rates and the stopping range of primary ions are compared with simulations. Correspondences and discrepancies of the experiment with the simulations are discussed.

INTRODUCTION

During the operation of accelerating facilities, their components are activated because of beam losses, which could lead to unnecessary personnel exposure. Thus the estimation of the activity levels is needed to design proper shielding and decide whether the access to the experimental area is possible.

The FLUKA simulation package [1, 2] is widely used for the estimation of radiation hazards. The physical models implied in the code are constantly being further developed. Therefore verification is needed to make sure that the simulations give reasonable results.

Activation studies of accelerator materials were started at GSI Helmholtzzentrum für Schwerionenforschung in Darmstadt within the preparation for the high-current heavy-ion Facility for Antiproton and Ion Research (FAIR). Several irradiation experiments on selected materials and under different irradiation conditions were completed [3-5].

Here we present the results of the uranium irradiation of aluminium targets. The aluminium was chosen because it represents a material with relatively low atomic number ($Z = 13$) that is expected to get less activated than high- Z materials studied in previous experiments. The aluminium components should be preferred in accelerator areas with high beam losses (e.g. extraction region, beam-diagnostics components, etc.).

The goal of the study was to measure the stopping range of uranium at different energies, to study the dependences of nuclides' production rates on depth and to compare the experimental results with simulations.

EXPERIMENT AND METHODS

Two types of targets were irradiated. The truncated cylinder covered with organic material (Fig. 1) was used to measure the stopping range. The experimental technique is based on the idea that ions leave the trace on the organic material, the position of maximum blackening corresponds to the maximum of energy deposition.

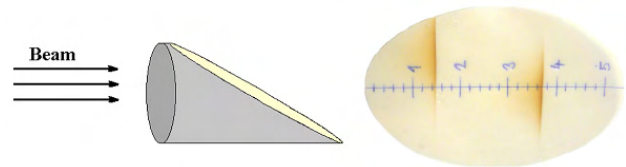


Figure 1: Truncated cylinder covered with organic material.

The cylinders assembled from discs (Fig. 2) were irradiated for depth profiling of the nuclides' production rates. The stack contained activation foils and spacers. The activation foils were used to get individual data-points for depth profiling, by measuring the γ -spectra of residual activity. The spacers were used to define the depth-points of the profiles by keeping the distance between the activation foils.

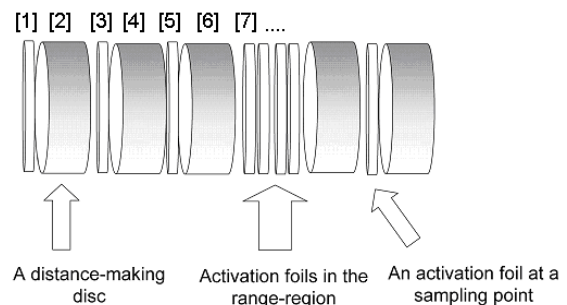


Figure 2: Scheme of the target for depth profiling of residual activity.

The irradiations were done at two energies of the primary ions: 500 MeV/u and 950 MeV/u. The truncated cylinder was irradiated two times by ions of both energies until the total number of projectiles on the target reached $\sim 2.5 \cdot 10^{11}$ ions for each energy. Two different cylindrical targets were irradiated for depth profiling of residual activity. The parameters of these irradiations are presented in Table 1.

*Work is supported by the Helmholtz International Center for FAIR within the framework of the LOEWE program launched by the State of Hesse.

[#]v.chetvertkova@gsi.de

MOMENTUM COLLIMATION IN A HIGH-INTENSITY COMPACT RAPID CYCLING PROTON SYNCHROTRON

J.Y. Tang[#], J.F. Chen, Y. Zou, IHEP, Beijing 100049, China

Abstract:

Momentum collimation in a high intensity RCS is a very important issue. Based on the two-stage collimation principle, a combined momentum collimation method is proposed and studied here. The method makes use of the combination of secondary collimators in both the longitudinal and transverse planes. The primary collimator is placed at a high-dispersion location of an arc, and the transverse and longitudinal secondary collimators are in a dispersion-free long straight section and in an arc, respectively. The particles with a positive momentum deviation will be scattered by a Carbon scraper and then cleaned by the transverse collimators, whereas the particles with a negative momentum deviation will be scattered by a Tantalum scraper and mainly cleaned by the longitudinal secondary collimators. This is due that a Carbon foil produces relatively more scattering than a Tantalum foil if the energy loss is kept the same. The relevant requirements on the lattice design are also discussed, especially for compact rings. The multi-particle simulations using both TURTLE and ORBIT codes are presented to show the physical images of the collimation method, with the input of the CSNS RCS ring.

INTRODUCTION

For high intensity proton synchrotrons, collimation systems are needed, not only to intercept particles that are outside prescribed betatron and momentum acceptances, but also to trap these particles with high efficiency. In this paper, the emphasis is on the momentum collimation for a high-intensity compact rapid cycling proton synchrotron.

For large synchrotrons such as LHC at CERN and main injector in FERMILAB, there are sufficient spaces to allocate a full two-stage momentum collimation system in one of the arcs [1-3]. However, for compact synchrotrons, the straight sections in arcs are much limited and there is no sufficient space to host a full two-stage momentum collimation system. Thus, simplified momentum collimation method is employed for the latter case. The two reference methods are: the ISIS method by using two-stage massive collimators [4]; the J-PARC method by using a standard two-stage collimation but with the secondary collimators in the downstream dispersion-free straight section [5]. The former has the two collimators within the same long dispersive straight section, and the latter has the primary collimator in one of the arc sections and shares the secondary collimators with the transverse collimation system. The new momentum collimation

method proposed here will be a combined collimation method: it will be a full two-stage collimation method, but with secondary collimators in one arc straight sections and one dispersion-free straight section. We take the CSNS/RCS as the example to study the collimation mechanism, but the method is general and applicable to other similar machines.

The China Spallation Neutron Source (CSNS) of several hundreds KW is to be constructed in Dongguan, Guangdong Province, China [6-7]. It is a short-pulse accelerator facility mainly consisting of an H⁺ linac and a proton rapid cycling synchrotron (RCS). The facility will be constructed in three phases (CSNS-I for 100 kW, CSNS-II for 200 kW, and CSNS-III for 500 kW, see Table 1.

Table 1: Main Parameters of CSNS

	CSNS-I	CSNS-II	CSNS-III
Beam power (kW)	100	200	500
Repetition rate (Hz)	25	25	25
Average current (μ A)	62.5	125	312.5
Linac beam energy (MeV)	80	130	250
Proton energy (GeV)	1.6	1.6	1.6
RCS accumulated particles	1.6×10^{13}	3.2×10^{13}	7.8×10^{13}

MOMENTUM COLLIMATION SCHEME

Combined Method for Momentum Collimation

The CSNS/RCS lattice of four-fold and all-triplet cells [8] has been designed to provide good conditions to place momentum collimators, with a high normalized dispersion at the middle points of the arcs that is good place the primary momentum collimator and sufficient space in the same straight section to place a secondary collimator.

The combined scheme for momentum collimation in the RCS for all the CSNS phases is detailed here: 1) Make use of the all-triplet lattice. 2) Using a thin Tantalum foil at negative momentum deviation (or negative X) to produce significant scattering but with little energy loss, this can help minimizing the decrease in Courant-Snyder invariant (or I_x) due to the longitudinal-horizontal coupling effect. 3) Using a thin Carbon foil at positive

[#] tangjy@ihep.ac.cn

AN EXPERIMENT AT SPS-HiRadMat AS A TOOL TO STUDY BEAM-MATTER INTERACTION

J. Blanco Sancho, CERN-AB, 1211 Geneva, Switzerland and
Ecole Polytechnique Federale de Lausanne, 1015 Station 1, Lausanne, Switzerland
R. Schmidt, CERN-AB, 1211 Geneva, Switzerland
N. A. Tahir, GSI, Planckstr. 1, 64291 Darmstadt, Germany

Abstract

The Large Hadron Collider and the future linear colliders deal with very high energy stored in the beams (on the order of several hundred MJoules for LHC) or very high power (for linear colliders). Beam sizes are small, for the LHC down to $10\ \mu\text{m}$, for linear colliders below one μm . It is important to understand the damage potential of such high energy beams to accelerator equipment and surroundings. Simulations have shown that in case of an impact of the full LHC beam onto a solid copper target can penetrate up to 35 m [1] as compared to 140 cm that is the typical penetration length for 7 TeV protons. It becomes evident that when working with high energy densities, it is no longer possible to neglect the hydro-dynamic process leading to a depletion of material in the target. For the calculation, a hybrid approach combining FLUKA [2] and BIG-2 [3] is proposed to treat HED problems. This approach can improve current simulations. It is foreseen to experimentally irradiate different materials with different beam intensities in the High Radiation to Materials (SPS-HiRadMat) [4] facility at CERN. These experiments will validate the simulation results by reproducing the density depletion along the beam path. The information obtained with these tests will be very useful in the understanding of the consequences of beam-matter interaction. Results could be applied to the LHC Beam Dump system, collimation, etc.

INTRODUCTION

Since the first electrostatic accelerators, 60 years ago, to the actual machines, the energy has been increasing from keV to TeV and currents have gone from mA to A. Actual accelerators, like LHC, operate at energies of some TeV with beam current of some hundred mA. Such multi TeV accelerators with very high current beams are required by particle physics for probing the standard model.

Such energetic beams, 362 MJ per beam in case of the LHC, are a new source of risk to damage the machine in case of failure, which is a major concern. The understanding of the risk is essential in order to design the protection systems of the machine correctly, to set admissible risk levels, and to determine the inventory of the spare parts needed to possibly replace the damaged equipment. The classical approach to address the damage caused by a particle beam is to calculate the temperature increase and induced stress using the energy deposition map obtained by Monte-Carlo

particle transport code. When the beam is long enough (tens of μm) this is no longer valid. Hydrodynamic effects start to play a role. The time constants of the hydrodynamic process are much shorter than the beam duration and thus the target material cannot be considered static during the whole interaction process (dynamic properties). Instead we combine the traditional approach of Monte-Carlo simulations with hydrodynamic simulations.

SPS-HIRADMAT

The High Radiation to Materials (HiRadMat) facility is dedicated to beam shock impact experiments. The project has been approved and the facility is currently under construction at CERN-SPS complex [5]. The facility is also part of the European Coordination for Accelerator Research & Development project (EuCARD). It is designed to allow testing of accelerator components, in particular those of LHC, to the impact of high-intensity pulsed beams. It will provide a 440 GeV proton beam or a 497 GeV/A ion beam. Beam properties are shown in table 1. The 440 GeV proton beam will have a focal size down to 0.5 mm, thus providing a substantial dense beam (energy/size). The transversal profile of the beam is considered to be Gaussian with a tunable sigma ranging from 0.5 mm to 2 mm.

This facility will allow to study High Energy Density physics as the energy density will be high enough to create plasma in the core of some materials (copper, tungsten) and to produce strong enough shock waves creating a density depletion channel along the beam axis (tunneling effect) [6, 7].

ENERGY DEPOSITION IN MATTER

Energy deposition in matter by particles is given by the evolution of the hadronic cascade from several TeV down to thermal energies. Most of the particle production takes place at energies below 1 GeV. Particles lose energy by multiple interaction mechanisms that can be grouped in two. Nuclear interactions (elastic and inelastic) are relatively rare and are treated in a discrete way by Monte-Carlo (MC) codes. The distance traveled by a particle before undergoing a nuclear interaction is modeled using the total cross-section that expresses the probability of interaction between two corpuscles. Energy loss by collisions and radiation, in case of charged particles, are mechanisms that

PROBABILITY OF INELASTIC NUCLEAR INTERACTIONS OF HIGH-ENERGY PROTONS IN ALIGNED CRYSTAL

R. Losito, W. Scandale[#], A. Taratin[‡], CERN, Geneva, Switzerland
for the UA9 Collaboration*

Abstract

A number of tests were performed in the North area of the SPS in view of investigating crystal-particles interactions for future application in hadron colliders. The rate of nuclear reactions was measured with 400 GeV proton beams directed into a silicon bent crystal. In this way the background induced by the crystal itself either in amorphous or in channeling orientation was revealed. The results provide fundamental information to put in perspective the use of silicon crystals to assist halo collimation in hadron colliders, whilst minimizing the induced loss.

INTRODUCTION

When charged particles enter a crystal with small angles θ relative to the crystal planes, their transverse motion is governed by the potential well $U(x)$ averaged along the planes. For angles smaller than the critical channeling angle $\theta_c = (2U_0/pv)^{1/2}$, where p , v are the particle momentum and velocity and U_0 the depth of the planar potential well, particles can be captured into the channeling regime and will move oscillating between two neighboring crystal planes. For moderate bending of the crystal, that is for $R < L/\theta_c$, where L and R are the length and the radius of curvature the crystal, the potential well is preserved and the channeling remains effective. In channeling regime, close collisions with the crystal atoms should be strongly suppressed.

In a crystal bent by the angle α , particle with $\theta \leq \alpha$ that cannot be channeled at the entry face of the crystal proceeds until the tangency point with the bent planes. Here two effects may take place: either the particle partially loses its transverse energy and gets trapped into the channel (volume capture) or its transverse direction is elastically reversed by the interaction with the potential barrier (volume reflection). For most of their path inside the crystal, volume reflected particles cross randomly the crystal planes except that at the tangency point.

Particles with larger incoming angles, which cannot be channeled neither reflected, traverse the entire crystal along a path uncorrelated to the crystalline structure and hence interact with it as if it was an amorphous medium.

In a two-stage collimation system a bent crystal used as primary deflector may deviate coherently the incoming halo at angles larger than what can be obtained with amorphous materials, either by channelling or by reflection process with an increase of the collimation efficiency that is the fraction of the halo collected by the

secondary absorber. Inefficiency is mostly governed by nuclear reaction rate inside the crystal itself. Criteria to minimize it are thus important when selecting the optimal crystal technology and mode of operation.

Hereafter we present results relative to a single strip silicon crystal, 1.94 mm long, bent along the (110) planes by $\alpha = 189 \mu\text{rad}$, well suited for UA9 test in the CERN-SPS [1]. The nuclear interaction rate was measured with 400 GeV/c protons in H8 beam line of the North area of the CERN-SPS as a function of the crystal orientation respect to the incoming direction of the particles [2].

INTERACTION RATE

Particles traversing a crystal along an amorphous orientation experience inelastic nuclear interactions with a probability $P_{in} \approx \sigma_{in} N_{am} L$ that is the product of the process cross-section by the target nuclear density and length. The Glauber approach provides the estimate $\sigma_{in} = 0.506 \text{ b}$ for 400 GeV/c protons [2], whilst for Si target the nuclear density is $N_{am} = 0.05 \times 10^{24} \text{ cm}^{-3}$. Thus, for a crystal length $L = 1.94 \text{ mm}$ one finds $P_{in} = 0.49\%$.

The nuclear density averaged along the trajectory varies by large factors when the particles travel with small angles relative to the crystal planes. For protons trapped in channeling states, the density drops as a Gaussian function of the distance x from the crystal planes:

$$D(x) = \frac{d_p}{\sqrt{2\pi}u_1^2} \exp\left(-\frac{x^2}{2u_1^2}\right),$$

where u_1 is the amplitude of thermal vibrations of the crystal atoms, $u_1 = 0.075 \text{ \AA}$ for a silicon crystal at a room temperature, d_p is the planar channel width. The width of the “nuclear corridor” across the planes is much smaller than the width of the channel itself: for the (110) Si, $d_p = 1.92 \text{ \AA}$ and $6u_1/d_p = 0.23$. Channeled particles with small transverse energies E_x travel in the potential well between nuclear corridors and cross a very small average density of nuclear targets. As the transverse energy E_x increases, the particles start interacting with nuclear corridors and cross a rapidly increasing average density of nuclear target, peaking at a value three times larger than N_{am} , when $E_x = U_0$. Finally, for $E_x > U_0$, the nuclear density decreases asymptotically towards N_{am} as E_x increases.

In the case of volume reflection the average nuclear density is N_{am} all along the particle trajectory except than in the tangency area, where it becomes significantly larger than N_{am} . Simulations show that the tangency area is rather short, only a few μm , and that in our 1.94 mm long crystal the increase of the average nuclear density is only a few percents.

[#]walter.scandale@cern.ch

[‡]on leave of absence from JINP, Dubna, Russia

*<http://greybook.cern.ch/programmes/experiments/UA9.html>

COMMISSIONING OF THE LHC WITH BEAM

V. Kain, CERN, Switzerland, on behalf of the LHC Commissioning Team

Abstract

After more than a year of repairing and preparing the Large Hadron Collider after a major technical problem, beams were injected again in November 2009. The commissioning plan for the 2009 to 2011 run was ambitious, aiming for centre-of-mass collision energies of 7 TeV and an integrated luminosity of 1 fb^{-1} . To date the LHC has not disappointed its user group or its designers. The first energy ramp to 1.2 TeV took place only 1 1/2 weeks after the start-up. A short technical break at the beginning of 2010 was followed by a series of commissioning highlights, including beams at 3.5 TeV, first collisions at 3.5 TeV, collisions with squeezed beams and injection of nominal bunch intensity. The major challenge for 2010 is to prepare the machine for higher and higher intensities to reach the target integrated luminosity by the end of 2011. This talk will give a short introduction to the LHC and its challenges and then focus mainly on the commissioning strategy, the preparation, the commissioning highlights, the status of the LHC and the plans for the coming months.

LHC NOMINAL PARAMETERS

The LHC surpasses existing accelerators in two aspects: the main dipole field is a factor 2 above other accelerators and the luminosity a factor 30.

The field of the LHC superconducting main dipoles has to be 8.3 T to keep 7 TeV protons in the vacuum chambers of the 27 km long accelerator installed in the former LEP tunnel. The design proton luminosity is $10^{34} \text{ cm}^{-2}\text{s}^{-1}$. This luminosity requires 3×10^{14} protons stored in the LHC which corresponds to a stored energy of about 360 MJ at 7 TeV - enough to cause serious damage in case it is lost in an uncontrolled way. One of the main accelerator systems is therefore the LHC machine protection system consisting of 100s of collimators installed around the LHC ring, 4000 Beam Loss Monitors (BLMs), absorbers in critical locations such as the beam dump region and the injection region and many other components. In total about 20'000 signals are connected to the beam abort system [1]. Figure 1 shows an overview of the LHC beam dumping system.

LHC BEAM COMMISSIONING

A short overview of the commissioning activities in 2008 and 2009 will be given. The focus will then be on the run 2010/11.

2008 and 2009

The LHC beam commissioning officially started on 10th of September 2008 with the first attempt to establish circulating beams. Preparations had been ongoing for a long time before. Long periods of hardware

commissioning and dry runs were followed by transfer line tests and LHC injection tests [2].

The 2008 commissioning activities were put to a sudden hold when on 19th of September a splice of a superconducting main busbar in one of the LHC sectors suffered from a thermal runaway during a typical powering test. The lateral damage caused by the incident was significant [3] and led to more than one year of shutdown for repair, consolidation and testing.

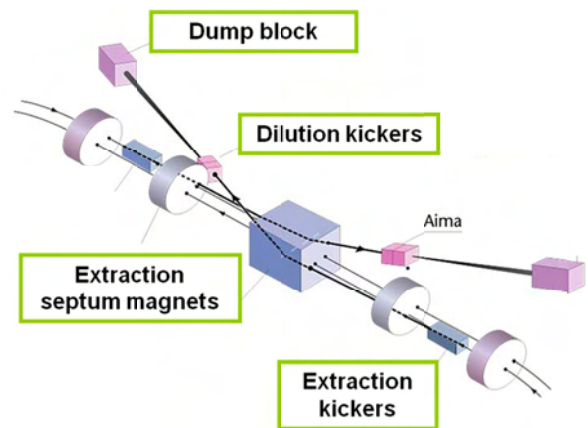


Figure 1: Overview of the LHC beam dumping system installed in the LHC point 6.

It was not until 20th of November in 2009 that the LHC could be started up again. The target energy during this period (governed by the status of the quench protection system) was 1.18 TeV. 18 days after start-up the first collisions at 1.18 TeV could be achieved.

2010/11- The Plan

The current plan for the run 2010/11 foresees protons for most of the time and ions towards the end of each year. The 2010 proton run will be finished end of October. November will be spent with ions. The current physics energy is 3.5 TeV per beam and the target β^* is 3.5 m (nominal β^* is 0.55 m).

The goal for the 2010/11 run is to collect 1 fmb^{-1} of data at 3.5 TeV per experiment. This requires a luminosity of $10^{32} \text{ cm}^{-2}\text{s}^{-1}$ and an intensity of 700 bunches with $10^{11} \text{ p}^+/\text{bunch}$. The stored energy at 3.5 TeV corresponding to this intensity is 30 MJ.

Obviously this ambitious goal can only be achieved with a strict, clean and reproducible machine setup and the machine protection system running at near nominal performance.

COMMISSIONING AND OPERATION OF THE LHC MACHINE PROTECTION SYSTEM

M. Zerlauth, R. Schmidt, J. Wenninger, CERN, Geneva, Switzerland

Abstract

The energy stored in the nominal LHC beams surpasses previous accelerators by roughly two orders of magnitude. The LHC relies on a complex machine protection system to prevent damage to accelerator components induced by uncontrolled beam loss. Around 20'000 signals feed directly or in-directly into the machine protection system. Major hardware sub-systems involved in machine protection include beam and powering interlock systems, beam loss and beam excursion monitors, collimators and the beam dumping system. Since the LHC startup in December 2009 the machine protection system components have been progressively commissioned with beam. Besides the usual individual component tests, global machine protection tests have been performed by triggering failures with low intensity beams to validate the protection systems. This presentation will outline the major commissioning steps and present the operational experience with beam of the LHC machine protection system.

MACHINE PROTECTION AT THE LHC

The first priority for the LHC machine protection systems (MPS) is to prevent equipment damage in the ring and during beam transfer from the pre-accelerator SPS [1]. Uncontrolled release of even a small fraction of the stored beam energy may cause serious damage to equipment. The nominal LHC proton momentum is a factor of seven above accelerators such as Tevatron and HERA, whereas the energy stored in the beams is more than a factor of 100 higher, see Figure 1. The beam intensity that leads to equipment damage depends on impact parameters and on the equipment hit by the beam. The damage level for fast proton losses is estimated to $\approx 2 \times 10^{12}$ p at 450 GeV, to $\approx 10^{11}$ p at 3.5 TeV and to $\approx 10^{10}$ p at 7 TeV. No special protection for the LHC would be required below these intensities. At 7 TeV the damage level is four orders of magnitude smaller than the nominal beam current. To evaluate the beam intensity to reach the damage level, a dedicated experiment was performed at the SPS confirming the numbers previously assumed for the damage threshold at 450 GeV [2].

The second priority of the machine protection is to protect superconducting magnets from quenching. At 7 TeV fast particle losses corresponding to a 10^{-8} - 10^{-7} fraction of the nominal beam intensity may quench superconducting magnets. This is orders of magnitude lower than for any other accelerator with superconducting magnets and requires a very efficient beam cleaning system. The LHC

will be the first accelerator requiring collimators to define the mechanical aperture through the entire machine cycle. A sophisticated scheme for beam cleaning and protection with many collimators and beam absorbers has been designed [3].

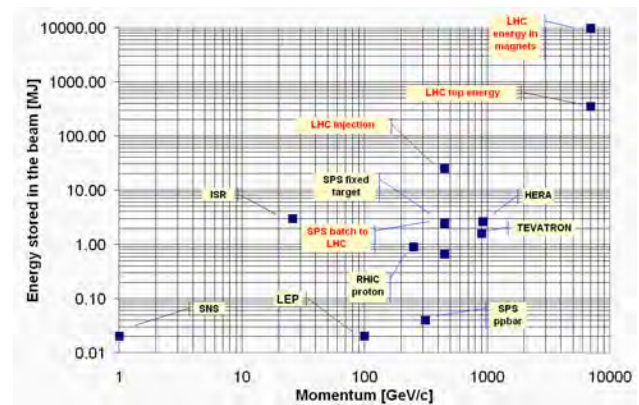


Figure 1: Stored beam energy as a function of the momentum for various accelerators.

LHC OPERATION IN 2010

In September 2008 an electrical problem in the interconnection between 2 main magnets lead to damage of over 50 magnets in one sector of the LHC which required a long repair and consolidation of the LHC of around 12 months [4]. The incident highlighted an issue affecting a large number of interconnections, as a consequence the operating beam energy of the LHC was reduced to 3.5 TeV for the LHC run of 2010-2011. The LHC will only operate at nominal energy from 2013 after a one-year shutdown in 2012 to repair all interconnections between the main dipole and quadrupole magnets in tunnel.

The aim of the LHC run in 2010/2011 is to integrate 1 fb^{-1} per experiment at 3.5 TeV. To reach this goal the LHC must operate at a luminosity of at least $10^{32} \text{ cm}^{-2}\text{s}^{-1}$ in 2011. To reach this luminosity target, approximately 400 bunches of nominal intensity (10^{11} protons) must be stored in each of the two LHC beams at 3.5 TeV. This corresponds to a stored energy of 20 MJ per beam, as compared to the nominal stored energy of 360 MJ. This target requires the LHC MPS to be fully commissioned in order to protect the LHC from damage by beams that exceed the damage level at 3.5 TeV by roughly 3 orders of magnitude.

OPERATIONAL EXPERIENCE AT J-PARC

Hideaki Hotchi^{*, 1)} for J-PARC commissioning team^{1), 2)},

¹⁾Japan Atomic Energy Agency (JAEA), Tokai, Naka, Ibaraki, 319-1195 Japan,

²⁾High Energy Accelerator Research Organization (KEK), Tsukuba, Ibaraki, 305-0801 Japan

Abstract

The J-PARC is a multi-purpose proton accelerator facility aiming at MW-class output beam power, which consists of a 400-MeV linac, a 3-GeV rapid cycling synchrotron (RCS), a 50-GeV main ring synchrotron (MR) and several experimental facilities (a materials and life science experimental facility; MLF, a hadron experimental hall; HD, and a neutrino beam line to Kamioka; NU). The beam commissioning of the J-PARC began in November 2006, and then the linac and RCS started a user operation for the MLF in December 2008. The current output beam power to the MLF is 120 kW. In this paper, the recent progress and operational experience in the course of our beam power ramp-up scenario such as beam loss control, machine activation and beam availability, especially obtained in the MLF user operation by the linac and RCS will be presented.

INTRODUCTION

The J-PARC is a multi-purpose proton accelerator facility aiming at MW-class output beam power. As shown in Fig. 1, the J-PARC accelerator complex [1] comprises a 400-MeV linac, a 3-GeV rapid cycling synchrotron (RCS), a 50-GeV main ring synchrotron (MR) and several experimental facilities (a materials and life science experimental facility; MLF, a hadron experimental hall; HD, and a neutrino beam line to Kamioka; NU).

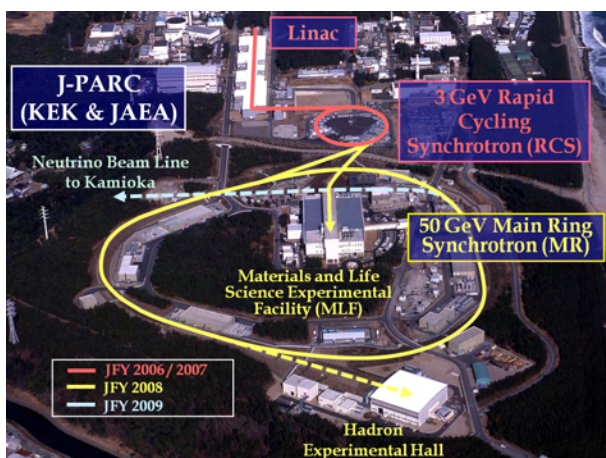


Figure 1: Bird's eye view of the J-PARC.

The linac consists of a H^- ion source, a radio-frequency quadrupole (RFQ), a drift tube linac (DTL) and

* hotchi.hideaki@jaea.go.jp

a separated-type drift tube linac (SDTL). The output energy is 181 MeV and the peak current is 30 mA at present. At full capability in the current configuration, the linac will produce 36 kW output at 181 MeV with 30 mA peak, 0.5 ms long and 56% chopper beam-on duty factor at 25 Hz repetition, which corresponds to 600 kW output at the RCS extraction energy (3 GeV). The upgrade of the front-end system to get 50 mA peak current as well as the installation of an annular coupled structure linac (ACS) for the energy recovery to 400 MeV, which are essential to achieve our final goal of 1 MW output at the RCS, are scheduled for summer maintenance periods in 2012 and 2013.

The linac beam is delivered to the RCS injection point, where it is multi-turn charge-exchange injected with a carbon stripper foil. The RCS accelerates the injected beam up to 3 GeV with 25 Hz repetition. The current injection energy is 181 MeV, for which the RCS will first aim at 300~600 kW output, and then drive for 1 MW output after upgrading the linac.

The 3-GeV beam from the RCS is mainly transported to the MLF to produce pulsed spallation neutrons and muons. A part of the RCS beam (typically 4 pulses every 3.64 s) is transported to the MR. The MR still accelerates the injected beam to 30 GeV, delivering it to the HD by a slow extraction and to the NU by a fast extraction. The output energy at the MR will be upgraded to 50 GeV in the second phase of the J-PARC project.

The beam commissioning of the J-PARC began in November 2006 and it has well proceeded as planned from the linac to the downstream facilities [2][3]. The linac and RCS started a user operation for the MLF with 4 kW output beam power in December 2008. Via a series of underlying beam studies with such a low intensity beam, the output beam power from the RCS to the MLF was increased to 120 kW in November 2009. Since then, our effort has been focused on a parameter tuning for higher-intensity beams (~300 kW) including a beam painting injection scheme in the RCS. In this paper, the recent progress and operational experience in the course of our beam power ramp-up scenario such as beam loss control, machine activation and beam availability, especially obtained in the MLF user operation by the linac and RCS will be presented (the status of the MR beam operation is presented in [4] in details).

CURRENT STATUS OF THE LINAC

Fig. 2 shows a typical residual radiation level in the linac, where the top value is a residual radiation level for 4 kW operation measured 6-hour after the beam shutdown, while

CONTROL AND PROTECTION ASPECTS OF THE MEGAWATT PROTON ACCELERATOR AT PSI

A.C. Mezger, M. Seidel, Paul Scherrer Institut, Villigen, Switzerland

Abstract

At the Paul Scherrer Institut a high intensity proton accelerator complex is routinely operated with a final kinetic energy of 590 MeV and with a beam current of 2.2 mA. In the future the beam current will be increased to 3 mA, which will then result in a beam power of 1.8 MW. Operating a facility at such a high beam power needs not only a performing and fast protection mechanism against failures but also protection against activation of the facility. This presents a particular challenge for the beam diagnostics since a high dynamic range of currents has to be handled. This paper will present the machine protection system together with several tools, control loops and procedures which are of utmost importance for minimizing the ever present losses in the facility.

A new challenge for our facility is the new ultra cold neutron (UCN) facility, which will come into operation later this year and which will require the switch over from one beam line to another for a duration of 8 seconds at full beam power. Using a short pilot pulse of a few milliseconds the beam position is measured and the beam centered in preparation for the long pulse. We will show the diagnostics that are involved and how we overcome the constraints imposed by the machine protection system.

INTRODUCTION

Any accelerator facility producing an intensive particle beam has to consider, besides beam loss leading to activation of the facility, a partial or complete loss of the particle beam leading to severe damage to the facility (Fig. 1). In our high power proton facility circa 10 milliseconds would be enough to melt stainless steel with

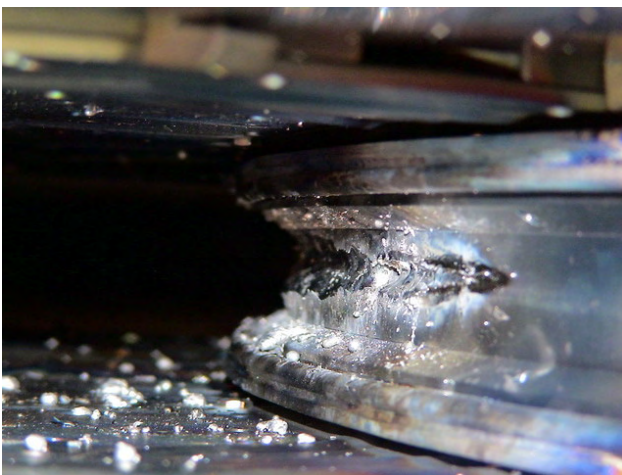


Figure 1: Cyclotron damage at injection, due to a lack of redundancy in the machine protection system.

a wrongly steered beam [1]. This could potentially occur due to the failure of components like magnets, RF components or other devices. Therefore, a system has to be implemented to protect the facility by switching off the particle beam within a few milliseconds to prevent damage. The whole system consisting of the machine protection system (MPS) itself, the devices delivering the signals for it (sensors) and the actuators shutting off the beam should be able to suppress the beam in less than 5 milliseconds. This demands for the individual components of the system reaction times in the sub-millisecond range. Furthermore the beam diagnostic devices covering many aspects of the beam and facility components and connected to the MPS have to evaluate the beam conditions and react also within a few milliseconds. These will be described later. However, in order to keep the number of “beam offs” as low as possible and therefore maintain also the high availability of the facility some compromises, where applicable, have been taken. An example of such a compromise is the suppression of “beam offs” when an acceleration cavity reflects its power for a very short time (in the order of 500 μ s). In addition to the fast behavior of the machine protection system, many other requirements have been defined for the necessary behavior of the machine protection system and will be presented later on.

This paper presents some aspects that have already been treated by previous papers, but tries to integrate these in a consistent way.

SAFETY PHILOSOPHY

Besides the protection of the facility against damage, many other systems are implemented. In our facility these systems comprise:

- Personal and radiation safety.
- Safety of the user facilities like the neutron spallation source (SINQ) or the new Ultra Cold Neutron (UCN) source.
- Patient safety systems.

All these systems have as final goal the shut off the beam when detecting any problem. However instead of considering all the systems as a whole, our policy maintains a clear separation of the individual systems. Moreover for shutting off the beam different actuators, which are monitored by the MPS for their proper functioning, are used.

This separation of concerns is of utmost importance for the licensing of the facility. It is easier to describe and convince the Swiss authorities of the correct behaviour and safety of the individual systems when these aspects are completely separated from the other systems. Besides the behaviour of these systems, only the integration of the

ACCELERATED PARTICLE TRACKING USING GPULIB

V. Ranjbar, I. Pogorelov, P. Messmer, K. Amyx,
Tech-X Corporation, Boulder, Colorado, USA

Abstract

A 4D version of BNL's spin tracking code SPINK [1] with limited elements has been successfully ported to a C++/GPU platform using GPULib [2]. This prototype used only quadrupoles, simple snakes, dipoles and drifts. We present the approach used to track spin and orbit degrees of freedom of polarized proton beams simultaneously. We also present recent results of prototyping a general-purpose particle tracking on GPUs, discussing our CUDA implementation of maps for single-particle dynamics in the Argonne National Lab's accelerator code ELEGANT [3] where a 40x speedup was achieved for single-particle-dynamics elements.

GENERAL PURPOSE COMPUTING ON GPU

In recent years, general purpose computing on graphics processing units (GPUs) has attracted significant interest from the scientific computing community because these devices offer a large amount of computing power at very low cost. Unlike general purpose processors, which are designed to address a variety of tasks ranging from control flow and bit manipulation operations to floating-point operations, GPUs are optimized to perform floating-point operations on large data sets. Instead of allocating a large amount of the on-chip real estate for large cache memory and control flow logic, GPUs dedicate a lot of resources to floating-point units. A GPU like the one found in the NVIDIA Tesla C2050 series consists of 15 vector processors with a vector length of 32 elements. Using predicated execution enables each vector element to execute its own flow through the program, providing the impression of 448 independent execution units.

The introduction of the Compute Unified Device Architecture (CUDA) by NVIDIA has made it possible for computational scientists without a deep knowledge of graphics oriented programming interfaces like OpenGL to take advantage of the high processing power offered by GPUs.

CUDA enables users to develop algorithms in C++ with a small set of language extensions. The developers write so-called *kernels*, code that executes on the GPU defining the behavior of a single thread of execution. Typically, a kernel is executed by thousands of threads concurrently and the GPU's thread manager maps them to the physical thread processors. The kernel is invoked on the host side, at which time it is determined how many threads will be executed. Memory management, data transfer and kernel invocations are all controlled by the host CPU. A special compiler, `nvcc`, translates kernels and host programs into

code that executes on the CPU and on the GPU. This architecture simplifies significantly the software development process for CUDA-enabled GPUs, but it still requires a detailed knowledge of the GPU's architecture in order to obtain good performance. For example, while the threads can be treated independently of each other, they are in fact executed on a Single-Instruction-Multiple-Data (SIMD) type architecture. E.g. on a C2050 card, 32 threads are executed using the same instruction stream, which means that diverging threads can lead to a large amount of stalled threads thus degrading performance. Also, one of the benefits of GPUs is their large memory bandwidth, but in order to take advantage of it, memory access of different threads has to be carefully aligned. Finally, many inherently sequential algorithms, such as cumulative sums of a vector, are straightforward to implement on a serial processor. However, optimization on a massively parallel system like GPUs requires carefully crafted routines. In order to free developers of the burden of low-level GPU code development, Tech-X developed GPULib, a library of GPU vector operations (<http://GPULib.txcorp.com>) [2]. While mainly designed to be used from within high-level languages, GPULib can also be used from C or Fortran.

GOALS OF THE CURRENT WORK

Our goal is to provide a set of fast orbit tracking kernels for ELEGANT and spin-orbit tracking classes for the Unified Accelerator Library (UAL) [4]. Using the UAL paradigm will make these classes usable by a wide variety of codes. The core spin transport function in SPINK, `Sprot()`, will be extracted translated to Templated C++ and turned into a self-contained class. These classes will wrap and self-contain core GPU kernels which will drive the numerically expensive particle pushes. These GPU kernels will be made available in future GPULib packages.

ELEGANT is an open-source, multi-platform code used for design, simulation, and optimization of FEL driver linacs, ERLs, and storage rings [3, 5]. The parallel version, PELEGANT [6, 7], uses MPI for parallelization and shares all source code with the serial version. Several new "direct" methods of simultaneously optimizing the dynamic and momentum aperture of storage ring lattices have recently been developed at Argonne [8]. These powerful new methods typically require various forms of tracking the distribution for over a thousand turns, and so can benefit significantly from faster tracking capabilities. Because the ability to create fully scripted simulations is essential in this approach, ELEGANT is used for these optimization computations.

AN EFFECTIVE SPACE CHARGE SOLVER FOR DYNAMION CODE

A. Orzhekhovskaya, W. Barth, S. Yaramyshev, GSI, Darmstadt, Germany

Abstract

An effective analytical and semi-analytical method for internal electrical field calculations was proposed for ellipsoidal shaped beam as well as for a beam of arbitrary longitudinal shape with an elliptical transverse cross section. This method combines acceptable accuracy with a high speed of computation. The existing version of the DYNAMION code uses the particle-particle method to calculate the electrical field, which needs a significant time for computation. A Semi-Analytical Solver (SAS) for the ellipsoidal bunch was introduced into DYNAMION code. It allows much faster beam dynamics simulations than the old. The DYNAMION parameter "macroparticle size" was investigated in combination with the new space charge algorithm. The beam dynamics simulations were performed through the 1st Alvarez tank of the GSI linac UNILAC using the standard and the new methods. The RMS emittance growth as a benchmark parameter shows sufficient agreement between both solvers.

INTRODUCTION

Fast and precise space charge solvers are especially important in the beam dynamics simulations for high current linear and circular accelerators, where space charge effects may dominate and lead to the emittance growth and beam losses. Space charge effects can be calculated using different analytical and numerical methods. Recently various modifications of the PIC solver are mainly used for the simulations. The advanced multiparticle code DYNAMION [1], dedicated to beam dynamics simulations in linacs, was created in 1985 in the Institute of Theoretical and Experimental Physics (ITEP, Moscow) and was developed in collaboration of ITEP and GSI Helmholtzzentrum fuer Schwerionenforschung (Darmstadt)

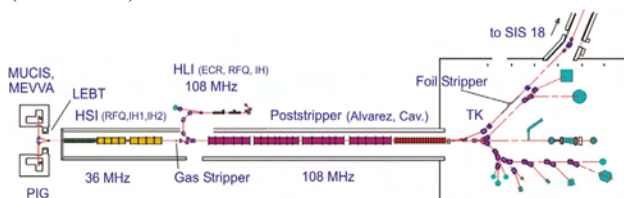


Figure 1: GSI – UNILAC.

Since 1991 the code DYNAMION is used for study, optimization and upgrade of the heavy ion high current GSI linac UNILAC (Fig. 1), serving as a high current injector for FAIR - International Facility for Antiproton and Ion Research at Darmstadt together with the synchrotron SIS 18 (Fig. 2). The UNILAC comprises high current injector (HSI; 2.2 keV/u - 1.4 MeV/u),

stripper section and poststripper accelerator (5 Alvarez type tanks; up to 11.4 MeV/u) [2,3].

For electrical field calculation the code DYNAMION uses recently two methods: the particle-particle interaction and the PIC solver. An analytical and Semi-Analytical space charge Solver (SAS) was originally created for beam dynamics simulations in the GSI synchrotron SIS18 and in FAIR rings SIS100, SIS300 [4-6]. This algorithm being implemented into the DYNAMION code allows also for fast and reliable beam dynamics simulations for linacs.

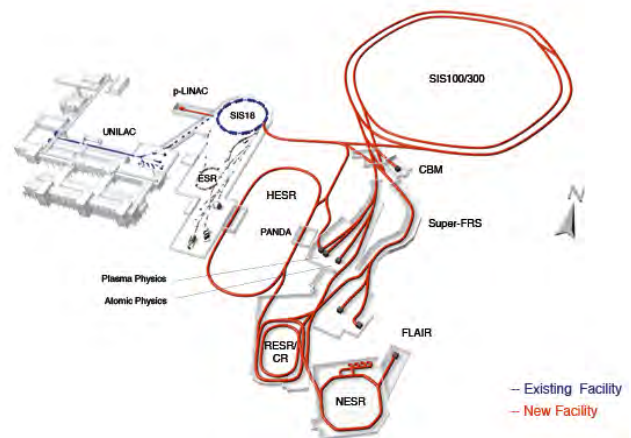


Figure 2: Scheme of GSI Helmholtzzentrum für Schwerionenforschung (Darmstadt, Germany) with existing and future facilities.

SEMI-ANALYTICAL SOLVER (SAS) FOR THE INTERNAL ELECTRIC FIELD CALCULATIONS

Kellogg's Formulae

A 3D ellipsoidal frozen bunch is considered; the charge density is given by

$$\rho(x, y, z) = \frac{Q}{4\pi abc} n(t),$$

where Q - total charge of the bunch, a, b, c - horizontal, vertical and longitudinal axis of the ellipsoid, $n(t)$ - analytical function, representing particle distribution, t - isodensity parameter

$$t = x^2/a^2 + y^2/b^2 + z^2/c^2, \quad 0 \leq t \leq 1.$$

The general formulae for the electrical field of such a bunch were derived by Kellogg [7]:

$$E_x = \frac{Q}{2} x \int_0^\infty \frac{n(T) ds}{(a^2 + s)^{3/2} (b^2 + s)^{1/2} (c^2 + s)^{1/2}},$$

$$E_y = \frac{Q}{2} y \int_0^\infty \frac{n(T) ds}{(a^2 + s)^{1/2} (b^2 + s)^{3/2} (c^2 + s)^{1/2}}, \quad (1)$$

CHALLENGES IN SIMULATING MW BEAMS IN CYCLOTRONS

Y. J. Bi ^{*}, Tsinghua University, Beijing, 100084, China & CIAE, Beijing, 102413, China & PSI
 A. Adelman [†], R. Dölling, M. Humbel, W. Joho, M. Seidel, PSI, Villigen, CH-5234, Switzerland
 T. J. Zhang, CIAE, Beijing, 102413, China; C. X. Tang, Tsinghua University, Beijing, 100084, China

Abstract

The 1.3 MW of beam power delivered by the PSI 590 MeV Ring Cyclotron together with stringent requirements regarding the controlled and uncontrolled beam losses poses great challenges with respect to predictive simulations. We describe a large scale simulation effort, which leads to a better quantitative understanding of the existing PSI high power proton cyclotron facility. Initial conditions for the PSI Ring simulations are obtained from a new time structure measurements and 18 profile monitors available in the 72 MeV injection line. The radial beam profile measurement which is just located in front of the extraction septum is compared with simulations. We show that OPAL (Object Oriented Parallel Accelerator Library) can precisely predict the radial beam pattern at extraction with a large dynamic range of 4 orders of magnitude. A large turn separation and a narrow beam size at the Ring extraction is obtained by adjusting parameters such as the injection position and angle, the flattop phase and the trim coils. A large turn separation and a narrow beam size are the key elements for reducing the beam losses to acceptable levels. The described simulation capabilities are mandatory in the design and operation of the next generation high power proton drivers.

INTRODUCTION

A three stage proton accelerator complex is operated at the Paul Scherrer Institut. The 590 MeV Ring cyclotron, routinely delivers 2.2 mA of proton current, which makes it the most powerful machine of this kind worldwide. The resulting strong, phase-independent energy gain per revolution gives good turn separation and hence a beam extraction with low beam losses in the order of 10^{-4} . The upgrade plans of the PSI facility foresee a stepwise increase of the beam intensity to 3.0 mA [1].

Benefiting from the the High Performance Computing (HPC) clusters available today, the powerful tool OPAL enables us to perform large scale simulations in complex high intensity accelerators [2]. OPAL is a tool for charged-particle optic calculations in accelerator structures and beam lines including 3D space charge. A new particle matter interaction model taking into account energy loss, multiple Coulomb scattering and large angle Rutherford scattering is now available. This model together with

the 3D space charge will significantly increase the predictive capabilities of OPAL.

THE PHYSICAL MODEL

To perform large scale simulations in complex high intensity cyclotrons, both space charge effect and the particle matter interaction should be considered carefully. The original version of OPAL can deal with not only single bunch space charge effects but also the effects of neighboring bunches [3], however, the particle matter interaction is missing. General-purpose Monte Carlo codes, e.g. MCNPX [4], FLUKA [5, 6], are developed to model the particle matter interaction, however they have limited capabilities to track the particle in both complex external and space charge fields. We extend OPAL in order to handle efficient particle matter interactions, hence collimator systems in high intensity accelerators can be modeled together with space charge.

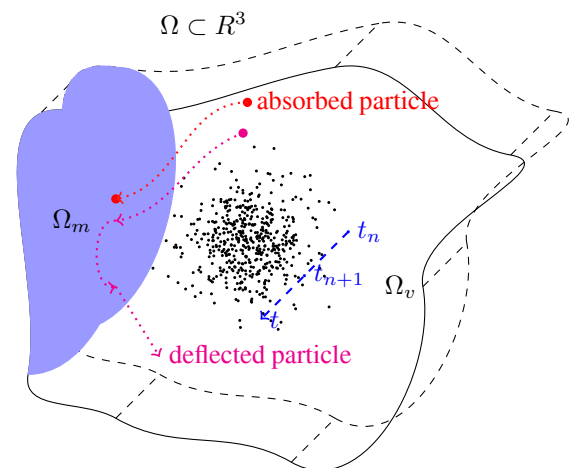


Figure 1: The beam and its surrounding region.

The Fig.1 describes the computational domain Ω surrounding the beam. It is divided into two sub-domains: the vacuum domain Ω_v and the material domain Ω_m . When the beam is passing collimator or in general 'material', some of the halo particle may go from the vacuum domain into the material domain. This part of the beam is then absorbed or deflected.

The flowchart with physical model in material is shown in Fig. 2. If the coordinate of a particle is in the material region, $x \in \Omega_m$, a temporal sub-stepsizes is defined as

^{*} bijj05@mails.tsinghua.edu.cn

[†] andreas.adelman@psi.ch

BEAM DYNAMICS AND DESIGN OF THE ESS LINAC

M. Eshraqi, M. Brandin, C. Carlile, M. Lindroos, S. Peggs, A. Ponton, K. Rathman, J. Swinarski, European Spallation Source, Lund, Sweden.

Abstract

The European Spallation Source, ESS, will use a linear accelerator delivering high current long pulses with an average beam power of 5 MW to the target station at 2.5 GeV in the nominal design. The possibilities to upgrade to a higher power LINAC at fixed energy are considered. This paper will present a full review of the LINAC design and the beam dynamics studies.

INTRODUCTION

The European Spallation Source, ESS, is a high current proton LINAC to be built in Lund, Sweden. The design is based on previous studies done by ESS-Scandinavia [1] and ESS-Bilbao [2] teams. In the new design the average beam current and the final beam energy have changed by at least a factor of two from the 2003 ESS design values (5 MW, 1 GeV, 150 mA, 16.7 Hz) [3]. Decreasing the beam current and increasing the beam energy simplifies the linac design and increases the reliability as well as leaving the upgrade scenario by increasing the beam current possible.

In the new design LINAC delivers 5 MW of power to the target at 2.5 GeV, with a nominal current of 50 mA. It is designed to include the ability to upgrade the LINAC to a higher power of 7.5 MW at a fixed energy of 2.5 GeV, by increasing the current from 50 to 75 mA. Increasing the beam current implies that in case of fixed power couplers the energy gain per cavity will decrease, to reach the fixed energy of 2.5 GeV extra cryo-modules will be added in the area reserved for this purpose, as illustrated in Fig. 1.

LINAC STRUCTURES

Proton Source and LEBT

It is foreseen to use an ECR, electron cyclotron resonance, proton source to produce up to 90 mA of beam current at 75 keV. The source will deliver pulses as long as 2 ms with a repetition rate of 20 Hz. One of their advantages is that they can operate in low vacuums of $O(10^{-4})$ Torr, enabling them to deliver very high currents. The absence of hot filaments increases the mean time between maintenance significantly [4]. These sources function is very reliable manner in terms of availability and current stability.

The Low Energy Beam Transport, LEBT, system is composed of two magnetic solenoids, it transports and matches the 75 keV beam out of source to the radio frequency quadrupole, RFQ, while minimizing emittance growth. The LEBT is equipped with magnetic steerers to adjust the beam

Table 1: Primary Parameters of Accelerating Structures

System	Energy MeV	Freq. MHz	β_{Geo}	No. of modules	Length m
Source	0.075	–	–	–	2.5
LEBT	0.075	–	–	–	1.6
RFQ	3	352.21	–	1	4.7
MEBT	3	352.21	–	–	1.0
DTL	50	352.21	–	3	19
Spokes	240	352.21	0.54	15	61
Low β	590	704.42	0.67	10	59
High β	2500	704.42	0.84	14	169

position and angle at the RFQ injection point, and includes beam diagnostics to measure the beam parameters between source and RFQ. Depending on the rise time of the source and the beam quality during the rise time a slow chopper might be added to deflect the low quality head and tail of the beam.

RFQ and MEBT

The first stage of the acceleration in ESS_{LINAC} will be performed by a radio-frequency quadrupole, RFQ. This four-vane RFQ operates at 352.21 MHz and boosts the proton beam from 75 keV to 3 MeV while it shapes the beam in a train of micro-pulses. The quality of the proton beam out of RFQ will have a significant impact on the particle dynamics throughout the rest of the LINAC. ESS has consequently put important R & D efforts in designing the RFQ. The RFQ is expected to maintain the transverse emittance of the beam, control and reduce the generation of halo, and shape the beam longitudinally to improve the efficiency of acceleration in the following structures. In addition very low loss in the RFQ walls is mandatory to prevent sparking and a possible thermo-mechanical stress.

A Medium Energy Beam Transport, MEBT, composed of four electromagnetic quadrupoles and two buncher cavities, at 352.21 MHz, matches the 3 MeV beam out of RFQ to the acceptance of the Drift Tube LINAC, DTL. Not requiring a chopper the MEBT will be the shortest possible to avoid the longitudinal blowup of the beam. At this energy, 3 MeV, neutron production is not an issue and pre-collimation can be easily performed, if necessary.

There are proposals to avoid the MEBT completely and couple the RFQ to the DTL directly, this option needs to ramp the voltage in RFQ, requiring a varying ρ , to match its phase advance to the one of DTL, and subsequently the acceleration

BEAM DYNAMICS OF SPL: ISSUES AND SOLUTIONS

P. A. Posocco, M. Eshraqi[#], A. M. Lombardi, CERN, Geneva, Switzerland
[#]and ESS Lund, Sweden

Abstract

SPL is a superconducting H- LINAC under study at CERN. The SPL is designed to accelerate the 160 MeV beam of LINAC4 to 4-5 GeV, and is composed of two families of 704.4 MHz elliptical cavities with geometrical betas of 0.65 and 1.0 respectively. Two families of cryo-modules are considered: the low-beta cryo-module houses 6 low-beta cavities and 4 quadrupoles, whereas the high-beta one houses 8 cavities and 2 quadrupoles. The regular focusing structure of the machine is interrupted at the transition between low beta and high beta structure and at 1.4 and 2.5 GeV for extracting medium energy beam. The accelerator is designed for max. 60 mA peak current (40 mA average) and max. 4% duty cycle, implying a very accurate control of beam losses. In particular the choice of the diagnostics and correction system, the maximum quadrupole gradient to avoid Lorentz stripping and the effect of the RF power delivery system on the beam quality are discussed in this paper.

INTRODUCTION

SPL, Superconducting Proton Linac [1], is a CERN multi user facility with the aim to produce at 5 GeV a high power proton beam suitable for a neutrino factory. Fixed target experiments are foreseen at lower energies, like ISOLDE at 1.4 GeV or Eurisol at 2.5 GeV.

LINAC4 [2] accelerates H- ions from 45 keV to 160 MeV in a sequence of normal conducting structures at 352.2 MHz and injects the beam into SPL: the H- are then accelerated from 160 MeV to 5 GeV by about 240 5 cells elliptical cavities (704.4 MHz) whose geometric β in the low energy part is equal to 0.65 and 1.0 above (see Figure 1). The nominal accelerating gradients are 19 and 25 MV/m respectively. The transition energy between the two families is set between 700 and 800 MeV, optimized in order to have the best beam dynamics and the most efficient acceleration [3]. At the moment two current scenarios are under study: while the final power is the same (4 MW), the peak current can be 32 or 64 mA, the latter being the highest among high power linac projects in the world running or under study (see Table 1).

A large community participates to the SPL design, including members of high power proton linac projects and of various Universities, companies and Institutes, all generally involved in electron and proton linac studies or in the technology of SC cavities.

SPL BEAM DYNAMICS

General Criteria

SPL beam dynamics was designed according to the following three general beam dynamics criteria:

Table 1: High Power Linac Projects in the World

Param.	Unit	SPL		SNS	ESS	Project X
		LC	HC			
ion		H-	H-	H-	p	H-
Energy	[GeV]	5	5	1	2.5	3
Beam power	[MW]	4	4	1.4	5	3
Rep. rate	[Hz]	50	50	60	20	CW
Av. pulse current	[mA]	20	40	26	50	1
P. pulse current	[mA]	32	64	38	50	10
Source current	[mA]	40	80	47	60	≤ 10 dc
Chopping ratio	[%]	62	62	68	/	10
Beam pulse	[ms]	0.8	0.4	1	2	100
Duty cycle	[%]	4	2	6	4	10

- The phase advance per period for zero current does not exceed 90 degrees in all planes to avoid beam envelope instabilities.
- The longitudinal phase advance is always smaller than the transverse. The ratio between the two is far from the peaks of Hofmann plots [4], avoiding resonances.
- The matching between the two cavity families is achieved by means of a smooth transition of the phase advance per meter.

Consequently:

- Maintaining the cavity voltage at its maximum except at the beginning of the low β and high β sections where the resulting phase advance would exceed 90 degrees, the longitudinal phase advance is reduced along the acceleration as the beam energy increases.
- Accordingly, the transverse phase advance is reduced in order to maintain the ratio. This is obtained by lowering the focalization. As the geometrical emittance decreases in the acceleration, the resulting average beam size remains almost constant along the linac.

THE IFMIF-EVEDA CHALLENGES AND THEIR TREATMENT

P. A. P. Nghiem*, N. Chauvin, O. Delferrière, R. Duperrier, A. Mosnier, D. Uriot,
 CEA/DSM/IRFU, 91191 Gif-sur-Yvette Cedex, France
 M. Comunian, INFN/LNL, Legnaro, Italy; C. Oliver, CIEMAT, Madrid, Spain

Abstract

One major system of the IFMIF project (International Fusion Materials Irradiation Facility) is its two accelerators producing the neutron flux by accelerating Deuteron particles up to 40 MeV against a Lithium target. In a first phase called EVEDA (Engineering Validation and Engineering Design Activity), a full scale prototype accelerating particles up to 9 MeV is being studied and constructed in Europe, to be installed in Japan.

Two unprecedented performances are required for the IFMIF-EVEDA accelerators: the very high power of 5 MW and very high intensity of 125 mA CW. That leads to numerous unprecedented challenges: harmful losses even for those as low as 10^{-6} of the beam, non-linear dynamics induced by very strong space charge forces, difficulties for equipment and diagnostic implementations in the high compact structure, need of specific RF tuning strategies in this context.

These issues are highlighted in this article, and the ways they are addressed are detailed.

INTRODUCTION

The IFMIF project (International Fusion Materials Irradiation Facility) is set in the context of the Fusion Broader Approach signed between Japan and Europe, aiming at studying materials which must resist to very intense neutron radiations in future fusion reactors. One objective is to construct the world most intense neutron source capable of producing 10^{17} neutrons/s at 14 MeV. A major system of this project is its two accelerators producing the neutron flux by accelerating Deuteron particles up to 40 MeV against a Lithium target. In a first phase called EVEDA (Engineering Validation and Engineering Design Activity), a full scale prototype accelerating particles up to 9 MeV is being studied and constructed in Europe, to be installed in Japan.

To produce the neutron flux equivalent to that of future fusion reactors, the required Deuteron intensity in the accelerators is very high, 125 mA CW, which, combined

with the required final energy, makes IFMIF-EVEDA the accelerators of the megawatt class at relatively low energy. This article points out how the simultaneous combination of these two very high intensity and very high power induces unprecedented challenges, but also provides exciting opportunity for HIB studies.

IFMIF MAIN FEATURES

The general layouts of the IFMIF-EVEDA accelerators are displayed in Fig. 1. In each of the two IFMIF accelerators, D^+ particles are first accelerated by the source extraction system, then by the long RFQ and finally the SRF-Linac composed of four cryomodules. The LEBT and MEBT have to focus and match the beam in the 6D phase space from an accelerating structure to another. The HEBT drives the beam to the Lithium target where, with the help of multipolar magnetic elements, the transverse beam density must be made flat in a well defined rectangle shape. The EVEDA accelerator is composed of exactly the same sections up to the first cryomodule, and a simplified HEBT which must properly expands the beam toward the Beam Dump.

In Fig. 1 are also indicated beam energies together with beam powers along the accelerators. Due to the very high beam intensity of 125 mA, the beam power is already 625 kW at the RFQ exit and 1.1 MW after the first cryomodule, to reach 5 MW after the 4th cryomodule. And that at relatively low energies of 5, 9 and 40 MeV, where space charge effects are still dominant.

That situation is unique when compared to worldwide linear accelerators in operation or planned. Figure 2 shows the beam power as a function of beam energy for the most powerful accelerators, while Fig. 3 gives for the same accelerators the generalised perveance K , relevant for judging space-charge forces. We can see that for a given energy, IFMIF-EVEDA has the highest beam power and the highest space charge regime. When considering beam power absolute values, IFMIF-EVEDA can be ranked second. But unlike any other accelerator, even for

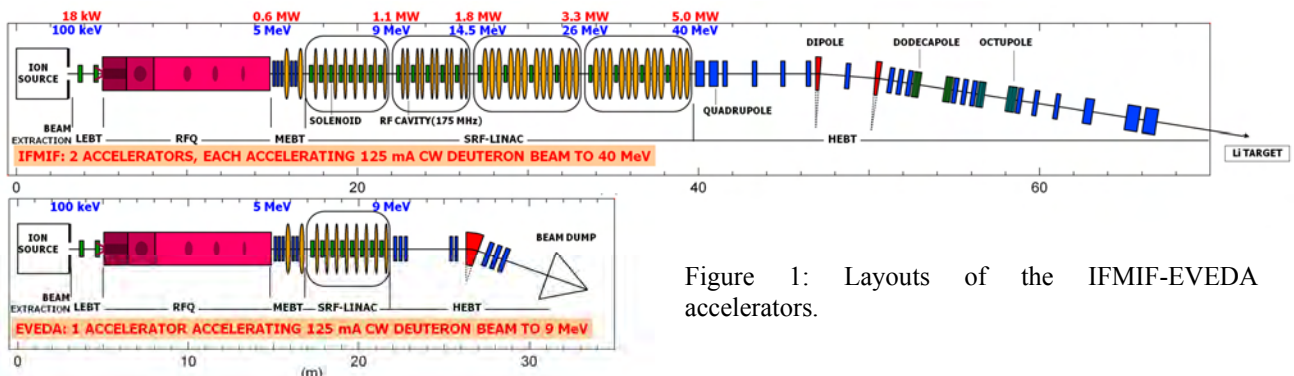


Figure 1: Layouts of the IFMIF-EVEDA accelerators.

* phu-anh-phi.nghiem@cea.fr

OVERVIEW OF BEAM OPTICS IN PROJECT-X SC CW LINAC*

J.-F. Ostiguy[†], N. Solyak, A. Vostrikov and J.-P. Carneiro
Fermilab, Batavia, IL 60510

Abstract

Project-X is a proposed multi-MW proton facility at Fermilab. Based on a new superconducting H⁻ linear accelerator, it would provide the foundation for a flexible long term intensity frontier physics research program. Two machine configurations have been developed. The first one involved a single 8 GeV, pulsed linac (9 mA peak, 1 ms @ 5 Hz pulses) followed by accumulation and acceleration to 60-120 GeV in the existing Main Injector synchrotron. The second -and currently favored one- replaces the single pulsed linac by a 3 GeV (10 mA peak, 1 mA average), continuous wave linac followed, up to 8 GeV, by either a rapid cycling synchrotron or a second (pulsed) linac. We present here an overview of beam optics for the 3 GeV CW linac. Alignment, field amplitude and phase tolerances are also addressed.

INTRODUCTION

The US elementary particle physics community strategic plan for the coming decade emphasizes research on three frontiers: the energy, intensity and cosmic frontiers. As the sole US site for accelerator based particle physics research, Fermilab's strategy features the development of a high intensity, multi-MW proton source. This new facility, dubbed Project-X, is based on a superconducting H⁻ linear accelerator. Project-X will provide the flexibility to support diverse intensity-frontier physics experiments, including a world leading program in neutrino physics. Ultimately, it would serve a basis for a future neutrino factory and/or muon collider. Specifically, the objectives of Project-X are:

- provide 2 MW of beam power at a beam energy of 60 to 120 GeV for long base line neutrino oscillation experiments
- provide > 1 MW of high intensity low energy protons for rare decay experiments operating simultaneously with the neutrino program.
- provide a path toward a muon source for a future Neutrino factory and/or a Muon collider: 4 MW of beam power at 5-15 GeV.

Historical Background

The genesis of Project-X is the Fermilab Proton Driver (PD), a concept developed at the beginning of the decade [1, 2]. The PD was an 8 GeV pulsed superconducting H⁻ linac used to inject and accumulate beam into the existing Main Injector synchrotron. To capitalize on the

* Work supported by U.S. DOE contract No. DE-AC02-07CH11359.

[†] ostiguy@fnal.gov

ILC (then TESLA) technology, the PD front-end frequency (325 MHz) was selected to be a submultiple of the 1.3 GHz ILC frequency. The PD featured a single four-fold jump in frequency to 1.3 GHz around 400 MeV with the bulk of the acceleration (from 2.4 to 8 GeV) subsequently handled with unmodified ILC cavities. An innovative scheme involving fast ferrite phase shifters for independent cavity phase and amplitude control was also introduced.

Project-X

At an early stage, Project-X retained many ingredients of the PD concept, most notably the 8 GeV pulsed linac. A subsequent series of reviews, studies and workshops led to the conclusion that the 8 GeV pulsed linac lacked the flexibility necessary to support both the near and long term Fermilab physics programs. An optimal energy for planned rare-decay experiments was deemed around 3 GeV. Perhaps more importantly, different experiments required simultaneous operation with vastly different beam timing structures. These considerations led to the current concept for Project-X (technically referred to as IC-2.2), and shown schematically in Fig. 1. It consists of a 3 GeV continuous-

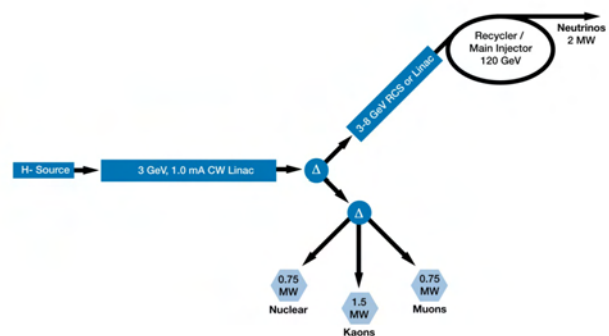


Figure 1: Project-X IC-2.2 conceptual diagram. Acceleration to 3 GeV is handled by linac operating in CW mode. Acceleration from 3 GeV to 8 GeV could be handled either by a pulsed linac, or by a rapid cycling synchrotron (linac option is shown).

wave (CW), 1 mA average, 10 mA peak linac, followed by rf separators to dispatch portions of the beam to different experiments. The chief advantage of CW operation is that it allows for arbitrarily complex beam pulse structures to be accelerated. The beam structure is imposed at low energy, before acceleration in the linac using a fast broadband chopper and can be modified more or less at will without altering the main linac operation. An added benefit of CW operation is that it is inherently more stable than pulsed operation. To reach 8 GeV, two options are being consid-

BEAM DYNAMICS IN THE FRIB LINAC*

R. C. York[#], X. Wu, Q. Zhao, M. Doleans⁺, F. Marti, E. Pozdeyev,
National Superconducting Cyclotron Laboratory, East Lansing, MI 48824, U.S.A.

Abstract

The Facility for Rare Isotope Beams (FRIB), a Department of Energy (DOE) national user facility to provide intense beams of rare isotopes for nuclear science researchers, is currently being established on the campus of Michigan State University (MSU). A superconducting driver linac will deliver cw beams of stable isotopes with an energy of >200 MeV/u at a beam power of 400 kW. Highly charged ions will be produced from an Electron Cyclotron Resonance Ion Source (ECRIS) with a total extraction current of several mA. Multiple charge states of heavier ions will be accelerated simultaneously to meet the final beam power requirement. The FRIB driver linac lattice design has been developed and end-to-end beam simulations have been performed to evaluate the machine performance. An overview of the beam dynamics is presented.

INTRODUCTION

The 2007 Long Range Plan for Nuclear Science had as one of its highest recommendations the “construction of a Facility for Rare Isotope Beams (FRIB) a world-leading facility for the study of nuclear structure, reactions, and astrophysics.” [1] FRIB, currently being established on the campus of Michigan State University (MSU) under a Cooperative Agreement between Department of Energy (DOE) and MSU, will be a DOE national user facility providing intense fast, stopped, and re-accelerated beams of rare isotopes for nuclear science researchers to understand the fundamental forces and particles of nature as manifested in nuclear matter, and to provide the necessary expertise and tools from nuclear science to meet national needs. Since the 2008 selection of MSU as the FRIB site, the driver linac layout has been evaluated and the double-folded configuration, as shown in Fig. 1, was chosen as the preferred alternative in 2010. The choice of

the driver linac layout was largely driven by goal to reduce overall project cost while maintaining the performance and upgrade potential.

The FRIB facility is based on a superconducting heavy ion linac with >200 MeV/u for all varieties of stable ions at beam power of 400 kW [2]. The uncontrolled beam loss specification for the cw, high power linac is ≤ 1 W/m to facilitate hands-on maintenance. To meet the beam intensity requirements, the FRIB linac will utilize simultaneous multi-charge-state acceleration for heavier ions. The driver linac will consist of a Front End to bring the beam energy to 0.3 MeV/u, three superconducting acceleration segments connected by two 180° bending systems to achieve a final beam energy of >200 MeV/u and a Beam Delivery System to transport the multi-charge-state beams to a fragmentation target, as shown in Fig. 1. The superconducting linac has an 80.5 MHz base frequency and utilizes four types of resonators with only one frequency transition to 322 MHz after the Linac Segment 1 of Fig. 1.

Several codes were used to design the driver linac lattice. The transport and matching in the Front End, the two 180° bending sections and the Beam Delivery System were performed using DIMAD, COSY and TRACE3D. The superconducting linac lattice was optimized for multiple charge state acceleration using a code developed at MSU. End-to-end beam simulations with high statistics have been performed using the code RIAPMTQ and IMPACT on high-performance parallel computers.

LINAC LATTICE DESIGN

The FRIB driver linac lattice design has been developed and evaluated through several evolutions [3,4]. The double-folded geometry was chosen to reduce overall project cost, and the beam dynamics of that design is discussed here.

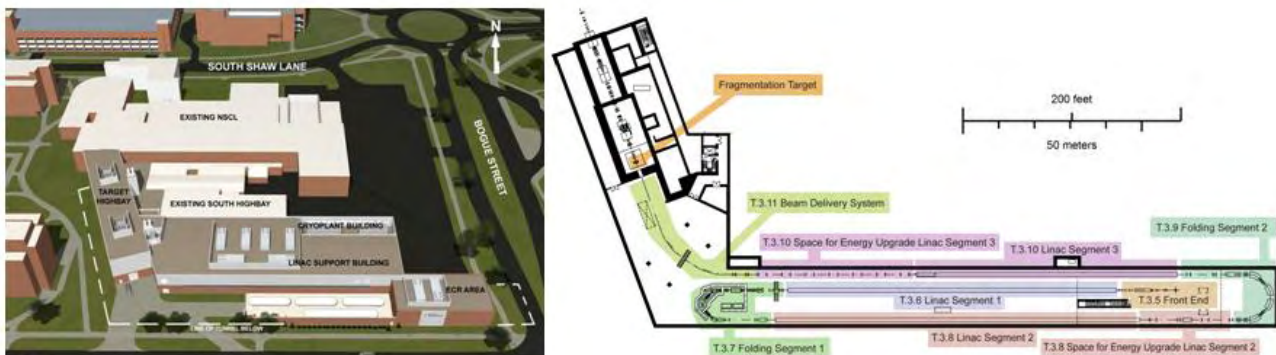


Figure 1: The planned FRIB surface buildings (left) and the layout of the double-folded superconducting driver linac in tunnel (right).

* Work supported by US DOE Cooperative Agreement DE-SC000661
[#]york@frib.msu.edu ⁺ now at ORNL, Oak Ridge, TN 37831, USA

OPERATIONAL EXPERIENCE WITH J-PARC INJECTION AND EXTRACTION SYSTEMS

P.K. Saha*¹⁾ for the J-PARC team^{1),2)},

¹⁾ Japan Atomic Energy Agency (JAEA), Tokai, Ibaraki 319-1195, Japan,

²⁾ High Energy Accelerator Research Organization (KEK), Tsukuba, Ibaraki 305-0801, Japan

Abstract

The Japan Proton Accelerator Research Complex (J-PARC) is now in a full operational stage and delivering relatively high power beam to all experimental facilities. There are two stages of injection and extraction schemes in the entire facility and each has very unique as well as common issues in terms of the design criteria in order to obtain a desire beam power in each stage and finally to ensure a stable and fair operation keeping the beam loss to an acceptable limit. There has been a lot of understandings and achievements so far through systematic beam studies and thus continuing the user operations with relatively a high power beam to all experimental facilities. However, for further higher and long term operation, there remains few issues as well as challenges to discuss. Uncontrolled beam loss due to the foil scattering at the RCS injection area, slow rise time and heating problem with the fast extraction kicker system as well as improvement of duty factor for the slow extraction operation in the MR can be mentioned.

INTRODUCTION

The Japan Proton Accelerator Research Complex (J-PARC) is a high intensity accelerator project consists of a 400 MeV linac (181 MeV at present), a 3 GeV rapid cycling synchrotron (RCS), a 50 GeV (30 GeV at present) main ring (MR) and several experimental facilities [1]. The experimental facilities include a Material and Life Science Experimental Facility (MLF), which utilizes a 3 GeV fast extracted beam from the RCS, while the neutrino (NU) and the hadron (HD) experimental facilities use 30 GeV fast and slow extracted beam, respectively, from the MR. The entire accelerator facility already entered into an operational mode ending with its overall initial beam commissioning aspects. The RCS is now operating with a beam power of 120 kW for the MLF and more than 200 kW equivalent beam power for the MR injection. The MR already achieved a maximum possible of 6 bunches injection and continuing NU operation with a beam power of more than 50 kW through Fast Extraction (FX) at 30 GeV. The Slow Extraction (SX) operation there also for the HD experimental facility with gradually improving the duty factor is in a good progress. On the other hand, a maximum beam power of 300 kW already been demonstrated in the RCS, while the MR also demonstrated a 100 kW operation for the neutrino experiment [2, 3].

There are two stages of injection and extraction in the

entire system. An H^- beam with a kinetic energy of 181 MeV from the linac is injected into the RCS. RCS has a charge-exchange H^- painting injection scheme in the injection period of 500 μ s. Accelerated is done up to a beam energy of 3 GeV and the beam is then simultaneously extracted for the MLF and MR injection by using a pulsed bending magnet placed in the extraction beam transport line. The MR has a multi-bunch injection scheme and starting with a 3 GeV injection, the beam is accelerated up to a maximum of 30 GeV at present. The beam is then delivered either to the neutrino experiment through FX mode or to the hadron experimental facility through SX mode.

In order to obtain a high power and high quality beam and eventually for a fair and stable operation, there are many issues and challenges in each accelerator especially, with the injection and extraction systems of both RCS and MR. Some of the issues are common but most of the issues are quite different in many aspects. Because of a charge-exchange scheme, the RCS injection system involves many more issues and thus needed to adopt a complicated and a sophisticated system as compared to the MR injection. The charge-exchange foil including the foil system itself is one of the most complicated issue in the RCS injection. On the other hand, the SX scheme of MR is quite different than the ordinary RCS extraction, where a high duty and a low loss operation are always big issues. The overall initial operational experiences with both injection and the extraction systems are satisfactory and there also has a lot of understandings through systematic beam studies and simulations especially, with a high power beam. However, there remains few urgent issues for further higher power and stable operation in the near future. The uncontrolled beam loss due to the foil scattering at the injection area during multi-turn injection period is one of main issue in RCS for high power operation. The leakage field from the extraction and injection magnets in RCS and MR, respectively, are two big issues. Furthermore, slow rise time of the FX kicker system, hitting problem in the kicker ferrite core are two recent issues and appear as direct limitations for high power SX operation to the NU experiment, where a high duty regardless of high power for the HD experimental facility is one of the key issue with SX operation in the MR.

RCS INJECTION AND EXTRACTION SYSTEMS

One key issue with the RCS injection is to keep the uncontrolled beam loss especially, from the foil scattering as low as possible. Based on detail study on the transverse

*E-mail address: saha.pranab@j-parc.jp

INJECTION PAINTING AND ASSOCIATED HW FOR 160 MeV PSB H⁻

C. Bracco, B. Balhan, J. Borburgh, C. Carli, E. Carlier,
R. Chamizo, M. Chanel, T. Fowler, B. Goddard, M. Hourican,
A.M. Lombardi, B. Mikulec, A. Newborough, D. Nisbet, R. Noulivos,
U. Raich, F. Roncarolo, L. Sermeus, M. Scholz, W. Weterings, CERN, Geneva, Switzerland

Abstract

Linac4 will replace the currently used Linac2 in the LHC injector chain. The motivation is to increase the proton flux availability for the CERN accelerator complex and eventually achieve the LHC ultimate luminosity goals. Linac4 will inject 160 MeV H⁻ ions in to the four existing rings of the PS Booster (PSB). A new charge-exchange multi turn injection scheme will be put into operation and requires a substantial upgrade of the injection region. Four kicker magnets (KSW) will be used to accomplish transverse phase space painting in order to match the injected beams to the required emittances. This paper presents hardware issues and related beam dynamics studies for several painting schemes. Results of optimization studies of the injection process for different beam characteristic and scenarios are discussed.

INTRODUCTION

The ultimate luminosity reach of the LHC foresees to increase the bunch intensity from 1.15×10^{11} protons (p⁺) to 1.7×10^{11} p⁺. One of the key intensity limitation is determined by the direct space charge effects at the PS Booster (PSB) for low energies. The replacement of the Linac2, currently injecting 50 MeV p⁺ into the PSB, with Linac4 will allow to increase the injection energy to 160 MeV [1]. This will mitigate the space charge effects and permit to increase the beam intensity at the Booster. Moreover, the conventional multi turn injection, used with Linac2, will be substituted by a H⁻ charge exchange injection system [2]. This consists of a horizontal closed orbit bump (chicane) and a thin carbon foil (stripping foil) converting hydrogen ions to protons by removing the electrons. The chicane is made up of four dipole magnets (BS), with 66 mrad deflection, which are located symmetrically around the stripping foil. A further attenuation of the space charge effects can be obtained controlling the distribution, in phase space, of the injected particles. The energy of the injected beam will be varied to fill the bucket with an equal density distribution (longitudinal painting) [3]. The H⁻ charge exchange allows to inject more times in the same phase space volume. An additional closed orbit bump will be used to fill first the centre and then the outer area of the ellipse in the transverse phase space (transverse painting).

The PSB has to provide beam to several users with different requirements in terms of beam intensity and emittance. Decay time modulation of four kicker magnets (KSW),

which are already installed in the PSB lattice, will allow to accomplish the transverse phase space painting to the required emittances [4].

PSB USERS BEAM REQUIREMENTS

Particles are accelerated up to 1.4 GeV in the PSB and then they can be either directed to the Proton Synchrotron (PS) or directly to the isotope facility ISOLDE. The Booster has to provide the PS with beams having different emittances and intensities, in order to fulfill the requirements of several users. Six beam types are foreseen for the Large Hadron Collider (LHC), during nominal and ultimate operation. Beams with extremely different characteristics are then needed for a number of fixed target experiments (CNGS, East and North area targets), the Antiproton decelerator (AD) and neutron time-of-flight facility (nTOF).

Linac4 supplies 1×10^{14} protons per pulse to the PSB, with a pulse length of 400 μ s. Protons need roughly 1 μ s to perform one turn in the Booster. Number of injection turns needed to fill the PSB rings, target intensities and emittances are summarized in Table 1 for the different users.

INJECTION TRANSVERSE PAINTING

The beam will be injected in the PSB with an angle of 66 mrad with respect to the axis of the circulating beam. The strength of the BS chicane magnets (RBEND) will be maximum during injection, corresponding to a -45.9 mm orbit bump, and will decrease linearly after the injection. Edge focusing effects will occur at the pole faces and perturb the vertical betatron oscillations. This perturbation can be compensated either with additional trim quadrupoles (active) or by a pole face rotation of the BS (passive) [5]. The studies presented in this paper refer to the passive compensation case, and to a pole face rotation of 66 mrad (SBEND).

In addition to the injection chicane, a horizontal painting bump is implemented. The height of the bump, at the beginning of the injection, depends on the beam and other injection parameters. The painting bump starts to decay already during injection to control the filling of the horizontal phase space. Vertical beam ellipse areas are partially filled without painting, letting the space charge forces reshuffle the particle distribution on successive turns. The following studies were performed to understand the effect of different KSW decay modulations on the beam emittance and to de-

SNS INJECTION FOIL EXPERIENCE

M.A. Plum, S.M. Cousineau, J. Galambos, S.-H. Kim, P. Ladd, C.F. Luck, C.C. Peters, Y. Polsky,
R.W. Shaw, Oak Ridge National Laboratory*, Oak Ridge, TN, USA
R.J. Macek, Los Alamos National Laboratory, Los Alamos, NM, USA
D. Raparia, Brookhaven National Laboratory, Upton, NY, USA

Abstract

The Spallation Neutron Source comprises a 1 GeV, 1.4 MW linear accelerator followed by an accumulator ring and a liquid mercury target. To manage the beam loss caused by the H^0 excited states created during the H^- charge exchange injection into the accumulator ring, the stripper foil is located inside one of the chicane dipoles. This has some interesting consequences that were not fully appreciated until the beam power reached about 840 kW. One consequence was sudden failure of the stripper foil system due to convoy electrons stripped from the incoming H^- beam, which circled around to strike the foil bracket and cause bracket failure. Another consequence is that convoy electrons can reflect back up from the electron catcher and strike the foil and bracket. An additional contributor to foil system failure is vacuum breakdown due to the charge developed on the foil by secondary electron emission. In this paper we detail these and other interesting failure mechanisms and describe the improvements we have made to mitigate them.

INTRODUCTION

The Spallation Neutron Source accelerator [1] comprises a 1 GeV, 60 Hz, H^- ion beam linac with a 1.5 MW design beam power, followed by an accumulator ring with charge-exchange injection to compress the 1 ms long pulses from the linac to ~ 700 ns. The present beam power is typically about 1 MW at 925 MeV. Corrugated nanocrystalline diamond stripper foils [2] have been in use from the beginning of formal operations in 2006. These foils were successfully used with no failures until May 3, 2009, shortly after increasing the beam power to ~ 840 MW. The first failure was quickly followed by two more, and the beam power was reduced to ~ 430 kW to prevent further foil system failures, and then to ~ 400 kW two days later after another failure. A mid-cycle foil change (a first for SNS) was executed on May 19, 2009 using a modified foil bracket, but the foil system continued to fail.

A team was assembled to investigate the failures and recommend modifications, which were put in place for the next run cycle starting in September 2009. The modified foils and brackets performed very well, and a single foil lasted for the entire September – December production run, which included operating at a beam

power of 1 MW. A single foil was also used for the subsequent February – June 2010 run cycle, with even more charge delivered to the neutron production target.

In this paper we discuss the causes of the foil system failures, and the modifications made to prevent them.

SNS STRIPPER FOIL SYSTEM

The nominally 17 mm x 45 mm x 0.30 mg/cm² stripper foils have three free edges and are mounted on L-shaped brackets that hang from pins on the foil changing mechanism. A photo of a first generation foil and bracket is shown in Fig. 1. The long arm and leg of this bracket style were designed to accommodate stripper foils that require support from thin carbon fibers that can be stretched across the arm and the leg. The diamond foils do not require fiber support.

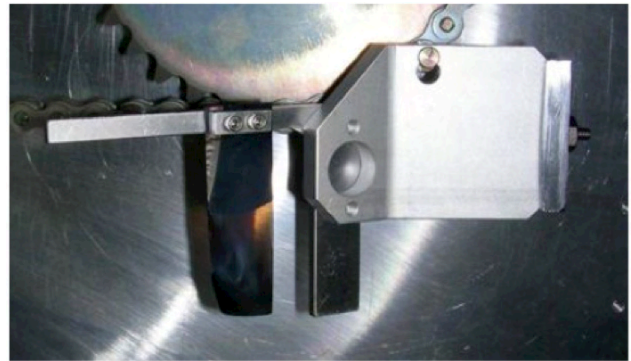


Figure 1: A first generation foil bracket mounted on the foil-changer mechanism. The long arm and leg of the L-shaped bracket were designed to stretch carbon fibers across the span to support foils if needed (not used in this case). (Figure reproduced from Ref. 3.)

When in use, the foil is positioned inside a strong (~ 0.25 T) magnetic field to control the beam loss caused by the partially stripped H^0 excited states created by the foil that, if not properly controlled, could strip to H^+ at some point downstream of the foil and outside the ring acceptance [4]. The magnetic field at the foil causes the excited states with $n \geq 5$ to strip within about a mm of the foil. Also, the foil is located in the falling field (downstream end) of the magnet, and the peak field of the next downstream magnet is less than the field at the foil, so that the surviving $n < 5$ states will not strip until they reach the secondary stripper foil, whereupon they can be properly transported to a beam dump.

*ORNL is managed by UT-Battelle, LLC, under contract DE-AC05-00OR22725 for the U.S. Department of Energy.

ADVANCEMENTS IN LASER TECHNOLOGY AND APPLICATIONS TO ACCELERATORS*

Yun Liu[#], SNS, Oak Ridge National Laboratory, U.S.A.

Abstract

A brief review on the emergent applications of laser technology to particle accelerators is provided. Important developments of key elements in laser technology that lead to the applications are described.

INTRODUCTION

Advancements in laser technology have dramatically expanded the applications of lasers to particle accelerators. Today, lasers have been used for accelerators in a broad range from operational systems such as nonintrusive particle beam diagnostics instruments, to elaborate applications with high technical readiness levels including, for instance, photoinjectors, a laser assisted foil-less charge exchange injection scheme and Compton scattering-based light sources, and finally to exotic topics such as laser driven electron/ion accelerators. This talk reviews recent experimental results achieved in the above applications, their requirements on laser parameters and challenges that require future laser technology development. Important technical elements such as the femto-second pulse generation, the burst-mode optical amplifiers, the beam combining from laser arrays, and the power enhancement optical cavity will be briefly described.

LASER TECHNOLOGY ADVANCEMENTS

Ultra-high-Intensity Pulsed Lasers

The remarkable progress in the application of lasers to accelerators was largely attributed to the invention of the chirped pulse amplification (CPA) technique [1]. Prior to CPA, the maximum laser peak power was below 1 GW and the maximum achievable laser intensity stayed around 10^{14} W/cm², a limitation due to the nonlinear effects and catastrophic optical damage of the optical components. The core of the CPA technique is that it stretches the pulse duration before the amplifier, maintains the intensity below the amplifier damage threshold, and compresses the pulse in air or vacuum to avoid any possible nonlinear effect. Today, CPA is the only technique for amplifying an ultrashort laser pulse up to the petawatt (10^{15} W) level. The main gain materials used in CPA are solid-state media such as Ti:sapphire or Nd:Glass, which can store about a thousand times more energy than dye or excimer lasers used earlier.

Table 1 lists the parameters of a few ultrahigh-intensity lasers in various facilities. Focusing petawatt pulses onto small spots can produce extreme power densities of 10^{18}

to 10^{21} W/cm². Such high power densities can accelerate electrons to relativistic speeds, generate MeV protons, and produce x-rays and gamma rays. As we see in the later part, many of the lasers in Table 1 have been used for these purposes.

Table 1: Ultrahigh Intensity Lasers

Facility	Laser Type	Peak Power	Pulse Width	Rep. Rate
UT Austin	Nd:Glass	1.1 PW	167 fs	10 Hz
HERCULES (U Michigan)	Ti:Sapphire	300 TW	30 fs	0.1 Hz
Vulcan (RAL)	Nd:Glass	1 PW	700 fs	
LLNL	Ti:Sapphire + Nd:Glass	1.5 PW	440 fs	10 Hz
Gekko (Osaka)	Nd:Glass	500 TW	500 fs	3-4 Hz
LOA	Nd:Glass	100 TW	25 fs	10 Hz
MPQ	Ti:Sapphire	20 TW	450 fs	10 Hz
PHLIX	Nd:Glass	1 PW	500 fs	
LULI	Nd:Glass	100 TW	300 fs	10 Hz
Ref. [2]	Yb Fiber	1 GW	700 fs	100KHz

Laser Array Beam Combination

In many applications such as the Compton scattering based light source or laser based collider design, (X-ray/ γ -ray) the yield and luminosity are important factors. Such applications require not only high peak power, but also high average power of the laser system.

Increasing the cavity volume will raise the laser power but this approach has a physical limitation. An alternative approach to building high power lasers is to use arrays of relatively lower power lasers. As a matter of fact, many large laser facilities obtain extremely high power intensities through beam combining of a large number of high power lasers. In general, beam combining requires that the beams from the array elements be combined to have the propagation characteristics of a single beam. One way of scaling up the laser power is to incoherently combine the laser beams via multiplexing in position, angle, wavelength or polarization. As an example, a 2-MW peak power was obtained by wavelength combing from 4 pulsed photonic crystal fiber lasers [3]. A drawback of the incoherent beam combining is that the brightness of the total beam from the laser array cannot exceed that of each individual beam.

The limitation of the brightness does not apply to mutually coherent beams since they occupy the same elements in phase space and behave as if they came from one coherent source. Therefore only coherent beam combining allows truly scalable output powers and diffraction-limited quality of the combined beams. Primary approaches to get mutually coherent beams are

* Work performed at Oak Ridge National Laboratory, which is managed by UT-Battelle, LLC, under contract DE-AC05-00OR22725 for the U.S. Department of Energy.

[#] liuy2@ornl.gov

FEASIBILITY OF 2 GeV INJECTION INTO THE CERN PS

S. Aumon, B. Balhan, W. Bartmann[#], J. Borburgh, S. Gilardoni, B. Goddard, M. Hourican, L. Sermeus, R. Steerenberg, CERN, Geneva, Switzerland

Abstract

The increase of the extraction energy of the CERN PSB to 2 GeV has been suggested as a method to increase the intensity of the LHC beam which can be obtained from the present injector complex. Such a change would require a redesign of the present PS proton injection system, which is already operating at close to its limits. The feasibility of a 2 GeV proton injection is discussed and a potential solution outlined. The implications on the injection equipment and on the performance in terms of beam parameters and losses are discussed.

INTRODUCTION

An increase in the extraction energy of the CERN PSB has been mooted [1] as a possible route to removing the space charge limit at injection into the CERN PS for the LHC beam. This could open a path to significantly increase the brightness of the beam for future LHC luminosity upgrades [2], and might be a cost-effective alternative to the SPL-PS2 injector complex upgrade route [3]. Many PSB systems would be affected by the increase from 1.4 GeV to 2 GeV; in addition, the beam transfer to the PS and in particular the PS fast injection system for p+ would need to be redesigned. The present injection scheme is outlined, and the constraints for a 2 GeV injection are presented. Two possible upgrade concepts are compared: injection into the same straight section SD42 as present, and injecting into the upstream straight section SD41 which has longer available drift space. The reasons for preferring an injection into the present straight section are presented. The feasibility of this solution is examined in terms of the required injection equipment performance, the available aperture, the impact on the injection of other beams and the requirements for modifications to associated beam instrumentation, vacuum and the injection line. Experimental studies on emittance blow up made with the present injection kicker are reported, which have implications for the choice of kicker operating mode (short-circuit or terminated) and on the necessity for an additional injection kicker system.

EXISTING 1.4 GeV INJECTION

The present injection into the PS is a classical horizontal plane fast bunch-to-bucket scheme to transfer protons only, using a closed orbit bump to approach the septum. The septum is located in a straight section with low horizontal β , which minimises the beam size but increases the effective septum width and hence required kick strength. The injection bump makes use of a bumper

magnet located just upstream of the septum, to allow injection with a large angle, required to fit the beam inside the aperture of the main lattice magnet downstream of the septum. The injection bump and trajectory are shown in Figures 1 and 2 for the LHC beam and high intensity beam, respectively, together with the physical aperture model of the PS in this region. It should be noted that the injected beam is not fully optically matched to the circulating beam.

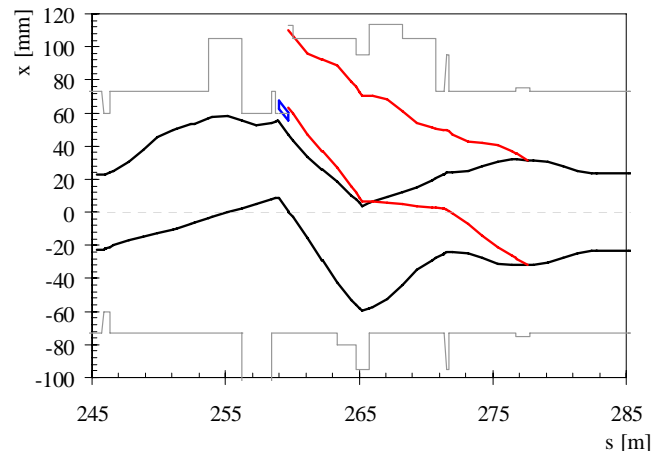


Figure 1: Existing injection bump and injected trajectory envelopes for 12.0 μm high intensity beam at 1.4 GeV.

CONSTRAINTS

The new injection should be at a rigidity 30% higher than at present, Table 1. The kicker rise time should not increase beyond 56 ns, to avoid losses from the 220 ns long bunches injected with 276 ns spacing. The injection should accept LHC beams at 2.0 GeV with a maximum emittance of 3.0 μm , and should also conserve the emittance of the 1 μm pilot beam. Ideally it should be possible to inject the large emittance high intensity beam at 2.0 GeV; it is essential that it be possible to continue to inject this beam at 1.4 GeV.

Table 1: Beam Characteristics and Constraints

	Present	Upgrade
Beam rigidity [Tm]	7.14	9.28
Kicker rise time [ns]	56	56
Normalised emittance LHC physics beam [μm] H / V	3.0 / 3.0	3.0 / 3.0
Normalised emittance LHC pilot beam [μm] H / V	1.0 / 1.0	1.0 / 1.0
Normalised emittance high intensity beam [μm] H, V	12 / 9	12 / 9

[#]wolfgang.bartmann@cern.ch

COUPLING IMPEDANCES OF A SHORT INSERT IN THE VACUUM CHAMBER

Y. Shobuda, JAEA/J-PARC center, Tokai-mura, Ibaraki 319-1195, Japan
Y. H. Chin and K. Takata, KEK, Tsukuba, Ibaraki 305-0801, Japan

Abstract

We have developed a theory to calculate both longitudinal and transverse impedances of a resistive short (typically shorter than the chamber radius) insert with cylindrical symmetry, sandwiched by perfectly conductive chambers on both sides. It is found that unless the insert becomes extremely thin (typically a few nm for a metallic insert) the entire image current runs on the thin insert, even in the frequency range where the skin depth exceeds the insert thickness, and therefore the impedance increases drastically from the conventional resistive-wall impedance. In other words, the wake fields do not leak out of the insert unless it is extremely thin.

INTRODUCTION

In proton synchrotrons, the inner surface of a short ceramic break is normally coated by a thin (typically about ten nm) Titanium Nitride (TiN) to suppress the secondary emission of electrons. The skin depth can be larger than the thickness of the TiN coating in low frequency, and the wake fields may interact with the outside world through the coating. It is thus important to construct a theory of resistive insert taking into account its thickness effects.

We have developed a theory to describe the impedance of a short insert by generalizing a theory of a gap, where the respective components are sandwiched by perfectly conductive chambers [1, 2]. The main difference between the gap and the insert is that the insert has a finite skin depth, and this skin depth effect will modulate how wake fields propagate in the chamber. Main objective of this paper is to study how the impedance of the insert will change from that of the conventional resistive-wall theory to that of a gap, when the thickness of the insert is changed compared to the skin depth.

In numerical examples shown in figures, unless specified otherwise, we consider a beam pipe radius $a = 5$ cm with an insert of length $g = 8$ mm, and conductivity $\sigma_c = 6 \times 10^6 / \Omega \text{ m}$. This can be a model for a short ceramic break with TiN coating in a copper beam pipe.

LONGITUDINAL IMPEDANCE

The longitudinal coupling impedance of the resistive short insert is expressed as

$$Z_{L,insert} = \frac{Z_0}{j\beta a k I_0^2(\bar{k}a)} / [Y_{pole} + Y_{cut} - \frac{2\pi \sqrt{j k \beta Z_0 \left(\sigma_c + j \frac{k \beta \epsilon'}{Z_0} \right) \tanh \sqrt{j k \beta Z_0 \left(\sigma_c + j \frac{k \beta \epsilon'}{Z_0} \right) t}}{k^2 \beta^2 g}], \quad (1)$$

where

$$Y_{pole} = - \sum_{s=1}^{\infty} \frac{4\pi a (1 - e^{-j \frac{b_{s,g}}{2a}})}{g b_s^2}, \quad (2)$$

$$Y_{cut} = - \frac{\int_0^{\infty} d\zeta \frac{4(1 - e^{-j w \sqrt{k^2 \beta^2 + \frac{\zeta}{(a+t)^2}}})}{\zeta \left(k^2 \beta^2 + \frac{\zeta}{(a+t)^2} \right) H_0^{(1)}(e^{j \frac{\zeta}{2}} \sqrt{\zeta}) H_0^{(2)}(e^{j \frac{\zeta}{2}} \sqrt{\zeta})}{g \pi (a+t)} \simeq \frac{2\sqrt{2}(1-j)}{\sqrt{k\beta g}}, \quad (3)$$

$Z_0 = 120\pi$, $k = \omega/c\beta$, $\bar{k} = k/\gamma$, ϵ' is the relative dielectric constant of the insert. Here, $b_s^2 = k^2 \beta^2 a^2 - j_{0,s}^2 = -\beta_s^2$, $j_{0,s}$ are s -th zeros of $J_0(z)$ and $H_m^{(1)}(z)$ is the Hankel function of the first kind. We should notice that b_s approaches $-j\beta_s$ for $j_{0,s} > k\beta a$.

At first, let us check the accuracy of the formula Eq.(1) by comparing with ABCI results [3]. Recently, ABCI has been upgraded and can now handle a resistive material inside a cavity. We choose the chamber thickness $t = 2$ mm, the relative dielectric constant of the insert $\epsilon' = 10$ and its conductivity $\sigma_c = 50$ [$\Omega \text{ m}$]. In order to simulate correctly, the mesh size should be sufficiently smaller than the chamber thickness. In our case, it is divided into ten meshes. At high frequency where the skin depth becomes smaller than the mesh size, ABCI cannot accurately simulate field behavior. That is about 1GHz for the present choice of mesh size. At higher frequency where the skin depth is smaller than the mesh size, the theory predicts the insert impedance better than the ABCI [1]. In ABCI, we put a huge cavity in the outside of the insert to simulate open space. Figure 1 shows the comparison results of the real (left) and the imaginary (right) parts of the impedance, respectively. Quite good agreements can be seen between the two results.

IMPEDANCES OF TWO DIMENSIONAL MULTILAYER CYLINDRICAL AND FLAT CHAMBERS IN THE NON-ULTRARELATIVISTIC CASE

N. Mounet, EPFL, Lausanne and CERN, Geneva, Switzerland
 E. Métral, CERN, Geneva, Switzerland

Abstract

Two dimensional electromagnetic models (i.e. assuming an infinite length) for the vacuum chamber elements in a synchrotron are often quite useful to give a first estimate of the total beam-coupling impedance. In these models, classical approximations can fail under certain conditions of frequency or material properties. We present here two formalisms for flat and cylindrical geometries, enabling the computation of fields and impedances in the multilayer case without any assumption on the frequency, beam velocity or material properties (except linearity, isotropy and homogeneity).

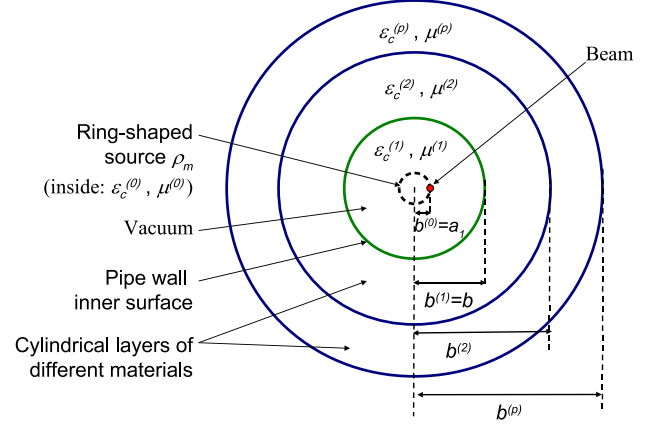


Figure 1: Cross section of the cylindrical chamber.

INTRODUCTION

In this old subject [1], the general formalism of B. Zotter [2] enables the analytical computation of the electromagnetic (EM) fields in frequency domain and the impedance created by a beam in an infinitely long multilayered cylindrical pipe made of any linear materials. Still, improvements of this formalism were possible for better accuracy and computational time, thanks in particular to a matrix formalism for the field matching. Also, it is possible to extend this theory to any azimuthal mode instead of only $m = 0$ and $m = 1$, enabling the computation of nonlinear terms in the EM force.

For multilayer flat chambers, the usual approach is to compute the beam coupling impedances thanks to a formula valid for an axisymmetric geometry multiplied by constant ‘‘Yokoya’’ form factors [3, 4], but this has been shown to fail in the case of non metallic materials such as ferrite [5] which is expected since Yokoya’s theory relies on hypotheses that can be wrong for certain materials and/or certain frequencies. Therefore, we show here how we can provide a more general theory of the multilayer flat chamber impedance, going beyond the single-layer case [4] or the double-layer one [6, 7]. We use similar ideas as for a cylindrical geometry and apply them to an infinitely long and large flat chamber.

Details on the derivations below can be found in [8, 9].

ELECTROMAGNETIC FIELDS IN A CYLINDRICAL MULTILAYER CHAMBER

We consider a point-like beam of charge Q travelling at a speed $v = \beta c$ along the axis of an axisymmetric infinitely long pipe of inner radius b , at the position $(r = a, \theta = 0, s = vt)$ in cylindrical coordinates. The source charge density is in frequency domain ($f = \frac{\omega}{2\pi}$), after the usual

decomposition on azimuthal modes [8, 10]

$$\rho(r, \theta, s; \omega) = \sum_{m=0}^{\infty} \rho_m = \sum_{m=0}^{\infty} \frac{Q \cos(m\theta) \delta(r - a_1) e^{-jks}}{\pi v a_1 (1 + \delta_{m0})}, \quad (1)$$

where $k \equiv \frac{\omega}{v}$, δ is the delta function, and $\delta_{m0} = 1$ if $m = 0$, otherwise. The space is divided into $N+1$ cylindrical layers of homogeneous, isotropic and linear media (see Fig. 1), each denoted by the superscript (p) ($0 \leq p \leq N$). The last layer goes to infinity.

The macroscopic Maxwell equations in frequency domain for the electric and magnetic fields \vec{E} and \vec{H} are written [2]

$$\begin{aligned} \text{curl} \vec{H} - j\omega \vec{D} &= \rho_m v \vec{e}_s, & \text{curl} \vec{E} + j\omega \vec{B} &= 0, \\ \text{div} \vec{D} &= \rho_m, & \text{div} \vec{B} &= 0, & \vec{D} &= \epsilon_c \vec{E}, & \vec{B} &= \mu \vec{H}, \end{aligned} \quad (2)$$

where [11]

$$\epsilon_c = \epsilon_0 \epsilon_1 = \epsilon_0 \epsilon_b [1 - j \tan \vartheta_E] + \frac{\sigma_{DC}}{j\omega(1 + j\omega\tau)}, \quad (3)$$

$$\mu = \mu_0 \mu_1 = \mu_0 \mu_r [1 - j \tan \vartheta_M]. \quad (4)$$

In these expressions, ϵ_0 (μ_0) is the permittivity (permeability) of vacuum, ϵ_b the real dielectric constant, μ_r the real part of the relative complex permeability, $\tan \vartheta_E$ ($\tan \vartheta_M$) the dielectric (magnetic) loss tangent, σ_{DC} the DC conductivity and τ the Drude model relaxation time [12].

From Maxwell equations, one gets for each mode m [13]

$$\begin{aligned} \left[\frac{1}{r} \frac{\partial}{\partial r} \left(r \frac{\partial}{\partial r} \right) + \frac{1}{r^2} \frac{\partial^2}{\partial \theta^2} + \frac{\partial^2}{\partial s^2} + \omega^2 \epsilon_c \mu \right] E_s &= \\ & \frac{1}{\epsilon_c} \frac{\partial \rho_m}{\partial s} + j\omega \mu \rho_m v, \\ \left[\frac{1}{r} \frac{\partial}{\partial r} \left(r \frac{\partial}{\partial r} \right) + \frac{1}{r^2} \frac{\partial^2}{\partial \theta^2} + \frac{\partial^2}{\partial s^2} + \omega^2 \epsilon_c \mu \right] H_s &= 0. \end{aligned}$$

VAN KAMPEN MODES FOR BUNCH LONGITUDINAL MOTION

A. Burov, FNAL*, Batavia, IL 60510, U.S.A.

Abstract

Conditions for existence, uniqueness and stability of bunch steady states are considered. For the existence uniqueness problem, simple algebraic equations are derived, showing the result both for the action and Hamiltonian domain distributions. For the stability problem, van Kampen theory is used [1-3]. Emerging of discrete van Kampen modes show either loss of Landau damping, or instability. This method can be applied for an arbitrary impedance, RF shape and beam distribution function Available areas on intensity-emittance plane are shown for resistive wall wake and single harmonic, bunch shortening and bunch lengthening RF configurations.

MAIN EQUATIONS

Let $H(z,p)$ be a Hamiltonian for longitudinal motion inside RF bucket distorted by the wake field:

$$\begin{aligned} H(z, p) &= \frac{p^2}{2} + U(z) + V(z, t); \\ U(z) &= U_{\text{rf}}(z) - \int \lambda(z') \mathcal{W}(z - z') dz'; \\ V(z, t) &= - \int \rho(z', t) \mathcal{W}(z - z') dz'. \end{aligned} \quad (1)$$

Here z and p are the offset and the momentum of a particle, $U(z)$ is the steady state potential with $U_{\text{rf}}(z)$ as its RF part, $\lambda(z)$ is steady state linear density, $W(z)$ is the wake function, $V(z, t)$ and $\rho(z, t)$ are small perturbations of the potential well and linear density. For the potential well $U(z)$, action I and phase φ variables can be found:

$$\begin{aligned} I(H) &= \frac{1}{\pi} \int_{z_{\min}}^{z_{\max}} \sqrt{2(H - U(z))} dz; \\ \Omega(I) &= \frac{dH}{dI}; \quad \frac{dz}{d\varphi} = \frac{\sqrt{2(H - U(z))}}{\Omega(I)}. \end{aligned} \quad (2)$$

The linear density λ and its perturbation ρ can be related to steady state phase space density $F(I)$ and its perturbation $f(I, \varphi, t)$:

$$\begin{aligned} \lambda(z) &= \int F(I) dp; \\ \rho(z, t) &= \int f(I, \varphi, t) dp. \end{aligned} \quad (3)$$

Below, the steady state distribution $F(I)$ is treated as an input function, determined either by cooling-diffusion

*Operated by Fermi Research Alliance, LLC under Contract No. DE-AC02-07CH11359 with the United States Department of Energy.

kinetics, or by injection. The perturbation $f(I, \varphi, t)$ satisfies the Jeans-Vlasov equation [4]:

$$\frac{\partial f}{\partial t} + \Omega(I) \frac{\partial f}{\partial \varphi} - \frac{\partial V}{\partial \varphi} F'(I) = 0. \quad (4)$$

Set of equations (1-4) assumes given input functions $U_{\text{rf}}(z)$, $W(z)$ and $F(I)$, while the steady state solution $U(z)$, $I(H)$, $\lambda(z)$ and all the eigenfunctions of the dynamic Jeans-Vlasov equation (4) are to be found.

To obtain the steady state solution, the following set of three equations is to be solved:

$$\begin{aligned} U(z) &= U_{\text{rf}}(z) - \int \lambda(z') \mathcal{W}(z - z') dz' \equiv U_{\text{RHS}}[\lambda]; \\ I(H) &= \frac{1}{\pi} \int_{z_{\min}}^{z_{\max}} \sqrt{2(H - U(z))} dz \equiv I_{\text{RHS}}[U]; \\ \lambda(z) &= 2 \int_{U(z)}^{H_{\max}} \frac{F(I(H))}{\sqrt{2(H - U(z))}} dH \equiv \lambda_{\text{RHS}}[I, U]. \end{aligned} \quad (5)$$

For any given input functions $U_{\text{rf}}(z)$, $W(z)$ and $F(I)$, the solution can be numerically found by means of a quasi-time method. Indeed, let it be assumed that initially there is no wake, so that the entire potential well is equal to the RF potential $U(z) = U_0(z) = U_{\text{rf}}(z)$. With that, initial action and linear density functions $I_0(H)$ and $\lambda_0(z)$ can be found from the 2nd and 3rd equations of the set (5). Then the following iteration procedure can be applied:

$$\begin{aligned} U_n(z) &= U_{n-1}(z) - \varepsilon (U_{n-1}(z) - U_{\text{RHS}}[\lambda_{n-1}]); \\ I_n(H) &= I_{\text{RHS}}[U_n]; \\ \lambda_n(z) &= \lambda_{\text{RHS}}[I_n, U_n] \quad ; \quad n = 1, 2, \dots \end{aligned} \quad (6)$$

If the solution exists, the process converges to it provided the convergence parameter $\varepsilon > 0$ is sufficiently small. When the steady state is found, the dynamical stability analysis can be performed by means of Jeans-Vlasov equation (4). Following Oide and Yokoya [5], the eigenfunctions may be expanded in Fourier series over the synchrotron phase φ :

$$f(I, \varphi, t) = e^{-i\omega t} \sum_{m=1}^{\infty} [f_m(I) \cos m\varphi + g_m(I) \sin m\varphi]. \quad (7)$$

With the zero-phase at the left stopping point,

$$\begin{aligned} z(I, \varphi = 0) &= z_{\min}(I); \quad z(I, \varphi = \pi) = z_{\max}(I); \\ z(I, -\varphi) &= z(I, \varphi); \quad p(I, -\varphi) = -p(I, \varphi), \end{aligned} \quad (8)$$

this yields an equation for the amplitudes $f_m(I)$:

$$\begin{aligned} [\omega^2 - m^2 \Omega^2(I)] f_m(I) &= \\ -2m^2 \Omega(I) F'(I) \sum_{n=1}^{\infty} \int dI' V_{mn}(I, I') f_n(I'); \end{aligned} \quad (9)$$

LONGITUDINAL PEAK DETECTED SCHOTTKY SPECTRUM

E. Shaposhnikova, T. Bohl and T. Linnekar, CERN, Geneva, Switzerland

Abstract

The peak detected Schottky spectrum is used for beam observation in the CERN SPS and now also in the LHC. This tool was always believed, however without proof, to give a good picture of the particle distribution in synchrotron frequencies similar to the longitudinal Schottky spectrum of unbunched beam for revolution frequencies. The analysis shows that for an optimised experimental set-up the quadrupole line from the spectrum of the peak detected signal is very close to the synchrotron frequency distribution inside the bunch - much closer than that given by the traditional longitudinal bunched-beam Schottky spectrum. The analysis of limitations introduced by a realistic experimental set-up is based on its realisation in the SPS.

INTRODUCTION

The so called “peak detected Schottky” (PD Schottky) signal is a beam diagnostics tool developed and used extensively in the SPS [1, 2] since the late seventies, especially during $p\bar{p}$ operation. This technique has already been used in the LHC.

The theory of Schottky signals for unbunched and bunched beams both in the longitudinal and transverse plane is well developed (e.g. [3]-[5]). In the case of an unbunched beam the longitudinal Schottky spectra gives the particle distribution in revolution frequencies and therefore in particle momentum. For the bunched beam, information about the momentum spread (dispersion) can also be extracted in most cases [6].

The PD Schottky is a special case of the bunched beam longitudinal Schottky signal, different from the usual technique since it uses only one selected piece of information from the beam current - its (average) peak amplitude. This method is in fact closer to the unbunched beam Schottky spectra in that it also provides almost direct information about the particle distribution in oscillation frequency, which for an unbunched beam is the revolution frequency and for a bunched - the synchrotron frequency [7]. The deviation of the PD Schottky spectrum from the synchrotron frequency distribution is mainly defined by the experimental set-up.

PEAK DETECTED SIGNAL

The peak detected signal is used as a beam diagnostics tool to control beam lifetime and stability and can also be used as input for Schottky diagnostics. In the SPS and LHC a simple circuit, Fig. 1, consisting of fast switching diode and capacitor detects the peak of the bunch current signal

from the wide-band pick-up. The spectrum is obtained using the dynamic spectrum analyser.

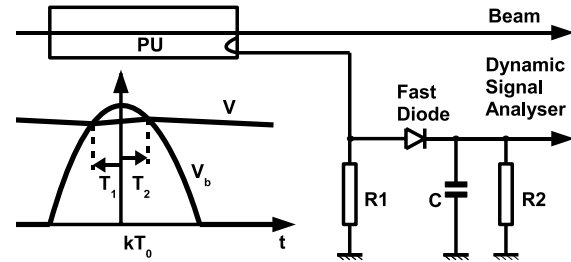


Figure 1: The simplified scheme of the bunch peak detection used for longitudinal Schottky signal in the SPS.

The parameters relevant to the Schottky measurements in the SPS and LHC and used in different examples below are presented in Table 1.

Table 1: The PD Schottky Parameters in the SPS and LHC

Parameter			SPS	LHC
revol. period	T_0	μs	23.0	88.9
RF harmonic	h		4620	35640
resistance	R_1	Ω	50	50
resistance	R_2	$\text{M}\Omega$	1.0	1.0
capacitance	C	pF	240	920
PD decay time	$1/\mu$	μs	240	920
PD growth time	$1/\alpha$	ns	12	12
acquisition time	T_a	s	1.6	3.2

The fast diode is open during the bunch passage with current I_b , when $V_b = I_b R_1 \geq V$. The voltage V measured at resistance R_2 during this time interval $(-T_1, T_2)$ can be found from the following equation (valid for $R_2 \gg R_1$)

$$\frac{dV}{dt} = \alpha(V_b - V), \quad (1)$$

where $\alpha C = 1/R_1 + 1/R_2$. The solution of eq. (1), valid for $-T_1 < t < T_2$, is

$$V(t) = \alpha \int_{-T_1}^t V_b(t') e^{-\alpha(t-t')} dt' + V(-T_1) e^{-\alpha(t+T_1)}. \quad (2)$$

with additional conditions

$$V(-T_1) = V_b(-T_1), \quad (3)$$

$$V(T_2) = V_b(T_2). \quad (4)$$

TRANSVERSE SCHOTTKY AND BTF MEASUREMENTS AND SIMULATIONS IN SPACE-CHARGE AFFECTED COASTING ION BEAMS

S. Paret, V. Kornilov, O. Boine-Frankenheim, GSI, Darmstadt, Germany
T. Weiland, Technische Universität Darmstadt, Darmstadt, Germany

Abstract

A study of the transverse dynamics of coasting ion beams with moderate space charge is presented. An analytic model based on the dispersion relation with a linear space-charge force is used to describe the impact of space charge on transverse beam transfer functions (BTFs) and the stability limits of a beam. The dielectric function obtained in this way is employed to describe the transverse Schottky spectrum with linear space charge as well. The difference between space charge and impedance effects is highlighted. An experiment performed in the heavy ion synchrotron SIS-18 at GSI to detect space-charge effects at different beam intensities is explicated. The measured transverse Schottky spectra, BTFs and stability diagrams are compared with the analytic model. The space-charge parameters evaluated from the Schottky and BTF measurements are compared with estimations based on measured beam parameters. Furthermore, particle tracking simulations demonstrating the impact of collective effects on the Schottky and BTF diagnostics are presented. The simulation results are used to verify the space-charge model.

INTRODUCTION

GSI's heavy ion synchrotron SIS-18 will serve as a booster for the projected FAIR accelerators [1]. For this purpose, the linear accelerator UNILAC and SIS-18 have to accelerate beams of unprecedented intensity. The accompanying collective effects may degrade the beam quality and cause particle losses due to instabilities. Therefore collective effects in ion beams are investigated at GSI.

In SIS-18, where the particle energy is low, space charge is a major concern as it is known to inhibit Landau damping of coherent beam instabilities [2, 3]. Furthermore the output of standard diagnostic tools for the accelerator operation, like Schottky diagnostics and beam transfer functions (BTFs), has to be interpreted taking into account space-charge effects. As shown in this report, an analytic model, related to the well known model for impedances, can be used to describe the impact of space charge on transverse Schottky or BTF signals as long as the nonlinear components of the self-field can be neglected. It allows also to retrieve the fractional part of the working point which cannot be read directly from the signals due to an intensity dependent distortion. In the next section this model introduced. The following sections an experiment and computer

simulations are described and their output is compared to the space-charge model. A more detailed discussion of the topics of this article can be found in Refs. [4, 5, 6].

LINEAR SPACE CHARGE AND BEAM DIAGNOSTICS

The current fluctuation in a coasting ion beam produces a longitudinal Spectrum, consisting of a series of bands at integer multiples, m , of the revolution frequency f_0 . Due to the incoherent betatron motion of the particles a fluctuation of the beam's dipole moment arises and leads to the transverse Schottky spectrum. At low intensity the side bands forming this spectrum are located at frequencies [7]

$$f_m^\pm = f_0(m \pm Q_f), \quad (1)$$

where the $+$ refers to the upper side band of the m^{th} longitudinal band and the $-$ to the corresponding lower side band. Q_f is the fractional part of the working point.

The Schottky bands of a beam devoid of collective effects reflect the momentum distribution of the beam. The rms width of the longitudinal Schottky spectrum reads

$$\sigma_m = m|\eta|f_0\sigma_p, \quad (2)$$

where we introduced the slip factor η and the relative momentum spread σ_p . The rms width of the side bands depends in addition on the full tune Q and the chromaticity ξ by virtue of

$$\sigma_{m,0}^\pm = |m \pm (Q_f\eta - \xi Q)|f_0\sigma_p. \quad (3)$$

Exciting a Schottky side band with noise or a time harmonic signal and division of the response by the excitation yields the transverse BTF [8]

$$r_0(z) = \mp \int_{-\infty}^{\infty} \frac{P_0(\tilde{z})}{z - \tilde{z}} d\tilde{z} \quad (4)$$

where $z = (f_{m,0}^\pm - f)/\sigma_m^\pm$ is the normalized frequency, P_0 the Schottky side band under consideration and z the particle momentum divided by σ_p . The BTF of a beam with a Gaussian momentum distribution is the complex error function [9],

$$r_0(z) = \mp i \sqrt{\frac{\pi}{2}} \left[1 - \operatorname{erf} \left(\frac{iz}{\sqrt{2}} \right) \right] e^{-z^2/2}. \quad (5)$$

STUDIES OF THE EFFECT OF 2ND HARMONIC ON THE E-P INSTABILITY AND RF CONTROL OF INSTABILITIES *

V. Danilov[#], Z. Liu, ORNL, Oak Ridge, TN, U.S.A.

Abstract

The dependence of the electron-proton instability threshold on the 2nd harmonic voltage and on the longitudinal profile in general is observed in the Spallation Neutron Source ring. Possible explanations of this phenomenon are discussed in the paper. The most optimal RF configuration to mitigate instabilities is presented.

INTRODUCTION

The Spallation Neutron Source (SNS) Ring was designed and optimized for very intense beams with the number of protons above 10^{14} per pulse. Once this intensity was reached, a few instabilities were observed [1], with the electron-proton (e-p) instability being the strongest. This instability depends on accumulation of electrons in the vacuum chamber, which, in turn, depends on the longitudinal beam distribution. There are many papers on this subject (see, e.g. [2]), and the identified mechanisms of accumulation for long proton bunches are separated into two classes: single pass and multipass accumulation (see, e.g. [2]). They are often interrelated, but we believe the first one is the main source of electron production in the SNS ring. In our paper we focus on the single pass accumulation and its dependence on the longitudinal beam distribution.

SINGLE PASS ELECTRON ACCUMULATION AND ITS DEPENDENCE ON THE BEAM DISTRIBUTION

The main process leading to large density electron accumulation is secondary emission of electrons from charged particles accelerated in the electric field of the proton beam. Predominantly, those particles are electrons from residual gas in the vacuum chamber, electrons scraped from the vacuum chamber by lost protons, etc. The yield is measured and described in many papers. Here we present a fit to the yield as a function of incident electron energy from [3]. Figure 1 shows the dependence of true secondary electron yield versus energy of the incident electrons with zero incident angle on stainless steel (SS) and titanium nitrate (TiN) coated SNS vacuum chambers (most of the SNS vacuum chamber in the ring is coated with TiN). The maximal yield is larger for the stainless steel but in our regions of interest of energies around 100 eV they almost coincide.

*Research sponsored by Laboratory Directed Research and Development Program of Oak Ridge National Laboratory, managed by UT-Battelle, LLC, for the U. S. Department of Energy under Contract No. DE-AC05-00OR22725.

[#]daniilovs@ornl.gov

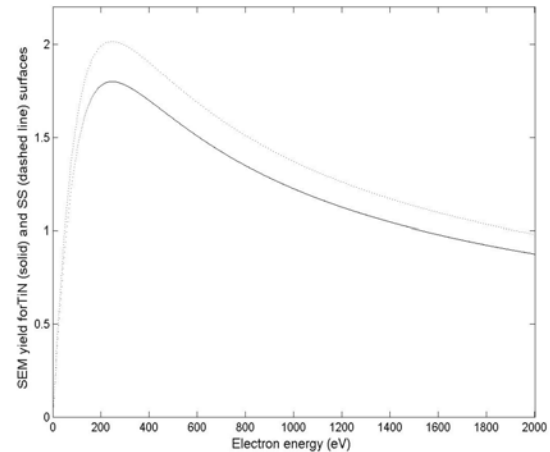


Figure 1: Secondary emission yields for stainless steel (dashed line) and titanium nitrate SNS coating (solid line) as a function of energy of incident electrons.

Most of the electrons due to secondary emission are generated at the trailing edge of the proton beam. The reason for this is simple – electrons near the walls of vacuum chamber are attracted by the proton beam as it passes by. Since the density of the beam is decreasing, the electrons are accelerated more during their pass into the beam than they are decelerated during their pass out of the beam. The resulting effect is that they acquire a rather large energy, and when they strike the opposite side of the wall there is enough energy to produce more than 1 electron on average per one strike.

The SNS maximum intensity ring beam can be approximated as a beam with $N=1.4 \cdot 10^{14}$ protons, a longitudinal distribution represented by an equilateral triangle with a trailing edge duration of 300 ns, and a round transverse distribution with r.m.s. radius 1 cm. The vacuum chamber radius is 10 cm. The incident electron energies at the trailing edge for these beam parameters range from 60 eV at the center of the beam, when the trailing edge begins, to 220 eV at the end. For the SNS chamber the yield for these energies ranges from 1 to 1.75.

More important is to find the average number of electrons, produced by one electron at the center of the beam, or the average trailing edge yield. We plot it as a function of the trailing edge slope (in this paper we always use linear longitudinal density of the trailing edge to make our estimates). It can be made longer or shorter by changing the 2nd harmonic RF in the SNS ring and for the same intensity and triangular (but lopsided) distribution it can vary from 0.5 to infinity in units of length of the trailing edge for a symmetric triangular distribution with the same total length.

SPALLATION NEUTRON SOURCE OPERATIONAL EXPERIENCE AT 1 MW*

J. Galambos, on behalf of the SNS team SNS-ORNL, Oak Ridge, TN, USA

Abstract

The Spallation Neutron Source (SNS) has been operating at the MW level for about one year. Experience in beam loss control and machine activation at this power level is presented. Also experience with machine protection systems is reviewed, which is critical at this power level. One of the most challenging operational aspects of high power operation has been attaining high availability, which is also discussed.

RAMP-UP HISTORY

The power ramp-up history for the SNS is shown in Fig. 1. Operation at the MW level has been routine for the past year. Initially the power increased quite rapidly, sometimes doubling over short periods. Careful residual activation measurements were performed during this ramp-up, both to understand the level of beam loss and to also provide a predictive basis for anticipating activation during the rampup. Generally the activation scales closely with beam loss monitor response. There were some cases of activation where beam loss was not detected, in which case, loss monitors were either added or moved closer to the beam pipe to increase sensitivity to loss detection.

Throughout the beam ramp-up history to-date, the beam power has not been limited by excessive beam loss.

ACTIVATION HISTORY

Linac

Beam loss was not expected in the superconducting linac (SCL). However early in the power rampup, activation was detected, and subsequent movement of the loss monitors close to the beam-pipe confirmed beam loss. Over the first one to two years the beam loss and resultant activation increased roughly proportional to the beam power.

In 2009, a running mode of reduced transverse focusing resulted in lower beam loss per Coulomb of accelerated beam and the activation levels have stabilized. Figure 2a shows this progression of SCL activation, overlaid on the beam power history. The activation levels are measured about once a month during scheduled maintenance days, and are 30 cm from contact. There is variability in the time from beam shutoff. Typically the measurements are 1-2 days after neutron production ends, but beam study periods at lower power levels typically run until 1-2 hours before the measurements.

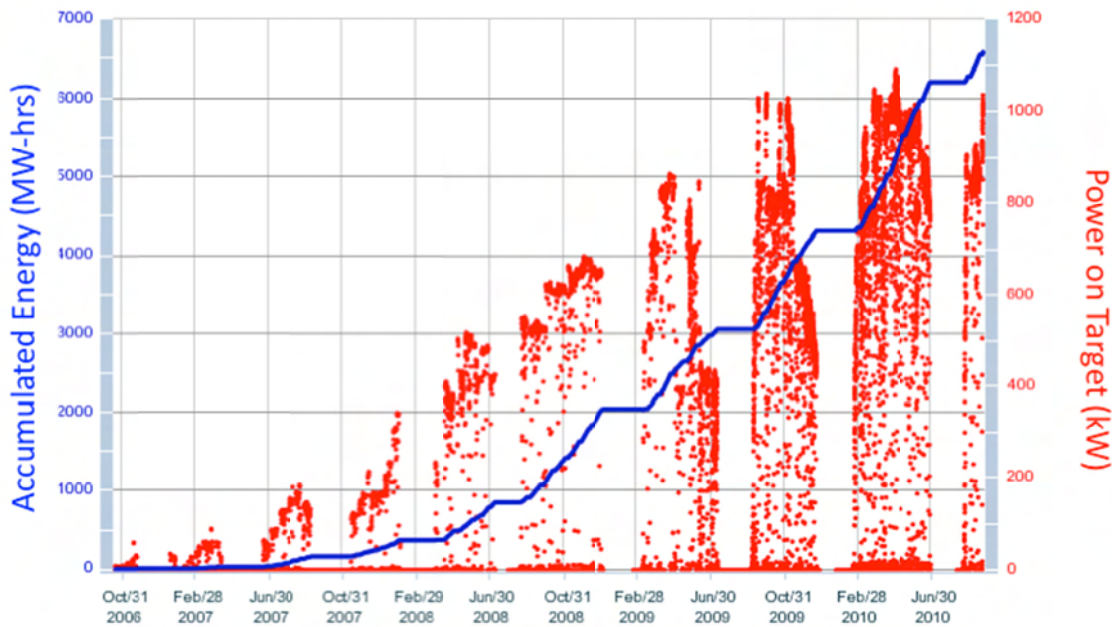


Figure 1: The history of the SNS power ramp-up to date.

* ORNL/SNS is managed by UT-Battelle, LLC, for the U.S. Department of Energy under contract DE-AC05-00OR22725.

HIGH POWER OPERATIONAL EXPERIENCE AT ISIS

D J S Findlay, on behalf of all staff in the ISIS Accelerator and Target Divisions,
 ISIS, Rutherford Appleton Laboratory, STFC, Oxfordshire OX11 0QX, UK

Abstract

Since 2008 ISIS has been running a second target station (TS-2) optimised for cold neutron production while continuing to run the original target station (TS-1) which began operating in 1984. The ISIS 800 MeV proton synchrotron cycling at 50 Hz produces a total beam power of 0.2 MW which is split between TS-1 and TS-2, 40 pps to TS-1 and 10 pps to TS-2. ISIS operations are described, including the first years of the new two-target-station operational régime.

INTRODUCTION

Although J-PARC [1], PSI [2] and SNS [3] are spallation neutron sources with higher power proton beams, ISIS [4] may still be the world's most productive spallation neutron facility in terms of science delivery, and since 2008 there have been two operational target stations at ISIS. Currently each year on average ~750 experiments are carried out involving ~1500 visitors who make a total of ~4500 visits (on average, very roughly, each visitor visits ISIS three times a year). These numbers include ~100 experiments and ~300 visits for the ISIS muon facility on TS-1. This paper summarises the experience at ISIS of running two target stations — experience that may be of interest to other facilities considering a second target station.

The ISIS First Target Station (TS-1) began operations in 1984, and since then neutron scattering work carried out on TS-1 has resulted in a total of ~9000 scientific publications.

The ISIS Second Target Station (TS-2) began operations in 2008. TS-2 was built to facilitate neutron scattering measurements on soft matter, biological samples, and advanced materials, and the target station is optimised for the production of high peak fluxes of cold neutrons in a way that was not possible on TS-1.

The key elements of the accelerator system at ISIS are as follows: H⁻ ion source at -35 kV, 665 keV 4-rod 202.5 MHz RFQ, 70 MeV 4-tank 202.5 MHz H⁻ drift tube linac, 52 m diameter 800 MeV proton synchrotron with six 1.3–3.1 MHz fundamental RF ferrite-loaded cavities and four 2.6–6.2 MHz second harmonic ferrite-loaded cavities. The key elements of target systems are as follows: a tantalum-coated tungsten plate primary target with two water moderators, a ~100°K liquid methane moderator and a 20°K liquid hydrogen moderator for TS-1; and a tantalum-coated tungsten cylinder primary target with a coupled hydrogen / solid methane moderator and a decoupled solid methane moderator for TS-2. There are twenty-six beam line instruments on TS-1 (both neutron and muon instruments), and currently seven neutron beam line instruments on TS-2; an additional six or seven instruments for TS-2 are foreseen under Phase 2

of the overall TS-2 project. ISIS is also host to MICE [5], the Muon Ionisation Cooling Experiment, an important step on the road to a practical neutrino factory. A schematic layout of ISIS is shown as Figure 1.

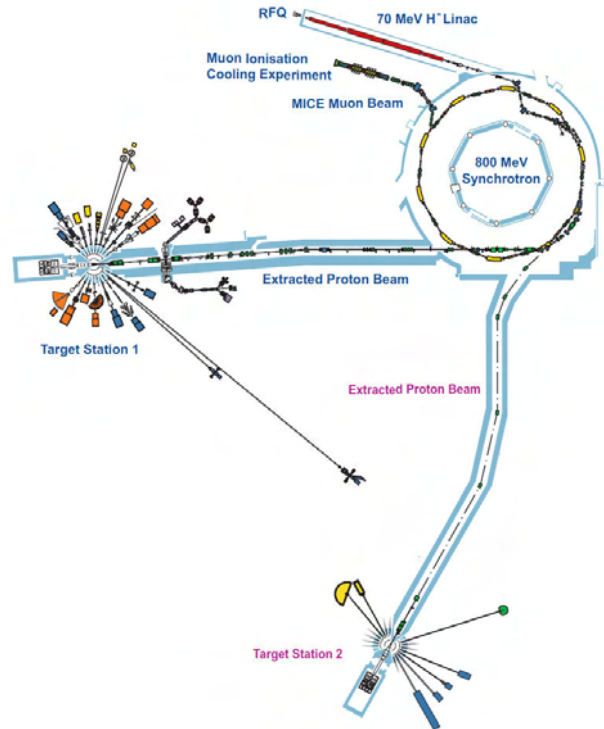


Figure 1: ISIS schematic layout.

AVAILABILITIES

Figure 2 (upper half) shows availabilities of the ISIS accelerator and target system over the past twelve years. (For each user cycle, ISIS machine availabilities are defined as (total number of beam pulses actually delivered to target) ÷ (total number of beam pulses originally scheduled to be delivered to target); everything that prevents beam from being delivered to target, e.g. off-time for re-tuning, accelerator faults, target faults, plant faults, and RAL site electricity supply faults, counts towards machine non-availability.) The average of the set of availabilities is 86%, and the standard deviation is 8%; availability appears to have become gradually worse with time. However, until and including 2003 there used to be the opportunity to add “run-on” to cycles with poor availabilities — whereby several “bad” days could be replaced by additional “good” days added to the end of the cycle — but this opportunity no longer exists. Adding run-on could lead to noticeable improvements in availabilities, as several days in a cycle several tens of days long can represent a ~10% effect. In order to make a

RECENT OPERATIONAL EXPERIENCE AT THE LANSCE FACILITY*

L. Rybarcyk[#], Los Alamos National Laboratory, Los Alamos, NM 87545, U.S.A.

Abstract

The Los Alamos Neutron Science Center (LANSCE) consists of a pulsed 800-MeV room-temperature linear accelerator and an 800-MeV accumulator ring. It simultaneously provides H⁺ and H⁻ beams to several user facilities that have their own distinctive requirements, e.g. intensity, chopping pattern, duty factor, etc.. This multi-beam operation presents challenges both from the standpoint of meeting the individual requirements but also achieving good overall performance for the integrated operation. Various aspects of more recent operations including the some of these challenges will be discussed.

INTRODUCTION

LANSCE is a multi-user, multi-beam facility that produces intense sources of pulsed, spallation neutron and proton beams in support of US national security and civilian research. It comprises a pulsed 800-MeV room temperature linear accelerator and 800-MeV proton storage ring and has been in operation for over 35 years. It first achieved 800-MeV beam on June 9, 1972. The facility, formerly known as LAMPF, routinely provided an 800 kW beam for the meson physics program. Presently, the LANSCE user facilities include:

- Proton Radiography (pRad) which provides high resolution, time-sequenced radiographs of dynamics phenomena,
- Weapons Neutron Research (WNR) that provides a source of unmoderated neutrons in the keV to multiple MeV range,
- Lujan which uses the proton storage ring (PSR) to create an intense, time-compressed proton pulse which is used to provide a source of moderated neutrons (meV to keV range),
- Isotope Production (IPF) which is a source of research and medical isotopes for the US, and
- Ultra-Cold Neutrons (UCN) which is a source of sub- μ eV neutrons for fundamental physics research.

The accelerator consists of separate H⁺ and H⁻ Cockcroft-Walton based injectors that produce 750-keV beams for injection into the 100-MeV drift tube linac (DTL). Each low energy beam transport (LEBT) contains magnetic quadrupoles for transverse focusing, a single-gap 201.25-MHz buncher cavity for initial bunching of the beam, and a beam deflector for "gating" beam into the linac. The H⁻ LEBT also contains a 16.77-MHz buncher for producing high-charge, individual micropulses and a slow-wave beam chopper for intensity modulating the H⁻ beams. The H⁺ and H⁻ beams are merged in a common LEBT that contains a single 201.25-MHz buncher cavity,

aka main buncher (MB), which performs the majority of the bunching for the standard linac beams and quadrupole magnets to achieve the final match into the linac. The DTL is an Alvarez style 201.25-MHz linac comprised of four independently powered tanks. The tanks contain magnetic quadrupoles in a FODO lattice. Following the DTL is a 100-MeV beam transport, aka the Transition Region (TR), which allows for independent matching, steering and phasing of the H⁺ and H⁻ beams into the next linac. It also contains a kicker magnet for extracting 100-MeV H⁺ beam for the IPF. Since there are currently no users of 800-MeV H⁺ beam, this magnet is operated in DC mode. Following the TR is the 805-MHz coupled-cavity linac (CCL) which accelerates beams up to 800 MeV. It consists of 44 independently powered modules, which have either two or four tanks. Each tank consists of a large number of identical accelerating and side mounted coupling cells. The magnetic quadrupole doublets, which are located between tanks, are arrayed in a FDO lattice. Beam steering magnets are located in the LEBT, TR and post linac beam transports.

Following the linac is a beam switchyard that employs DC magnets to separate the H⁺ and H⁻ beams. Pulsed kicker magnets are then used to direct H⁻ beam during some macropulses to the pRad or UCN facilities. Unkicked H⁻ beam pulses are directed toward the PSR or WNR facilities.

The proton storage ring (PSR) is an 800-MeV accumulator ring. It is a 10-sided FODO design with a 90.2 m circumference and employs a single ferrite loaded RF cavity operated at $h=1$. Two ferrite-loaded inductive inserts are employed to provide additional space-charge compensation of the beam. Direct H⁻ injection with injection painting is used in combination with a hybrid-boron-carbon (HBC) stripper foil[1] to achieve low-loss operation with better than 95% injection efficiency. The HBC foil produces acceptable first-turn losses with very good lifetime. Typically, the PSR operates at 20 Hz and provides beam to the Lujan spallation neutron target with one bunch containing $>3.3 \times 10^{13}$ protons.

RECENT OPERATIONS

The accelerator was designed to operate at 120 Hz. However, for the last several years has operated at 60 Hz due to limitations of the Burle 7835 power triode used in high-power amplifiers in the DTL. Typical beam macropulse length is 625 μ s which at 60 Hz requires ~5% linac RF duty factor. Peak beam currents are ~13 mA. Table 1 contains a summary of the typical beams parameters for the various user facilities presently in operation.

*Work supported by DOE under contract DE-AC52-06NA25396.

[#]lrybarcyk@lanl.gov

MEASURING CORRELATIONS BETWEEN BEAM LOSS AND RESIDUAL RADIATION IN THE FERMILAB MAIN INJECTOR*

Bruce C. Brown, Guan Hong Wu, Fermilab, Batavia, IL 60510, USA

Abstract

In order to control beam loss for high intensity operation of the Fermilab Main Injector, electronics has been implemented to provide detailed loss measurements using gas-filled ionization monitors. Software to enhance routine operation and studies has been developed and losses are logged for each acceleration cycle. A systematic study of residual radiation at selected locations in the accelerator tunnel have been carried out by logging residual radiation at each of 142 bar-coded locations. We report on fits of the residual radiation measurements to half-life weighted sums of the beam loss data using a few characteristic lifetimes. The data are now available over a multi-year period including residual radiation measurements repeated multiple times during three extended facility shutdown periods. Measurement intervals of a few weeks combined with variable delays between beam off time and the residual measurement permits sensitivity to lifetimes from hours to years. The results allow planning for work in radiation areas to be based on calibrated analytic models.

BASIC RELATIONSHIPS

The orbits used in Main Injector operation are quite stable. Most beam loss is at or near the injection energy of 8 GeV. Losses are dominated by the uncaptured beam loss from slip stack injection, beam in kicker gaps and 8 GeV beam lifetime issues. Variations are frequently due to small changes in the Booster beam quality. As a result, we will assume that the local geometry and energy of losses are always the same. Improvements in removal of beam from kicker gaps by anti-damping and improved collimation is responsible for the long term trends. With this assumption, the relation between Beam Loss Monitor (BLM) readings and residual radiation in the tunnel is fixed. We will explore our ability to correlate one BLM reading and residual radiation at some nearby point.

We illustrate this argument using Fig. 1 where we see a simulation of the residual radiation from beam loss in the collimation region of the Main Injector. Lost beam which was scattered by the primary collimator upstream is mostly captured in the secondary collimators but beam is also lost in other devices. The radiation fields for prompt radiation, residual radiation and absorbed dose are very similar.

The basis for linearly relating loss and residual radiation lies in the following arguments:

1. For a fixed loss pattern (as assumed), the prompt radiation field produced by losses will produce a distribution of isotopes in the devices near the beam. The number of radioactive nuclei will be proportional to the beam lost.

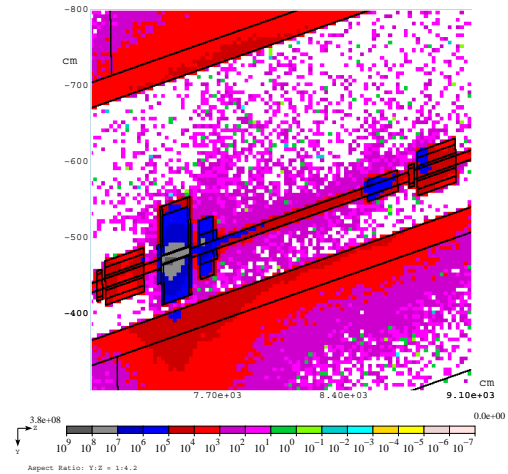


Figure 1: MARS simulation of loss region near Main Injector secondary collimator.

2. This radiation field will also produce ionization in nearby Beam Loss Monitors (BLM's) and the ionization signal will also be proportional to the number of lost protons.
3. The radioactive nuclei will emit radiation including gamma rays which can be detected by the Geiger counter used to monitor residual radiation. At each monitor point, the efficiency with which the Geiger counter records signals due to the spatial pattern of isotopes and the spectra of the radioactive decays is dependent only on the isotope being detected.

MEASUREMENTS

Residual Radiation Data

In preparation for higher intensity operation for the Main Injector neutrino program (NuMI), residual radiation measurements were undertaken beginning in 2004 to identify loss issues. Locations of interest were identified. A radiation meter was purchased with two internal Geiger tubes (for measurements from 50 micro-Roentgen/hr to 100 Roentgen/hr), a bar code reader to identify monitoring locations and memory to store results. Bar coded tags were installed. Measurements with this system have been carried out as access time permitted since 10 October 2005 [1]. For some accesses, the delay between beam loss and residual radiation measurement was a couple of hours. Intermediate

* Operated by Fermi Research Alliance, LLC under Contract No. DE-AC02-07CH11359 with the United States Department of Energy.

OPERATIONAL PERFORMANCE OF THE LHC COLLIMATION

S. Redaelli*, R.W. Assmann, R. Bruce, A. Rossi, D. Wollmann, CERN, Geneva, Switzerland

Abstract

The collimation system of the CERN Large Hadron Collider (LHC) is the most advanced cleaning system built for accelerators. It consists of 98 two-sided and 2 one-sided movable collimators of various designs and materials, for a total of 396 degrees of freedom (2 motors per collimator jaw), that provide a multi-stage cleaning of beam halo as well as a crucial role for the LHC machine protection. Collimators can be moved with functions of time to guarantee the optimum settings during energy ramp and betatron squeeze. The system has been commissioned with proton beams for the 3.5 TeV LHC runs and has ensured a safe operation, providing a close to nominal cleaning performance in the initial LHC operational phases. In this paper, the system performance achieved in the early LHC commissioning in the 3 MJ stored energy regime is presented.

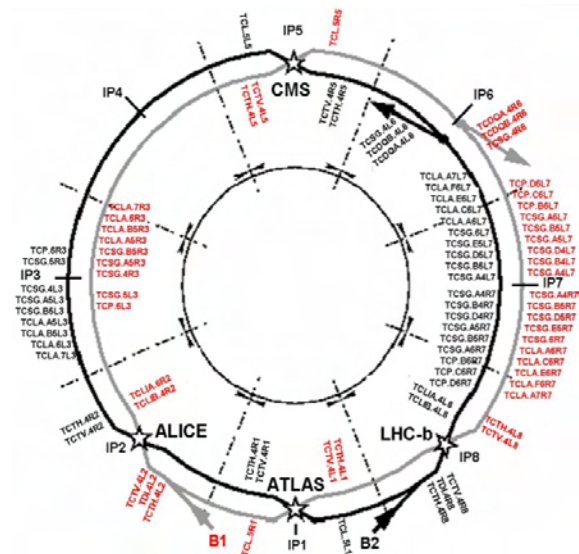


Figure 1: LHC layout with collimator locations [2].

INTRODUCTION

The collimation system of the Large Hadron Collider (LHC) has been designed to fulfill the high energy challenge of 362 MJ stored beam energy. A complex and distributed system is needed to achieve the required cleaning performance and to ensure the passive machine protection [1]. The system saw the first exciting beam commissioning in 2009 and has become fully operational in 2010. In this paper, the preliminary analysis of the collimator performance achieved with the operation in the 2–3 MJ regime is presented. After a brief recapitulation of the system layout, the strategy for the collimator setting calculation is presented and the concept of beam-based parameters is introduced. The cleaning performance achieved at 3.5 TeV is then presented and some conclusions are drawn.

LHC COLLIMATION SYSTEM LAYOUT

The LHC collimation system layout is given in a companion paper [1]. An illustrative scheme with the collimator locations around the ring, taken from [2], is given in Fig. 1. Hundred movable collimators with different roles are installed (Table 1). The back-bone of the system is provided by two warm interaction regions (IRs): the momentum (IR3) and betatron (IR7) cleaning IRs, with 28 collimators per beam. Robust primary (TCP) and secondary (TCSG) collimators made of a Carbon fiber composite (CFC) define the momentum and betatron cuts for the beam halo. Additional high-Z material absorbers (TCLA) protect the superconducting magnets downstream of the warm insertions. In the experiment interaction regions (IR1/2/5/8),

Table 1: List of Movable LHC Collimators

Functional type	Name	Plane	Num.	Material
Primary IR3	TCP	H	2	CFC
Secondary IR3	TCSG	H	8	CFC
Absorbers IR3	TCLA	H,V	8	W
Primary IR7	TCP	H,V,S	6	CFC
Secondary IR7	TCSG	H,V,S	22	CFC
Absorbers IR7	TCLA	H,V	10	W
Tertiary IR1/2/5/8	TCT	H,V	16	W/Cu
Physics debris absor.	TCL	H	4	Cu
Dump protection	TCSG	H	2	CFC
	TCDQ	H	2	C
Inj. prot. (lines)	TCDI	H,V	13	CFC
Inj. prot. (ring)	TDI	V	2	C
	TCLI	V	4	CFC
	TCDD	V	1	CFC

local protection is provided by 16 tertiary (TCT) collimators and by 4 physics debris absorbers (IR1 and IR5 only). Injection and dump protection elements are installed in IR2, IR8 and IR6. Various passive absorbers and masks are also available for dedicated local protections (not discussed here).

The collimators are installed in a variety of azimuthal orientations (see Fig. 2) and materials (CFC, Cu, W). Robust TCP and TCSG collimators sit at about 6 and 7 sigmas from the circulating beams (minimum full gap at 3.5 TeV is 3 mm, see the IR7 case in Fig. 3). Higher-Z collimators, more efficient to catch electromagnetic showers but also more fragile against beam losses, have typical settings above 10 sigmas.

* Stefano.Redaeli@cern.ch

BEAM LOSS AND RESIDUAL DOSE AT 100 KW USER OPERATION IN THE J-PARC ACCELERATOR

K. Yamamoto and J-PARC Beam Commissioning Team, J-PARC, Tokai-mura, Japan

Abstract

The accelerator facilities in J-PARC have been commissioned since January 2007. According to the progress of beam commissioning and construction of accelerators and experimental facilities, operational beam power becomes larger. The RCS produces 120 kW beam to MLF and the MR provides 50 kW beam to Neutrino target. In such high intensity operation, Linac ACS section, RCS injection and arc section, and MR collimator section become slightly higher residual dose area. We try to improve these losses before it is too late.

INTRODUCTION

The Japan Proton Accelerator Research Complex (JPARC) project is a joint project of Japan Atomic Energy Agency (JAEA) and High Energy Accelerator Research Organization (KEK). The accelerator complex consists of a linac (an acceleration energy is 181 MeV so far and it will upgrade to 400 MeV by installing Annular Coupled Structure linac (ACS) in 2013), a 3 GeV Rapid-Cycling Synchrotron (RCS), and a 50 GeV synchrotron Main Ring (MR) [1]. The beam commissioning of accelerator facilities started in January 2007. Construction of J-PARC facilities and beam commissioning were continued, now acceleration beams are provided to a materials and life science experimental facility (MLF) for the neutron experiments, a hadron experimental hall, and a neutrino target which produces a neutrino beam to Kamiokande. In

this paper, we present the histories of operational beam power and residual dose distributions after operation of these three accelerators.

LINAC

The J-PARC linac commissioning started in January 2007. The beam power of linac was increased with the advance of commissioning and construction of other facilities. Figure 1 shows the history of linac output power and residual dose rate since January 2007.

Residual dose values were chosen at some representative points. During the beam commissioning period from January 2007 to November 2008, we only used low repetition beam for commissioning and there were no significant residual dose. But when we started high duty user operation at a repetition rate of 25 Hz, more than 200 $\mu\text{Sv/h}$ dose rate was observed at the first bending magnet of the Linac – 3GeV RCS Beam Transport (L3BT) line (Blue plot in Fig. 1). We found that the residual dose on the inside (a H- beam direction) of the magnet was smaller than that on the outside (a proton beam direction) of the magnet. From the distribution of residual dose on the magnet, we considered that the source of this dose distribution was caused by the loss of proton beam. This proton beam was generated by the scattering of H- beam and the residual gas in the transport line between the ion source and Radio Frequency Quadru-

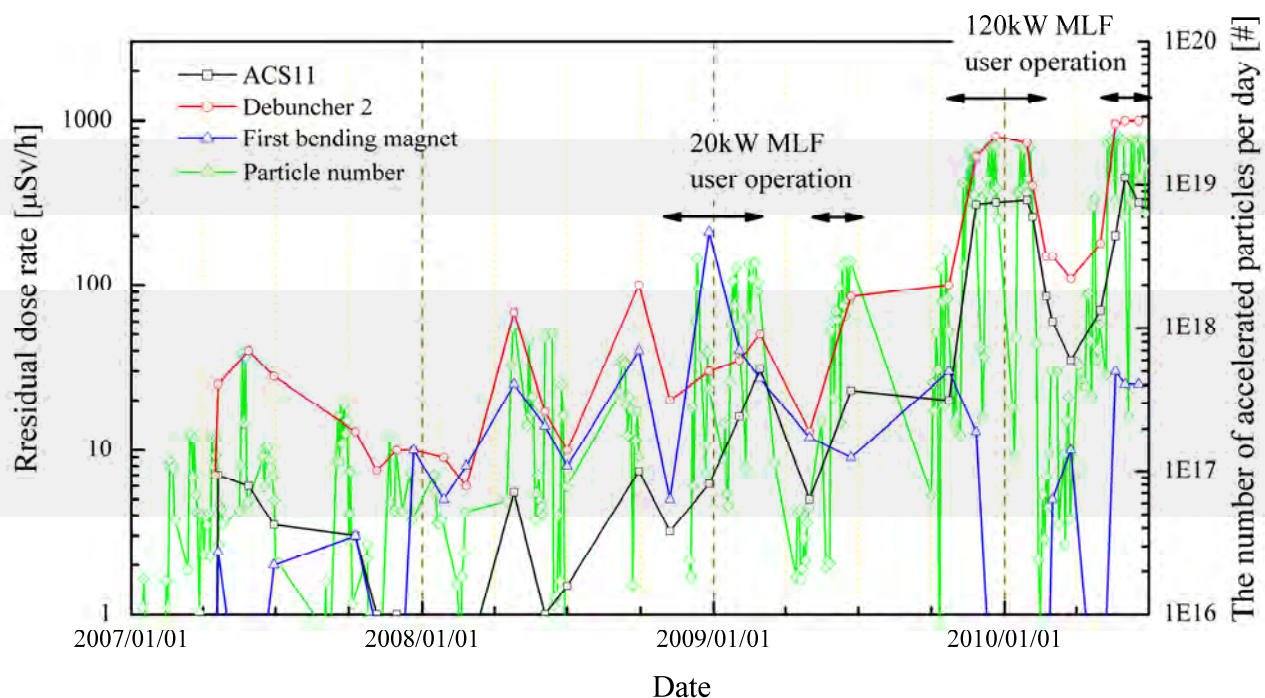


Figure 1: History of the linac operation and residual dose.

LINAC4 COMMISSIONING STRATEGY

J.B. Lallement, G. Bellodi, M. Eshraqi, M. Garcia Tudela, A.M. Lombardi, P. A. Posocco, E. Sargsyan, J. Stovall, CERN, Geneva, Switzerland

Abstract

Linac4 is a 160 MeV H^- ions accelerator, which will replace the 50 MeV proton Linac (Linac2) as injector for the CERN complex from 2016. The higher output energy together with charge-exchange injection will allow increasing beam intensity in the following machines. Linac4 is about 100 m long, normal-conducting, and will be housed in a tunnel, 12 m below ground, on the CERN Meyrin site. The low energy front-end, consisting of a 45 keV source, a 3 m long RFQ and a 3 MeV chopper line, will be commissioned starting next year in a temporary location. It will then be moved to the tunnel at the end of 2012 and the commissioning in situ will be done progressively with the installation of the accelerating structures. The preparation of 4 commissioning stages (12, 50, 100, and 160 MeV) is of key importance to meet the goals of beam performance and reliability. An extensive campaign of simulation is in progress to define the necessary measurements and the required diagnostics accuracy for a successful set-up of the transverse and longitudinal parameters of the machine. This paper presents the results of the simulations and the measurement strategy.

INTRODUCTION

Linac4 is a normal conducting, 160 MeV H^- ions accelerator, presently under construction at CERN which will upgrade the proton accelerator complex replacing the 50 MeV Linac2 and provide higher intensity beams [1]. The low energy front-end is composed of a 2 MHz rf volume source, a two solenoids Low Energy Beam Transport, a 3 MeV Radio Frequency Quadrupole resonating at 352.2 MHz and a Medium Energy Beam Transport, housing a beam chopper device. The acceleration up to 160 MeV is provided by three Drift Tube Linac tanks, a Cell Coupled Drift Tube Linac (21 tanks coupled in 3's) and 12 Pi-Mode Structure tanks. The first commissioning stage will start next year with the 3 MeV test stand. During this stage, the RFQ will be commissioned as well as the chopper-line. A dedicated detector, the Beam Shape and Halo Monitor, will characterize the performance of the chopper. The high energy part (from 3 to 160 MeV) will be commissioned in 2013, when the accelerating structures are installed in the tunnel. In the following we give some highlights of the simulation work done for the preparation of the commissioning.

COMMISSIONING STAGES

Linac4 will be commissioned in several stages, starting from the low energy end (3 MeV test stand) and after alternating phases of commissioning at intermediate

energies (12, 50, 100,160 MeV) and installations. The different stages are detailed below:

- Stage1: 3 MeV test stand, commissioning of the source, LEBT, RFQ and chopper line. This stage of the commissioning, starting next year, will take place in the PS south hall and will last until installation in the tunnel will start at the end of 2012.
- Stage2: The LEBT, RFQ and chopper line will be re-commissioned in the tunnel (2013).
- Stage3: The DTL tank1 (12 MeV) will be installed and commissioned.
- Stage4: DTL tanks 2&3 are installed and commissioned.
- Stage5: CCDTL is installed and commissioned.
- Stage6: PIMS is installed and commissioned.

AVAILABLE DIAGNOSTICS

Besides the permanent diagnostics (listed in table 1), a movable diagnostic bench has been foreseen as part of the Linac4 commissioning plan to characterize the H^- beam properties at the exit of the front end (RFQ and MEBT) at 3 MeV and of the first DTL tank at 12 MeV. The low energy end is the most critical for beam quality control (50% of the emittance growth happens before 3 MeV) and also the most critical for housing diagnostics (free space for non-active equipment is limited to a minimum in order to avoid the effects of uncompensated space charge forces). The bench will be composed of two sections: a spectrometer and a straight line. The spectrometer line will be used for longitudinal plane measurements of the beam energy spread and average energy with the purpose of cross-calibrating the Time Of Flight measurements and to find the set point of the rf structures (buncher + DTL tank) characterisation. The straight line will be used to characterize the beam trajectory, its emittance with a slit and grid system and transverse profile, the intensity and the longitudinal shape. The layout of the bench is shown in Figure 1.

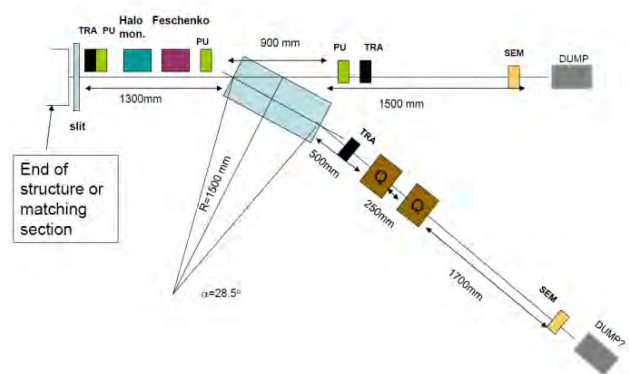


Figure 1: Diagnostic bench layout.

EFFECT OF SPACE CHARGE ON TRANSVERSE INSTABILITIES

V. Balbekov[#], Fermilab, Batavia, IL 60510, U.S.A.

Abstract

Transverse instability of a bunched beam is discussed in the paper with space charge effects taken into account. It is assumed that the Space Charge Impedance is a dominant part of the entire beam coupling impedance, which is a very characteristic case for high-brightness proton synchrotrons. Equation of intra-beam oscillations is derived and investigated including shape and frequency of the head-tail modes. Special attention is focused on Landau damping and threshold of possible instability.

INTRODUCTION

Transverse coherent instability of a bunched beam have been studied first by C. Pellegrini [1] and M. Sands [2] with intra-bunch degrees of freedom taken into account, but without space charge effects. A solution with these effects was presented later by F. Sacherer using boxcar model [3]. A crucial part of the space charge in Landau damping and instability threshold of bunched beams was demonstrated first in Ref. [4] for rather high synchrotron frequency. Later the problems were studied in Ref. [5-7], the last presenting most detailed study of the role of space charge impedance in the bunched beams instabilities.

Space Charge Impedance (SCI) is a part of an entire beam coupling impedance, which takes into account only local electromagnetic field carried by a beam. It is a purely imaginary value not depending on frequency and unable to cause the beam instability by itself. Real part of the impedance is just the one directly responsible for the instability. In principle, any retarding (wake) field is capable to generate such an addition. However, SCI can drastically affect intra-bunch coherent oscillations (head-tail modes) including their frequency, shape, and particularly threshold of possible instability. The effect is especially important in proton synchrotrons where SCI, typically, constitutes a significant or even dominant part of the impedance. Under these assumptions, the wake field can be treated as a small perturbation which controls mutual motion of the bunches (collective beam modes) including the instability growth rate. Just from this standpoint the problem is treated in this work. Incoherent space charge tune shift is used further as a convenient measure of the SCI.

COASTING BEAM LANDAU DAMPING

It is a well known fact that, at dominant SCI, transverse instability of a coasting beam is possible if space charge tune shift about exceeds the incoherent tune spread:

$$\Delta Q_{incoherent} > C \times \delta Q, \quad C \approx 1 \quad (1)$$

This relation has a simple physical explanation:

[#]balbekov@fnanl.gov

Self-sustaining coherent oscillations of a beam are impossible if their frequency falls within a range of incoherent betatron frequencies.

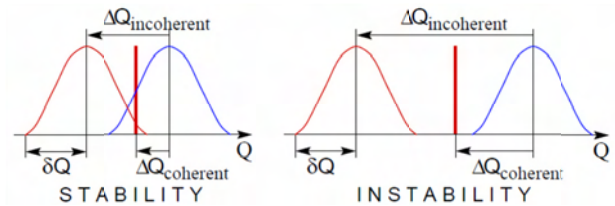


Figure 1: Landau damping origin of coasting beams.

Figure 1 is provided to illustrate the statement. Blue curve present a bare tune distribution, red one – the same distribution shifted by space charge force, and vertical red line depicts the coherent tune. Two cases are possible as it is shown in the picture. At comparably low intensity, the coherent tune could not leave the incoherent range (left-hand figure). Then the attendant electric field would excite *contra-phase* oscillations of particles, which individual tunes are located either lower or higher the coherent one. That would result a quick transfer of energy from coherent form to incoherent one, that is the beam heating and decay of the coherence. This effect is known as Landau Damping (LD). It does not arise at higher intensity when the coherent frequency leaves the incoherent range (right-hand figure). Then the coherent field excites *in-phase* oscillations of all the particles, supporting the coherence and creating conditions for instability. As it is seen from the picture, corresponding instability condition is

$$|\Delta Q_{incoherent} - \Delta Q_{coherent}| > \delta Q \quad (2)$$

This relation can be written down as Eq. (1) because $\Delta Q_{coh} \ll \Delta Q_{incoh}$ in practice. Coefficient C depends on the bunch shape being about 1.2–1.1 for Gaussian distribution truncated on the level of $(3-5)\sigma$.

BUNCHED BEAM LANDAU DAMPING

There is no doubt that above declared principle is valid for bunched beams as well. However, very different physical phenomena can be responsible for incoherent tune spread of coasting and bunched beams. In first case, the main source is, usually, momentum spread multiplied by chromaticity. However, as it was shown in Ref. [1] and [2], the instability threshold of bunched beams does not depend on chromaticity at all (though the instability growth rate can drastically depend on it). It means also that averaged in synchrotron phase tunes of the particles and corresponding tune spread only can affect coherent transverse motion of the bunch.

HEAD-TAIL BUNCH DYNAMICS WITH SPACE CHARGE

Vladimir Kornilov and Oliver Boine-Frankenheim,
 GSI, Planckstr. 1, 64291 Darmstadt, Germany

Abstract

Significant progress has been made recently in the understanding of the effects of direct space charge on the transverse head-tail bunch dynamics. Different analytic approaches for head-tail modes in bunches for different space-charge parameter regimes have been suggested. Besides head-tail eigenmode characteristics, Landau damping in a bunch exclusively due to space charge has been predicted. In this contribution we compare results of particle tracking simulations with theoretical predictions for the eigenfrequencies and eigenfunctions of head-tail modes in a Gaussian bunch. We demonstrate the space-charge induced Landau damping in a bunch and quantify damping rates for different modes and space-charge tune shifts. Under conditions below the mode coupling threshold we study the head-tail instability with space charge. Our results show that the space-charge induced damping can suppress the instability for moderately strong space charge. For strong space charge the instability growth rates asymptotically reach constant values, in agreement with theoretical predictions.

INTRODUCTION

The standard head-tail theory, i.e. the model of Sacherer [2, 3], does not include the effect of an incoherent tune spread on head-tail modes. A model for the head-tail instability with arbitrary space charge has been suggested in Ref. [4], for a bunch in a square-well potential and an airbag bunch distribution in the longitudinal phase space. Only in recent works [5, 6] analytical treatments of head-tail modes with space charge for realistic bunch distributions (as e.g. Gaussian) have been proposed. However, numerical simulations appear to be indispensable for a comprehensive stability analysis in different beam parameter regimes and with various collective effects taken into account. Here, we present particle tracking simulations for head-tail modes in a Gaussian bunch with space charge. We use two different particle tracking codes, PATRIC [7] and HEADTAIL [8], in order to compare different numerical implementations. As an exemplary instability driving source, the resistive-wall impedance is considered. In this work we consider the single-bunch head-tail instability for the parameters well below the threshold for mode coupling.

An important phenomenon, discussed in Refs. [5, 6], is Landau damping in a bunch exclusively due to space charge. In a coasting beam space charge can not provide Landau damping of its own, even if the coherent frequency

overlaps the tune spread induced by nonlinear space charge [9]. In the case of a bunch, the synchrotron motion plays an important role and the space-charge tune spread due to the longitudinal density profile provides Landau damping. Here, we demonstrate this Landau damping in particle tracking simulations and examine its role for the stability of head-tail modes at moderate and stronger space charge.

BUNCH SPECTRUM WITH SPACE CHARGE

There is no simple analytical answer for the space-charge effect on head-tail modes in bunches with an arbitrary bunch profile $\lambda(\tau)$. However, such a theory could be very useful for code validation and for the interpretation of simulation results. An analytical solution for head-tail modes in bunches with arbitrary space charge has been derived in Ref. [4]. The model assumes an airbag distribution in the longitudinal phase space and a square-well (or barrier) potential and thus a constant line density, which means a constant ΔQ_{sc} . The longitudinal momentum distribution has two opposing flows of particles $[\delta(v_0 - v_b) + \delta(v_0 + v_b)]$, the synchrotron tune in this bunch is $Q_s = v_b / (2\tau_b R f_0)$, where τ_b is the full bunch length and f_0 is the revolution frequency. The model considers “rigid flows”, i.e. only dipole oscillations without variation in the transverse distribution of the flows are included. It also assumes that all betatron tune shifts are small compared to the bare tune $|\Delta Q| \ll Q_0$. The resulting tune shift due to space charge (without impedances) is given by

$$\Delta Q = -\frac{\Delta Q_{sc}}{2} \pm \sqrt{\frac{\Delta Q_{sc}^2}{4} + k^2 Q_s^2}, \quad (1)$$

where “+” is for modes $k \geq 0$.

In order to verify the space-charge implementation for long-time simulations with a particle tracking code, we have introduced the barrier-airbag bunch distribution in both PATRIC and HEADTAIL codes. For the transverse space charge force, the “frozen” electric field model was used, i.e. a fixed potential configuration which follows the mass center for each single slice. This approach is justified for the “rigid-slice” regime and can be considered as a reasonable approach for moderate and strong space charge [10, 5]. A round transverse cross-section and a homogeneous transverse beam profile were used in the simulations in this work. An excellent agreement between the airbag theory [Eq. (1)] and simulations has been achieved, a detailed description of the code validation was presented in

THE STUDY OF THE SPACE CHARGE EFFECTS FOR RCS/CSNS

S. -Y. Xu, S. -X. Fang, S. Wang[#]

Institute of High Energy Physics (IHEP), Beijing, 100049, China

Abstract

RCS is a key component of CSNS. In this kind of high intensity RCS, the beam is space charge dominated, and the space charge effects are the main source of beam loss. Many simulation works were done for the study of space charge effects for CSNS/RCS by using code ORBIT and SIMPSONS.

INTRODUCTION

The China Spallation Neutron Source (CSNS) is an accelerator-based facility. It operates at 25 Hz repetition rate with an initial design beam power of 100 KW, and is capable of upgrading to 500KW. CSNS consists of a 1.6 GeV Rapid Cycling Synchrotron (RCS) and a 80 MeV linac, which can be upgraded to 250-MeV for beam power upgrading to 500 KW. RCS accumulates 80 MeV injection beam, and accelerates the beam to the design energy of 1.6 GeV, and extracts the high energy beam to the target. The lattice of the CSNS/RCS is a triplet based four-fold structure. Table 1 shows the main parameters of the lattice [1].

Due to the high beam density and high repetition rate, the rate of beam loss must be controlled to a very low level. In this kind of high power RCS, especially in the low energy end, the beam is space charge dominated, and the space charge effects can result in emittance growth and halo formation, which may contribute to beam losses. The space Charge effects are the most important issue of CSNS/RCS, which limit the maximum beam intensity, as well as the beam power. Many simulations works were done to study the space charge effects of CSNS/RCS by using the codes ORBIT and SIMPSONS. The simulation results are the foundation of physics design and the choice of design parameters.

SPACE CHARGE EFFECTS DURING INJECTION

In order to decrease the longitudinal beam loss, the longitudinal injection scenario with 50% chopping rate is adopted. In the CSNS, anti-correlated painting is employed to obtain a large transverse beam size which can significantly reduce the space charge tune shift of the accumulated beam. The emittance is painted from small to large in horizontal direction, while from large to small in vertical direction during 200-turn injection in 0.39 ms, with peak linac beam current of 15 mA.

During injection, the kinetic linac beam is fixed, while the kinetic energy of the synchronous particle in the CSNS/RCS varies with the dipole field B of the RCS:

$$E_K = E_0(\sqrt{1 + 6.569B^2(T) - 1}) \quad (1)$$

where E_0 is the rest energy of proton.

Table 1: Main Parameters of the Lattice

Circumference (m)	227.92
Superperiod	4
Number of dipoles	24
Number of long drift	12
Total Length of long drift (m)	75
Betatron tunes (h/v)	4.86/4.78
Chromaticity (h/v)	-4.3/-8.2
Momentum compaction	0.041
RF harmonics	2
RF Freq. (MHz)	1.0241~2.444
RF Voltage (kV)	165
Trans. acceptance ($\mu\text{m}\cdot\text{rad}$)	540

To obtain a uniform longitudinal distribution, to reduce the transverse space charge effects, the starts of injection should be carefully chosen. By comparing the longitudinal distribution with different start time, -0.14 ms was chosen, and the beam is injected from -0.14 ms to 0.25 ms. The deviations of the kinetic energy of the injected particle from that of the synchronous particles in the RCS during injection are shown in Fig. 1 (a). Figure 1 (b) shows the beam distribution in the longitudinal phase space at the end of injection.

In case of no space charge effects, to obtain a uniform distribution in horizontal and vertical phase space, the bump functions are given by:

$$x(t) = x_0 \sqrt{\frac{t}{t_{inj}}}, \quad 0 \leq t \leq t_{inj} \quad (2)$$

$$y(t) = y_0 \sqrt{\frac{t_{inj} - t}{t_{inj}}}, \quad 0 \leq t \leq t_{inj} \quad (3)$$

where t_{inj} is the injection time, and x_0, y_0 are the radiuses of the normalized horizontal and vertical phase space.

[#] wangs@ihep.ac.cn

SIMULATION OF SPACE CHARGE EFFECTS IN JPARC

K. Ohmi, S. Igarashi, Y. Sato, KEK, Tsukuba, Japan

Abstract

Nonlinear space charge interaction in high intensity proton rings causes beam loss, which limits the performance. Simulations based on the particle in cell (PIC) method have been performed for JPARC-Rapid Cycle Synchrotron (RCS) and Main Ring (MR). Whole acceleration processes are 20 msec and 1 sec for RCS and MR, respectively. Long-term simulation is necessary for the processes. We show results of the long-term simulation using ordinary method with step by step potential calculation and frozen model.

INTRODUCTION

Increasing the intensity of JPARC gradually, space charge effects are being crucial issue. The intensity is achieved 300kW and 100kW for RCS and MR, respectively, in Summer 2010. The target intensity of JPARC is 1MW and 0.72 MW (30GeV) for RCS and MR, respectively. The bunch population is $N_p=4.17 \times 10^{13}$ at the target. The repetition rate is 25 Hz and 0.45 Hz. The collimators are designed to be 4 kW and 450 W for RCS and MR, respectively. That of the beam transport line from RCS to MR is 2kW. Previous simulations [1,2,3] showed the loss limit is to tight, especially in MR. The collimators will be upgraded in the future to 2-4 kW in MR. Hurdle toward the target intensity seems to be very high even the update of the collimators. Close linking of the both ring, RCS and MR, is necessary to achieve the high performance. In this paper, we report the space charge simulation of RCS and MR using a code developed by one of the authors (K.O.) named SCTR [4]. The parameters of RCS and MR are summarized in Table 1.

Table 1 Parameter List of J-PARC RCS and MR

	RCS	MR
Kinetic Energy (GeV)	0.4-3	3-30
Circumference (m)	349	1567
Bunch population, N_p	4.17×10^{13}	4.17×10^{13}
Number of bunch (Harm.)	2 (2)	8 (9)
Repetition (Hz)	25	0.45
Beam power (MW)	1	0.72
Emittance (collimation)(m)	$\sim 324 \times 10^{-6}$	$< 65 \times 10^{-6}$

SIMULATION CODE

The simulation code has been developed since 2007 [3]. The potential solver is based on FACR (Fourier Analysis and Cyclic Reduction) algorithm. The boundary is square perfect conducting wall. The potential is normalized by

$$\Phi = \frac{N_p r_p}{\beta^2 \gamma^3} \lambda(z) \phi(x, y : s) \quad (1)$$

where β and γ are relativistic factors. The potential is assumed to be proportional to the line density of the beam, $\lambda(z)$, normalized by 1. The transverse potential ϕ is given by solving two-dimensional Poisson equation,

$$\Delta_{\perp} \phi = \rho, \quad (2)$$

where ρ is the projected particle density in the transverse plane normalized by 1.

The space charge force is calculated by the gradient of the normalized potential and the dynamical variables are transferred by difference equations as follows,

$$\frac{\Delta p_x}{\Delta s} = -\frac{\partial \Phi}{\partial x}, \quad \frac{\Delta p_y}{\Delta s} = -\frac{\partial \Phi}{\partial y}, \quad \frac{\Delta p_z}{\Delta s} = -\frac{\partial \Phi}{\partial z} \quad (3)$$

The transformations of the lattice elements, drift space, magnets and cavities are expressed by 6 dimensional symplectic map. The azimuthally step Δs should be shorter than the beta function. Since the beta function is in the range of 2.5-20 m and 4-30 m for RCS and MR, respectively, Δs is chosen ~ 1 m.

Two types of computers were used for the simulation. One is PC with dual multi-core CPU's; 2x8 and 2x6 cores. The other is Blue Gene L. Typically 1024 CPU's (Power PC 440) connected by a fast network. Two simulation methods are used depending on the two types of computers. One is ordinary method: i.e., the potential is calculated every azimuthally steps. PC is used for the simulation. In Blue Gene computer, the potential is calculated every 50 turns element by element and is frozen till next 50 turns.

BEAM LOSS SIMULATIONS FOR RCS

Proton LINAC delivers the beam with energy of 181 MeV to RCS in 2010. The target intensity of RCS and MR is realized after energy upgrade of LINAC to 400 MeV in 2012. In this paper we perform beam loss simulation for the beam injected at 400 MeV. Figure 1 shows the acceleration and cavity voltage in RCS [3]. The turn number 15,000 corresponds to the acceleration time 25ms. The cavity voltage of the first and second harmonics are expressed by

$$V(z) = V_1 \cos(2\pi Hz / C + \phi) + V_2 \cos(4\pi Hz / C) \quad (4)$$

where $z=s-vt$.

MULTI-RIBBON PROFILE MONITOR USING CARBON GRAPHITE FOIL FOR J-PARC

Y. Hashimoto[#], S. Muto, T. Toyama, D. Arakawa, Y. Hori, Y. Saito, M. Shirakata, M. Uota,
Y. Yamanoi, KEK/J-PARC, Tsukuba/Tokai, Japan

S. Ohya, UBE Industries, Ltd., Organic Specialty Materials Research Laboratory, Ichihara, Japan
D. Ohsawa, Kyoto University, Radioisotope Research Center, Kyoto, Japan

M. Mitani, Minotos Engineering, Kunitachi, Japan

Y. Sato[†], National Institute of Radiological Sciences, Chiba, Japan

T. Morimoto, Morimoto Engineering, Iruma, Japan

Abstract

We developed a secondary-electron-emission type beam profile monitor with a thin graphite ribbon target having a thickness of 1.6–2.0 μm . It clearly measured high-intensity beams up to 1×10^{13} ppb at a beam energy of 3 GeV with good linearity of the electron-emission yield. The energy deposition in this intense case was fairly small, 5.1×10^{-3} J/bunch/foil. The monitors were installed at injection beam transport (3–50 BT) for main ring (MR) primarily to measure the injection beam profiles by a single pass. A standard-size target has 32-channel ribbons 1.5–3 mm wide, with a length of 200 mm or more. The charge signal produced on the target was transmitted via a 34-channel coaxial cable assembly 400 m long to a signal processor without amplification. This paper describes the characteristics of the graphite, the target fabrication, and the results of beam measurements.

greater because of the larger beam size. More importantly, uniform electron emission is required over such a large area. In light of all these requirements, a specially developed graphite was chosen as the target material because of its low atomic number (6), high heat endurance, and small minimum thickness (1.6 μm).

INTRODUCTION

In designing for secondary-electron-emission target, besides its material, target shape means wire or ribbon is worthy of consideration. Thin wires are typically employed [1, 2] because of they cause little beam loss. When handling high-intensity beams of more than 1×10^{13} particles per bunch (ppb) in GeV-class accelerators, the profile of not only the beam's core but also its tail becomes more important because of beam loss concerns. For high sensitive detection, a ribbon-type target [3, 4] is more suitable than a wire type's.

Although a ribbon's larger surface, as compared to that of a wire, can be advantageous for highly sensitive measurement, beam loss increases in proportion to the ribbon's width. To reduce beam loss, a material of lower atomic number is preferable, and target thickness should be decreased. Generally, the higher the melting point of a material, the more durable it is against heat load. Resistance to heat fatigue is desirable. On the other hand, the space charge effect on emitted dense electrons becomes significantly greater than it is for of an ordinary wire target, because the ribbon and electrode for electron capture are constructed in parallel. To overcome this effect, the potential applied to the electrode should be increased. In a high-intensity accelerator such as J-PARC, the target area becomes as large as $200 \times 200 \text{ mm}^2$ or

[#]yoshinori.hashimoto@kek.jp

[†]deceased

THIN GRAPHITE TARGET



Figure 1: Graphite having thickness of 1.6 μm .

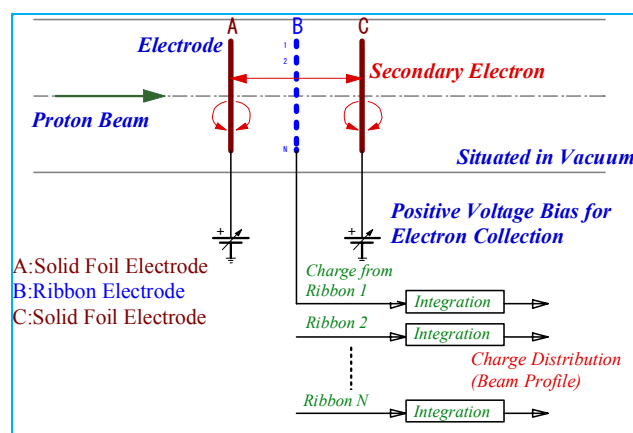


Figure 2: Detector configuration.

Graphite

The graphite was specially made by UBE Industries, Ltd. It has remarkable characteristics of flexibility and self-support, as shown in Fig. 1. These features are attributed primarily to its toughness, which results from the larger crystallites in its composition. Its firing temperature was 2600 $^{\circ}\text{C}$, and the maximum size

A TIME-RESOLVED SEM MONITOR WITH LARGE DYNAMIC RANGE*

M. Hori[†], Max-Planck-Institut für Quantenoptik, Garching, Germany and
 Department of Physics, University of Tokyo, Japan
 K. Hanke, CERN, Geneva, Switzerland

Abstract

CERN's Linac4 will provide 160-MeV H^- beams of intensity $N = 2 \times 10^{14}$ ions s^{-1} . Before this beam can be injected into the existing CERN Proton Synchrotron Booster (PSB), a beam chopper must be used to remove some sequences of 0.5-ns-long micro-bunches from it. We developed a monitor to measure the time structure and spatial profile of the chopped beam, with respective resolutions $\Delta t \sim 1$ ns and $\Delta x \sim 2$ mm. Its large active area $40 \text{ mm} \times 40 \text{ mm}$ and dynamic range also allows investigations of beam halos. The beam was first allowed to strike a carbon foil, and the resulting secondary electrons were accelerated by sets of parallel grid electrodes. The electrons then struck a phosphor screen, and the scintillation light was guided to a thermoelectrically cooled, charge-coupled device camera. The sub-nanosecond time resolution was attained by applying high-voltage pulses to the grids. The monitor has been tested with 700-ps-long UV laser pulses, and a 3-MeV proton beam provided by a tandem.

INTRODUCTION

In the planned design of Linac4 [1, 2, 3, 4], a H^- beam is accelerated to energy $E = 3$ MeV in a radiofrequency quadrupole (RFQ) which is excited at frequency $f_e = 352.2$ MHz. The beam emitted from the RFQ output thus consists of a train of 500-ps-long micro-bunches that each contain 10^9 ions and are spaced by intervals of $f_e^{-1} = 2.8$ ns. A beam chopper [1, 5] positioned downstream of the RFQ is planned to remove 133 consecutive micro-bunches out of every 352 in the beam. It is here crucial to remove all the ions in the bunches, as the ions would otherwise miss the longitudinal acceptance of the PSB, strike its inner walls, and radioactivate the accelerator. In this paper, we describe a monitor [6] which characterizes and validates the time evolution of the spatial profile of this chopped beam. More technical details can be found in Ref. [6].

* Work supported by European Community-Research Infrastructure Activity (CARE, RII3-CT-2003-506395), the Grant-in-Aid for Creative Basic Research (10NP0101) of Monbukagakusho, the European Young Investigator Awards (EURYI) of the European Science Foundation, and the Munich Advanced Photonics Cluster of the Deutsche Forschungsgemeinschaft (DFG).

[†] Masaki.Hori@cern.ch

MONITOR PRINCIPLE AND CONSTRUCTION

In this monitor, the H^- ions were first allowed to strike a carbon foil of thickness $t_d = 50 \mu\text{g} \cdot \text{cm}^{-2}$ (Figure 1) which was placed at a 45-degree angle with respect to the H^- beam. The secondary electrons emitted from the foil were moved out of the path of the H^- beam and collected on a phosphor screen. The image of the scintillation light propagated along a fiber optic conduit, and was photographed by a charge-coupled device (CCD) camera. CCD's and phosphor screens are normally used as integration devices because of their slow (ms-scale) response times. In this monitor, however, a resolution $\Delta t \sim 1$ ns was attained by applying high voltage (HV) pulses of sub-nanosecond rise or fall times on a grid electrode and the phosphor screen, which controlled the flow of secondary electrons from the foil to the phosphor [7]. The monitor could be gated off during the strong H^- micro-bunches, and turned on within ~ 500 ps to verify whether there were any residual particles in the chopped bunches. The CCD normally had a dynamic range of $\sim 10^4$ against single micro-bunches of the beam. As we shall described below, this could be further increased by many orders of magnitude by exposing the CCD over several micro-bunches.

Initial acceleration of the electrons was provided by a grid [8] which was positioned parallel to the carbon foil at a distance $l \sim 7$ mm from it, and in the path of the H^- beam. The grid consisted of 25 graphite filaments of diameter $d = 5 \mu\text{m}$ (manufactured by Toray Industries K.K.). Calculations showed that the filaments would heat up ($T > 2000$ °C) and break, if the full RFQ beam intensity of $I = 70$ mA were focused into a 1-mm-diameter spot on their surface. The filaments would easily survive at $d \sim 10$ mm and reduced values of the duration $\Delta t_m \sim 100$ ns and repetition rate $f_r \leq 1$ Hz of the RFQ macro-pulses. We plan to validate the chopped beam at this reduced intensity, once the RFQ is constructed.

Next the electrons traversed a series of grids, including one with a specific structure which allowed 1-kV pulses of sub-nanosecond fall time to be applied to it. The grid surface of $50 \text{ mm} \times 50 \text{ mm}$ was segmented into four $12.5 \text{ mm} \times 50 \text{ mm}$ strips, parallel to the wires. The segments were connected to four gold striplines printed by thick-film methods on the ceramic frame. The widths and thicknesses of the segments were carefully adjusted to attain a characteristic impedance $Z_0 = 50 \Omega$. The grid potential could thus be driven with an avalanche diode switch (Kentech Instruments HMP1/s/v), which simultaneously

NON-INVASIVE BEAM PROFILE MEASUREMENTS USING AN ELECTRON-BEAM SCANNER

W. Blokland, ORNL*, Oak Ridge, TN 37831, U.S.A.

Abstract

Two electron scanners, one for each plane, have been installed in the SNS (Spallation Neutron Source) Ring to measure the profile of the high intensity proton beam. The SNS Ring accumulates 0.6 μ s long proton bunches up to 1.6×10^{14} protons, with a typical peak current of over 50 Amp during a 1 ms cycle. The measurement is non-destructive and can be done during production. Electron guns with dipoles, deflectors, and quadrupoles scan pulsed electrons through the proton beam. The EM field of the protons changes the electrons' trajectory and projection on a fluorescent screen. Cameras acquire the projected curve and analysis software determines the actual profile of the bunch. Each scan lasts only 20 nsecs, which is much shorter than the proton bunch. Therefore the longitudinal profile of the proton bunch can be reconstructed from a series of scans made with varying delays. This talk will describe the theory, hardware and software of the electron scanner, as well as the results and progress made in improving the measurements.

INTRODUCTION

The electron scanner is a non-destructive alternative to a profile measurement instrument such as the wire-scanner. As such the electron scanner can run without restriction in regards to the beam intensity during neutron production. Electrons are accelerated up to 75 keV and scanned through the proton beam at a 45 degree angle, as shown in Fig. 1.

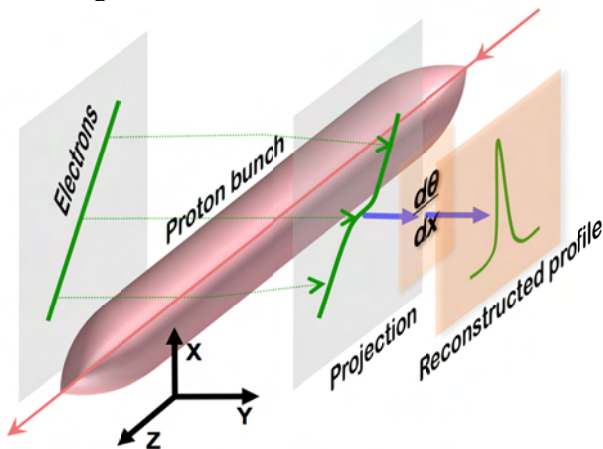


Figure 1: The deflection of the electrons.

The electron beam does not have to be tilted to derive the profile. However, the tilting makes the analysis easier and more accurate. For a vertical beam, the electrons are mostly deflected back on the same vertical trace and one

* ORNL/SNS is managed by UT-Battelle, LLC, for the U.S. Department of Energy under contract DE-AC05-00OR22725

must analyze the density distribution of the electrons along the vertical scan to derive the profile, see also [1]. Figure 2 shows simulated examples of both approaches. The figure shows the change in projection due to the deflection of the electrons for different beam widths "s" as well as the distribution density if the electron scan was vertically projected.

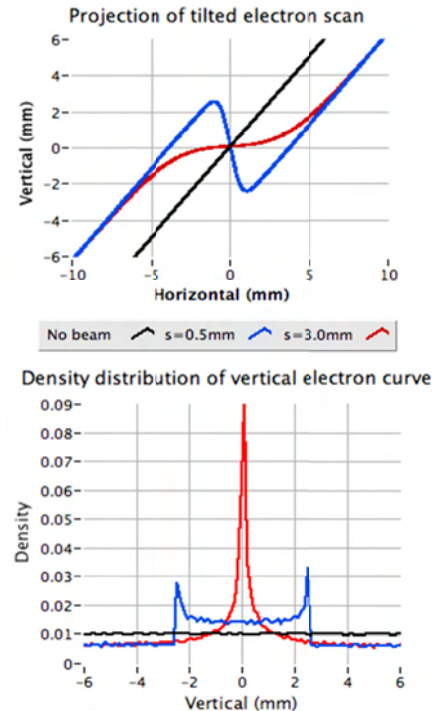


Figure 2: Simulation of the deflected electrons. The top figure shows the curve when scanned at 45 degrees, while the bottom figure shows the density distribution for a vertical scan.

By tilting the electron beam, the transverse profile can be derived from the angle of deflection of the electron beam passing by or through the proton beam. The derivation is shown in [2] and assumes that the path of the electrons is approximately straight, the net energy change to the electrons by the proton beam is close to zero, and the effect of the proton magnetic field can be neglected. The equation is as follows:

$$\frac{d\theta}{dx} = \int_L \frac{e}{mv^2} \cdot \frac{\delta(x,y)}{\epsilon_0} dy$$

where e is the electron charge, m is the electron mass, v is the velocity, $\delta(x,y)$ is the proton beam density distribution, and θ is the electron beam deflection angle. Thus the profile is reconstructed by taking the derivative of the curve.

CURRENT AND TRANSMISSION MEASUREMENT CHALLENGES FOR HIGH INTENSITY BEAMS

P.-A. Duperrex*, M. Gandel, D. Kiselev, Y. Lee, U. Müller, PSI, Villigen, Switzerland

Abstract

Current measurements for high intensity beams present some challenges for monitors located behind a target due to the heat load from the scattered particles. The resulting resonance drifts make accurate current and transmission measurements very difficult. These problems will become more severe with higher intensity beam operation (3mA, 1.8MW) in the PSI cyclotron. This paper presents the techniques that have been developed to overcome this problem. The present solution is based on an innovative scheme to measure on-line the resonator gain and to correct the estimate of the current.

INTRODUCTION

Beam current measurements are one of most fundamental measurements for the cyclotron. They are used to measure the transmission at different parts of the beam lines, in particular the transmission at a 4 cm thick graphite target (the so-called target E) for muon and pion production. Transmission measurements at this point are very important. If a portion of the beam were to bypass the target E, the beam footprint on the next target (the SIN-Q spallation neutron source target) could be reduced. This would lead to an overheating of the SIN-Q target surface. Thus, to avoid such possible damage, the transmission at this point must be carefully monitored.

One of the current monitors used for the target E transmission measurement is placed in vacuum behind the graphite target. This monitor, called MHC5, is subject to heavy heat load due to the energy deposition of the scattered particles. The temperature could reach 200°C due to poor heat conduction and low emissivity of the monitor. The resulting mechanical thermal expansion induces a drift of the resonance frequency. The amplification factor of the resonator is then modified leading to a calibration drift. Because of the dynamic nature of this effect, it was not possible to solve this problem by calibrating the monitor at different beam intensities.

Based on these observations, a new current monitor with improved cooling was designed and built. It has an active water cooling system, its surface was blackened to increase the radiation cooling and its mechanical structure was improved for better heat conduction. Temperature sensors were also installed to monitor the cooling efficiency. Simulations and laboratory tests were also performed so that temperature variations would not affect the resonance characteristics of the monitor.

Even with these improved cooling features, the monitor

exhibited some anomalous gain drifts up to 30% during operation at high current (>1mA). This problem will be more severe for future high intensity beam operation (3 mA). For this reason, it was necessary to implement a drift compensation that could deal with these dynamic changes.

RESONATOR AND HEAT LOAD

Measurement Principle

The current monitor consists of a re-entrant resonator, symmetric around proton beam pipe. The open-end gap in the beam pipe couples some of the wall current into the resonator. This gap acts also as a capacitor and determines the resonance frequency. The resonance frequency is set to 101.26 MHz, the 2nd harmonic of the proton beam bunch frequency. This harmonic is used because of the better signal-to-noise ratio, the RF noise components from the generator being mainly at the odd harmonics. No significant shape dependency of the 2nd harmonic amplitude for relatively short beam pulses is expected [1]. The oscillating magnetic field in the resonator is measured using a magnetic pick-up loop, the signal being proportional to the beam current. Advantages of such resonator are that its construction is simple and it is rugged with respect to radiation. Disadvantages are that it is sensitive to temperature and it is not an absolute measurement; the signal has to be calibrated using another current monitor.

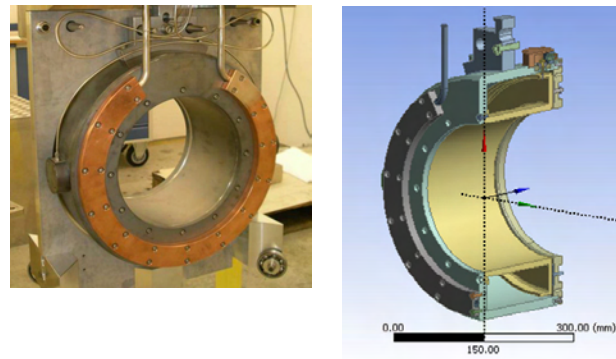


Figure 1: Current monitor ready for installation with the water cooling circuitry at the beam entry side (left). The cavity structure is shown in a half-cut drawing (right).

Mechanical Design

The monitor is made of aluminium (Anticorodal 110), with a 10µm coating layer of silver to improve the electrical conductivity. The inner diameter is 225mm, the outer diameter 420mm, its height 224mm. The capacitor

*pierre-andre.duperrex@psi.ch

STUDIES OF INDUCED RADIOACTIVITY AND RESIDUAL DOSE RATES AROUND BEAM ABSORBERS OF DIFFERENT MATERIALS

M. Brugger, D. Forkel-Wirth, S. Roesler*, J. Vollaire, CERN, Geneva, Switzerland

Abstract

The FLUKA particle interaction and transport code is capable to calculate in one and the same simulation interactions at LHC energies as well as the associated hadronic and electromagnetic particle showers from TeV energies down to energies of thermal neutrons. Sophisticated models for nuclear interactions predict the production of radio-nuclides of which the built-up and decay, along with the associated electromagnetic cascade, can also be calculated in the same simulation. The paper summarizes applications of FLUKA to assess activation around LHC beam absorbers, such as the beam dumps, and presents results of measurements performed during LHC operation.

INTRODUCTION

Modern particle interaction and transport codes such as FLUKA [1,2] allow one to predict radioactivity and associated residual dose rates caused by high energy beam losses in accelerator components in great detail. Phenomenological models of high energy hadronic interactions linked to sophisticated generalized cascade, pre-equilibrium and fragmentation models are able to describe the production of individual radioactive nuclides with good accuracy (often within less than 20%), as comprehensive benchmark studies have demonstrated. The calculation of induced radioactivity has thus become an integral part of design studies for high energy beam absorbers. Results provide valuable information on material choices, handling constraints and waste disposal and allow an early optimization of components in order to increase the efficiency of the later operation of the facility while keeping doses to personnel as low as reasonably achievable. The present paper gives examples of both generic studies with FLUKA for different absorber materials as well as studies for collimators and absorbers of the Large Hadron Collider (LHC).

BENCHMARK STUDY

The unique features of FLUKA for the computation of induced radioactivity and residual dose rates were extensively benchmarked at the CERF facility. At this facility a positively charged hadron beam of 120 GeV interacts in a copper target creating a stray radiation field which can be used for a large variety of studies, among others the activation of material samples. Different materials commonly used for accelerator components and shielding (copper, iron, aluminum, *etc.*) were irradiated and their activation measured by gamma spectrometry

and with dose rate instruments at different cooling times.

Furthermore, the irradiation as well as the radioactive build-up and decay were simulated with FLUKA and results compared to the experimental data [3,4]. The benchmark showed that FLUKA predicts specific activities of individual nuclides within 20-30% in many cases and is also able to reproduce residual dose equivalent rates. An example for the latter is given in Fig. 1 [4].

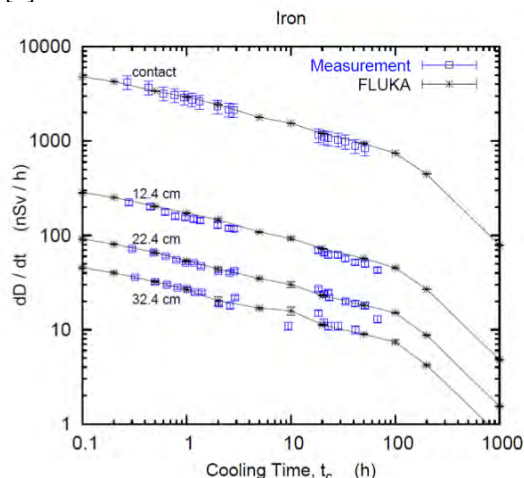


Figure 1: Residual dose equivalent rates as function of cooling time on contact to an iron sample and at three different distances as measured and as calculated with FLUKA [4].

GENERIC ACTIVATION STUDY

Calculations with a generic collimator allowed the assessment of different jaw materials on the activation properties of the entire assembly and the associated residual dose rates [5]. The geometry consists of two rectangular, vertical jaws of a length of 120 cm made of carbon, copper or tungsten. The cooling system is approximated by two copper plates with an artificially reduced density, in order to account for its actual design based on water-cooled pipes, fixed to the jaws with stainless steel clamps. The entire assembly is finally placed into a stainless steel tank. Figure 2 shows a cross sectional view through the geometry. While the jaws and copper plates are pure materials, the following elemental composition is used for all stainless steel components (given in percent by mass): Cr (15.0%), Ni (14.0%), Mn (2.0%), Mo (3.0%), Si (1.0%), P (0.045%), C (0.03%), S (0.03%), Fe (remaining fraction). The geometry also includes a tunnel wall which, however, is of minor importance due to its small contribution to the dose rate close to the absorber as well as to low-energy neutron activation of the absorber.

*Stefan.Roesler@cern.ch

RECENT MARS15 DEVELOPMENTS: NUCLIDE INVENTORY, DPA AND GAS PRODUCTION*

N.V. Mokhov[#], Fermilab, Batavia, IL 60510, U.S.A.

Abstract

Recent developments in the MARS15 code are described for the critical modules related to demands of hadron and lepton colliders and Megawatt proton and heavy-ion beam facilities. Details of advanced models for particle production and nuclide distributions in nuclear interactions at low and medium energies, energy loss, atomic displacements and gas production are presented along with benchmarking against data.

PHYSICS MODEL DEVELOPMENTS

The focus of recent developments to the MARS15 code [1] was on particle production in nuclear interactions at low and medium energies crucial for an accurate description of radiation effects in numerous applications at particle colliders and high-power beam facilities [2]. Substantial improvements have been done to the MARS code event generator LAQGSM [3], the quark-gluon string model. These include low-energy projectiles (p, γ , and heavy ions), near-threshold kaon production, low-energy pions for precision experiments and a neutrino factory, inverse reactions, cross-sections of light nuclear projectiles, light target nuclei (hydrogen, deuterium, and tritium), machine-independent form, and thorough tests on various platforms. An example of benchmarking [4] is shown in Fig. 1 for a quite difficult case of kaon production in the near-threshold region on deuterium in comparison to the ANKE spectrometer data at COSY-Julich [5]. The agreement is amazingly good.

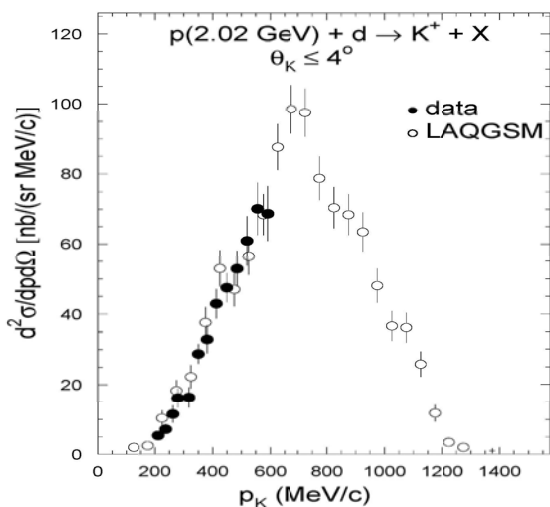


Figure 1: Double differential cross sections of produced K^+ mesons in interactions of protons with deuterium.

*Work supported by Fermi Research Alliance, LLC under contract No. DE-AC02-07CH11359 with the U.S. Department of Energy.

[#]mokhov@fnal.gov

Electromagnetic shower (EMS) module – crucial in energy deposition calculations practically in all applications – has been substantially extended. The exclusive and hybrid modelling options have been added for all EMS processes and all photo- and electro-nuclear hadron and muon production reactions with user-controlled material-dependent switches between the exclusive, inclusive and hybrid modes. The appropriate choice of these parameters substantially reduces variance and improves a computational efficiency.

Electromagnetic interactions of heavy-ion beams, recoil nuclei and fragments generated in nuclear interactions are, in many cases, the most important contributor to radiation effects. In MARS15, knock-on electron production above the material/projectile-dependent thresholds is accurately modelled, with remaining (restricted) energy loss treated continuously down to 1 keV. The ionization energy loss model for an arbitrary projectile has been further updated [6] with a modified Thomas-Fermi expression for ion effective charge based on that by Pierce and Blann, and taking into account available information on probabilities of different ion charge states for few-electron heavy ions at intermediate energies. Fig. 2 shows calculated dE/dx vs data for various particles in silicon at energy 1 keV/A to 1 GeV/A.

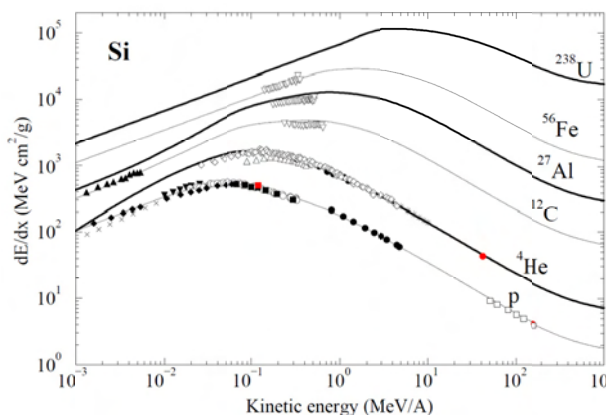


Figure 2: Ionization energy loss of projectiles from protons to uranium in silicon.

Other developments to MARS15 include a new flux-to-dose conversion module based on recent publications [7-10]; user-defined irradiation and cooling times for residual dose; extended Graphical-User Interface (GUI); extended geometry module for a higher accuracy in very complex configurations in a presence of arbitrary magnetic and electric (RF) fields; extended lists of built-in materials and nuclide distributions; adjustments to run the code in a machine-independent fashion on 32- and 64-bit platforms.

STUDIES OF MATERIAL PROPERTIES UNDER IRRADIATION AT BNL LINEAR ISOTOPE PRODUCER (BLIP)*

N. Simos[#], H. Kirk, H. Ludewig, BNL, Upton, NY 11973, USA
N. Mokhov, P. Hurh, J. Hylan, J. Misek, FNAL, Batavia, IL 60510, USA

Abstract

Effects of proton beams irradiating materials considered for targets in high-power accelerator experiments have been under study using the Brookhaven National Laboratory's (BNL) 200 MeV Linac. The primary objectives of the study are to (a) observe changes in physio-mechanical properties (b) identify possible limits of proton fluence above which materials cease to maintain integrity, (c) study the role of operating temperatures in inducing radiation damage reversal, and (d) correlate radiation damage effects between different irradiating species on materials by utilizing reactor and particle accelerator experience data. These objectives being addressed in the latest material irradiation study linked to the Long Baseline Neutrino Experiment (LBNE). Observations on materials considered for high-power targets and collimators, including preliminary observations of the LBNE study are presented.

INTRODUCTION

High-performance targets under consideration to intercept multi-MW proton beams of a number of new particle accelerator initiatives depend almost entirely on the ability of the selected materials to withstand both the induced thermo-mechanical shock and simultaneously resist accumulated dose-induced damage which manifests itself as changes in material physio-mechanical properties. The increased demand imposed on the targets of high-power accelerators, which amounts to an order of magnitude over the experience from accelerator experiments to-date, combined with the physical limitations characterizing most common materials have led to an extensive search and experimentation with a number of new alloys and composites. In addition this search included renewed focus and interest on materials such as graphite which has been used extensively in both particle accelerators as target material and in nuclear reactors as a moderator. Driving the renewed interest in graphite is the variety of its lattice structure which may have a significant influence on its ability to operate safely at the increased demand levels of beam-induced shock and irradiation flux.

Proton irradiation effects on a wide array of materials considered to support high power experiments have been studied extensively using the BNL 200 MeV proton beam of the Linac and utilizing the target station of the Linear Isotope Producer (BLIP).

Based on the Linac/BLIP parameters, and depending on the mode of operations in conjunction to the BNL accelerator complex, 20-24 kW of proton beam power (~95-100 μ A current) are effectively used to irradiate target materials under consideration. The objectives of the material irradiation studies include:

(a) the identification and quantification of potentially present fluence and/or flux thresholds which may limit certain materials from operating for extended periods under MW-level operating conditions. Specifically, focus in the identification of such threshold was prompted by observations made on materials such as graphite and carbon-carbon composite which, based on reactor experience data, should have been able to maintain integrity at much higher integrated dose but appeared to be limited by a proton fluence threshold,

(b) the potential role that target operating temperature may play in inducing the reversal or "healing" of radiation damage that the material undergoes due to the beam exposure. Experimental results of studies to-date using the BNL Linac beam to irradiate special alloys and composites revealed that certain lattice structures are capable of undergoing a reversal of the induced damage that is prompted by a threshold temperature which is capable of mobilizing the radiation-induced defects in the material and thus enabling the restoration of the original physical properties and

(c) the correlation of damage different irradiating species, such as energetic protons or neutrons, induce on materials as well as the energy dependence of irradiation damage. Nuclear reactor experience data on materials such as graphite exposed to primarily thermal neutrons when compared with experience data from accelerator targets where energetic protons are interacting with the same materials reveal differences in the damage rate which could be attributed to the irradiating species, the particle energy or both. Recent experimental results on graphite and carbon-carbon composites irradiated using the 200 MeV protons at BNL BLIP indicated that a threshold fluence appears to exist at $\sim 0.5 \times 10^{21}$ protons/cm² beyond which these materials, which have survived much greater fluences in nuclear reactor environments, experience serious structural degradation.

Prompted by the BNL experimental data on graphite and carbon-composites and by the observed NuMI graphite target neutron yield reduction which has been attributed to progressive target radiation damage, the interest in understanding the behavior of these materials under proton irradiation and quantifying the fluence limitations that appear to play a role has been renewed.

*Work supported by the U.S. Department of Energy.
#simos@bnl.gov

BEAM-LOSS CRITERIA FOR HEAVY-ION ACCELERATORS AND ACTIVATION OF DIFFERENT MATERIALS*

I. Strašák^{#†}, V. Chetvertkova[†], GSI Helmholtzzentrum für Schwerionenforschung,
Darmstadt, Germany

E. Mustafin, GSI Helmholtzzentrum für Schwerionenforschung, Darmstadt, Germany

M. Pavlovič, Slovak University of Technology, Bratislava, Slovakia

Abstract

Assessment of the radiation hazards from activated accelerator components due to beam-losses is a serious issue for high-energy hadron facilities. Important radiation-safety principle ALARA (As Low As Reasonably Achievable) calls for minimizing exposure to people. That is why the uncontrolled beam-losses must be kept on the reasonable low level. The beam-losses below 1 W/m are considered as a tolerable for “hands-on” maintenance on proton accelerators. The activation of the heavy-ion accelerators is in general lower than the activation of the proton machines. In our previous work, we estimated the “hands-on” maintenance criteria for heavy ions up to uranium in stainless steel and copper by scaling the existing criterion for protons. It was found out that the inventory of the isotopes and their relative activities do not depend on the primary-ion mass but depend on the target material. For this reason in the present work the activation of other important accelerator construction materials like carbon, aluminium and tantalum was studied using the FLUKA code.

INTRODUCTION

Activation of accelerators due to uncontrolled beam losses during normal operation is an important issue especially for high-energy hadron accelerators [1-4]. The residual activity induced by lost beam particles is a dominant source of exposure to personnel and one of the main access restrictions for “hands-on” maintenance [1].

Quantification of the residual activity provides fundamental information that can be used in several ways: (1) to specify the tolerable beam losses in the machine, (2) to optimize the choice of construction materials, or (3) to estimate the necessary “cooling” time after turning off the beam. All these three measures are important with respect to the reduction of personnel exposure.

The well known available information is that activation caused by uncontrolled beam losses uniformly distributed along the beam line on the level of 1 W/m can be accepted for high-energy proton accelerators as tolerable to ensure the “hands-on” maintenance [5]. The effective-dose rate in the vicinity of the activated accelerator components then should not significantly exceed 1 mSv/h for a typical operating period of an accelerator followed by a reasonable “cooling down” time before the “hands-on” maintenance (100 days irradiation / 4 hours cooling /

30 cm distance) [6-8]. The beam-loss criteria for heavy-ion accelerators were specified by scaling the 1 W/m criterion for protons [8-10].

In the frame of the FAIR project (Facility for Antiproton and Ion Research) [11] extensive experimental studies [12-14] and Monte Carlo simulations [8-10] of the residual activity induced by high-energy heavy ions in copper and stainless steel were performed at GSI Darmstadt. The simulations were performed by FLUKA [15, 16] and SHIELD [17, 18] codes. It was shown that the induced residual activity decreases with increasing primary-ion mass and with decreasing energy [8-10]. Besides that it was found out that the isotope inventory and their relative activities depend on the target material.

The results presented in this paper follow the previous studies [8-10] and give information about the residual activity induced in other materials: carbon, aluminium and tantalum. These materials are important for the construction of collimators [19, 20] and in addition aluminium also for the construction of beam pipes [21].

BEAM-LOSS CRITERIA FOR HEAVY-ION ACCELERATORS

FLUKA and SHIELD codes were used for simulation of the residual activity induced by various projectiles in two target configurations representing: (1) a beam pipe of an accelerator and (2) a bulky accelerator structure like a magnet yoke, a magnet coil or a collimator. The purpose of the simulations was to compare heavy ions with protons [8-10]. The target materials were stainless steel (beam pipe and bulky target) and copper (bulky target) representing the most common construction materials used for basic accelerator components. The assumed stainless-steel composition was C (0.07%), Mn (2.0%), Si (1.0%), Cr (18%), Ni (9.5%), and S (0.03%) in addition to iron (stainless steel 304). The simulations were performed for ^1H , ^4He , ^{12}C , ^{20}Ne , ^{40}Ar , ^{84}Kr , ^{132}Xe , ^{197}Au and ^{238}U at energies from 200 MeV/u up to 1 GeV/u. The residual activity and the effective-dose rate at the distance of 30 cm from the beam-pipe outer surface were calculated at different time points [8]. The activity was scored by both codes whereas the dose rate only by FLUKA.

Beam-Loss Criteria for Beam Pipes

The assumed beam-pipe geometry was a 10 m long tube made of stainless steel, 10 cm inner diameter, 2 mm wall thickness. The glancing angle between the incident beam particles and the inner surface of the beam pipe was 1 mrad. The irradiation time was 100 days. The beam

*Work supported by the EU program EuCard, WP 8, ColMat
[#]i.strasik@gsi.de [†]On leave from Johann Wolfgang Goethe
Universität, Frankfurt am Main, Germany

EXPERIENCE WITH MOVING FROM DPA TO CHANGES IN MATERIAL PROPERTIES*

Meimei LI[#], Argonne National Laboratory, Argonne, IL 60439, U.S.A.

Abstract

Atomic displacements by high energy particles induce formation of point defects and defect clusters of vacancies and interstitial atoms in a crystalline solid. The damaged microstructure results in significant changes in materials physical and mechanical properties. Besides displacement damage, nuclear transmutation reactions occur, producing He and H gas atoms that can have pronounced effect on materials performance. Radiation effects in materials have been studied using various irradiation sources, e.g. fission, fusion and spallation neutron sources, high-energy ions and electron beams, etc. With different types of bombarding particles, radiation damage correlation is essential so that radiation effects produced by different irradiation sources can be compared and data can be transferred or extrapolated. The parameter commonly used to correlate displacement damage is the total number of displacements per atom (dpa). Irradiation-induced changes of material properties are measured as a function of dpa. Considering that several aspects of radiation exposure can give rise to property changes, the extent of radiation damage cannot be fully characterized by a single parameter. This paper will discuss damage correlation under various irradiation environments, key irradiation parameters and their effects on irradiation-induced property changes.

INTRODUCTION

Radiation damage is produced by energetic particles, such as neutrons, ions, protons, or electrons, interacting with a crystalline solid. An energetic particle transfers recoil energy to a lattice atom, so-called primary knock-on atom (PKA), and the PKA displaces neighbouring atoms, resulting in an atomic displacement cascade. The displacement threshold is typically about a few tens of electron volts [1]. Atomic displacements by high energy particles induce the formation of point defects and defect clusters of vacancies and interstitial atoms. The displacement cascade event occurs within picoseconds. With time, diffusion processes take place and irradiation-induced defects recombine or cluster to form more stable damage structures, e.g. dislocation loops, dislocation networks, voids, helium bubbles, precipitates, etc. The damaged microstructure results in significant changes in physical and mechanical properties of a material. In addition to the displacement damage, nuclear transmutation reactions occur, producing helium and hydrogen gas atoms and solid impurities. The production

of helium and hydrogen can have pronounced effect on materials performance even at low concentrations [2,3].

Radiation damage has been studied using various irradiation sources, e.g. fission neutrons in nuclear reactors (e.g. liquid metal fast reactors, gas-cooled and water-cooled mixed-spectrum reactors), fusion neutrons in a D-T fusion neutron source, spallation neutron sources, ion irradiation with accelerators, and high-energy electron beams, etc. Nuclear fission reactors are by far the most commonly-used irradiation facilities. A number of simulation irradiation techniques have been developed for materials research, particularly when there is lack of prototypic irradiation facilities. For instance, material development for fusion reactors, which currently are still in the development stage, has been made primarily in thermal or fast fission reactors. Fusion reactors have significantly higher neutron energy (14.1 MeV) than fission reactors (< 2 MeV). Radiation effects expected to be produced by intense 14.1 MeV neutrons from a fusion reactor have been simulated with low-energy fission neutrons in existing reactors [4]. Another way to obtain radiation effect information in materials is through the use of accelerators. High energy proton accelerators have been used for irradiation studies of fusion reactor materials [5]. Energetic ions are used to simulate neutron irradiation damage for various other reasons, such as minimization of high residual radioactivity, low-cost, better-controlled irradiation conditions, and declined availability of neutron irradiation sources.

High energy protons produce spallation reactions in the target, leading to high-level radiation damage, a large amount of deposited energy, and production of H and He and other transmutation products. This extremely aggressive irradiation environment poses a significant challenge for the target design of high-energy accelerators. Graphite is a candidate material in a number of target designs [6]. The structural behaviour of graphite, e.g. strength and ductility, dimensional stability, susceptibility to cracking, is a complex function of the source material, manufacturing process, chemical environment, temperature, and irradiation conditions. Although extensive knowledge exists on the irradiation effects in graphite, the assessment of the radiation resistance of the high energy proton beam target (e.g. the Neutrons at the Main Injector (NuMI) target) is however, difficult, as most of the information available on radiation effects in materials is based on nuclear fission reactor irradiations, while the irradiation conditions in the NuMI facility is considerably different from nuclear reactor irradiations. The potential impact of radiation damage on

*Work supported by the U.S. Department of Energy, Office of Nuclear Energy under Contract DE-AC02-06CH11357.

[#] mli@anl.gov

INJECTION AND EXTRACTION FOR THE EMMA NS-FFAG

K. Marinov, S. I. Tzenov and B. D. Muratori,
STFC Daresbury Laboratory and Cockcroft Institute, UK

Abstract

EMMA (Electron Machine with Many Applications) is a prototype non-scaling electron FFAG being commissioned at Daresbury Laboratory. Ns-FFAGs have great potential for a range of new applications in many areas of science, technology, manufacturing and medical applications including the next generation high energy proton and heavy ion accelerators for accurate and effective particle beams cancer therapy, muon accelerators for the study of the physics and chemistry of advanced materials and accelerator driven subcritical reactors (ADSRs). This paper summarizes the design of the extraction and injection transfer lines of EMMA as well as the associated septa and kickers. The ALICE energy recovery linac prototype is used as the injector to EMMA, with energy range from 10 to 20 MeV. Because this is the first non-scaling FFAG constructed, it is crucial to study as many of the electron beam properties as feasible, both at injection and after acceleration in an extraction line. To do this, a complex injection line was designed consisting of a dogleg to extract the beam from ALICE, a matching section, a tomography section and some additional dipoles and quadrupoles to transport the beam to the entrance of EMMA. Similarly the design of the extraction line and its diagnostics are described.

INTRODUCTION

EMMA is currently being commissioned at Daresbury Laboratory, UK, to demonstrate the world's first operation of a new concept in accelerator design called non-scaling FFAG, (ns-FFAG) [1,2]. Ns-FFAGs were first designed to provide very rapid acceleration for muon beams and have since been further developed for a wide range of potential applications. These range from the next generation high energy proton and heavy ion accelerators for accurate and effective particle beam cancer therapy (PAMELA [3]), an accelerator for a muon facility for the study of the physics and chemistry of advanced materials, to accelerator driven subcritical reactors (ADSRs). In ADSRs, fission is enabled by high energy proton beams spallating neutrons from a target embedded in a thorium fuelled reactor [4]. Ns-FFAGs have also been adopted as the baseline design for an international neutrino factory [5]. First, the "proof of principle" accelerator EMMA must be demonstrated, this is summarised in [6].

INJECTION LINE

The ALICE to EMMA injection line, shown in Figure 1, consists of a dogleg to extract the beam from the ALICE accelerator, a tomography section and finally a short dispersive section consisting of two dipoles, prior to

the injection septum [7]. After the dogleg, the beam is matched into a tomography diagnostic via four quadrupoles. The purpose of this section is twofold: Firstly, to provide a quick and precise measurement of the Twiss parameters, and secondly to make emittance and transverse profile measurements. This creates a 'fixed point' in the line after which, if the tomography section is matched correctly, the Twiss parameters at all energies should be the same. This is useful because of the requirement to inject at a range of energies, which gives different Twiss parameters depending on the amount of RF focusing from the ALICE linac cavities and how far off-crest they are. The rest of the line after the tomography section can then be used to optimise the slightly different, energy dependent, injection parameters.

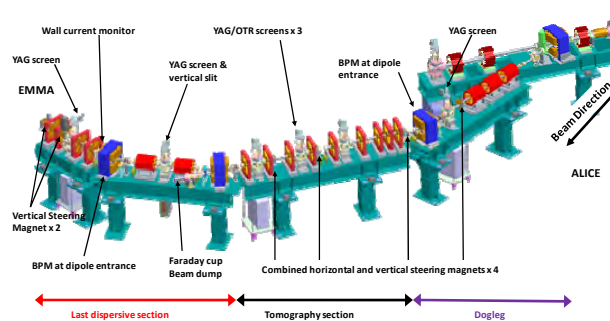


Figure 1: ALICE to EMMA injection line.

In order to improve the study of the physics of ns-FFAGs, it is important to minimise the energy spread of the beam at the start of the injection line. By carefully choosing the phases of the two ALICE linac cavities, it was possible to achieve an energy spread less than 0.05 % (5 keV at 15 MeV). This has not yet been repeated at all other energies but there is no reason to think it will not be possible to achieve the same as all that is done is a simple elimination of the correlated energy spread and the uncorrelated one remains constant.

MODELLING

The results reported in this section are from the tracking code FFEMMAG developed S. Tzenov at Daresbury Laboratory and described in [8]. Other studies of injection and extraction into the EMMA ring [9,10] using different codes give broadly similar results.

Single Turn Injection

The basic elements of the injection system are a septum magnet and two kicker magnets, located in two successive long straight sections immediately after the long straight section where the septum is inserted. The extraction system is simply a mirror image of the injection one.

DESIGN STATUS OF THE PEFP RCS*

J. H. Jang[#], H. J. Kwon, H. S. Kim, Y. S. Cho, PEFP/KAERI, Daejeon, Korea
 Y. Y. Lee, BNL, Upton, New York 11973, U.S.A.

Abstract

The 100-MeV proton linac of the proton engineering frontier project (PEFP) can be used as an injector of a rapid cycling synchrotron (RCS). The design study of the RCS is in process. The main purpose of the RCS is a spallation neutron source. The initial beam power is 60 kW where the injection and extraction energies are 100 MeV and 1 GeV, respectively. It will be extended to 500 kW through the upgrades of the injection energy to 200 MeV, the extraction energy to 2-GeV, and the repetition rate from 15 Hz to 30 Hz. The slow extraction option is also included in the design for basic and applied science researches. This work summarized the present design status of the PEFP RCS. In the introduction, the present status of the PEFP project is briefly summarized.

INTRODUCTION

Proton Engineering Frontier Project (PEFP) is the 100-MeV proton linac development project which was launched at 2002 and will be finished at 2012 [1]. As an extension plan of the linac, we are considering a rapid cycling synchrotron (RCS). The main purpose of the RCS is a spallation neutron source which can be used in the fields of the material science, bio technology, chemistry, etc.

The PEFP proton linear accelerator consists of two parts. The low energy part includes an ion source, a low energy beam transport (LEBT), a 3-MeV radio frequency quadrupole (RFQ), and a 20-MeV drift tube linac (DTL) [1]. The high energy part consists of seven DTL tanks which accelerator proton beams from 20 MeV to 100 MeV. The 20-MeV linac system has been successfully installed and tested at the KAERI site. The fabrication of the remaining DTL tanks will be finished in this year and the test of the DTL tanks is in progress. A medium energy beam transport (MEBT) system will be installed after the 20-MeV DTL. It includes a 45-degree bending magnet in order to extract 20-MeV proton beams. 100-MeV proton beams will be guided into beam lines by another 45-degree dipole magnet which is located after the last DTL tank. The 20-MeV or 100-MeV proton beams are distributed respectively into 5 target rooms. The main characteristics of PEFP beam lines is using AC magnets to distribute proton beams into 3 target rooms in both 20-MeV and 100-MeV beam lines. The schematic plot of the PEFP linac and beam lines is given in Figure 1. The basic parameters of the linac are summarized in Table 1.

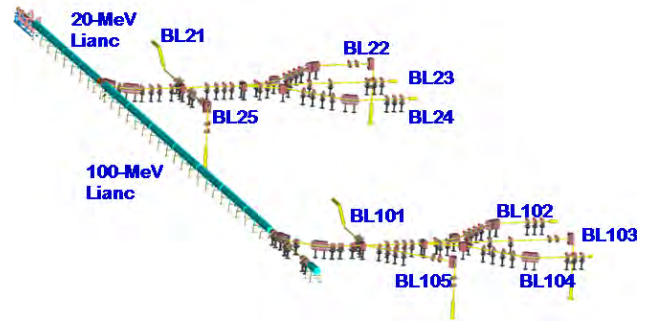


Figure 1: Schematic plot of the PEFP linac and beam lines.

Table 1: Basic Parameters of PEFP Linac

Parameter	Value
Particle	Proton
Beam Energy	100 MeV
Operation Mode	Pulsed
Max. Peak Current	20 mA
Pulse Width	<1.33 ms (< 2.0 ms up to 20 MeV)
Max. Beam Duty	8% (24% up to 20 MeV)

Gyeongju city which is located in the south-eastern part of Korea hosted the project in January 2006. The geological surveys of the site and the site-dependent plan such as the facility layout and access road have been completed for the civil construction. The general arrangement of the accelerator and beam utilization buildings and conventional buildings are also completed. Figure 2 shows the bird's eye view of the PEFP accelerator research center. Now the construction of each building is in progress.



Figure 2: PEFP accelerator research center.

*This work was supported by Ministry of Education, Science and Technology of the Korean government

[#]jangjh@kaeri.re.kr

NON-SCALING FFAG AND THEIR APPLICATIONS*

D. Trbojevic,[†] Brookhaven National Laboratory, Upton, New York, USA

Abstract

Examples of the Non-Scaling Fixed Field Alternating Gradient (NS-FFAG) in applications are shown. NS-FFAG designs, with beam passing either once or just a few turns, are shown: the medical gantries in the cancer therapy, Re-circulating Linac Accelerators (RLA) with droplets or race track, and a muon accelerating ring with distributed RF cavities. A small permanent magnet proton cancer therapy machine and one GeV racetrack with superconducting magnets are presented as examples of NS-FFAG with larger numbers of turns. Consideration of the possible use of the NS-FFAG for storage rings for protons or pions for longitudinal manipulations is assessed.

INTRODUCTION

This report describes possible applications of the Non-Scaling Fixed Field Alternating Gradient (NS-FFAG) accelerators. In recent years there has been a clear revival of the previous concept of the FFAG's, developed mostly in the 1950's [1, 2, 3] mostly with a Midwestern Universities Research Association (MURA). More recent information about Scaling FFAG (S-FFAG) concept can be found elsewhere [4]. In the second chapter, a concept of the NS-FFAG is described. It includes a description of the linear properties of the structures, explains the rationale of the large momentum acceptance and small aperture requirements. In the basic concept description of the tune, time of flight, dispersion and amplitude functions variations with a momentum are shown. Applications of NS-FFAG's are divided into two categories: where a beam passes through the structure one or a few times, or where the beam has multiple - hundreds of turns. This distinction comes as a consequence of the tune variations with momentum. Although the NS-FFAG is a linear machine with a large dynamical aperture and large momentum acceptance the integer crossings of the tunes represents a problem. This comes from misalignment of more than 20-40 μm or from the magnetic field error larger than $\delta B/B > 10^{-3}$. The following chapter describes NS-FFAG examples with a single or a few beam passes: the carbon/proton medical gantries for the cancer therapy, the RLA either race-track or droplets, an RLA for electron ion collider acceleration, thirteen turns NS-FFAG muon accelerator made of triplet combined function magnets, and finally a storage ring to capture muons from pion decays, which is fully described in the program Phase Rotated Intense Slow Muon

(PRISM) beam in Japan [5]. The higher momentum pions, of few hundred MeV/c (idea of C. Ankenbrandt -Muon Inc.), could be stored in the same fashion as in the PRISM and from a decay of relativistic pions obtain muons with a smaller momentum spread. The spectrum that ranges from about 100% to about 50% of the pion momentum. So a NS-FFAG ring with a momentum acceptance of 50% and a high RF voltage would capture most of the decay muons from an injected pion beam in no more than 6 turns. The third chapter describes NS-FFAG for non-relativistic beams where a larger number of turns is assumed. A proton accelerator for the cancer therapy made of NS-FFAG made with permanent Halbach magnets, and a 1 GeV superconducting race track are described. Additional heavy-ion acceleration replacing long and very expensive superconducting linac was just noted (more information is available in the previous publication [6]). From the particle tracking of all the examples at the central momentum, where usually the momentum compaction is equal to zero becomes a clear possibility for using NS-FFAG as a storage ring for longitudinal beam manipulations as the momentum aperture is $\delta p/p = \pm 50\%$.

BASIC CONCEPT OF THE NS-FFAG

In S-FFAGs the tunes ν_x and ν_y are constant with a zero chromaticity for all particle energies as the orbits radii scale with energy but with the field index $|n| \sim 500$. This necessarily makes the field nonlinear. The benefit of the NS-FFAGs is due to the relationship $\Delta x = D_x \Delta p/p$, where Δx is the radial beam offset, D_x is the lattice dispersion function and $\Delta p/p$ is the fractional momentum deviation. The value for Δx may be kept less than ± 50 mm for a $\Delta p/p = \pm 60\%$, if the D_x is < 0.08 m. The dispersion function or the dispersion action H is well controlled, similar to the request for the minimum of the H in the light source lattice. The NS-FFAG has a very strong focusing structure to obtain small values of D and β , and hence small magnet sizes. Linear magnetic field dependence with respect to the radial axis $B \propto r$ is an additional simplification. The strongest focusing, smallest dispersion, and best circumference is achieved by the combined function magnets in the triplet FDF where in the middle is a larger defocusing main bending element surrounded by two smaller focusing combined function magnets with opposite bend [8], as shown in Fig. 1.

In the non-scaling case the magnetic fields are linear even though they lead to a substantial range of tunes; that is acceptable in an accelerator for muons because the acceleration has to take place very rapidly, and therefore betatron resonances are traversed so fast that they have very little

*Work performed under a Contract Number DE-AC02-98CH10886 with the auspices of the US Department of Energy.

[†] dejan@bnl.gov

COMMISSIONING AND OPTIMIZATION OF THE LHC BLM SYSTEM

E.B. Holzer, B. Dehning, E. Effinger, J. Emery, C.F. Hajdu,
 S. Jackson, C. Kurfürst, A. Marsili, M. Misiowiec, E. Nebot Del Busto, A. Nordt,
 C. Roderick, M. Sapinski, C. Zamantzas, CERN, Geneva, Switzerland
 V. Grishin, IHEP, Protvino, Russia and CERN

Abstract

Due to rapid progress with the LHC commissioning in 2010, set-up beam intensities were soon surpassed and damage potential was reached. One of the key systems for machine protection is the beam loss monitoring (BLM) system. Around 4000 monitors are installed at likely or critical loss locations. Each monitor has 384 associated beam abort thresholds (12 integrated loss durations from 40 μ s to 84 s for 32 energy intervals). A single integrated loss over threshold on a single monitor aborts the beam. Simulations of deposited energy, critical energy deposition for damage or quench and BLM signal response backed-up by control measurements determined the initial threshold settings. The commissioning and optimization of the BLM system is presented. Test procedures were used to verify the machine protection functionalities. Accidental magnet quenches were used to fine-tune threshold settings. The most significant changes to the BLM system during the 2010 run concern the injection, the collimation and the beam dump region, where hardware changes and threshold increases became necessary to accommodate for increasing beam intensity.

INTRODUCTION TO THE LHC BLM SYSTEM

The main function of the LHC BLM system [1] is damage protection. Additionally, quenches of superconducting magnets have to be avoided. The BLM system's response is critical for short and intense particle losses, while at medium and longer loss durations it is assisted by the quench protection system and the cryogenic system. The system changes its beam abort thresholds automatically, corresponding to the beam energy, and allows to follow the loss duration dependent quench levels of the superconducting magnets (signal integration times from 40 μ s to 84 s). The detectors are ionization chambers (IC) and secondary emission monitors (SEM), which are 70000 times less sensitive. In order to give operations a threshold tuning possibility, the 'applied thresholds' are derived from pre-set 'master thresholds' by multiplication with a 'monitor factor' (MF). $MF \leq 1$ is enforced. Typically, $MF = 0.1$ on cold magnets. Master thresholds are always set safely below damage level (at least a factor 10 for losses up to 100 ms), typically to three times the quench level. 'Families' of monitors have the same master thresholds. They protect same elements with same monitor locations from similar loss scenarios. Table 1 summarizes the monitors and fami-

lies. ICs which are not used for beam interlock are installed in the dump lines, for future upgrade elements or redundant monitors with RC signal delay. The BLM system is extensively used for operation verification and machine tuning. The following data sets are available: Logging (one value every second for nearly all integration times); post mortem (online 80 ms and offline 1.72 s of 40 μ s integrals); collimation buffer (80 ms of 2.6 ms); capture data (80 ms of 40 μ s or 5.2 s of 2.6 ms) and extraction validation or XPOC buffer (80 ms of 40 μ s). Logging data is also used for online display.

Table 1: Monitors and Families

Monitors	Purpose	# Monitors	# Families
IC	interlock (97%) observation (3%)	3592	122
SEM	observation	289	22

COMMISSIONING AND SYSTEM VALIDATION TESTS

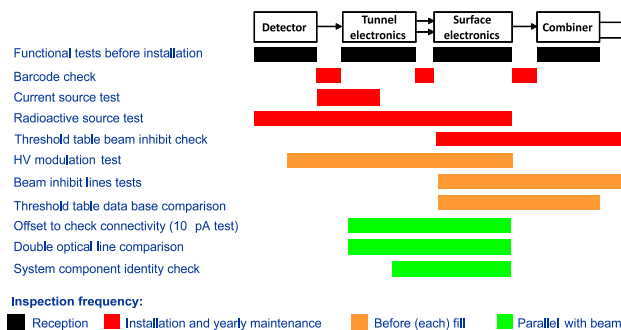


Figure 1: Overview of the most important BLM testing procedures. The colored bars show which part of the system is tested at which frequency.

Commissioning of the BLM system (2008, 2009 and beginning of 2010) was advancing in parallel with the beam commissioning of the LHC [2]. The machine protection functionalities of the BLM system had been phased in. This way, they provided the required protection level for each stage of the commissioning, without compromising the machine availability. The input to BIS (Beam Interlock System) from individual monitors was switched from 'masked' to 'unmasked' in stages. At the end of the 2009 run the LHC was operating with most of the channels unmasked. The continuous (during beam operation) acquisition system self tests became operational during the 2009 run. The reg-

STATUS REPORT OF THE RAL PHOTO-DETACHMENT BEAM PROFILE MONITOR*

C. Gabor[†], STFC, ASTeC, Rutherford Appleton Laboratory (RAL), Oxfordshire, UK,
 G.E. Boorman, A. Bosco, Royal Holloway, University of London, UK
 J.K. Pozimski, P. Savage, Imperial College London of Science and Technology,
 Blackett Laboratory, UK
 A.P. Letchford, STFC, RAL Isis Neutron Source, Oxfordshire, UK

Abstract

The Rutherford Appleton Laboratory (RAL) is developing a front end suitable for High Power Proton Applications HPPA. The main components are an H^- ion source with up to 60 mA current at 65 keV, a transport section to match the beam to an RFQ with 3 MeV output energy and a LEBT comprising a chopper system with several buncher cavities. Photo detachment can be used as a non-destructive diagnostics method. The paper reports on progress with a beam profile monitor that is placed in a pumping vessel right after the ion source at the intersection to the Low Energy Beam Transport (LEBT). This diagnostics tool consists of mirrors inside the vacuum to scan the laser beam through the beam, the actual detector to measure photo detached electrons, laser and optics outside the vacuum and electronics to amplify and read out the signal. The paper summarizes the experimental set-up and status, discusses problems and presents recent measurements.

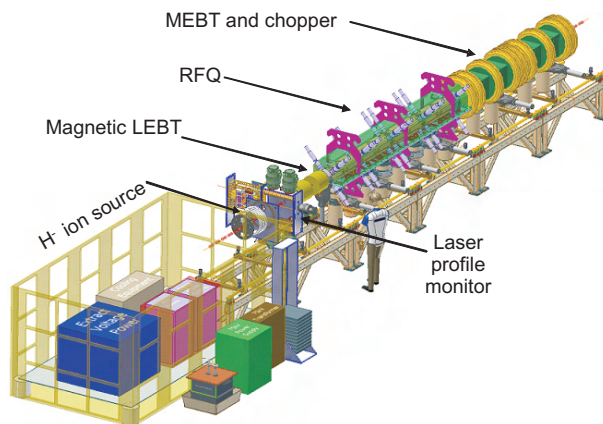


Figure 1: Overview of the FETS set up. The main elements are a Penning type ion source, 3 solenoid LEBT, RFQ and the MEFT consisting of quadrupoles, four buncher cavities and a combined slow/ fast chopper. It is intended to use photo-detachment as a non-destructive diagnostics method applying to a beam profile monitor and an emittance scanner at 3 MeV beam energy.

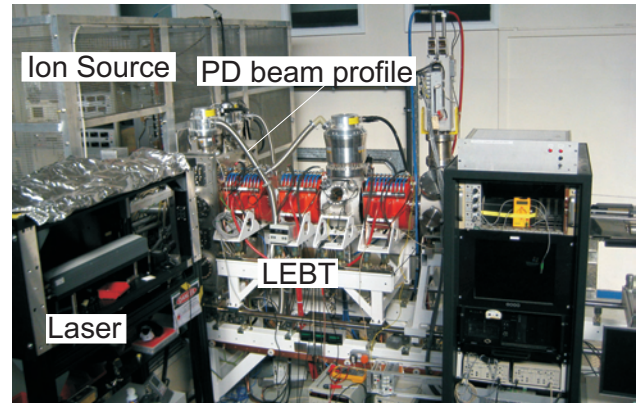


Figure 2: Recent set-up of ion source, differential pumping vessel which hosts also the beam profile monitor.

INTRODUCTION

High Power Proton Particle Accelerators in the megawatt range have many applications including drivers for spallation neutron sources, neutrino factories, transmuters (for transmuting long-lived nuclear waste products), and energy amplifiers[2, 3]. FETS is RALs contribute to the development of HPPAs but also to prepare the way for an upgrade to the Isis accelerator and to contribute to the U.K. design effort on neutrino factories.

The Front End Test Stand FETS project[1], located at RAL, is to demonstrate that chopped low energy beams of high quality can be produced. FETS (see Fig. 1) consists of a 60 mA Penning Surface Plasma Ion Source, a

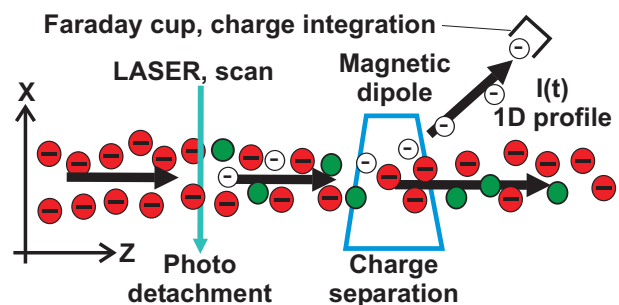


Figure 3: Basic principle of photo detachment ion beam diagnostics The H^- ions get neutralized by laser light. The diagnostics is in general a three stage process: detachment, charge separation and detection.

* work supported by Institute of Applied Physics with a laser loan

[†] christoph.gabor@stfc.ac.uk

BEAM INDUCED FLUORESCENCE PROFILE MONITOR DEVELOPMENTS

P. Forck*, C. Andre, F. Becker, R. Haseitl, and B. Walasek-Höhne
GSI Helmholtzzentrum für Schwerionenforschung, Darmstadt, Germany

Abstract

As conventional intercepting diagnostics will not withstand high intensity ion beams, the non-destructive Beam Induced Fluorescence (BIF) method for transverse profile monitoring was extensively developed during the last years at the GSI heavy ion facility. Tests with various ions in the energy range from 1.4 MeV/u to 750 MeV/u were done. An overview of the general performance and the technical realization is given. Fluorescence spectra of nitrogen and rare gases were recorded, using an imaging spectrograph and wavelength selected beam profiles were obtained. The recorded transverse profiles coincides for all working gases with the exception of *He*. The background contribution by beam induced neutrons and γ s was investigated.

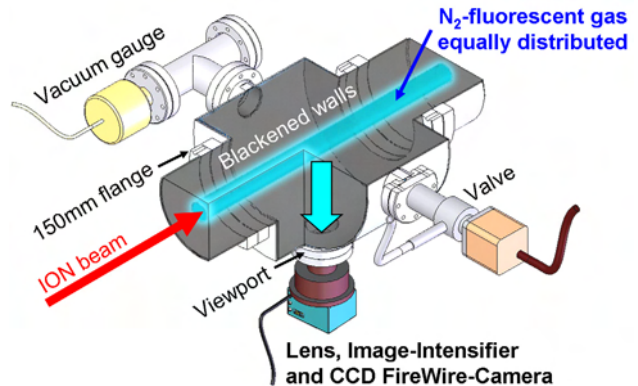


Figure 1: Scheme of a BIF Monitor for horizontal beam profile determination as installed at GSI.

BIF METHOD OVERVIEW

Non-destructive transverse profile measurements are preferred not only for single-pass diagnostics at different locations in a transfer line, but also to enable time resolved observations of a stored beam within a synchrotron. The essential reason for non-destructive diagnostics is the large beam power available at modern hadron accelerators, which excludes the usage of traditional intercepting methods like scintillation screens, SEM-grids or wire scanners due to the high risk of material damage during irradiation by the total beam intensity.

As an alternative to these traditional devices a Beam Induced Fluorescence (BIF) Monitor was realized and its properties were investigated in detail during the last years. A BIF Monitor is schematically depicted in Fig. 1. Due to the electronic stopping power the residual gas is ionized and left in an excited state with a certain probability. Optical photons emitted due to de-excitation can be used for transverse profile determination. But only those photons emitted towards the camera are detected, resulting in a solid angle $\Omega \approx 10^{-4}$ and single photon technologies have to be applied. The spatial resolution is adapted to the beam parameters over a wide range by choosing an appropriate optical magnification ratio. An important boundary condition is the depth of field, which has to cover the entire beam diameter. The BIF method was investigated by different authors for profile measurements at cw-LINACs [1, 2, 3], pulsed LINACs [4, 5], cyclotron facilities and has been tested at synchrotrons as well [6, 7, 8].

* p.forck@gsi.de

TECHNICAL REALIZATION

In order to detect single photons an image intensified camera has to be used. One technical principle is the MCP-based image intensifier. In these devices the photon are converted to an electron at a photo-cathode and accelerated to a Multi-Channel-Plate (MCP). This might be either a single MCP having an $\sim 10^3$ -fold amplification of photo-electrons or a double MCP stack with $\sim 10^6$ -fold amplification, the latter one is suited for single photon detection. The electron avalanche hits a phosphor screen to create photons again which are finally observed by a standard CCD camera. The installations at GSI Ion LINAC comprises of either a tri-alkali photo-cathode S20 or bi-alkali photo-cathode in front of a double MCP stack of 25 mm diameter [9]. A standard lens system (in most cases Pentax C1614ER with focal length $f = 16$ mm) provides a reproduction scale of typically $250 \mu\text{m}$ per pixel [4]. For some of the experiments other lens system are used, e.g. with enhanced UV transmission (LINOS inspec.x with $f = 50$ mm). The spatial resolution is about $100 \mu\text{m}$ (with respect to the beam location), mainly determined by the internal resolution of the double MCP intensifier arrangement. The resolution on the photo-cathode acting as the image plane is about 30 line-pairs per mm (lp/mm). CCD cameras with a digital interface (FireWire of GigE) are used to provide a loss-less data transport and adequate trigger possibilities [10].

As an alternative to MCP-based image intensifiers segmented photo-multipliers are used by other authors [6, 11]. As a third possibility a modern electron-multiplying CCD camera (emCCD) was considered [12, 13]: The amplification of the photo-electrons is realized by a chain of avalanche diodes between the CCD matrix and the ADC.

FIRST MEASUREMENTS OF NON-INTERCEPTIVE BEAM PROFILE MONITOR PROTOTYPES FOR MEDIUM TO HIGH CURRENT HADRON ACCELERATORS*

J. M. Carmona[#], A. Ibarra, I. Podadera, CIEMAT, Madrid, Spain

Z. Abou-Haidar, M. A. G. Alvarez, A. Bocci, B. Fernández, J. García López, M.C. Jiménez-Ramos, CNA, Sevilla, Spain

Abstract

In the frame of the IFMIF-EVEDA [1] accelerator project (a 125 mA, 9 MeV, 175 MHz (CW) deuteron accelerator) CIEMAT has designed and tested two types of non-interceptive optical monitors based on gas fluorescence. This beam diagnostic technique offers a non-invasive beam profile characterization for medium to high current hadron beams. Both monitors have been tested at CNA cyclotron [2] using 9 MeV deuterons up to 40 μ A and 18 MeV protons up to 10 μ A. Profile measurements were carried out under high radiation background because the target and profilers were close to each other in the experimental setup.

In this paper, a brief description of fluorescence profile monitors (FPMs) together with the first beam measurements including systematic scans on beam current and pressure are presented.

INTRODUCTION

A high power beam (e.g. 1.125 MW for IFMIF-EVEDA) is potentially harmful for any interceptive diagnostic even though operated at low duty cycle. Hence, non-interceptive diagnostics needs development to be used during nominal operation of the accelerator.

A beam profiler based on the fluorescence of the residual gas in one of the best candidates due to its intrinsically high versatility. As a consequence of the beam particles passing through the vacuum pipe, the residual gas particles are excited. Photons are produced due to the de-excitation of the gas molecules or atoms of this residual or injected gas. The light emitted can be collected and used for the determination of the beam profiles without intercepting the beam. This technique has already been tested at high-energy proton and heavy ion accelerators [3-5].

Two fluorescence profile monitors prototypes have been designed and developed at CIEMAT and tested with beam for the first time at Centro Nacional de Aceleradores (CNA) in Sevilla. Both monitors are designed to be used under low level light environments being the image optical properties easily changed by means of a simple lens change.

Although the beam current during experiments was lower than IFMIF-EVEDA, the rest of parameters like energy, cross sections, branching ratios of transitions or efficiencies among others will be the same, with the

exception of vacuum pressure. Since the number of photons produced during the beam-gas interaction increases linearly proportional with the beam current and pressure, an extrapolation to high current scenarios will be straightforward without having uncertainties in other parameters.

The objective of these tests is to demonstrate the capability of measuring deuteron profiles with closest conditions available to IFMIF-EVEDA ones.

FPM PROTOTYPE DESIGNS

Prototype FPMs developed are based on a custom intensified Charge Injection Device (CID) camera and on a Photo Multiplier Tube (PMT) linear array. A brief description of both prototypes can be found in next subsections.

Custom ICID Based Profiler

As standard commercial intensified cameras do not satisfy the detector requirements (like sensor reliability under radiation environments) a custom intensified camera has been developed. A Proxitronic image intensifier was coupled to a radiation hard CID camera model 8726DX6. The Proxitronic intensifier unit selected has a bialkali photocathode and a P46 phosphor screen with a quartz input window. The whole system is called intensified CID (ICID).

PMT Based Profiler

The second prototype is based on a linear multianode PMT coupled to a lens. The 32 channel PMT H7260 from Hamamatsu Photonics with a Bialkali photocathode and quartz input windows was selected. For the charge integrator and data acquisition a PhotoniQ IQSP482 from Vertilon Corp. was chosen. The PMT array is mounted in an interface board together with the lens objective in a custom design and compact assembly for a safe handling interface.

The movable interface board improves the operation of the lens by changing the minimum focusing distance of operation.

EXPERIMENTAL SETUP

The FPM prototypes were installed at the end of the experimental line of the cyclotron just upstream the rotating wire scanner (BPM-83 from NEC Corp.) in order to crosscheck the profiles acquired by the FPM. The beam was stopped at the end of the line with a faraday cup (FC) of aluminium plus a thin layer of graphite. Both FPMs

*Work supported by Spanish Ministerio de Ciencia e Innovacion
Project No ENE2009-11230/FTN

[#]jm.carmona@ciemat.es

IPM SYSTEMS FOR J-PARC RCS AND MR

K. Satou, S Lee, T. Toyama, KEK, Tsukuba, Japan
H. Harada, N. Hayashi, A. Ueno, JAEA, Tokai, Japan

Abstract

Residual gas Ionization Profile Monitors (IPMs) are used at the J-PARC RCS and MR. The IPM is one of the most promising nondestructive profile monitor. However, usage in the high power accelerator like J-PARC, whose beam intensity will overcome $4E13$ particle per bunch, is challenging, because interferences with the space charge electric field of the intense beam should be carefully estimated.

The overview of the systems and the present statuses are described. The external electric field error of the RCS IPM, and the issue on contaminations on the electron collection mode are also discussed.

INTRODUCTION

The residual gas Ionization Profile Monitors (IPMs) are employed in Rapid Cycling Synchrotron (RCS) and in Main Ring synchrotron (MR) of J-PARC. The IPM uses the charged particles generated by the interaction of beam with the residual gas in the vacuum chamber. The external electric field with high uniformity are required to project the particles across the beam to a detector which mounted on the horizontal and the vertical plane. The IPM is one of the most ideal diagnostics because it induces no beam loss.

However, due to its quite complicated collection process, collecting the charged particles in the strong space charge electric field by the intense beams, it needs cross checking with other profile monitors like Multi Wire Profile Monitor (MWPM). If the space charge electric field is weak, then the effect becomes negligible with increasing a high voltage for particle collection (HV). However, the maximum space charge electric field of the J-PARC beam will reach to that of the order of 1 MV/m depending on the bunching factor. The usage in such a high space charge electric field is challenging.

There are two mode operations, ion collection and electron collection. The usage of the ion collection mode in a high power synchrotron is reported in Ref. [1].

At present, the ion collection mode are mainly used at the RCS and the MR, however, with increasing the intensity of the beam, the electron collection with guiding magnetic field (B_g) will be required [2]. As for the RCS, the electron collection mode with the B_g is also adopted.

After introducing the present IPM system, an issue on the particle collection error by the external electric field of the RCS IPM and large contaminations on the electron collection mode without the B_g measured at the MR IPM are presented.

OVERVIEW OF THE SYSTEM

Schematic drawing of the horizontal IPM system is shown in Fig. 1.

In the RCS, two IPMs are installed to measure horizontal and vertical profile. The locations of the RCS IPMs are shown in Fig. 2. The horizontal IPM is at the arc section where the dispersion function is 3.9 m. The new IPM system will be installed in the straight section where the dispersion is zero. As for the MR, two IPM systems, horizontal and vertical, have been installed at the straight section where the dispersion is zero, and the new IPM system has installed during this summer shut down at the arc section where the dispersion is 2.1 m. This IPM is not yet operated. The locations of the MR IPMs are shown in Fig. 3.

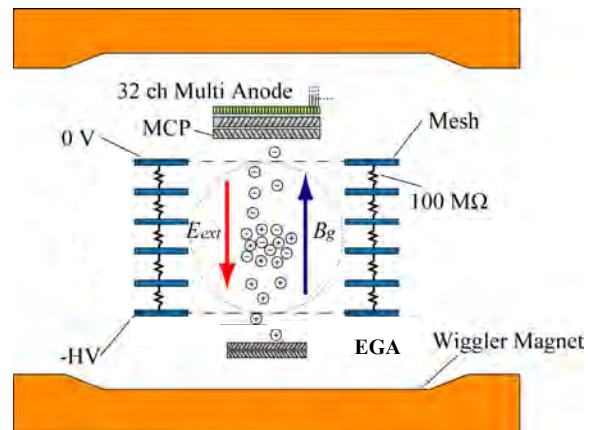


Figure 1: The schematic drawing of the IPM with magnet.

A set of the electrodes connected with the resistors is used to produce the external electric field to collect charged particles. The gap size of the electrodes is equal to the diameter of the beam window which is 297 mm for the RCS IPM and 130 mm for the MR IPM, respectively. The maximum HV for the RCS IPM and the MR IPM are 45 kV and 50 kV, respectively. By changing the polarity of the HV, both the positive ions and the electrons are collected. At present, the operating HV is limited to under 30 kV for the MR IPM to meet the internal criteria for electrical facilities. However, it will be upgraded sooner.

Rectangular chevron type microchannel plate (MCP) with multi strip anode is used for signal multiplication and signal read out. The active area of the MCP is $81 \times 31 \text{ mm}^2$. As for the RCS, the 3 MCPs are used to measure the large emittance beam of $216 \pi \text{ mm mrad}$. One 32ch multi-anode (anode width is 2.5 mm) type

BEAM INSTRUMENTATION FOR HIGH-INTENSITY, MULTI-GeV SUPERCONDUCTING LINACS*

E. Gianfelice, B. Hanna, V. Scarpine, J. Steimel, R. Webber, M. Wendt[#],
Fermilab, Batavia, IL 60510, U.S.A.

Abstract

A number of high-intensity, multi-GeV superconducting RF (SRF) proton or H⁻ linacs are being developed or proposed throughout the world. The intensity frontier, having been identified as one leg of the future of particle physics, can be addressed by the development of such a linac. All these accelerators will place strict demands on the required beam diagnostics, especially in the development of none or minimum invasive monitors such as beam profile and halo monitors.

An H⁻ / proton beam test facility is currently under construction and commissioning at Fermilab. It serves as a test bed for the development of critical beam manipulation and diagnostics components for the anticipated Project X, Fermilab's SRF multi-MW, multi-GeV linac. The paper will discuss the beam diagnostic needs for these high-intensity linacs in particular the role of the Project X test facility for development and testing of these beam instrumentation systems.

INTRODUCTION

Table 1: High Power SRF Linacs

	SNS	SPL	ESS	Myrrha	PX
E [GeV]	1,3	5	2.5	0.6	3
P [MW]	3	4	5	2.4	3
I _{pulse} [mA]	42	40	50	n/a	n/a
I _{ave} [mA]	2.5	0.8	2	4	1
duty fact. [%]	6	2	4	CW	CW
pulse len. [ms]	1	0.4	2	n/a	n/a
rep. freq. [Hz]	60	50	20	n/a	n/a

Table 1 gives an (incomplete) overview of existing (SNS) and planned high power SRF linacs for protons or H⁻. Some of the high level parameters presented are anticipated after upgrades or improvements. All facilities have a multi-MW beam power at high kinetic energies and therefore operate beams with high risk potential to damage or destroy accelerator components, if missteered or of insufficient quality. Already small beam losses can cause major trouble in close proximity of SRF accelerating structures. As a rule of thumb the maximum beam loss along the SRF linac should not exceed an equivalent of 1 W/m.

A precise control and high stability of the guide fields

is mandatory, and has to be verified by a set of reliable beam diagnostics, distributed along the linac. Essential are the measurement of

- Beam trajectory – BPMs
- Beam phase, TOF – BPMs, WCM, EO-methods
- Beam intensity – toroids, WCM
- Beam losses – BLM / TLM (e.g. ion chamber)
- Beam profile / emittance and halo – SEM, wire scanner, Allison scanner, slits, laser diagnostics, e-beam scanner, IPM, vibrating wire, etc.
- Bunch profile and tails – Feschenko monitor, laser diagnostics

Most beam parameters can be diagnosed with non-invasive, i.e. electromagnetic methods, or by detecting particle showers outside the vacuum system. The non-invasive measurement of transverse and/or longitudinal profiles however, remains challenging, particular if photo detachment methods (laser diagnostics) cannot be applied, i.e. monitoring of proton beams. The cryogenic environment of a SRF linac gives additional challenges for the beam instrumentation hardware, thus the segmentation and warm diagnostics sections along the linac are crucial. Except for simple BPM pickups and BLM detectors outside the beam vacuum system, no beam diagnostic detectors are foreseen in the cryogenic parts of the planned SRF linacs. Even if located in warm sections, but still nearby SRF structures, invasive diagnostics may produce too much unwanted spill of dissociated material, and can contaminate the niobium surface of the cavities. And finally, invasive diagnostics are of very limited use in the final, high beam power sections of the accelerator, just because of too high residual losses, even a single wire interacting with <0.1 % on a multi-MW beam produces kW beam losses.

PROJECT X

Fermilab's anticipated high intensity accelerator future is called "Project X" [1]. Major goals are the support of high energy physics (HEP) at the intensity frontier to study rare processes (kaon and muon physics), research in nuclear physics and energy, as well as a staged path towards science at the energy frontier, i.e. utilize Project X as a source for a neutrino factory and/or muon collider.

Central element of the Project X accelerator complex will be a 3 GeV SRF CW linac, accelerating H⁻ to 3 MW beam power (see Figure 1). A system of magnetic and RF beam splitters feeds various experiments simultaneously, as well as a pulsed SRF linear accelerator extension – in favour to a RCS – to accumulate H⁻ particles using foil or laser stripping at 8 GeV into the existing Recycler / Main Injector ring accelerators.

*This work supported by the Fermi National Accelerator laboratory, operated by Fermi Research Alliance LLC, under contract No. DE-AC02-07CH11359 with the US Department of Energy.
[#]manfred@fnal.gov

BEAM-BEAM SIMULATIONS FOR FUTURE ELECTRON-ION COLLIDER eRHIC*

V. Ptitsyn, Y. Hao, V.N. Litvinenko, BNL, Upton, NY 11973, U.S.A.

Abstract

The future electron-ion collider eRHIC - under design at BNL - will collide the electron beam accelerated in energy recovery linacs with protons or ions circulating in the RHIC storage ring. The beam-beam effects in the linac-ring configuration have a number of unique features. For the in-depth studies of the beam-beam effects and the resulting luminosity limitations, we developed a dedicated simulation code. We studied the effects of the mismatch, the disruption and the pinching on the electron beam. Relevant dynamics of the proton beam, including the kink instability in combination with incoherent beam-beam effects, was also explored in detail. In this paper we describe the main features of our simulation code and present the most important simulations results.

INTRODUCTION

Several designs of electron-ion colliders are under development in the world [1]. The design of electron-ion collider eRHIC at BNL adds an electron accelerator, based on energy recovery linacs (ERLs), to the existing heavy ion accelerator complex RHIC [2]. The eRHIC design uses a so-called linac-ring collision scheme. The electron beam, accelerated in the ERL, passes a collision point just once, while the proton (or ion) beam circulates in a ring and passes the collision point on every turn. There may be several collision points in the collider, although in this paper we show the simulation results for the case of one electron-proton collision.

Since the electron beam goes through the collision point(s) only on one pass, the allowed strength of the beam-beam force acting on the electron beam can be much larger than for electrons circulating in a storage ring. Thus a typical beam-beam limit for electrons in circular colliders can be surmounted. The resulting eRHIC luminosity in the linac-ring scheme is considerably larger than that in the ring-ring scheme. Present eRHIC design aims at the luminosity of e-p collisions exceeding $10^{34} \text{ cm}^{-2} \text{ s}^{-1}$.

The studies of the beam-beam interactions in the linac-ring collision scheme is very important eRHIC R&D item. Since there has been no collider based on the linac-ring collision layout, there is no any operational experience with the linac-ring beam-beam interactions and the related machine performance limits. Thus all features of beam collisions in the linac-ring scheme have to be thoroughly studied during the machine design. This would allow to determine the maximum achievable luminosity and to identify and address possible problems originating from

the beam-beam interactions. One should note that the linac-ring collider scheme have been considered in previous years for accelerator designs, for example, as possible design for B-factory. Hence, the specific features of the linac-ring beam-beam interactions had been also studied [3,4]. For eRHIC, the following features of the beam-beam interactions have to be considered and investigated:

- The electron beam disruption. The level of the disruption should be acceptable for the electron beam transport and deceleration in the ERL.

- The electron beam pinch, the related enhancements of the luminosity and the beam-beam effect on the proton beam.

- The kink instability of the proton beam.

- The effect of fluctuating electron beam parameters (intensity, transverse emittance) on the proton beam.

A comprehensive study of the list above require a full-blown simulations of the beam-beam effects including the nonlinearity of beam-beam force, the variation of beta-function throughout the collision region, synchrotron oscillations of the proton beam, chromaticity and amplitude-dependence of proton betatron tunes. A code EPIC was created [5] to carry out the detailed and time-efficient studies of the beam-beam effects in eRHIC. The following section provides description of the EPIC simulation code. In later sections we present some results of the beam-beam simulations and discuss the influence of those results on the collider design.

THE BEAM-BEAM INTERACTION MODEL AND SIMULATION CODE

The EPIC code takes into account two considerable asymmetries in the eRHIC collision scheme. One is the asymmetry of the strength of the beam-beam force acting on the electrons and the protons. Both in terms of the beam-beam parameters ($\xi_p=0.015$, $\xi_e = 2.2$), and in the terms of the disruption parameters ($D_p = 0.007$, $D_e = 27$) the beam-beam effect on the electron beam is much stronger compared with that on the hadron beam. Because of the strong beam-beam effect the electron beam gets disrupted during the pass through the collision region. In contrary to that, the beam-beam effect on the protons is moderate, and the effect of the interactions becomes important on the scale of thousands and million turns. The strong asymmetry of the beam-beam effects is used in the EPIC simulation code to separate the study of one pass effect of the electron beam disruption and multi-turn effect of the beam-beam interaction on the proton (ion) beam.

* Work supported by Brookhaven Science Associates, LLC under Contract No. DE-AC02-98CH10886 with the U.S. Department of Energy.

COMPUTATIONAL CHALLENGES FOR BEAM-BEAM SIMULATION FOR RHIC*

Y. Luo, W. Fischer, Brookhaven National Laboratory, Upton, NY USA

Abstract

In this article we will review the computational challenges in the beam-beam simulation for the polarized proton run of the Relativistic Heavy Ion Collider (RHIC). The difficulties in our multi-particle and million turn tracking to calculate the proton beam lifetime and proton beam emittance growth due to head-on beam-beam interaction and head-on beam-beam compensation are presented and discussed. Solutions to obtain meaningful physics results from these trackings are proposed and tested. In the end we will present the progress in the benchmarking of the RHIC operational proton beam lifetime.

INTRODUCTION

The Relativistic Heavy Ion Collider (RHIC) accelerates and collides ions and polarized protons. For the experiments the figure of merit in the polarized proton run is $LP_B^2 P_Y^2$, where L is the luminosity and $P_{B,Y}$ are the polarizations of the Blue and Yellow beams respectively. Since its first polarized proton run at 100 GeV in 2003, the polarized proton luminosity has increased by an order of magnitude. And the proton polarization reached 55% and 34% at 100 GeV and 250 GeV.

The main limits to the luminosity improvement in the RHIC polarized proton run are the beam-beam interaction effect, the nonlinear effect from the lattice, and the parameter modulations. To further increase the proton luminosity [1], we would like to reduce the β^* at the interaction points from current 0.7 m to 0.5 m, and to increase the bunch intensity from current 1.5×10^{11} to 2.0×10^{11} and perhaps beyond. An upgrade of the polarized proton source has been started to increase the proton current by an order of magnitude and the polarization by about 5% to 85-90%.

For the polarized proton runs, the working point is chosen to provide good beam lifetime and maintain the proton polarization. The current working point is constrained between 2/3 and 7/10. When the proton bunch intensity is above 2×10^{11} , there will not be enough tune space between 2/3 and 7/10 to hold the beam-beam tune spread. One solution is to adopt head-on beam-beam compensation [2]. The idea is to introduce a low energy electron beam to collide with the proton beam to compensate the proton-proton beam-beam effects. Our preliminary simulation study shows that head-on beam-beam compensation with the e-lenses can significantly reduce the large beam-beam tune spread. However, considering that the e-lenses

are strong nonlinear elements, their effects on the proton beam dynamics and lifetime have been carefully studied.

Since beam-beam effect has played a more and more important role in the polarized proton run in RHIC, numeric simulation studies are needed to understand the current RHIC operations and to predict the effect of head-on beam-beam compensation. In the article we will review the computational challenges in our beam-beam simulation. With limited computing resource and computing time, some approaches and new algorithm to reduce the statistic fluctuations in the calculated beam lifetime and emittance are presented and tested. Progress in the benchmarking of RHIC operational proton beam lifetime is also reported.

CHALLENGES IN SIMULATION

To reproduce the observations in the real operations, a robust simulation code and a realistic lattice model are needed. For RHIC, the lattice model should include the correct linear optics, all non-linear magnetic field errors, and all known parameter modulations.

To save the computing time, we adopt a weak-strong beam-beam model although the two proton beams have similar populations. Considering β^* is comparable to the RMS bunch length at IP6 and IP8 in the polarized proton run, we adopt the 6-D weak-strong synchro-beam map a la Hirata to calculate the beam-beam kicks.

Our simulation code is SimTrack [3], which is a C++ library for the optics calculation and particle trackings in the high energy accelerators. The particle motion in the magnetic elements is tracked with the 4th order symplectic integration. To save computing time, multipoles are treated as thin lenses. Particles are tracked element by element.

Dynamic aperture has been frequently used to judge the stability of lattice and the effect of beam-beam interaction in RHIC [4]. Comparing to multi-particle tracking of a 6-D Gaussian distribution, it only needs a small amount of computing time. The shortcoming of dynamic aperture is that it does not give information of emittance evolution. And there is not a clear calibration between dynamic aperture and beam lifetime. Online measurement of dynamic aperture with beam is also time-consuming.

Actually in the operations of a collider, the beam intensity, the transverse and longitudinal beam sizes, and the luminosity are all directly measured. And in a long-term multi-particle tracking of a 6-D Gaussian distribution bunch, they are well defined and can be calculated too. Therefore, these parameters are suitable for the purpose of benchmarking simulation codes and comparing operation observations and simulation results.

* This work was supported by Brookhaven Science Associates, LLC under Contract No. DE-AC02-98CH10886 with the U.S. Department of Energy.

SIMULATION OF SPACE-CHARGE EFFECTS IN THE PROPOSED CERN PS2*

J. Qiang[†], R. D. Ryne, LBNL, Berkeley, CA 94720, USA

U. Wienands, SLAC, Menlo Park, CA 94025, USA

H. Bartosik, C. Carli, Y. Papaphilippou, CERN, Geneva, Switzerland

Abstract

A new proton synchrotron, the PS2, was proposed to replace the current proton synchrotron at CERN for the LHC injector upgrade. Nonlinear space-charge effects could cause significant beam emittance growth and particle losses and limit the performance of the PS2. In this paper, we report on simulation studies of the potential space-charge effects at the PS2 using three-dimensional self-consistent macro-particle tracking. We will present the computational model used in this study, and discuss the impact of space-charge effects on the beam emittance growth, especially due to synchro-betatron coupling, initial longitudinal painted distribution, and RF ramping schemes.

INTRODUCTION

The PS2 with higher injection energy (4 GeV) was proposed to replace the current proton synchrotron with 1.4 GeV injection energy for LHC upgrade at CERN [1]. Space-charge effects have been identified as the most serious intensity limitation in the PS and PS Booster [2], since nonlinear space-charge effects in high intensity hadron beams can cause significant emittance growth and particle losses. These effects put a strong limit to the attainable intensity for the proposed synchrotron accelerator. Exploring the space-charge effects through long-time self-consistent particle tracking will help shed light on the source of emittance growth and particle losses (e.g. space-charge driven resonance) and help provide means to overcome these effects through improved accelerator design or compensation schemes.

COMPUTATIONAL MODELS

In this study, we have used the IMPACT code and the MaryLie/IMPACT (ML/I) code developed at Lawrence Berkeley National Laboratory for simulation studies. The IMPACT code is a parallel particle-in-cell code suite for modeling high intensity, high brightness beams in RF proton linacs, electron linacs and photoinjectors [3]. It consists of two parallel particle-in-cell tracking codes IMPACT-Z and IMPACT-T (the former uses longitudinal position as the independent variable and allows for efficient particle advance over large distances as in an RF linac, the latter uses time as the independent variable and is needed to

accurately model systems with strong space charge as in photoinjectors), an RF linac lattice design code, an envelope matching and analysis code, and a number of pre- and post-processing codes. Both parallel particle tracking codes assume a quasi-electrostatic model of the beam (i.e. electrostatic self-fields in the beam frame, possibly with energy binning) and compute space-charge effects self-consistently at each time step together with the external acceleration and focusing fields. The 3D Poisson equation is solved in the beam frame at each step of the calculation. The resulting electrostatic fields are Lorentz transformed back to the laboratory frame to obtain the electric and magnetic self-forces acting on the beam. There are six Poisson solvers in the IMPACT suite, corresponding to transverse open or closed boundary conditions with round or rectangular shape, and longitudinal open or periodic boundary conditions. These solvers use either a spectral method for closed transverse boundary conditions [4], or a convolution-based Green function method for open transverse boundary conditions [5]. The parallel implementation includes both a 2D domain decomposition approach for the 3D computational domain and a particle-field decomposition approach to provide the optimal parallel performance for different applications on modern supercomputers. Besides the fully 3D space-charge capability, the IMPACT code suite also includes detailed modeling of beam dynamics in RF cavities (via field maps or z-dependent transfer maps including RF focusing/defocusing), various magnetic focusing elements (solenoid, dipole, quadrupole, etc), allowance of arbitrary overlap of external fields (3D and 2D), structure and CSR wake fields, tracking multiple charge states, tracking multiple bin/bunches, Monte-Carlo simulation of gas ionization, an analytical model for laser-electron interactions inside an undulator, and capabilities for machine error studies and correction. For the purpose of studying space-charge effects in a synchrotron ring, the IMPACT code was extended to include thin lens kicks for multipole elements and RF cavities, multi-turn simulation, dynamic RF ramping, and lumped space-charge kicks.

The MaryLie/IMPACT (ML/I) [6] is a hybrid code that combines the beam optics capabilities of MARYLIE with the parallel 3D space-charge capabilities of IMPACT. In addition to combining the capabilities of these codes, ML/I has a number of powerful features, including a choice of Poisson solvers, a fifth-order RF cavity model, multiple reference particles for RF cavities, a library of soft-edge magnet models, representation of magnet systems in terms of coil stacks with possibly overlapping fields, and wakefield

* Work partially by the US Department of Energy through the US LHC Accelerator Research Program (LARP) under Contract No. DE-AC02-05CH11231.

[†] jqiang@lbl.gov

WAKE FUNCTIONS FOR LAMINATED MAGNETS AND APPLICATIONS FOR FERMILAB BOOSTER SYNCHROTRON*

A. Macridin[†], P. Spentzouris, J. Amundson, Fermilab, Batavia, IL, USA
 L. Spentzouris, D. McCarron, Illinois Institute of Technology, Chicago, IL, USA

Abstract

The Fermilab Booster beam is exposed to magnet laminations, resulting in impedance effects much larger than resistive wall effects in a beam pipe. We present a calculation of wake functions in laminated magnets, which show large values at distances of the order of a few meters, but decrease quickly to zero beyond that. Therefore, strong in-bunch and nearest-bunch effects are present. We show realistic Synergia simulations of the Booster using these wake functions and space-charge solvers appropriate for the various geometries of the constituent elements of the machine. The simulation of tune shifts is in good agreement with experimental data. We find that wake fields in the Booster magnet laminations strongly increase beam emittance and have the potential to cause significant beam loss.

INTRODUCTION

Due to the high complexity of accelerators, simulations which employ large computers and sophisticated algorithms are required in order to understand and make predictions about beam dynamics. Besides high order maps to describe single particle propagation through accelerators, simulations should also consider collective effects such as space charge (SC) forces and wake field interactions. These problems can be addressed with the Synergia code developed at Fermilab [1]. Synergia is an extensible multi-language framework which incorporates a large collection of physical models, specialized modules and numerical libraries.

The Booster synchrotron is a 40 year old machine placed at near the beginning of the Fermilab accelerator chain, now typically running with beam intensities roughly twice the design value. Due to the strong demand for increasing intensity, investigation of collective effects in the Booster is of paramount importance.

A peculiarity of the Booster is the parallel-planes vacuum chamber formed by its laminated magnets [2]. Different authors stress the importance of wake effects in laminated structures [3, 4, 5, 6, 7]. While their analysis

is based on the analysis of impedance functions defined in frequency space, complex Synergia simulations require knowledge of distance dependent wake functions.

Recently, measurements of tune shifts in the Booster indicate the presence of quadrupole wake effects specific to geometries without circular symmetries [8]. While the quadrupole influence on the betatron tune shift has been discussed before in the context of resistive wall wakes [9], for Booster simulations it is important to study the effect in structures with laminations.

In the first part of the paper we calculate the impedance and wake functions for Booster laminated magnets. The wake fields are large and oscillate in sign at distances on the order of the bunch length, and decay quickly at large distances. This implies that in-bunch and nearest-neighbor-bunch wake interactions are predominant.

The second part shows results of Synergia simulations of the Booster at the injection energy. We find that the coherent vertical tune decreases with increasing beam intensity, while the horizontal tune is almost constant, in close agreement with experiment [8]. Synergia simulations also show that the wake has the potential to cause significant beam loss in Booster and strongly increases the beam emittance.

WAKE FUNCTIONS FOR LAMINATED MAGNETS

Formalism

The wake functions describe the effect of the electromagnetic field created by a particle moving through an accelerator beam pipe upon the trailing particles. We consider a parallel-planes beam pipe as a suitable approximation for the Booster magnets. If the distance between the leading and trailing particle is $|z|$, the momentum of the trailing particle traversing a structure of length L will be modified by:

$$c\Delta p_z = -qQW^{\parallel}(z) \quad (1)$$

$$c\Delta p_x = -qQ(W_x^{\perp}(z)X - W_x^{\perp}(z)x) \quad (2)$$

$$c\Delta p_y = -qQ(W_y^{\perp}(z)Y + W_y^{\perp}(z)y) \quad (3)$$

Here Q (q) and (X, Y) ((x, y)) represent the charge and the transverse displacement of the leading (trailing) particle respectively. \parallel and \perp denote the longitudinal and the transverse directions. The higher order terms in the displacement are neglected. For this particular geometry, only two wake functions, $W_x^{\perp}(z)$ and $W_y^{\perp}(z)$, are needed for the transverse directions (Eq. 2 and Eq. 3). This is a con-

* This work was supported by the United States Department of Energy under contract DE-AC02-07CH11359 and the ComPASS project funded through the Scientific Discovery through Advanced Computing program in the DOE Office of High Energy Physics. This research used resources of the National Energy Research Scientific Computing Center, which is supported by the Office of Science of the U.S. Department of Energy under Contract No. DE-AC02-05CH11231 and of the Argonne Leadership Computing Facility at Argonne National Laboratory, which is supported by the Office of Science of the U.S. Department of Energy under contract DE-AC02-06CH11357.

[†] macridin@fnal.gov

A NEW PARADIGM FOR MODELING, SIMULATIONS AND ANALYSIS OF INTENSE BEAMS

E. Nissen, B. Erdelyi, Department of Physics, Northern Illinois University, Dekalb, IL 60115, USA

Abstract

Currently when the effects of space charge on a beam line are calculated the problem is solved using a particle in cell method to advance a large number of macroparticles. If quantities such as space charge induced tune shifts are desired it is difficult to determine which of the many variables that make up the beam is the cause. The new method presented here adds the effects of space charge to a nonlinear transfer map, this allows us to use normal form methods to directly measure quantities like the tune. This was done using the code COSY Infinity which makes use of differential algebras, which allow the direct calculation of how the tune depends on the beam current. The method involves finding the high order statistical moments of the particles, determining the distribution function, and finally the potential. In order to advance the particles as accurately as possible a fast multipole method algorithm is used. In this talk we present the new methods and how they allow us to follow the time evolution of an intense beam and extract its nonlinear dynamics. We will also discuss how these methods can improve the design and operation of current and future high intensity facilities.

INTRODUCTION

The purpose of this study is to create a method whereby the effects of space charge in a particle beam are included in the transfer map of the machine the beam is passing through. Currently the transfer map governs the motion of single particles in the machine, which is useful for steering, bare tunes, dynamic apertures, and many other quantities of interest governing the motion of single particles. Creating this new space charge added map will allow for the analysis of the effects of space charge on quantities that are directly extracted from the map using normal form methods such as tunes and chromaticities.

The calculation of the space charge effect involves first creating a distribution of particles which will serve as proxies for the beam. These are used to calculate the distribution function throughout the beam pipe, the distribution function is then integrated with an appropriate Green's function to determine the potential. The potential is used to find the electric fields, which are used to create an electric field map which is applied to the map of the element using Strang splitting. We will begin with an overview of the process before examining some results.

SOFTWARE ENVIRONMENT

The software being used is COSY Infinity 9.0 [1]; this package uses differential algebras to perform exact numerical differentiation as well as to create Taylor models of the elements in question. Differential algebras work by creating vectors with their elementary mathematical operations redefined in such a way that they retain the derivatives of each quantity as they move through an algorithm. This allows for not only non-linear Taylor maps, but for coordinate transforms to normal form coordinates that retain any variable dependences that the original map had. These Taylor models allow for high order transfer maps, as well as non-linear normal form transformations. The easy inclusion of non-linearity in the transfer maps, which allows outside calculation using differential algebras makes the task of adding space charge to the transfer map significantly less cumbersome than a traditional code.

DISTRIBUTION CALCULATION

In order to create a map of the effects of space charge in a region, the distribution must be calculated within that region. We use a set of discrete test particles as proxies for the distribution which can be used to calculate the Taylor series.

The particles are formed into a Taylor series using their statistical moments. If two distributions have the same moments, mathematically they are identical [2]. The moments are calculated by,

$$M_{nm} = \sum_{i=1}^{N_{particles}} x_i^n y_i^m. \quad (1)$$

If we assume that the distribution is a Taylor series of the form, $\rho(x, y) = \sum_i \sum_j C_{ij} x^i y^j$, then the moments can be connected to the coefficients with the equation,

$$M_{nm} = \sum_i \sum_j \int_{-x_r}^{x_r} \int_{-y_r}^{y_r} C_{ij} x^{n+i} y^{m+j} dx dy, \quad (2)$$

where x_r and y_r are the x and y boundaries. This is trivially integrated, forming a matrix equation. This matrix is inverted using truncated single value decomposition, which gives the proper values for the Taylor series coefficients. This is the same way that the coefficients are found for three dimensions.

CHALLENGES OF RECONCILING THEORETICAL AND MEASURED BEAM PARAMETERS AT THE SNS ACCELERATOR FACILITY

A. Aleksandrov, Oak Ridge National Laboratory, Oak Ridge, TN 37830, USA

Abstract

The Spallation Neutron Source (SNS) is steadily approaching its design beam power of 1.4 MW without encountering major of the models used for the accelerator design and tuning. Nevertheless, it is surprisingly difficult to reconcile many of the measured beam parameters with the model prediction. In this paper we discuss several examples of such discrepancies, ranging from a simple single particle tracking to beam emittance measurements. We also present our approach to resolving some of the issues from a diagnostics standpoint.

INTRODUCTION

The intention of this talk was to initiate a discussion during a joint session of the Computational Challenges and the Beam Diagnostics and Instrumentation working groups on the issues of reconciling measured beam parameters with computer simulations. This topic is not new and has been a subject of intense discussion during every HB workshop.

The SNS accelerator, recently commissioned, is one of the newest and highest intensity proton machines in existence. Advanced computer simulation tools were used during its design, and it is equipped with a comprehensive set of beam diagnostics. This makes the SNS accelerator a practical, state-of-the-art example for reconciliation of high intensity beam simulation with measurements. Due to length limitations we will only discuss problems related to the SNS linac in this document.

The SNS is running at 1 MW and no problems are expected up to the design beam power of 1.4 MW. This success is a confirmation of the general validity of the models used for the accelerator design and tuning. At the same time, our commissioning and initial operation experience shows that it is surprisingly difficult to reconcile many of the measured beam parameters with the model predictions. The important questions to ask are: Are the models we used as design tools capable of predicting major beam parameters in the operational accelerator? If yes, are they accurate and powerful enough to predict beam loss? Do we need to have such accurate models? If yes, do we believe it is realistic to obtain such a high level of accuracy, should we even try? We can not give answers to these questions in this document but will provide some practical examples to illuminate several aspects of the problem: The accuracy of the models, the reliability of the measured data, the uncertainty in the knowledge of the machine state and the initial distribution.

BEAM DYNAMICS SIMULATION

There are many computer codes available these days powerful code PARMILA was the main simulation tool for the SNS linac design. Some other codes were used for simulation of beam dynamics in linear and circular accelerators. Some of them can run on parallel computers and track tens of millions of particles with 3D space charge calculations. An older and less for verification of the design stability and for error tolerance studies, such as IMPACT, LINAC and TRACE-3D. End-to-end simulations with different initial distributions demonstrated good agreement between the codes. Expectations have been high, based on quick and successful commissioning of the linac, that the same models can accurately predict the beam parameters in the real accelerator, maybe even beam halo and losses. These expectations have not materialized so far, and there is a growing understanding that a different kind of computer model is required for predicting behavior of real beams in real accelerators.

A real machine is characterized by a very large number of parameters, the precise values of which are not known. A few examples are RF phases and amplitudes, magnet strengths and offsets, etc. A common practical way to determine these values is to fit the model to the available experimental data by varying the parameters of interest in the model. To solve this optimization problem a large number of runs are required, preferably in real time with live data in the control room. This is unrealistic for end-to-end simulations with large numbers of particles and 3D fields, even with modern computing capabilities. But this is exactly the modern trend in simulation code development: End-to-end simulations with huge numbers of particles and 3D-field calculations. The motivation for increasing the number of simulated particles and mesh density is to increase the accuracy of electro-magnetic field calculations, which defines the final accuracy of particle motion in the model. This is the correct approach for modeling an ideal accelerator. But in a real machine, very often the model accuracy is defined by knowledge of the actual hardware parameters, and therefore increasing the number of simulated particles and the mesh density does not improve the accuracy of the model predictions. As a result of growing computer power requirements for modern accelerator design codes, it becomes impractical to use them for real machine simulation. In practice we have to use a combination of codes or pieces of codes for modeling different aspects of beam dynamics in different portions of the SNS linac. At present, these pieces are not connected and there is no convenient framework for the data analysis with good optimization capabilities.

BEAM DYNAMICS SIMULATION IN SARAF PHASE-I PROTON/DEUTERON 4 MEV LINAC COMMISSIONING

J. Rodnizki, A. Kreisel, Soreq NRC, Yavne 81800, Israel

Abstract

The SARAF accelerator is designed to accelerate both deuteron and proton beams up to 40 MeV. Phase I of SARAF consists of a 4-rod RFQ (1.5 MeV/u) and a prototype superconducting module housing 6 half-wave resonators (HWR) and 3 superconducting solenoids (4-5 MeV). Beam Dynamics TRACK simulation, for a proton and a deuteron beam, tailored to the present available field amplitude at each cavity, were used to evaluate and tune the linac. The simulation is a key factor to reach a stable high intensity CW beam. The ions energy and energy spread were measured using the Rutherford scattering technique. The measured energy gain and the energy spread at the RFQ exit and along the PSM were in good agreement with the beam dynamics simulations.

INTRODUCTION

SARAF (Soreq Applied Research Accelerator Facility) is currently under construction at Soreq NRC. It will consist of up to 40 MeV high current (up to 4 mA) CW, 176 MHz RF superconducting linac of protons and deuterons. The linac status and technical description of its components are given in [1]. Phase one of the SARAF linac includes a 20 keV/u proton/deuteron ECR ion source, a LEBT, a 3.8 m long 1.5 MeV/u four rods RFQ and a Prototype Superconducting Module (PSM) with six $\beta = 0.09$ HWRs, a Diagnostic plate (D-plate), Beam Dumps (BD) and a temporary beam line. The main components of Phase I are shown in Fig. 1.

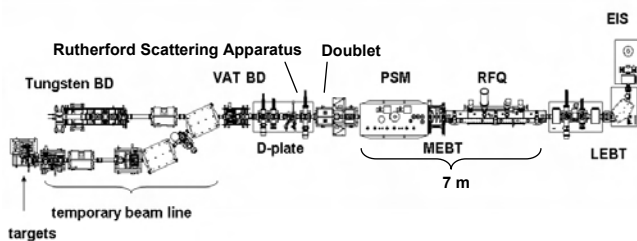


Figure 1: Phase I of the SARAF linac.

Beam dynamics simulations were vital during the conditioning efforts of phase I. At each step of the operation the low level RF amplitude and phase were varied to achieve the beam dynamics design. The electromagnetic fields were simulated using CST MWS and the presented beam dynamics simulations were done using TRACK [2].

The simulations were applied for:

1. Analysis of the RFQ beam transmission as function of the RFQ power.

2. Optimization of the RFQ field flatness to achieve better transmission and lower losses downstream the RFQ.
3. Exploring and calibrating the voltage at each cavity as a function of the low level RF signal.
4. Beam dynamics design of the fields configuration according to the achievable measured voltage in each cavity.

ANALYSIS OF RFQ BEAM OPERATION

A comparison of proton beam dynamics simulation to a measurement in 2007 is presented in Fig. 2 top. It shows good agreement at the low power region and a reduction in the measured transmitted current in the high power region relative to the simulated value [3]. The expected value was extracted from beam dynamics simulations with homogenous fields along the RFQ.

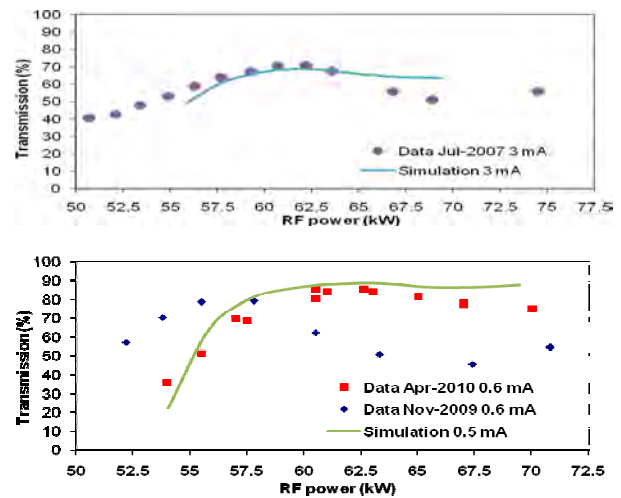


Figure 2: Proton transmitted current as function of RFQ power. Comparison of data and simulation for high current 3mA (top) and low current ~0.5 mA (bottom).

Prior to 2009 measurements the bottom electrodes were re machined due to high parasitic fields that eliminated CW deuteron beam operation. The quadrupole electrodes design, so called ‘mini-vane’, has a cooling water channel drilled inside. The mini-vanes allow a good cooling of the electrodes and avoids misalignment caused by heating. In the SARAF RFQ mini-vanes design the distance between the bottom electrodes and the stems with the negative RF polarity (each second stem) was too small (around 5 mm). This resulted in parasitic fields between the bottom electrodes and the stems, which are higher than the fields between the electrodes, as proved by RF simulations.

To solve this problem local cutting of the bottom electrodes back side along each second stem reduced

MEASUREMENT AND SIMULATION IN J-PARC LINAC

M. Ikegami*, KEK/J-PARC, Tokai, Japan
 H. Sako, A. Miura, G. Wei, JAEA/J-PARC, Tokai, Japan

Abstract

In J-PARC linac, significant transverse emittance growth and halo formation are observed with the design peak current of 30 mA. In the previous study, the most probable cause of the beam quality deterioration was identified as the longitudinal mismatch at MEBT with a help of particle simulations. Based on this finding, we have performed a retuning of MEBT buncher amplitudes experimentally, and have succeeded in mitigating the emittance growth and halo development. It demonstrates that a particle simulation is helpful in identifying the mechanism behind the experimentally observed beam quality deterioration in a high-intensity proton linac, and setting the direction for the practical tuning for it.

INTRODUCTION

J-PARC linac consists of a 50-keV negative hydrogen ion source, a 3-MeV RFQ (Radio Frequency Quadrupole linac), a 50-MeV DTL (Drift Tube Linac), and a 181-MeV SDTL (Separate-type DTL) [1]. While its design peak current is 30 mA, it started its user operation in December 2008 with the reduced peak current of 5 mA. We have been increasing its beam power since then, and it is currently operating with the peak current of 15 mA [2].

As reported in the previous workshop of this series [3], we experienced a significant emittance growth in DTL followed by halo development in SDTL in a demonstration operation with the design peak current of 30 mA. Distinctive features of this phenomenon are as follows;

- Absence of halo development in DTL in spite of the significant emittance growth in this section
- Absence of emittance growth in SDTL despite the significant halo development in this section

This phenomenon is assumed to be space-charge-driven, because it has not been observed with the lower peak current of 5 mA.

In the previous study [3], we have concluded from an extensive particle simulation that the emittance growth and halo development are likely to be caused by a longitudinal mismatch at MEBT (Medium Energy Beam Transport) between RFQ and DTL. The simulation has shown that a longitudinal mismatch leads to a transverse mismatch oscillation due to space-charge coupling, and then drives a halo development. This mechanism explains why the halo development is delayed until the beam reaches SDTL. How-

ever, we could not perform an experiment to retune the longitudinal matching at that time because the peak current was limited to 5 mA due to a sparking problem in RFQ [4]. As RFQ is recovering and the peak current has been increased to 15 mA, we have tried to mitigate the emittance growth and halo development experimentally by retuning the buncher cavities in MEBT. We have observed the qualitatively same beam quality deterioration with the peak current of 15 mA, although the degrees of emittance growth and halo development are naturally more modest than those observed with 30 mA.

In this paper, we present experimental results in the tuning performed base on the findings in a particle simulation described in the reference [3].

ORIGINAL MATCHING AT MEBT

The layout of MEBT is shown in Fig. 1 schematically. We have two buncher cavities in MEBT to perform a longitudinal matching between RFQ and DTL. Originally, the amplitude and phase of bunchers were set with an amplitude-phase scan tuning with monitoring the output beam energy. The beam energy was measured with TOF (Time Of Flight) methods using two downstream FCT's (Fast Current Transformers). An FCT detects the beam phase, and we use two FCT's just after the buncher under tuning for the TOF measurement. The present monitor layout in MEBT is found in the reference [5].

As the buncher cavity has only an RF gap, the resulting phase scan curve is a simple sinusoidal curve. Then, it is easy to find its effective gap voltage and synchronous phase from the measurement. The synchronous phases are set to -90 degree, and the amplitudes are set to the design values determined from Trace3D calculation [6]. In the Trace3D calculation, we assume twiss parameters obtained with PARMTEQM simulation at the exit of RFQ [7].

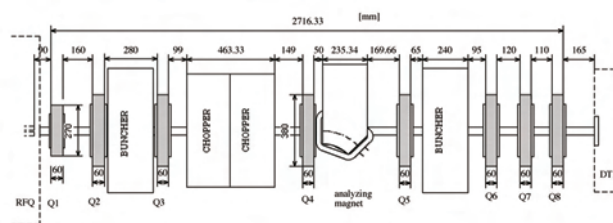


Figure 1: The schematic layout of MEBT.

* masanori.ikegami@kek.jp

BEAM MEASUREMENT AND SIMULATION AT THE SNS

A. Shishlo[#] on behalf of SNS Accelerator Group, ORNL, Oak Ridge, TN 37831, U.S.A.

Abstract

The overview of the Spallation Neutron Source (SNS) linac lattice, diagnostics, and beam dynamics is presented. The models and model-based tuning procedures of the warm and superconducting parts of the SNS linac are discussed. There are significant discrepancies between simulated and measured losses in the superconducting part of the linac. The possible reasons for these losses and their relation to the beam dynamics are discussed.

INTRODUCTION

At present time the SNS accelerator complex routinely delivers 1 MW proton beam to the mercury target which makes it the most powerful pulsed spallation source in the world. The SNS accelerator consists of a 1 GeV linac and an accumulator ring. This paper will discuss the SNS linac structure, the beam dynamics, comparison between models and measurements, and losses in the SNS linac.

SNS LINAC

The SNS linac includes a front-end, six 402.5 MHz drift tube tanks (DTL), four 805 MHz coupled cavity linac (CCL) sections, and two sections of a superconducting linac (SCL) with cavities designed for relativistic factors 0.61 and 0.81 (so-called medium- β and high- β SCL sections). The structure and design output energies are shown in Fig. 1. The DTL and CCL are room temperature RF structures. The SCL cavities operate at a temperature of 2°K. The SNS front-end (FE) consists of a negative hydrogen-ion source, a low energy beam transport line (LEBT), an RFQ that accelerates the H⁻ beam to an energy of 2.5 MeV, and a medium energy beam transport line (MEBT) that matches the beam for the DTL entrance. The ion source and RFQ are designed to deliver 38 mA peak current, but now the FE can provide up to 45 mA which we are not using in production.

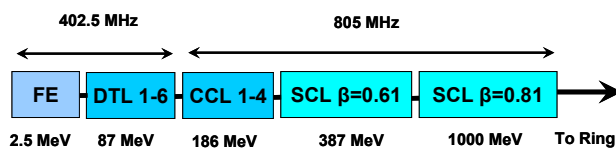


Figure 1: SNS linac structure.

SNS Linac Beam Dynamics

A primary goal in the SNS linac design was to minimize potential damage and radioactivation of the accelerator resulting from beam halo generation and uncontrolled losses [1]. According to the design

[#]shishlo@ornl.gov

parameters, the losses should not exceed 1 W/m. Some conditions were imposed to minimize halo generation [1]:

- The zero-current phase advances (transverse and longitudinal) per period never exceed 90°.
- To avoid the second order parametric resonance, the transverse and longitudinal phase advances do not cross except in DTL tank 1 and CCL module 4 where matching considerations prevail.
- The transverse and longitudinal phase advances per meter are smooth functions along the linac. This feature minimizes possible mismatches and helps to create a current independent design.

Other source of potential halo and emittance growth are resonant modes. They can develop in the beam itself and cause beam energy exchange between transverse directions. The analysis of such resonances for 52 mA peak current showed that the SNS linac is too short for noticeable beam degradation [1].

The analysis of the beam dynamics of the superconducting part revealed a surprisingly tolerant design [2]. The deviation of the electric fields of the SCL cavities from the design values by as much as $\pm 30^\circ$ appears to have minimal effect on the beam performance. This low sensitivity is, in part, a direct result of the nature of the SCL linac where each cavity's phase can be adjusted individually. In contrast, the normal-conducting DTL and CCL are synchronous structures where each gap in any cavity is phase-locked to its neighbor, and its phase is not adjustable.

SNS Linac Beam Diagnostics

A suite of beam diagnostics devices defines what kind of information we can get for analysis and for tuning the linac. The available SNS linac beam diagnostics include:

- Beam-position monitors (BPM). The 60 SNS linac BPMs are able to measure the beam position, beam intensity, and beam phase on a mini-pulse-by-mini-pulse basis. The ability to measure the beam phase is an absolute necessity to tune up RF phases of linac cavities.
- The SNS linac Beam Current Monitor (BCM) system consists of 10 fast current transformers. The accuracy of the current measurement is not enough to see beam losses below the 1% level.
- Wire Scanners (WS) are used for interceptive measurements of transverse beam profiles in the MEBT, DTL, and CCL. Wire scanners in the MEBT measure the charge of electrons stopped in the wire and all other WSs measure charge induced by secondary emission from the wire.
- To measure transverse beam profiles in the SCL, 'laser wire' (LW) stations are used. LW uses a non-intrusive method based on photo-ionization of the

ADVANCED BEAM DYNAMICS SIMULATIONS WITH THE DYNAMION CODE FOR THE UPGRADE AND OPTIMIZATION OF THE GSI-UNILAC

S. Yaramyshev, W. Barth, G. Clemente, L. Dahl, L. Groening, S. Mickat, A. Orzhekhovskaya, H. Vormann, GSI, Darmstadt, Germany
 A. Kolomiets, S. Minaev†, ITEP, Moscow, Russia
 U. Ratzinger, R. Tiede, IAP, Frankfurt, Germany

Abstract

With the advanced multi-particle code DYNAMION it is possible to calculate beam dynamics in linear accelerators and transport lines under space charge conditions with high accuracy. Special features as data from the real topology of RFQ electrodes, drift tubes, quadrupole lenses, misalignment and fabrication errors and consideration of field measurements lead to reliable results of the beam dynamics simulations. Recently the DYNAMION code is applied to the upgrade and optimization of the GSI UNILAC as an injector for the Facility for Antiproton and Ion Research at Darmstadt (FAIR). An operation of the FAIR requires for the increase of the beam- intensity and -brilliance coming from the UNILAC (up to a factor of 5).

End-to-end simulations for the whole linac (from ion source output to the synchrotron entrance) allow for the study and optimization of the overall machine performance as well as for calculation of the expected impact of different upgrade measures, proposed to improve the beam brilliance. The results of the beam dynamics simulations by means of the DYNAMION code are compared with the recent measurements, obtained after upgrade of the High Current Injector (HSI) in 2009.

INTRODUCTION

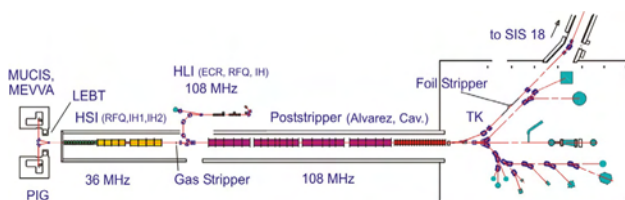


Figure 1: Schematic overview of the GSI UNILAC and experimental area.

Besides two ion source terminals and a low energy beam transport system (LEBT) the UNILAC-HSI comprises a 36 MHz IH-RFQ accelerating the ion beam from 2.2 keV/u up to 120 keV/u and a short 11 cell adapter RFQ (Super Lens). The IH-DTL, consisting of two separate tanks, accelerates the beam up to the final HSI-energy of 1.4 MeV/u. After stripping and charge state separation the Alvarez DTL provides for beam acceleration without significant particle loss. The transfer line (TK) to the SIS 18 is equipped with a foil stripper

and another charge state separator system [1].

The HSI was commissioned in 1999 aiming for 15 mA of U^{4+} beam current. However the measured uranium beam current never exceeded 6.5 mA.

In 1999-2003 an extended experimental program dedicated to improve the overall UNILAC performance for heavy ion high current operation lead to an U^{73+} intensity of 2.0 emA at the injection to SIS 18. Before foil stripping 4.5 emA of U^{28+} beam intensity was achieved. An optimized total particle transmission of up to 50% was reached, while a design performance of about 90% was expected. The beam losses mainly happen in the front-end area of the HSI [2].

NUMERICAL INVESTIGATIONS AND FACILITY UPGRADE

Recently, for the operation of the GSI-accelerator chain as an injector for the FAIR facility, a considerable increase of the heavy ion beam brilliance of up to a factor of 5 at the end of the UNILAC is required [3].

HSI Upgrade I (2004)

Since 1999 detailed computer simulations using the DYNAMION code [4] were performed to determine the source of beam intensity limitations. The simulations were verified by beam parameters, measured during the UNILAC operation. It was demonstrated that the bottleneck of the whole facility is the front-end system of the HSI. As a result, a partial RFQ upgrade program took place in 2004. It was mainly directed to the improvement of the rf-performance, but also included a new design of the input radial matcher (IRM), dedicated to optimize the beam dynamics in the focusing quadrupoles in front of the RFQ and to improve the matching itself [5].

The rf-performance of the HSI-RFQ was significantly improved after replacement of the electrodes. Minor changes of the IRM (approx. 1% of the RFQ length) lead to 15% increase of the maximum beam intensity at the RFQ output (with the same beam from the ion source). The prediction of the numerically calculated optimization of the RFQ electrode profile and beam matching was confirmed. The beam dynamics codes were approved.

HSI Upgrade II (2009)

The FAIR program requires an increased HSI U^{4+} beam current of up to 18 mA. The results of numerical investigation demonstrated a necessity of an essential upgrade of the RFQ electrode profile for the FAIR requirements. Simulations, done by means of the

† Sergey Minaev sadly passed away on March 11, 2010

DESIGN OF THE T2K TARGET FOR A 0.75-MW PROTON BEAM*

C.J. Densham[#], M. Baldwin, M.D. Fitton, M. Rooney, M.L. Woodward,
 STFC Rutherford Appleton Laboratory, Chilton, Didcot, OX11 0QX, UK
 A. Ichikawa, Department of Physics, Kyoto University, Kyoto 606-8502, Japan
 S. Koike, T. Nakadaira, High Energy Accelerator Research Organisation (KEK),
 1-1 Oho, Tsukuba, Ibaraki 305-0801, Japan

Abstract

The T2K experiment began operation in April 2009 [1]. It utilises what is projected to become the world's highest pulsed power proton beam at 0.75 MW to generate an intense neutrino beam. T2K uses the conventional technique of interacting a 30 GeV proton beam with a graphite target and using a magnetic horn system to collect pions of one charge and focus them into a decay volume where the neutrino beam is produced. The target is a two interaction length (900 mm long) graphite target supported directly within the bore of the first magnetic horn which generates the required field with a pulsed current of 320 kA. This paper describes the design and development of the target required to meet the demanding requirements of the T2K facility. Challenges include radiation damage, stress waves, design and optimisation of the helium coolant flow, and integration with the pulsed magnetic horn. Conceptual and detailed engineering studies were required to develop a target system that could satisfy these requirements.

T2K SECONDARY BEAMLINER

A primary 30 GeV proton beam is used to generate a secondary beam of pions by interaction with a two interaction length graphite target [2]. The target station houses the target and three magnetic horns as shown in Figure 1. The proton beam enters the target station through a proton beam window which separates the beamline vacuum from the target station and decay volume which is filled with helium at atmospheric pressure. Between the window and the first horn assembly containing the target is a graphite baffle/collimator to protect the downstream components in the event of a miss-steered beam. The target is supported directly inside the bore of the first magnetic horn, which directs pions of the required sign in a forward direction. The second and third horns further focus the pion beam which decays to generate the ν_μ beam as the pions traverse a 96 m long decay volume. The remnant hadron beam is deposited in a hadron absorber or beam dump situated at the far end of the decay volume. Approximately one third of the beam power is transmitted into the kinetic energy of secondary particles including pions, another third is deposited in the beam dump and the remainder into the decay volume walls and target station shielding. Less than 5% of the proton beam power is deposited in the target itself as heat.

The beam window, baffle, target and magnetic horns are supported beneath shielding modules to permit replacement and to accommodate a potential change in off-axis angle for the facility if desired for a future upgrade. Each support module assembly is contained within the helium vessel. The building is equipped with a remotely operated crane to enable these highly activated components to be lifted from the beam line and lowered into a Remote Maintenance Area adjacent to the beam line.

The beam window, target and horns installed for Phase I have been designed for operation at an average beam power of 750 kW. The T2K roadmap foresees an upgrade to 1.66 MW by 2014 and there is an ambition to achieve 3-4 MW within the lifetime of the facility. Since the target station, decay volume and hadron absorber are fixed installations and cannot be maintained or replaced after activation, they were all designed for operation at the highest envisaged beam power of 4 MW.

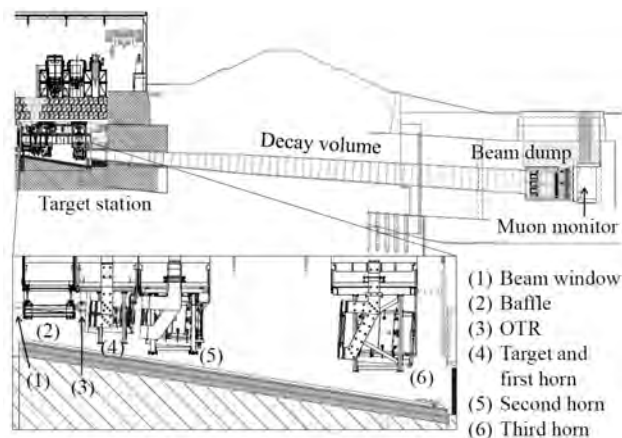


Figure 1: T2K secondary beam line.

TARGET DESIGN ISSUES

Nuclear grade IG430 [3] graphite was chosen as the pion production target material for T2K since it is able to withstand the stress waves generated in it by the pulsed proton beam. The power density generated by the pulsed proton beam is approximately proportional to the atomic number, consequently a low-Z material is favoured for the pion production target. Graphite has an attractive combination of high thermal conductivity, high heat capacity, low expansion coefficient, low modulus and a sufficiently high strength which is retained at high temperatures. The main disadvantage of graphite compared with e.g. beryllium is that it suffers

*Work supported by Science & Technology Facilities Council, UK

[#]chris.densham@stfc.ac.uk

BEAM DUMP DEVELOPMENT FOR A KOREAN PROTON ACCELERATOR*

C-S. Gil[#], J.H. Kim, D.H. Kim, J-H. Jang, KAERI, Daejeon, Korea

Abstract

A beam dump for a 20 MeV, 4.8 mA proton beam had been manufactured in Korea. The beam dump was made of graphite for low radioactivity, and was brazed to copper for cooling. The IG 430 graphite and Oxygen Free High Conductivity (OFHC) copper were brazed using a TiCuSil filler metal, which is a compound of 4.5% titanium, 27% copper, and 68.8% silver [1]. The beam dump was designed by placing two graphite plates 30 cm × 60 cm in size at an angle of 15 degrees in order to reduce the peak heat flux in the beam dump [2,3,4]. Also, a 100 MeV proton beam dump was designed with copper of high heat conductivity.

INTRODUCTION

A proton accelerator is under construction in Korea. In 2012, the energy of the proton beam will be raised up to 100 MeV, and the average current will be 1.6 mA. A 20 MeV proton beam is currently being tested. Dumps for the 20, 100 MeV proton beams have been designed for the Korean proton accelerator. A beam dump for the 20 MeV, 4.8 mA proton beam was manufactured to minimize radioactivity using graphite. The detailed specifications of the 20, 100 MeV beam dumps including activation analyses will be presented in this paper.

20 MeV BEAM DUMP

The conceptual design of the beam dump for the 20 MeV, 4.8 mA proton beam is shown in Fig. 1. The angle between two beam dump plates is 15 degrees and the peak heat flux in the beam dump plates is 200 W/cm². The beam profile in the beam dump is presented in Fig. 2.

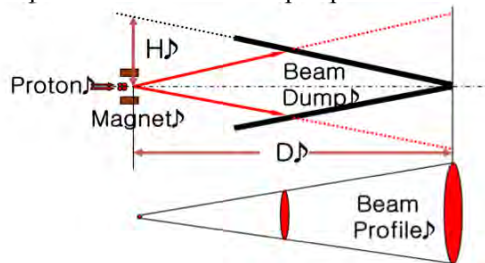


Figure 1: Conceptual design of the beam dump.

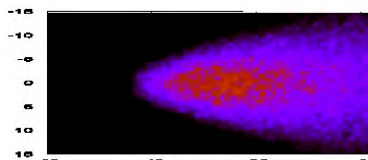


Figure 2: The beam profile in the beam dump.

Specifications

The beam dump for a 20 MeV proton beam was designed using the following specifications.

- Beam dump materials: Graphite (IG 430), Copper (OFHC), SUS 304.
- Brazing filler metal: TiCuSil (Titanium: 4.5 %, Copper: 27.7 %, Silver: 68.8 %).
- Two plates (30 cm × 60 cm, angle 15°)
- Average power: 96 kW (20 MeV, 4.8 mA)
- Peak heat flux in the beam dump: 200 W/cm².
- Maximum temperature: Graphite 223 °C, Copper 146 °C, Cooling water 85 °C.

Figure 3 shows four graphite beam dump blocks and the beam dump arrangement.

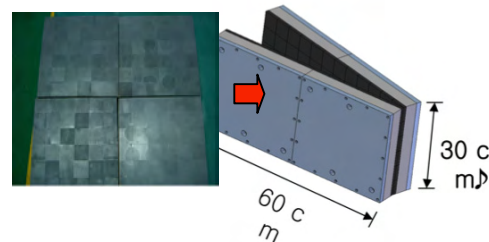


Figure 3: Manufactured graphite beam dump blocks and the beam dump arrangement.

Brazing

The beam dump was designed to minimize radioactivity at the surrounding materials of the beam dump as well as the beam dump itself. Graphite was selected as the proton beam facing material for low radioactivity. However, graphite is not a good material for water cooling due to its low heat conductivity and high hygroscopicity. To resolve these problems, the brazing of graphite and copper was considered. The brazing of graphite and copper is not easy due to their different thermal expansion rates at high brazing temperatures. The stresses of graphite and copper with their thicknesses at the brazing progress were analyzed with ANSYS code [5]. Figure 4 shows the different stresses during the brazing process based on thickness. The tensile stress of graphite during the copper brazing is the lowest at around 1 cm of graphite. The graphite stresses due to the brazing copper are not sensitive to the copper thicknesses. The graphite

*This work has been performed under the frontier project sponsored by MEST.

[#]csgil@kaeri.re.kr

NEW DESIGN OF A COLLIMATOR SYSTEM AT THE PSI PROTON ACCELERATOR

Y. Lee*, D. Reggiani, M. Gandel, D. C. Kiselev, P. Baumann, M. Seidel, A. Strinning, S. Teichmann, PSI, Villigen, Switzerland

Abstract

PSI is gradually upgrading the 590 MeV proton beam intensity from the present 2.2 mA towards 3 mA, which poses a significant challenge to the reliable operation of the accelerator facility. Of particular concern is the collimator system which is exposed to the strongly divergent beam from a muon production target. It shapes an optimal beam profile for low-loss beam transport to the neutron spallation source SINQ. The current collimator system absorbs about 14 % of the proton beam power. Consequently, the maximum temperature of the collimator system exceeds 400 C at 2.2 mA, which is close to the limit set for safe operation. In this paper, we present a new collimator system design which could withstand the proton beam intensity of 3 mA, while fulfilling the intended functionality. Advanced multiphysics simulation technology is used for the geometric and material optimizations, to achieve the lowest possible actual to yield stress ratio at 3 mA. A sensitivity study is performed on the correlation between the beam misalignments and the reliability of the accelerator components in the proton downstream region.

INTRODUCTION

The ring cyclotron at PSI generates 590 MeV proton beam with the beam current up to 2.3 mA. The protons are guided to collide with solid targets, in order to generate high flux muons and neutrons for various research purposes. Figure 1 shows the beamline elements at the PSI proton accelerator between the 4 cm thick graphite muon generation target (Target E) and the bending magnet (AHL).

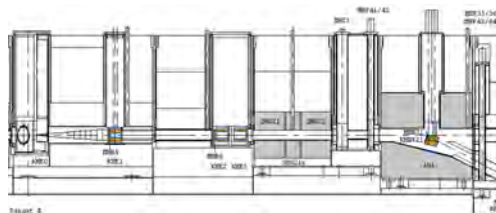


Figure 1: The beamline elements at the PSI proton accelerator between the muon generation target (Target E) and the bending magnet (AHL). The Q21 and Q22 are quadrupole magnets.

As the proton beam hits Target E, it diverges via elastic and inelastic Coulomb scatterings. While the scattered secondary particles are absorbed by the two collimators KHE0

and KHE1, the divergent direct beam must be collimated by the collimator system composed of KHE2 and KHE3. This is to protect the accelerator components and the proton channel between Target E and the neutron production target SINQ.

The collimator system composed of KHE2 and KHE3 is made of OFHC copper and absorbs approximately 14 % of the total proton beam power. In 2009, 1.3 MW (590 MeV/2.3 mA) proton beam power was routinely used at PSI. The thermal load which the collimator system must sustain is then close to 200 kW. The maximum temperature is estimated to reach up to 700 K (430 C) which is about 50 % of the melting temperature of the OFHC-copper. The planned proton beam intensity upgrade at PSI therefore poses a significant challenge to the stable operation of the accelerator facilities, due to the enhanced thermal load from proton beam stopping at the collimator system. In this paper, we propose a collimator design which further optimizes the basic design concept presented in Ref. [1], which could sustain the thermal load from the planned 1.8 MW (590 MeV/3.0 mA) beam upgrade.

WORKING PRINCIPLES

A quarter model of the present collimator system composed of KHE2 and KHE3 is shown in Fig. 2. The colli-

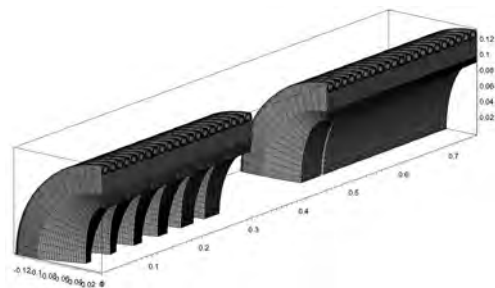


Figure 2: A quarter of the collimator system model: The KHE2 (left) at the beam entry side and the KHE3 at the beam exit side (right).

mator system must stop the 590 MeV protons completely, which would otherwise directly hit the accelerator components behind. Therefore, it should be longer than the projected stopping range of a 590 MeV proton in copper, which is calculated to be 25 cm by MCNPX [2]; see Fig. 3. The KHE2 reduces the beam power before the protons impinges on KHE3, and the final collimation is done in KHE3. In order to remove the beam stopping power from the collimator, active water cooling through brazed stainless steel pipes is applied. The KHE2 is exposed to higher

* yong-joong.lee@psi.ch

THE DESIGN OF BEAM COLLIMATION SYSTEM FOR CSNS/RCS*

Na Wang[#], Sheng Wang, Nan Huang, Qing Qin, IHEP, Beijing, China

Abstract

China Spallation Neutron Source (CSNS) accelerator consists of a 80 MeV linac and a 1.6 GeV Rapid Cycling Synchrotron (RCS), which is designed to produce beam power of 100 kW with a repetition rate of 25 Hz. For such a high intensity RCS, beam loss and control are of primary concern. A two-stage collimation system is designed to localize the beam losses in a restricted area, and keep the uncontrolled losses less than 1 W/m at the other part of RCS. The detailed design of the beam collimation system is presented, including the compare among different schemes. Key issues which affect the collimation efficiency are analyzed, and the collimation efficiency and beam loss distribution are studied by using the code ORBIT.

INTRODUCTION

The CSNS [1] requires a total number of 1.56×10^{13} protons for the target beam power of 100 kW. In designing the RCS, one of the primary concerns is machine component radioactivation caused by uncontrolled beam losses [2]. To allow hands on maintenance, beam loss around the machine should not exceed 1 W per meter. Another important concern is the beam loss during the single turn extraction. Smaller beam emittance at extraction allows less exigent kicker strength and small beam loss at extraction. In order to achieve the low loss requirement around the ring and well constrained extraction beam extension, a two stage collimation system is designed to localize the beam losses in well shielded regions of the machine [3].

Table 1: The Main Parameters of the CSNS Ring

Parameters	Symbol, unit	Value
Inj./Ext. energy	E_{inj}/E_{ext} , GeV	0.08/1.6
Circumference	C , m	228
Beam population	N_p , $\times 10^{13}$	1.56
Harmonic number	h	2
Repetition frequency	f_0 , Hz	25
Betatron tune	ν_x/ν_y , cm	4.86/4.78
Ring acceptance	ε , $\pi\text{mm}\cdot\text{mrad}$	540

Simulations are performed to predict the cleaning efficiency of the two-stage collimation system and the beam loss pattern around the CSNS ring. Both the collimators geometry and arrangement are optimized for minimizing the extent of the escaping halo. The nominal

parameters of CSNS used in the simulation are shown in Table 1.

COLLIMATION SYSTEM DESIGN

RCS lattice is four fold structure, and it is good for provide a separate section for accommodating collimation system. The schematic layout of the RCS ring is shown in Fig. 1. The four straight sections are designed for beam injection, collimation, extraction, and RF systems, respectively. There are an 11 m and two 3.8 m dispersion free drift space. A long drift space and a short one next to it are dedicated to transverse collimators. The collimation system is located downstream of injection region. Figure 2 shows the lattice functions along a superperiod.

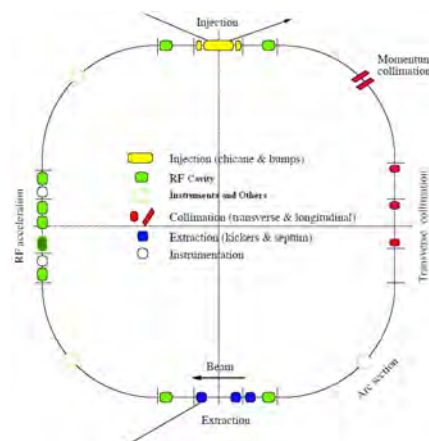


Figure 1: Schematic layout of the SNS accumulator ring.

Another straight section with large dispersion function in the arc section before the transverse collimation is dedicated to momentum collimation. As the majority of the losses in the RCS ring are due to transverse space charge halos, and longitudinal beam loss is not necessary for 100 kW beam, the momentum collimation will not be included in the primary stage, but the space is preserved for further consideration. Further studies are needed.

A set of four movable scrapers made of 0.17 mm tungsten plates acts as primary collimators for increasing the divergence of the incident halo protons. Four secondary 0.4 m long copper collimators are located downstream of primary collimator as absorbers. The layout of the collimators in the straight section is shown schematically in Fig. 2. The collimators are set to around $350 \pi\text{mm}\cdot\text{mrad}$ for the primary and around $400 \pi\text{mm}\cdot\text{mrad}$ for the secondary jaws. The physical aperture of the ring is designed with $540 \pi\text{mm}\cdot\text{mrad}$ acceptance and 1% momentum deviation.

*Work supported by the National Foundation of Natural Sciences contract 10725525 and 10605032

[#]wangn@ihep.ac.cn

REVIEW OF INSTABILITY MECHANISMS IN ION LINACS

R. Duperrier*,
CEA Saclay,
91191 Gif sur Yvette, France

Abstract

An important issue for the new high power class ion linac projects is the preservation of the beam quality through the acceleration in the linac. An extremely low fraction of the beam (from 10^{-4} down to 10^{-7}) is sufficient to complicate the hands on maintenance in such accelerator. This paper reviews the instability mechanisms in Ion Linacs. Basics rules for the definition of their architecture and the results applied to existing machines and projects are covered.

INTRODUCTION

High power ion linacs have become increasingly attractive in recent years. Among the possible applications are heavy ion drivers for thermonuclear energy [1] or rare ion beam production [2, 3], transmutation of radioactive wastes [4], neutrino physics [5] and the spallation sources of neutrons for matter research [6, 7, 8]. High intensity charged particle beams can develop extended low density halos. The existence of halos can have serious consequences for the hands on maintenance. Beam dynamics for such accelerators requires an exhaustive research of the different mechanisms that may induce beam loss from 10^{-4} down to 10^{-7} . The control of these mechanisms is the main guideline for the design of high power linacs. Among the different sources of beam loss, instabilities induced by the coupling of the beam and the accelerator working points are a major concern. This paper reviews the instability mechanisms in Ion Linacs. Basics rules for the definition of their architecture and the results applied to existing machines and projects are covered.

SPACE CHARGE NON LINEARITIES

As a particle beam is a charge and current distribution, it acts as a source term in Maxwell equations and generates self fields or space charge fields. The effect of space charge is essentially a low energy issue for two reasons: transversally, the self magnetic force tends to compensate the repulsive self electric force when the ions become relativistic and, longitudinally, the bunch length increases with the energy which corresponds to a reduction of the beam charge density. It is worth noting that beam waists may affect this statement at high energy. In essence, self fields are a strong function of the particle distribution and only an uniform beam density may produce linear fields but this case is only valuable for theoretical investigations. The non

*romuald.duperrier@cea.fr

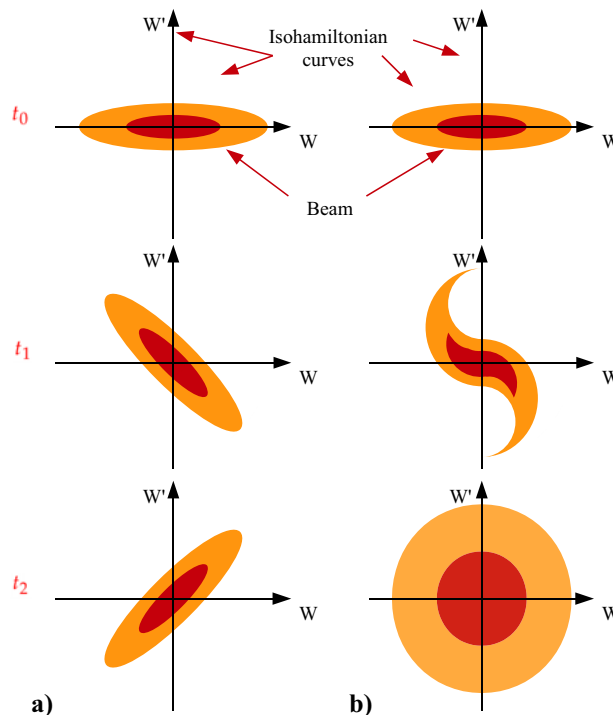


Figure 1: Evolution in phase space of a mismatched beam in case of a linear (a) or a non linear (b) force.

linear nature of self fields induces a spread of the tune shift. One importance consequence is that if each particle isn't located in phase space on an isohamiltonian curve which is matched to its own energy, a filamentation will occur and provoke an emittance growth (see figure 1). After a relaxation time which corresponds to a few focusing period when the space charge is important [11], a new equilibrium is reached and the emittance remains constant until a new mismatch is applied to the beam. This mechanism is applicable to the longitudinal focusing force of the cavities or any non linear force. Even if this phenomena could induce an emittance growth, it doesn't correspond to an instability mechanism. In this paper, a beam loss mechanism will be assumed to be an instability when the solution of the equation of the motion for the particles or the beam envelop corresponds to an exponential like behavior. It is worth noting that the impact on the motion of the instability changes significantly the initial conditions and the necessary conditions for the instability may vanish. The exponential like behavior is then transitional.

LOSS CONTROL AND RELIABILITY ISSUES IN HIGH INTENSITY LINACS

M. Comunian, INFN/LNL, Legnaro, Italy

Abstract

New projects like IFMIF or the new generation of Spallation Neutron Source require high power beams with high availability and reliability. To achieve these results one needs low beam losses and a good control beam dynamics.

This paper focuses on the important characteristics and critical beam dynamics design issues for the high intensity linacs. In particular the techniques used for the loss control at the design stage, with the emphasis on the physical phenomena like emittance growth and halo. The reliability issue will be addressed with practical examples from the low energy and high current IFMIF-EVEDA project and comparing this case with higher energy projects.

INTRODUCTION

The emittance growth and the halo control is an issue in the new high intensity Linac like IFMIF [1] and ESS [2], for that the design is very important to mitigate the beam losses.

In this way is it possible to keep induced radioactivity to a low level and to retain hands-on maintenance of the accelerator with personal safety and environmental protection for ground, water and air.

A low emittance also guarantee a good beam quality for the experimental setup that is an issue for high energy accelerators, on the other hand the final emittance is not so important for low energy accelerators with an high power target to heat up.

To guarantee hands-on maintenance the level of beam loss must be in average below 1W/m, but this figure is valid only at high energy instead for a low energy the safe level of beam losses can be relaxed.

A low level of beam losses is also necessary to protect machine part from beam related break, like radiation structural damage and thermal damage of superconducting components.

EMITTANCE GROWTH AND HALO CONTROL

Transverse Emittance Control

The transverse emittance is created in the accelerator source and is mainly due to fact that the beam is created in a magnetic fields, in this way by the conservation of angular moment, the beam at the source exit present an emittance different from zero. After the beam creation, the source extraction electrodes, the level of neutralization in the low energy beam transport, the magnets aberrations and last but not least the space charge, increase the

transverse emittance. More in general all the non linear self E.M. fields and external E.M. fields increase the transverse emittance.

In the RFQ (Radio Frequency Quadrupoles) accelerator the transverse emittance is almost constant, the only zone where the emittance can increase is in the "coupling gap section", these abrupt interruptions in the electrodes are presents in very long, respect to the wavelength, RFQ.

In the MEBT (Medium Energy Beam Transport) Transport, from the RFQ to the following Linac, DTL (Drift Tube Linac) or SC (Super Conducting) cavities, the transverse emittance typically increase, this is due to the fast change in the phase advance per meter, from a very short focusing period (inside the RFQ) to a more long focusing lattice, like inside the DTL, or still more longer focusing period inside the SC cavities. To avoid the problem is it necessary to reduce the period length in the following linac, by increasing the final period in the RFQ reducing the focusing force and/or rising the final RFQ energy.

In the DTL part of the linac the transverse emittance is constant, due to the regular focusing lattice design.

In the SC part of the linac the transverse emittance should be conserved, but this is more challenging due to the longer focusing period.

Another small source of transverse emittance growth is the change in the RF frequency along the linac, due to non linear effects of the E.M. Bessel components that double by doubling the frequency, for the same beam size.

Longitudinal Emittance Creation and Control

The longitudinal emittance is formed in the RFQ and the final value can be control by using a longer shaper section with a right numbers of longitudinal phase advance rotations. In the case of high intensity RFQ the longitudinal space charge phenomena can increase quite fast the emittance due to the presence of baffles in the phase space that also induce fast longitudinal losses. In this way a long shaper section in a high intensity RFQ get more losses, i.e. low longitudinal capture, than low final longitudinal emittance.

The part of the beam that is not captured longitudinally can be scraped out at the end of the gentle buncher by reducing the RFQ small aperture "a", in this way that part of the beam is removed at low energy and induce only a small activation of the structure.

The longitudinal emittance can be transported, from the end of the shaper, up to the end of the RFQ without increase, due to the regular longitudinal focusing scheme, if is avoided a fast change in the synchronous phase inside the RFQ.

DYNAMICS OF INTENSE INHOMOGENEOUS CHARGED PARTICLE BEAMS*

E.G. Souza, A. Endler, R. Pakter[†], F.B. Rizzato

Instituto de Física, Universidade Federal do Rio Grande do Sul, Brazil

R.P. Nunes, Instituto de Física e Matemática, UFPel, Universidade Federal de Pelotas, Brazil

Abstract

Inhomogeneous cold beams undergo wave breaking as they move along the axis of a magnetic focusing system; the largest the inhomogeneity, the soonest the breaking. The present analysis however reveals that the wave breaking time is very susceptible to beam mismatch. It is shown that judiciously chosen mismatches can largely extend beam lifetimes. The work includes some recently discussed issues: the presences of fast and slow regimes of wave breaking, and the role of thermal velocity distributions in space-charge dominated beams. In all instances, the theory is shown to be accurate against simulations.

INTRODUCTION

It is well known that magnetically focused beams of charged particles can relax from non-stationary into stationary flows with the associated particle evaporation [1]. This is the case for homogeneous beams with initially mismatched envelopes flowing along the magnetic symmetry axis of the focusing system. Gluckstern [2] showed that initial oscillations of mismatched beams induce formation of large scale resonant islands [3] beyond the beam border: beam particles are captured by the resonant islands resulting in emittance growth and relaxation. A closely related question concerns the mechanism of beam relaxation and the associated emittance growth when the beam is not homogeneous. On general grounds of energy conservation one again concludes that beam relaxation takes place as the coherent fluctuations of beam inhomogeneities are converted into microscopic kinetic and field energies [4]. Recent works actually show that in the case of cold beams relaxation proceeds in two basic steps. Firstly, wave breaking itself pushes particles off the beam. Secondly, ejected particles are heated up as they absorb energy from macroscopic coherent oscillations of the remaining beam core. Wave breaking is therefore the key feature in the relaxation of cold inhomogeneous beams since it produces those particles that will later form the relaxing beam halo.

Two instances leading to wave breaking in inhomogeneous beams have been identified. Originally, a threshold was obtained in terms of gradients in the amplitude of waves propagating across the beam [5, 6]. While below the threshold breaking is absent, above the threshold it is fast.

As particles largely displaced from their equilibrium positions are released, they overtake each other in less than one plasma wave cycle. Density singularities and wave breaking are thus created, and particles are pushed off the beam. A more thorough analysis however shows that not only amplitude gradients, but also the formerly neglected gradients of the spatially varying frequency of the density waves is a key factor determining wave breaking [7, 8]. The physical process is different from the previous, as one shows that no threshold exists in this latter case. Particles slowly move out of phase due to small differences in their oscillatory frequencies, until a time when one eventually overtakes another. At that instant the infinite density peak is again formed generating the breaking.

In all the previous discussion, no particular attention is directed toward beam size; the basic interest was the role of beam non uniformity on wave breaking. One should note, however, that since wave breaking is essentially dictated by compressions and rarefactions of beam densities, it may be quite possible that expansions or contractions of the beam transversal size has a noticeable effect on the process. In particular we will show that, contrarily to the homogeneous beam case where envelope mismatch is an undesirable feature, for inhomogeneous beams it may largely delay wave breaking, extending beam lifetime. Analytical treatment can be made if one considers crystalline cold beams which have been attracting a growing amount of interest lately [9]. We shall therefore expose our case with aid of this type of system, introducing moderate temperatures later to study warmer, but space-charge dominated beams.

BEAM PROFILE AND WAVE BREAKING

Consider an axially symmetric, collisionless, unbunched beam moving with constant velocity along z . Ignoring longitudinal smoother gradients, one obtains the relevant fields with help of Gauss's law as one considers the larger transversal gradients. The equation for the radial motion of any cylindrical layer of the beam thus takes the form [8]

$$r'' = -\kappa r + \frac{Q(r)}{r}, \quad (1)$$

primes indicating derivatives with respect to z for stationary beams. $Q(r)$ is a measure of the total charge up to the present radial layer position. It reads $Q(r) = KN(r)/N_t$, where $K = N_t q^2 / \gamma^3 m \beta^2 c^2$ is the beam perveance, with $N(r)$ denoting the number of particles up to radial coordinate r , and N_t their total number. q and m denote the beam

* Work supported by CNPq and FAPERGS, Brazil, and by AFOSR, USA, grant FA9550-09-1-0283.

[†] pakter@ifufrgs.br

HEBT LINES FOR THE SPIRAL2 FACILITY. WHAT TO DO WITH ACCELERATED BEAMS?

L. Perrot[#], J.L. Biarrotte, IPNO-IN2P3-CNRS, Orsay, France
 P. Bertrand, G. Normand, GANIL, Caen, France
 E. Schibler, IPNL-IN2P3-CNRS, Villeurbanne, France
 D. Uriot, SACM/IRFU/DSM/CEA, Saclay, France

Abstract

The SPIRAL2 facility at GANIL-Caen is now in its construction phase, with a project group including the participation of many French laboratories (CNRS, CEA) and international partners. The SPIRAL2 facility will be able to produce various accelerated beams at high intensities: 40 MeV Deuterons, 33 MeV Protons with intensity until 5mA and heavy ions with $A/Q=3$ up to 14.5 MeV/u until 1mA current. We will present the final status of the high energy beam transport lines of the new facility. Various studies were performed on HEBT and beam-dump concerning beam dynamics, safety and thermo-mechanicals aspects. New experimental areas using stable beams and the cave dedicated to radioactive ion production will be presented according the scientific program.

INTRODUCTION

The construction phase of SPIRAL2 is already launched within a consortium formed by CNRS, CEA and the region of Basse-Normandie in collaboration with French, European and international institutions [1, 2]. The facility will deliver high intensity rare isotope beams for fundamental research in nuclear physics, high intensity stable heavy ions beams, and high neutron flux for multidisciplinary applications. SPIRAL 2 will give access to a wide range of experiments on exotic nuclei, which have been impossible up to now. In particular it will provide intense beams of neutron-rich exotic nuclei (10^6 – 10^{10} pps) created by the ISOL production method. The extracted ion beams will subsequently be accelerated to higher energies (up to 20 MeV/nucleon) by the existing CIME cyclotron, typically 6–7 MeV/nucleon for fission fragments. A low energy branch will be build to transport the beam to the DESIR hall. High intensity stable isotope beams and high power fast neutrons are other major goals of the facility. After two years of preliminary study, and following the decision to launch the construction phase, a complete design of the driver accelerator is presently under way [3]. This paper describes the studies performed on the high energy beam transport lines which deliver stable beams to experimental areas, radioactive production cave and beam dump.

GENERAL LAYOUT OF THE DRIVER ACCELERATOR

The driver accelerator delivers CW beams of deuterons (40 MeV, 5 mA) and heavy ions ($A/q=3$, 14.5 MeV/A, 1 mA). The injector is composed of two ion sources (deuterons and heavy ions) and a common RFQ cavity (88 MHz) [4]. The superconducting LINAC is composed of two sections of quarter-wave resonators (QWR), beta 0.07 and 0.12 at the frequency of 88 MHz, with room temperature focusing devices [5, 6]. After the LINAC, ions are transported using various high energy beam transport (HEBT) lines according to experimental programs. Beams can be transported to the beam-dump, to experimental areas like the Neutrons For Science (NFS) area, the Super Separator Spectrometer (S3) or to the converter of the radioactive ions production area.

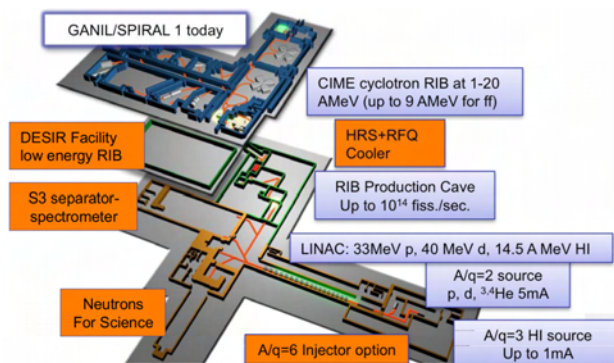


Figure 1: General scheme of the SPIRAL2 facility.

It must be noticed that in a second phase of SPIRAL2, a heavy ions source with $A/q=6$ will be built with its associated injector. The LINAC will accelerate these ions up to 8.5 MeV/u. This point must be taken into account for the design of the HEBT lines.

SPIRAL2 HEBT LINES

This paper will only focus on the beam transport description after the superconducting LINAC. In a first subsection we will give a compilation of the beam characteristics at the LINAC exit. In a second subsection, we will give the structure of the HEBT.

The well known TRACEWIN code is used for all beam dynamics calculations [7].

[#]perrot@ipno.in2p3.fr

FIRST LEBT SIMULATIONS FOR THE BILBAO ACCELERATOR ION SOURCE TEST STAND

I. Bustinduy, D. de Cos, J. Feuchtwanger, J.L. Munoz, F.J. Bermejo, ESS-Bilbao, Spain
 S. Lawrie, D. Faircloth, A. Letchford, J. Pozimski, STFC/RAL, Chilton, Didcot, Oxon, UK
 S. Jolly, P. Savage, Imperial College of Science and Technology, UK
 J.Back, Warwick University, UK
 J. Lucas, Elytt Energy, Madrid, Spain
 J.P. Carneiro, IkerBasque Foundation, Chicago, USA

Abstract

The proposed multi-specimen Low Energy Transport System (LEBT) consists of a series of solenoids with tunable magnetic fields, used to match the characteristics of the beam to those imposed by the RFQ input specification. The design of the LEBT involves selecting the number of solenoids to use and their fixed positions, so that a set of fields that provides the desired matching can be found for any given conditions (different currents, input emittances, etc). In this work we present the first simulations carried out to design the Bilbao Accelerator LEBT, which were performed using several codes (TRACK, GPT, Trace2D). The best configuration is discussed and evaluated in terms of the degree of matching to the RFQ input requirements.

INTRODUCTION

As a continuation of the ITUR ion source test stand [1], a front end test stand (FETS) for proton is being currently designed and constructed in Bilbao (Spain), comprising a Low Energy Beam Transport (LEBT), a Radio-Frequency Quadrupole (RFQ) [2] and a High Speed Chopper [3]. The aim is to produce chopped proton beams of up to 75 mA current, up to 2 ms pulse length, and 50 Hz repetition rate.

The aim of the LEBT, placed between the ion source and the RFQ, is to match the beam characteristics to the RFQ input specification. This paper summarizes the latest advances on the Bilbao Accelerator LEBT design. Several aspects of the current design status will be covered, including the magnetic structure, cooling system, and beam dynamics simulations.

MAGNETIC STRUCTURE

The Bilbao Accelerator LEBT is composed of a series of solenoids placed at fixed positions, producing tunable magnetic fields. The number of solenoids used will be discussed later in this paper. Figure 1 shows the layout for the 4-solenoid configuration.

Following the work in [4], the solenoids present a smaller internal radius (involving more turns) at the ends than in the centre. This way, the magnetic field profile along the axis is flatter than the one achieved with a uniformly shaped solenoid, which would present a typical

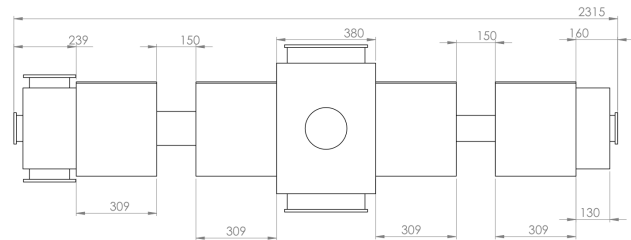


Figure 1: Proposed layout of the LEBT. The aperture of the first two magnets is 134 mm and 100 mm for the last two ones.

bell-shaped magnetic field profile. Besides, the variable radius approach creates a magnetic field that remains confined within the solenoid limits, avoiding perturbations on any nearby elements (e.g. other solenoids and the vacuum pump).

In order to save beam-line space, the proposed design includes the ability to nest dipoles and solenoids together. Therefore, the LEBT is composed of two types of elements:

- Two single solenoids, presenting an aperture of 134 mm, placed at the first and second positions of the LEBT.
- Two dipole-solenoid assemblies, composed by a solenoid integrated together with a set of two crossed (x-y) dipoles of the $\cos\theta$ type (similar to typical structure used for superconducting magnets). The dipoles are capable of steering the beam to correct for misalignment of the beam line components, reaching a deflection of up to $\pm 4^\circ$ for protons. These elements will be used at the third and fourth positions of the LEBT. The presence of the dipoles limits the aperture to 100 mm, which may be assumed due to the fact that the first two solenoids reduce the transverse dimensions of the beam.

The proposal for the solenoid design includes an iron yoke with ferromagnetic end plates. The preliminary analysis indicates that a relatively large current density is required in order to obtain the desired magnetic field. Therefore, we have opted for solenoids made of 16 independently cooled internal coils. Each of the coils will be cooled by an

A NEW POSSIBILITY OF LOW-Z GAS STRIPPER FOR HIGH-POWER URANIUM BEAM ACCELERATION AS ALTERNATIVE TO C FOIL

H. Okuno*, N. Fukunishi, A. Goto, H. Hasebe, H. Imao, O. Kamigaito, M. Kase, H. Kuboki, Y. Yano,
RIKEN Nishina Center, Wako, Japan
A. Hershcovitch, BNL, Upton, NY, USA

Abstract

The RIKEN accelerator complex started feeding the next-generation exotic beam facility RIBF (RadioIsotope Beam Factory) with heavy ion beams from 2007 after its successful commissioning at the end of 2006. Many improvements carried out from 2007 to 2010 increased the intensity of various heavy ion beams. However, the available beam intensity, especially of uranium beams, is far below our goal of 1 pμA (6×10^{12} particle/s). In order to achieve it, upgrade programs are already in progress; the programs include the construction of a new 28-GHz superconducting ECR ion source and a new injector linac. However, the most serious problem of a charge stripper for uranium beams still remains unsolved, despite extensive R&D works. The equilibrium charge state in a gas stripper is considerably lower than that in a carbon foil due to the density effect of the latter. However, a gas stripper is free from the problems related to lifetime and thickness uniformity. These merits motivated us to develop a low-Z gas stripper to achieve a higher equilibrium charge state even in gases. We measured the electron-loss and electron-capture cross sections of U ion beams in He gas as a function of their charge state at 11, 14, and 15 MeV/u. The extracted equilibrium charge states from the cross point of the two lines of the cross sections were promisingly higher than those in N₂ gas by more than 10. We believe that the difficulty in the accumulation of about 1 mg/cm² of low-Z gases can be overcome by using a plasma window.

INTRODUCTION TO RI BEAM FACTORY

The RIKEN Nishina center for Accelerator-Based Science constructed the RIBF (RadioIsotope Beam Factory) [1] aiming to realize a next-generation facility that can provide the most intense RI beams, which is the highest in the world, at energies of several hundred MeV/nucleon over the entire range of atomic masses. The RIBF requires an accelerator complex that can accelerate ions over the entire range of masses and deliver 80-kW uranium beams at an energy of 345 MeV/nucleon. Figure 1 shows a bird's eye view of the RIBF. The left part is the old facility that was completed in 1990. Using the four-sector K540-MeV RRC (RIKEN Ring Cyclotron) [2] with the two injectors, RILAC (RIKEN Linear ACcelerator) [3] and the AVF cyclotron [4], many experiments were carried with RI beams of light ions because the RRC can accelerate relatively light

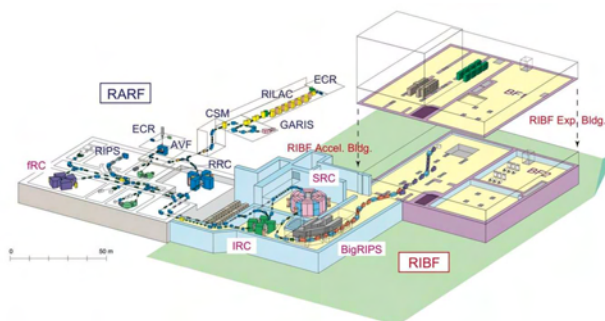


Figure 1: Bird's eye view of RI Beam Factory.

ions up to 100 MeV/u, which is the lower limit for RI beam production. In order to expand the mass range for RI beam production up to uranium, three ring cyclotrons, the fRC (fixed-frequency Ring Cyclotron) [5], IRC (Intermediate Ring Cyclotron) [6], and SRC (Superconducting Ring Cyclotron) [7], were designed and constructed as energy boosters for the RRC. The SRC is the first ring cyclotron in the world using superconducting sector magnets with the largest bending power.

The design and construction of the RIBF accelerators started from 1997, and the accelerator building was completed at the end of March 2003. In November 2005, we reached an important milestone: the superconducting sector magnets for the SRC were successfully excited at the maximum field level. The first beam was obtained on December 28, 2006 [8, 9]. Many improvements were carried out to increase the beam intensity and to commission new beam species to meet the requirements of different experiments. Table 1 shows a list of beams accelerated thus far. These beams were used in many nuclear experiments such as the discovery of 45 new isotopes [10] and the study of the halo structure and large deformation of extremely neutron rich Ne isotopes [11, 12]. Our goal is to achieve a beam intensity of 1 pμA for the entire atomic range. We reached the target intensity for He and O and about one fourth of the target intensity for Ca. However, the beam intensity of U beams is still very low, suggesting that we need to adopt drastic measures.

INCREASING INTENSITY OF URANIUM BEAM

From our operational experience, mentioned in the previous section, the key issues to be addressed for increasing

* okuno@riken.jp

PARAMETRIC STUDY OF A TWO-STAGE BETATRON COLLIMATION FOR THE PS2

J. Barranco, Y. Papaphilippou, CERN, Geneva, Switzerland

Abstract

Beam losses are a major limiting factor in the performance of any high intensity synchrotron. For the new CERN Proton Synchrotron 2 (PS2), an overall low loss design has been adopted. However, it is unavoidable that due to different processes a certain fraction of particles leave the beam core populating the so-called beam halo. A collimation system removes in a controlled way all particles outside the prescribed betatron and momentum acceptances. This article presents a two-stage betatron collimation design as an optical device for different long straight section layouts. Parametric studies for the different main design parameters are presented and their influence in the expected cleaning efficiency of the system is analyzed and compared to the accepted thresholds of admissible losses.

INTRODUCTION

Optics design of collimation systems has been extensively treated in previous works [1, 2, 3], and codes (e.g. DJ [4]) were developed in order to minimize the escaping halo between different stages of a collimation system. The relative phase advance between the different collimation stages is pointed out in all cases as a key parameter to maximize the cleaning efficiency. Nevertheless, in small and medium size accelerators space constraints are tight, preventing an optimal collimation system design. The new racetrack CERN PS2 will feature a two-stage betatron collimation system in one of the two long straight sections with fixed optics. In this article the main relevant optics parameters of a betatron collimation system are discussed and evaluated to optimize the cleaning efficiency in the PS2.

OPTICS MODEL OF A COLLIMATION SYSTEM

A collimation system is intended to absorb particles outside defined limits (so-called beam halo) before they reach the magnets, damaging and radioactivating them. The most common way to do that is to place blocks of certain materials as the closest element to the beam to intend to absorb these particles in a controlled way. However, it is unavoidable that a certain fraction of this halo will be outscattered back to the vacuum chamber after losing energy and with an increased divergence. For this reason a second stage located at a certain retraction from the first is needed to trap these scattered particles. A two stage betatron collimation system is designed for the PS2 where the primaries act as pure scatterers increasing the divergence of the particle, and thus the probability of being absorbed in the second

stages. For the present study, each collimator is composed by two parallel movable straight jaws.

The collimation process and the main optics parameters involved can be summarized in the following points.

- Due to different diffusion processes [5], particles leave the beam core drifting towards larger amplitudes with a certain diffusion velocity (v_{diff}). The collimators define the minimum transverse acceptance seen by the beam during along the ring (Fig. 1). Assuming a slow diffusion process [2], particles will impact first tangentially to the collimator jaws (red dots in Fig. 1). Additional collimators at different azimuthal angles could be added to assure the same acceptance in any radial direction.

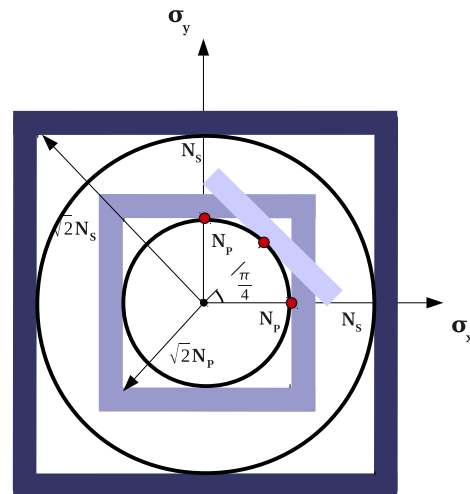


Figure 1: Transverse view of a two stage collimation system in number of betatronic sigmas (with $\sigma = \sqrt{\beta\epsilon}$). The half aperture of primary collimators in both planes is $N_p \sigma$ and $N_s \sigma$ for the secondaries. In a slow diffusion process the beam halo particles will impact first tangentially to the jaw, i.e. in its middle point.

- At a certain excursion the particle finally hits the primary collimator and gets scattered to larger amplitudes. Depending on the particle's divergence at the jaw collimation, the impact would be at the front or along the edge. In both cases it is possible to define an impact parameter (d) as in Fig. 2.
- For systems where primaries are meant to be only scatterers, the length (l_p) should be adjusted to provide enough divergence to reach the secondaries with the fewer number of passages through them, while assuring the own survival of the scrapers.

OPERATION OF THE J-PARC MAIN RING WITH THE MODERATE BEAM POWER: PREDICTIONS AND OBSERVATIONS

A.Molodozhentsev, KEK, Tsukuba, Japan

Abstract

The routine operation of J-PARC Main Ring for the Neutrino experiments has begun from April 2010, providing the moderate beam power at the maximum energy of 30GeV. The obtained beam power, extracted from the machine at this stage for the '6 bunches' operation with the repetition time of 3.3 sec, is about 110kW. Total power of the lost beam is just 100Watt, localized at the MR collimation system, which is in good agreement with predictions. After the summer shutdown 2010 the number of bunches, accelerated in the J-PARC Main Ring, will be increased up to 8. The expected beam power for the 'Neutrino' experiments will reach 140kW, which is the basis for the continuous routine operation of MR during 2010.

To optimize the machine performance, providing minimum particle losses during the injection and acceleration processes, the computational model of the J-PARC Main Ring has been established. The combined effects of the machine resonances and the space charge of the beam at the injection energy have been studied for different scenarios of the machine operations with the moderate beam power.

In frame of this report the comparison between predictions, based on the corresponding simulations, and measured beam losses is analyzed for different 'bare' tunes. The linear decoupling 'proof-of-principal' correction scheme and the obtained experimental results are discussed for the case of the moderate beam power of the J-PARC Main Ring. The predicted and obtained budget of the beam losses for the machine operation with the moderate beam power is presented. Finally, the basic scenario for the high beam power operation is discussed shortly.

INTRODUCTION

J-PARC Main Ring (MR) should provide acceleration of the proton beam from the injection energy of 3GeV up to the maximum extraction energy of 50GeV. At the early operation stage of MR the maximum energy is limited by 30GeV. The accelerated proton beam is delivered to the 'Neutrino Experiment' and to the 'Nuclear and Particle Physics Experiments' by using the 'fast' and 'slow' extraction techniques, respectively. For the 'phase-1' operation of the J-PARC Complex the 300kW beam power is produced by the rapid cycling synchrotron (RCS), which accelerates the proton beam from 181MeV up to 3GeV with the repetition rate of 25Hz providing 2 bunches per pulse. According to the design specification of the J-PARC Complex, only about 5% of the average RCS beam power is used by MR. The beam, extracted from RCS, is injected to MR by using the single-turn injection technique. The total beam power in MR at the

injection energy of 3GeV for the case of the '8-bunches' operation will be 14.5kW (1.25e13 protons per bunch). At the energy of 30GeV the maximum expected beam power for the 'phase-1' of the MR operation is 140kW.

The MR performance for the low-beam intensity case, predicted by the computational MR model [1], has been compared with the measured characteristics of the MR including the beam survival at the injection energy for different betatron tunes. The obtained results, which represent the effects of the machine resonances, will be discussed in this report.

For the MR operation the significant contribution of the 'sum' linear coupling resonance $Q_x+Q_y=43$ to the particle losses has been predicted and observed at the early stage of the machine commissioning. The correction approach, based on the local vertical bump of the circulating orbit at the location of the sextupole magnets, has been proposed and tested successfully for J-PARC Main Ring.

The tune scanning analysis has been performed for different operation scenario of the machine with the maximum equivalent beam power of 100kW at the extraction energy of 30GeV. This analysis has been made for both the computational MR model and for the real machine operation. The obtained results will be also discussed in this report. Finally, the optimum machine performance has been established providing minimum particle losses, localized at the Main Ring collimation system. The observed power of the lost beam during the injection and acceleration processes is about 100Watt, which is much below the capacity limit of the MR collimation system. The obtained experimental result agrees with the predictions, based on the MR computational model for the moderate beam power.

MAIN RING OPERATION WITH 'ZERO' BEAM INTENSITY

The J-PARC Main Ring commissioning process was started in 2008 from 'zero' beam intensity, which is just about 1% from the design intensity. The 'direct' injection scheme without bump-magnets, which change the circulating orbit in the injection straight section of the ring, has been used to inject the beam into MR. The lattice properties have been studied and compared with the results of the computational model of the machine [2].

The Main Ring computational model has been developed, representing the synchrotron with the realistic machine imperfections including measured field data and measured alignment error for each magnet. The measured properties of the MR focusing structure are in reasonable agreement with the simulated values, in particular the closed orbit distortion, the beta functions in the horizontal and vertical directions, linear chromaticity of the machine

LONG TERM SIMULATIONS OF THE SPACE CHARGE INDUCED BEAM LOSS EXPERIMENT IN THE SIS18

G. Franchetti*, O. Chorniy, I. Hofmann, W. Bayer, F. Becker, P. Forck, T. Giacomini, M. Kirk, T. Mohite, C. Omet, A. Parfenova, P. Schütt, GSI, Darmstadt, Germany

Abstract

In this proceeding we present the simulations of the experiment made in the SIS18 synchrotron on the effect of the space charge in a bunched beam stored for one second. The simulations attempt to reproduce 4 sequences of measurements with 4 different types of beams at different intensities using sextupole driven resonances. Our results confirm the conclusions from previous measurements at the CERN-PS using octupoles driven resonances. Some conclusion on the beam physics case are addressed.

INTRODUCTION

An extensive experimental campaign on space charge and resonances has taken place in 2006-2008 on the SIS18 synchrotron at GSI. The purpose of this study was to provide experimental data for code benchmarking and to investigate experimentally the basic beam loss and emittance increase mechanism acting on a beam during long term storage. The beam dynamics mechanism is believed to be trapping or scattering [1, 2, 3]. While these effects were subject of early investigations mainly as single particle effects, only recently it has been proposed that incoherent space charge can drive a periodic resonance crossing in a bunch [4]. In order to disentangle the effect of the synchrotron motion from that of the space charge, we have performed 4 separated set of measurements characterized by the presence or absence of high intensity as well as of the synchrotron motion. First results of these measurements were presented in HB2008 [5]. Here we present the full campaign and the associated simulation results. The details on the experimental campaign, the parameters characterizing the beam and a more detailed discussion on the simulations are documented in the extensive paper Ref. [6]. The necessity of consolidating the beam loss prediction is very important for the SIS100 synchrotron and its magnet field quality requirement [7, 8]. Uncontrolled beam loss is required to be within a 5% budget in order to mitigate a progressive vacuum degradation, dangerous for beam lifetime. Therefore the mechanism studied here plays an important role for the discussion on the nonlinear components in magnets, residual closed orbit distortion as well as in the resonance compensation strategy.

* g.franchetti@gsi.de

EXPERIMENTAL RESULTS AND SIMULATIONS

Low Intensity Coasting Beams

The experimental campaign consisted in measuring the time evolution of a well controlled bunched beam for several tunes taken in the neighborhood of the resonance $3Q_x = 13$. The beam used is composed of $^{40}\text{A}^{18+}$ with KV emittances at injection of $\epsilon_x = 19$ mm-mrad, $\epsilon_y = 14$ mm-mrad. The injection energy is of 11.28 MeV/u. In order to be able observe a beam distribution broadening, a beam smaller than the SIS18 acceptances ($A_x \simeq 200$ mm-mrad, $A_y \simeq 50$ mm-mrad) was created. Transverse beam profiles are measured with the intra-beam profile monitor (IPM) [9], while the longitudinal profile is measured with a beam position monitor. The operational condition of the full campaign have been set so to compensate the natural chromaticity in order to study only the pure space charge driven effects. The third order resonance in this experiment is already excited by natural errors, which are not known by previous measurements. We have used data on beam loss in order to construct a model of the nonlinear lattice of SIS18. In Fig. 1a we show a tune scan of the beam response after 1 second storage, the curves show the emittance ratio and the beam survival. Around the third order resonance beam loss becomes substantial because of the reduction of the separatrix [10]. The pattern of beam loss and the beam loss stop band can be modeled when the resonance is driven by one localized sextupolar error, which we assume as the source of the resonant dynamics. By monitoring the beam loss a stop-band of $\Delta Q_x \simeq 0.12$ due to the 3rd order resonance $3Q_x = 13$ was found. The titled shape of the beam loss curve around the third order resonance is created by some extra detuning made by the chromatic correction sextupoles and other high order nonlinearities. From the simplified model we find that the presence of only the chromatic correction sextupoles creates a too strong effect on the simulated tilting of the beam loss curve. Hence we have included and properly excited an octupolar error in the same location of the sextupolar error. The location of these two nonlinear components has been taken arbitrary as we do not possess more information on the machine nonlinearities and their location. However, with this model, we simulated the experiment with results shown in Fig. 1b. Note in both pictures Figs. 1a,b the error-bars, which are estimated as described in Ref. [6]. The large error-bars in Fig. 1a are the results of beam fluctuation typical of low intensity. The error-bars in Fig. 1b are originated by the

HIGH INTENSITY STUDIES ON THE ISIS SYNCHROTRON, INCLUDING KEY FACTORS FOR UPGRADES AND THE EFFECTS OF HALF INTEGER RESONANCE

C.M. Warsop, D.J. Adams, I.S.K. Gardner, B. Jones, R.J. Mathieson, S.J. Payne, B.G. Pine, C.R. Prior*, G.H. Rees*, A. Seville, H.V. Smith, J.W.G. Thomason, R.E. Williamson, ISIS and *ASTeC, Rutherford Appleton Laboratory, Oxfordshire, UK

Abstract

ISIS is the spallation neutron source at the Rutherford Appleton Laboratory in the UK. Operation centres on a high intensity proton synchrotron, accelerating 3×10^{13} ppp from 70-800 MeV, at a rep. rate of 50 Hz. Studies are under way looking at many aspects of high intensity behaviour with a view to increasing operational intensity, identifying optimal upgrade routes and understanding more about fundamental intensity limitations. Present work is assessing the possibility of increasing beam power by raising injection energy into the existing ring (to ~180 MeV), with a new optimised injector. Progress on calculations and simulations for the main high intensity topics is presented, including: space charge and emittance evolution in the transverse and longitudinal planes, beam stability, and injection optimisation. Of particular interest is the space charge limit imposed by half integer resonance, for which the latest experimental and simulation results are reviewed.

HIGH INTENSITY STUDIES AT ISIS

Present ISIS Status and Operations

Following the commissioning of the ISIS second target station in 2008, the ISIS accelerators now supply beam for two neutron target stations [1]. Beam power is being increased to accommodate the new users, and central to this is the high intensity optimisation of the ring, particularly the dual harmonic RF (DHRF) system and associated beam dynamics. Typical operational beam intensities are now 220-230 μA with well controlled losses (~5%). As machine performance is better understood, intensities should approach 240 μA .

The ISIS synchrotron has a circumference of 163 m, composed of 10 superperiods. It accelerates $\sim 3 \times 10^{13}$ ppp (protons per pulse) from 70-800 MeV, on the 10 ms rising edge of the sinusoidal main magnet field. At a repetition rate of 50 Hz this corresponds to an average beam power of ~0.2 MW. Charge-exchange injection takes place over 130 turns, with painting over both transverse acceptances, which are collimated at about 300π mm mrad. Nominal tunes are $Q_{h,v}=(4.31, 3.83)$, but these are varied during the cycle using trim quadrupoles. Peak incoherent tune shifts due to space charge are estimated at $\Delta Q_{inc} \approx -0.4$. The beam is essentially unbunched at injection, and is 'adiabatically' captured by the DHRF system. Two bunches are accelerated by the $h=2, 4$ systems, with peak design voltages of 160 and 80 kV/turn respectively. The $h=2$ frequency sweep is 1.3-3.1 MHz. The second harmonic

system increases trapping efficiency and improves the bunching factor. The machine operates below transition ($\gamma_t=5.034$) and with natural chromaticities ($\xi_x \approx \xi_y \approx -1.4$). Three fast kickers extract the beam in a single turn, via a vertical septum magnet.

High intensity rings studies address three main areas: increasing intensity for present operations, studying higher intensity potential for the existing ring with a new injector, and assessing options for adding a new ring aiming at ≥ 1 MW beam powers. Underpinning this work is a programme of code development, experiments and diagnostics improvements to allow study of beam loss mechanisms. Many of the concerns for future upgrades coincide with those for current operations.

ISIS Injection and Megawatt Upgrades

The age and associated risk of breakdown are motivating plans to replace large sections of the ISIS 70 MeV linac. Such a replacement could be combined with an overall upgrade to the injector and injection system into the existing ISIS ring. If the injection energy were to be increased (~180 MeV), and injection optimised, there is the prospect of substantially increased beam power (perhaps ~0.5 MW). Although there are numerous potential problems with such a scheme, it could offer a high value upgrade path. Increases in beam power may also carry through to later upgrades. This option is the subject of current studies and is discussed below.

For beam powers in the megawatt regime, ISIS upgrades would make use of an additional 3.2 GeV RCS. Direct injection from the present 800 MeV ring would provide beam powers of ~1 MW. The 3.2 GeV ring could then be adapted for multi-turn charge-exchange injection from a new 800 MeV linac, and provide beam powers of 2-5 MW. Appropriate designs have been described in [2] and will be studied in more detail in due course.

HIGH INTENSITY ISSUES FOR INJECTION UPGRADES

A set of *working parameters* is assumed for the injection upgrade study: whether these are optimal, or the proposed intensities are practical, is to be determined. The starting point is a new 180 MeV injector, with chopped beam injection into the present ring. A suitable linac design has been established [2], which defines the injected beam parameters. *Provisional* working values for intensity are 8×10^{13} ppp, corresponding to 0.5 MW. Other (flexible) working assumptions are: acceleration from 180-800 MeV, a sinusoidal main magnet field, injection

TUNE RESONANCE PHENOMENA IN THE SPS AND RELATED MACHINE PROTECTION

T. Baer*, CERN, Geneva, Switzerland and University of Hamburg, Germany
 B. Araujo Meleiro, T. Bogey, J. Wenninger, CERN, Geneva, Switzerland

Abstract

The 7 km long CERN Super Proton Synchrotron (SPS) is, apart from the LHC, the accelerator with the largest stored beam energy worldwide of up to 3 MJ. In 2008, an equipment failure led to a fast tune shift towards an integer resonance and an uncontrolled loss of a high intensity beam, which resulted in major damage of the accelerator. Distinct experimental studies and simulations provide clear understanding of the beam dynamics and the beam loss patterns at different SPS tune resonances. Diverging closed orbit oscillations, a resonant dispersion and increased beta beating are the driving effects that lead to a complete beam loss in as little as 3 turns ($69 \mu\text{s}$). At the moment, the commissioning of a new turn-by-turn position interlock system which will counteract the vulnerability of the SPS is ongoing.

In this paper, mainly the dynamics of beam losses at different tune resonances and machine protection related aspects are discussed. The beam dynamics at tune resonances are only briefly addressed, a more detailed description is given in [1]. A very comprehensive description of theory, methodology, experiments, simulations and results is given in [2].

INTRODUCTION

On June 27th, 2008 an equipment failure in the SPS led to the uncontrolled loss of a high intensity beam at 400 GeV with a total beam energy of about 2.1 MJ. The vacuum chamber of a main bending magnet was punctured in the vertical plane (cf. Fig. 1) and the magnet had to be replaced. Cause of the incident was a freeze of the main timing system that inhibited the beam extraction after acceleration and resulted in an unintended tune shift towards the $Q = 26$ integer tune resonance during the ramp down of the magnets. An analysis of the data from the beam loss monitoring system revealed that the beam was lost in less than 20 ms which is the time resolution of the system [3].

The incident points out a vulnerability of the SPS to fast beam losses and the challenge of machine protection against tune resonances.

BEAM DYNAMICS AT TUNE RESONANCES

Dedicated experiments were made to understand the beam dynamics at different tune resonances in the SPS.

* contact: Tobias.Baer@cern.ch

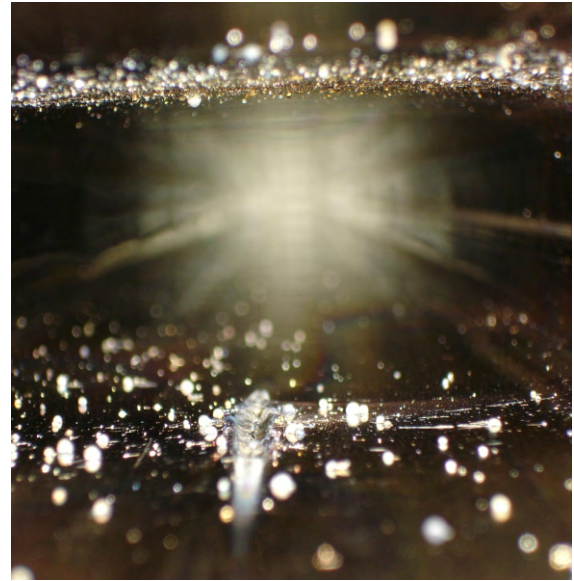


Figure 1: Impact of a 2.1 MJ beam. Over a length of about 10 cm the vacuum chamber is punctured. Metal droplets contaminate the vacuum chamber.

Figure 2 depicts the special threat of beam losses due to integer tune resonances.

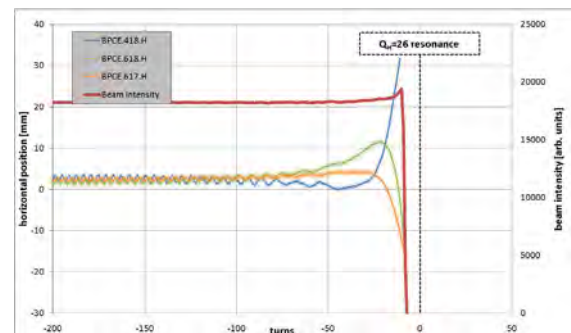


Figure 2: Beam intensity and horizontal turn-by-turn beam position at three particular beam position monitors (BPMs). The horizontal tune is decreased linearly by about $-2 \cdot 10^{-3}/\text{turn}$. The beam is lost at a tune of about $Q_H = 26.015$. **The complete beam is lost within 3 turns after the first beam losses start.**

Measurement conditions: beam energy: 450 GeV, bunch intensity: $1.0 \cdot 10^{10}$ protons, 12 bunches.

The graph shows the horizontal beam position at three particular BPMs close to the $Q_H = 26$ integer tune resonance and the corresponding beam intensity. The horizontal tune is decreased linearly and the beam position starts

HIGH INTENSITY BEAM PHYSICS AT UMER

B. L. Beaudoin, S. Bernal, M. Cornacchia, K. Fiuza, I. Haber, R.A. Kishek, T.W. Koeth, M. Reiser, D.F. Sutter, H. Zhang, and P.G. O'Shea, Institute for Research in Electronics and Applied Physics, University of Maryland, College Park, MD 20742, U.S.A.

Abstract

We report on progress of studies of transverse and longitudinal space-charge beam physics at the University of Maryland electron ring (UMER), a low-energy, high current recirculator. The transverse beam dynamics studies include measurements of betatron and dispersion functions as well as linear resonances for a number of beam currents. We also discuss the implementation of induction focusing for the longitudinal containment of the lowest current beam. When complemented with optimized orbit steering, this longitudinal beam focusing has made possible to extend the number of turns from 100 to more than 1,000, limited mostly by electronics. Some of the results presented are compared with calculations and simulations with the computer codes ELEGANT and WARP.

INTRODUCTION

The University of Maryland Electron Ring (UMER) is a high intensity circular machine that is dedicated to the study of long path length space-charge dominated beam and accelerator physics on a small scale [1]. Understanding how space-charge modifies beam transport from the “zero current” linear optics theory to a regime of highly depressed tune is of fundamental interest to transporting high current bright beams for long distances.

Table 1 summarizes the parameters of the beams currently under study in UMER. The values in the last two columns result from calculations in a uniform focusing model [1]. All beams have pulse duration close to 100 ns, with a 60 Hz repetition rate. Further, the beams are injected with a single-turn scheme involving a fast magnetic kicker and 2 wide-aperture magnetic quadrupoles [2]. The diagnostics employed consist of 14 fast capacitive beam position monitors (BPMs) located every 64 cm around the 11.52 m-circumference ring except for three locations that are fitted with glass breaks. At one of these locations, roughly half way around the ring and labelled “RC10”, a fast wall current monitor is employed to measure the AC component of the circulating beam current.

Table 1: Parameters of 3 Electron Beams in UMER at 10 keV and Nominal Operating Bare Tune of 6.6

Beam Current	Norm. RMS Emittance	Av. Beam Radius	Tune Depression
0.6 mA	$0.4 \pm 20\% \mu\text{m}$	1.6 mm	0.86
6.0	$1.3 \pm 10\%$	3.4	0.63
21	$1.5 \pm 10\%$	5.2	0.31

In one case (0.6 mA), we have the additional capability of longitudinal confinement of the beam through inductively-produced voltage pulses applied at the bunch ends. As discussed below, longitudinal focusing dramatically increases the transport distance. Additional details of this topic can be found in Ref. [3].

The paper is organized as follows: in the first two sections we present results of transverse beam dynamics (lattice functions and linear resonances); in the third section we summarize the implementation of longitudinal focusing for the low current beam, including a brief discussion of a simple 1D model and space charge waves, and in the last section we present the summary and conclusions.

LATTICE FUNCTIONS

The techniques employed for measuring betatron and dispersion functions in UMER are standard [4], but the space-charge tune depressions at injection are not (see Table 1).

We use quadrupole-current scans to determine the betatron function, and energy scans to calculate the dispersion function. The following well-known approximation [4], as applied to UMER, relates the betatron function at a given quadrupole to the changes in coherent tune ($\Delta\nu$) and quadrupole strength ($\Delta k \propto \Delta I_{\text{Quad}}$) when the latter is sufficiently small:

$$\beta_{x,y} [\text{cm}] = \pm 317 \frac{\Delta V_{x,y}}{\Delta I_{\text{Quad}} [A]}. \quad (1)$$

We obtain $\beta_x = 13.7 \pm 4.6$ cm, $\beta_y = 18.2 \pm 1.9$ cm from a quadrupole scan near halfway around the ring at the standard operating point (ring quadrupole current equal to 1.819 A) for the 6.0 mA beam. Calculations with the code Elegant [5] yield $\beta_x = 23.9$ cm, $\beta_y = 41.3$ cm. Betatron beating from mismatch is most likely the reason for the differences, with a small contribution (not included in Elegant) from defocusing by image forces.

With 72 quadrupoles in UMER, measuring the betatron function is clearly tedious, even more so if this has to be repeated for all beam currents. Thus, other techniques like those based on the response matrix are being explored. But other questions arise when applying standard techniques to beams with high space-charge. For example, if we consider Eq. (1), it could be assumed that to first order there is no change in the contribution to focusing from space charge as the external focusing is varied. In addition, the contribution from linear space-charge to the tune variation (numerator in Eq. (1)) would

INTERPLAY OF SPACE-CHARGE AND BEAM-BEAM EFFECTS IN A COLLIDER *

A.V. Fedotov[#], M. Blaskiewicz, W. Fischer, T. Satogata, S. Tepikian
Brookhaven National Laboratory, Upton, NY 11973, USA

Abstract

Operation of a collider at low energy or use of cooling techniques to increase beam density may result in luminosity limitation due to the space-charge effects. Understanding of such limitation became important for Low-Energy RHIC physics program with heavy ions at the center of mass energies of 5-20 GeV/nucleon. For a collider, we are interested in a long beam lifetime, which limits the allowable space-charge tune shift. An additional complication comes from the fact that ion beams are colliding, which requires careful consideration of the interplay of direct space-charge and beam-beam effects. This paper summarizes our initial observations during experimental studies in RHIC at low energies.

INTRODUCTION

Design of several projects which envision hadron colliders operating at low energies such as NICA at JINR [1] and Electron-Nucleon Collider at FAIR [2] is under way. In Brookhaven National Laboratory (BNL), a physics program, motivated by the search of the QCD phase transition critical point, requires operation of the Relativistic Heavy Ion Collider (RHIC) with heavy ions at very low energies corresponding to $\gamma=2.7-10$ [3].

In a collider the maximum achievable luminosity is typically limited by beam-beam effects. For heavy ions significant luminosity degradation, driving bunch length and transverse emittance growth, comes from Intrabeam Scattering (IBS). For Low-Energy RHIC such IBS growth can be effectively counteracted with electron cooling [4]. If IBS were the only limitation, one could achieve a small hadron beam emittance and bunch length with the help of cooling, resulting in a dramatic luminosity increase. However, as a result of low energies, direct space-charge force from the beam itself is expected to become the dominant limitation [5]. In fact, similar limitations may become important even in future high-energy electron-ion colliders when strong cooling is employed to boost the luminosity [6, 7].

Also, the interplay of both beam-beam and space-charge effects may impose an additional limitation on the achievable luminosity lifetime. Thus, the understanding at what values of the space-charge tune shift one can operate in the presence of beam-beam effects in a collider is of great interest for all of the above projects.

Operation of RHIC for Low-Energy physics program started in 2010 which allowed us to have a first look at the combined impact of beam-beam and space-charge effects on beam lifetime experimentally.

LUMINOSITY LIMITATIONS

Space Charge

In general, the space-charge force can change the oscillation frequencies of individual particles (incoherent effect) as well as frequencies of collective beam oscillations. This can lead to rather complex phenomena of space-charge driven resonances, as well as complicates response to the resonances driven by other mechanisms. These effects are mostly of concern for space-charge dominated beam transport and high-intensity storage rings operated close to the space-charge limit associated with low-order machine resonances. Although some of the effects may become important for long beam lifetime in a collider. For discussion of these effects see, for example, Refs. [8-10] and references therein.

A convenient figure of merit for direct space charge effects in circular accelerator is the incoherent direct space-charge tune shift. For a Gaussian transverse distribution, the maximum incoherent space-charge tune shift can be estimated using the following formula:

$$\Delta Q_{sc} = -\frac{Z^2 r_p}{A} \frac{N_i}{4\pi\beta^2 \gamma^3 \varepsilon} \frac{F_c}{B_f}, \quad (1)$$

where F_c is a form factor which includes correction coefficients due to beam pipe image forces (the Laslett coefficients), r_p is the proton classical radius, A and Z are the atomic mass and charge numbers, N_i is the number of ions per bunch, ε is the un-normalized RMS emittance and B_f is the bunching factor (mean/peak line density). Here we assume $F_c=1$.

When the space-charge tune shift becomes significant, the beam can overlap resonances, leading to large beam losses and poor beam lifetime. For machines where the beam spends only tens of milliseconds in the high space-charge regime, the tolerable space-charge tune shift can be as large as $\Delta Q_{sc}=0.2-0.5$. However, for a long storage time, the acceptable tune shifts are much smaller. Beam lifetimes of a few minutes have been achieved with tune shifts of about 0.1 [11].

Beam-beam

Each time the beams cross each other, the particles in one beam feel the electric and magnetic forces due to the

*Work supported by the U.S. Department of Energy
[#]fedotov@bnl.gov

APPLICATION OF A LOCALIZED CHAOS GENERATED BY RF-PHASE MODULATIONS IN PHASE-SPACE DILUTION*

S.Y. Lee, Indiana University, Bloomington, IN 47405, USA

K.Y. Ng, Fermilab, Batavia, IL 60510, USA

Abstract

Physics of chaos in a localized phase-space region is exploited to produce a longitudinally uniformly distributed beam. Theoretical study and simulations are used to study its origin and applicability in phase-space dilution of beam bunch. Through phase modulation to a double-rf system, a central region of localized chaos bounded by invariant tori are generated by overlapping parametric resonances. Condition and stability of the chaos will be analyzed. Applications include high-power beam, beam distribution uniformization, and industrial beam irradiation.

INTRODUCTION

ALPHA, under construction at IU CEEM, is a 20-m electron storage ring. [1] The project calls for storing a tiny synchrotron-radiation-damped bunch to be extended to about 40 ns with uniform longitudinal distribution. RF barriers should be the best candidate for bunch lengthening. Unfortunately, this ring is only 66.6 ns in length, and the widths of the barriers must be of the order of 10 ns or less. The risetime of the barrier voltage will therefore be a few ns, or the rf generating the barrier voltage will be in the frequency range of a few hundred MHz. Ferrite is very lossy at such high frequencies and is therefore unsuitable for the job. Even if another material could be substituted, the barriers of such narrow widths would require very high rf peak voltage; the rf system would be very costly.

Another way to achieve bunch lengthening is to perform phase modulation of the rf wave so as to produce a large chaotic region at the center of the rf bucket, but bounded by well-behaved tori. The beam at the bucket center will be blown up to the much larger chaotic region. If true chaoticity is achieved, the particle distribution will be uniform. Such an idea has been demonstrated experimentally at the IUCF Cooler ring in 1997, [2] where a double-rf system was used and the diffusion was found rather sensitive to the phase difference $\Delta\phi_0$ between the two rf waves. In this paper, the modulation method is further investigated by first determining the choice of $\Delta\phi_0$, and next analyzing the condition and stability of the localized chaotic region.

THE MODEL

The model to be studied is described by the Hamiltonian $H = H_0 + H_1$, where [3]

$$H_0 = \frac{1}{2}\nu_s\delta^2 + \nu_s \left\{ 1 - \cos\phi - \frac{r}{h} [1 - \cos(h\phi + \Delta\phi_0)] \right\},$$

$$H_1 = a\delta\nu_s \sin(\nu_m\theta + \eta). \quad (1)$$

*Work supported by the US DOE under contracts DE-FG02-92ER40747, DE-AC02-76CH030000, and the NSF under contract NSF PHY-0852368.

Here r is the ratio of the two rf voltages, h is the ratio of the two rf harmonics, ν_s is the small-amplitude synchrotron tune in the absence of the second rf, ν_m is the phase modulation tune, η is the modulation phase, a is the modulation amplitude, ϕ is the rf phase, δ is the canonical momentum offset, and θ advances by 2π per revolution turn. This model entails a number of parameters. In this paper, however, we restrict ourselves to the special case of $r = 1/2$, $h = 2$, $\nu_m/\nu_s = 2$, and $\eta = 0$, thus leaving behind only the phase offset $\Delta\phi_0$ and the modulation amplitude a .

Choice of $\Delta\phi_0$

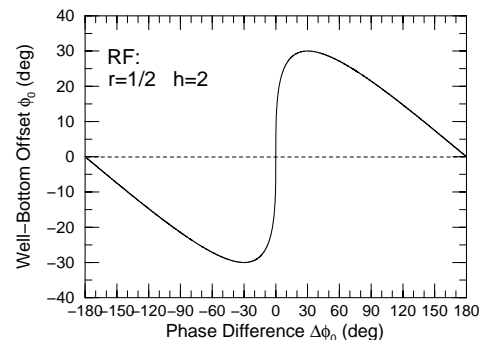
The action at the bottom of an rf potential well $V(\phi)$ is zero and so are the *resonance strengths* generated by phase modulation (see Fig. 4 below). Since the bunch will be tiny, it will be difficult to be driven into parametric resonances if it sits at the bottom of the rf potential. This explains why a two-rf system is necessary. The phase difference $\Delta\phi_0$ between the two rf's shifts the potential-well bottom away from the center of the longitudinal phase space, where the tiny bunch is located. The action at the bunch is now finite. Thus the farther the potential-well bottom is shifted, the larger the resonant strengths.

To generate a large region of chaoticity, the eventual modulation amplitude a will be large. However, a perturbative approach is taken in the analysis so as to get a ballpark understanding of the mechanism. For the unperturbed Hamiltonian, the position of the potential-well bottom ϕ_0 is given by $V'(\phi_0)/\nu_s = \sin\phi_0 - r \sin(h\phi_0 + \Delta\phi_0) = 0$, and is at a maximum when $V''(\phi_0) = 0$. This leads to the solution $\phi_0 = \pm \sin^{-1} r$. The corresponding phase difference between the two rf's is therefore (see Fig. 1)

$$\Delta\phi_0 = \frac{\pi}{2} - h \sin^{-1} r. \quad (2)$$

When $h = 1/r = 2$, the largest offset of well bottom is $\phi_0 = \pm 30^\circ$ and the corresponding phase difference between the two rf's is $\Delta\phi_0 = \pm 30^\circ$. Simulations show that diffusion of a tiny bunch at the phase-space center is possible when $20^\circ \lesssim |\Delta\phi_0| \lesssim 50^\circ$. In below, we first study the case of $\Delta\phi_0 = 30^\circ$, and attempt another value later.

Figure 1: Offset of potential-well bottom ϕ_0 as a function of rf phase difference $\Delta\phi_0$ at $h = 1/r = 2$.



OPTICAL STOCHASTIC COOLING IN TEVATRON*

V. Lebedev[#], Fermilab, Batavia, IL 60510, U.S.A.*Abstract*

Intrabeam scattering is the major mechanism resulting in a growth of beam emittances and fast luminosity degradation in the Tevatron. As a result in the case of optimal collider operation only about 40% of antiprotons are used to the store end and the rest are discarded. Beam cooling is the only effective remedy to increase the particle burn rate and, consequently, the luminosity. Unfortunately neither electron nor stochastic cooling can be effective at the Tevatron energy and bunch density. Thus the optical stochastic cooling (OSC) is the only promising technology capable to cool the Tevatron beam. Possible ways of such cooling implementation in the Tevatron and advances in the OSC cooling theory are discussed in this paper. The technique looks promising and potentially can double the average Tevatron luminosity without increasing its peak value and the antiproton production.

COOLING REQUIREMENTS

The Tevatron luminosity evolution is driven by interplay of the following major effects: the intrabeam scattering, the residual gas scattering, the RF noise and the beam-beam effects. They determine the initial luminosity lifetime of about 5-7 hours. The optimal store duration is about 16 hours and about 40% of antiprotons are burned in the particle interactions (due to luminosity). The rate of antiproton production has achieved its design value and its further growth looks extremely challenging and impossible without a major upgrade to the Antiproton source. Thus a further luminosity growth cannot be attained without beam cooling. The cooling should result in a controlled decrease of emittances so that the beams would stay at the maximum acceptable beam-beam parameter, ξ , in the course of entire store. That would allow us to burn in the luminosity ~80% of antiprotons and, consequently, to double the average luminosity. The required cooling times (in amplitude) are: for protons - 4 and 8 hour, and for antiprotons - 4.5 and 1.2 hour for the longitudinal and transverse degrees of freedom, correspondingly. Typical Tevatron store has $2.7 \cdot 10^{11}$ protons and 10^{11} antiprotons in a bunch with the rms bunch length increasing from 45 to 60 cm. Achieving the required cooling rates with stochastic cooling calls for the bandwidth of ~200 MHz which cannot be obtained in the presently tested micro-wave stochastic cooling. Electron cooling of 1 TeV (anti)protons requires ~500 MV electrons which is an expensive and extremely challenging project.

In this paper we consider a possibility of OSC suggested in Ref. [1] and later developed in Ref. [2]. Its use for the Tevatron was considered in Refs. [3] and [4].

* Work supported by the U.S. Department of Energy under contract No. DE-AC02-07CH11359
[#]val@fnal.gov

A suggestion to test it experimentally is reported in Ref. [5]. First we consider theory developments required for a beam optics optimization and, then, possible implementations for undulators and optical amplifiers.

Note that the OSC damps normally only horizontal and vertical degrees of freedom and the vertical cooling is achieved through the x - y coupling. In this case the horizontal motion has to be damped twice as fast resulting in the required horizontal cooling time of 4 and 0.6 hour for protons and antiprotons, correspondingly.

TRANSFER MATRIX

The OSC of an ultra-relativistic beam assumes [1] that the beam radiates an electromagnetic radiation in a pickup undulator. Then, the radiation is amplified in an optical amplifier (OA) and produces a longitudinal beam kick in a kicker undulator. The path length difference between the light and the beam is adjusted so that a particle would interact with its own radiation. The kick is always in the longitudinal direction and the transverse cooling is achieved by coupling between transverse and longitudinal motion. The longitudinal - horizontal coupling is assumed below. The motion symplecticity binds up the transfer matrix elements so that only 10 of 16 of them are independent. In the absence of RF between points 1 and 2 the matrix between them can be expressed through the Twiss parameters of the points and the partial slip-factor between them, η_{12} , so that:

$$\mathbf{M} = \begin{bmatrix} M_{11} & M_{12} & 0 & M_{16} \\ M_{21} & M_{22} & 0 & M_{26} \\ M_{51} & M_{52} & 1 & M_{56} \\ 0 & 0 & 0 & 1 \end{bmatrix}, \quad \mathbf{x} = \begin{bmatrix} x \\ \theta_x \\ s \\ \Delta p/p \end{bmatrix}, \quad (1)$$

$$\begin{aligned} M_{11} &= \sqrt{\frac{\beta_2}{\beta_1}} (\cos \mu + \alpha_1 \sin \mu), \\ M_{22} &= \sqrt{\frac{\beta_1}{\beta_2}} (\cos \mu - \alpha_2 \sin \mu), \\ M_{12} &= \sqrt{\beta_1 \beta_2} \sin \mu, \\ M_{21} &= \frac{\alpha_1 - \alpha_2}{\sqrt{\beta_1 \beta_2}} \cos \mu - \frac{1 + \alpha_1 \alpha_2}{\sqrt{\beta_1 \beta_2}} \sin \mu, \\ M_{16} &= D_2 - M_{11} D_1 - M_{12} D_1', \\ M_{26} &= D_2' - M_{21} D_1 - M_{22} D_1', \\ M_{51} &= M_{21} M_{16} - M_{11} M_{26}, \\ M_{52} &= M_{22} M_{16} - M_{12} M_{26}. \end{aligned} \quad (2)$$

Here $\beta_{1,2}$ and $\alpha_{1,2}$ are the beta-functions and their negative half derivatives at the points 1 and 2, $D_{1,2}$ and $D'_{1,2}$ are the dispersions and their derivatives, and μ is the betatron phase advance between points 1 and 2. The matrix elements are enumerated similar to a 6x6 matrix but the elements related to the vertical motion (decoupled from

ELECTRON COOLED BEAM LOSSES PHENOMENA IN COSY

Yu. Senichev, R. Gebel, B. Lorentz, R. Maier, M. Nekipelov, D. Prasuhn, F. Rathmann, H. Stockhorst, Institute for Nuclear Physics, FZJ, Julich, Germany

Abstract

Experimentally it has been shown the achievable intensity of electron cooled beams at COSY is restricted by three main beam loss phenomena: the initial losses just after injection during 5-10 s of beam cooling, the coherent self-excited oscillation of cooled beam and the long-term losses $\sim n \times 1000$ s. In this work we study the first and third types of loss and compare the theoretical and experimental results.

INTRODUCTION

The problem of the electron cooled beam losses in COSY leading to not clearly short lifetime of a beam was already repeatedly investigated [1]. For the first time one has sounded, that the electron beam can not only cool the ion beam, but also heat it up in paper [2], where this phenomena was named "electron heating". Many authors suggest explaining it by the nonlinearity of an electron beam field but not specifying what it does mean [3], except [4] in which the assessment of nonlinear resonances influence due to an electron beam is made.

The COSY ring is operating for medium energy experiments in the energy range 45-2500 MeV. During regular operation of the ring for experiments, the time spend at injection energy is about 100 ms short enough, that in the past no optimization of beam lifetime was carried out. At higher energies the beam lifetime is significantly longer, and no special measures are needed. To investigate the situation for the planned spin filtering studies, the status of beam lifetime at injection energy was studied. Recently the careful study to understand the beam lifetime of the proton beam at COSY injection energy of 45 MeV was undertaken.

In given work the results can be divided on two parts: experimental on measurement of beam lifetime and the theoretical part which has been directed on creation of mathematical model and treatment of experimental results. Following chronology of results receiving we begin with an experimental part. In theoretical investigation we are based on the concept of the isolated resonances with bridge between them due to diffusion arising because of scattering on residual gas. Besides it is assisted also with the additional e-beam chromaticity induced by an electron beam itself. In addition very low relative displacement of e- and p-beams can play strengthening role in losses of p-beam since it leads to excitation of odd resonances and decreases the distance between adjacent separatrix.

PROBLEM STATEMENT

At carrying out of experiments we at once tried to allocate the possible reasons for beam losses: fast immediate loss of particles in a single collision and

leaving of stable region (dynamic or physical aperture) and slow blow-up of a beam which is caused by multi-acts process. Against the slow blow-up of beam there was an argument that it can be compensated by suitable cooling systems whereas the immediate loss of particles can not. In other words the real reason for particle losses maybe one-act process resulting in the output of a particle from under influences of cooler. The processes which cause immediate loss of particles are: hadronic interaction, single Coulomb scattering, multiple scattering, recombination and energy loss. We have compared possible probability of each process and have concluded the dominant processes which determine the achievable beam lifetime are the single Coulomb and multiple scattering. In presence of a sufficient electron cooling in COSY the multiple scattering can also be neglected, as scattered particles will be cooled back to the core of the beam before the next collision takes place. However this process also is left among candidates as under certain conditions electronic cooling cannot compensate this process.

FIRST BEAM LIFETIME MEASUREMENTS AT COSY

The 184 m long COSY ring is divided into 8 sections. In each section one quadrupole mass spectrometer measurement was taken to determine the partial pressure distribution of the rest gas. This gas distribution was then scaled with the overall 40 total pressure gauge measurements to obtain a realistic distribution of partial pressures all around the ring. The contribution of the 9 most abundant gases was used together with the Twiss parameters from a MAD code of the ring to calculate the contributions to the beam lifetime $\tau = 1/(\Delta\sigma_c d_i f_b)$ with the real target density d_i , the revolution frequency of the beam f_b and Coulomb loss cross section $\Delta\sigma_c$.

Measurements of the beam lifetime were carried through with and without a D_2 target of density $2 \cdot 10^{14}$ atoms/cm². The time behaviour of the stored beam current measured by a beam current transformer (BCT) was fit with an exponential decay function to yield the beam lifetime. The measured beam lifetimes are $\tau(\text{with target}) = (321.3 \pm 0.4)\text{s}$ and $\tau(\text{without target}) = (4639 \pm 69)\text{s}$, which is about a factor ~ 15 smaller than the calculated beam lifetime. More details can be found in [5,6].

The possible explanations of the discrepancy of measurement and prediction based on single Coulomb scattering losses are: overestimation of the local acceptance or/and insufficient beam cooling.

Two different methods to measure the acceptance of the COSY ring were used: measurements with a single turn angle kick of the beam using a fast kicker magnet and measurement of beam lifetime versus position of scrapers.

TESTING MATERIAL PROPERTIES WITH HIGH ENERGY BEAMS IN HIRADMAT AT CERN

R. Losito, O. Aberle, A. Bertarelli, R. Catherall, F. Cerutti, A. Dallochio, I. Efthymiopoulos, S. Evrard, B. Goddard, C. Hessler, C. Maglioni, M. Meddahi, T. Stora, V. Vlachoudis, CERN, Geneva, Switzerland

Abstract

HiRadMat is a new facility under construction at CERN that will provide the users with the possibility to investigate the behavior of materials when irradiated with pulsed high energy and high intensity beams extracted from the CERN SPS. The need for such a facility was raised by the LHC collimation project to expand our present knowledge about the resistance of materials under impact with high energy protons. This paper will discuss the material parameters for which a deeper knowledge would be needed for extensive use in high-energy accelerators, and the kind of test that can be conducted in HiRadMat to improve this knowledge. In particular we will discuss destructive testing, meaning test of materials beyond the limit of rupture or at phase change, and damage testing that should reveal changes in materials properties due to long term irradiation below the rupture limit. The facility could be used as well for calibration of radiation detectors like BLMs. The main difficulty connected with the test is how to observe material changes. Some preliminary ideas on on-line and post-irradiation tests will be outlined.

INTRODUCTION

The construction of the LHC at CERN has raised interesting questions about the resistance of materials to accidental beam impact. The energy stored in the beams, already at a very early stage of operation, is such that even a single nominal bunch ($\sim 10^{11}$ protons) can cause significant damage to the materials used for the most common equipment. For this reason the LHC has been equipped with a complex protection system where the level of protection of the machine depends on several factors, the main being beam energy and intensity. In order to understand how to fix the limits among the different levels of protection, several studies and tests have been performed [1].

The first question in the line was to decide how to classify damage to materials. Several laboratories classify radiation damage according to the DPA (Displacement Per Atom) calculated through simulation codes like MARS [2] or PHITs [3]. CERN groups pragmatically decided to consider that, at least for metallic materials, “a clear sign of melting” [4] could be more convenient. It is in fact not possible to measure the DPA, and the estimate through different codes may bring results that differ by orders of magnitude [5], and would oblige to include in the limits large safety factors that may become overwhelming for practical use. In addition, for accidental beam impact, melting or structural damage are much

more of concern than DPA, which is an effect depending rather on integrated dose.

The pragmatic approach has the advantage to be verifiable by testing materials in a beam with known characteristics. An experiment conducted in 2004 by the LHC Machine Protection team (see [4]) assessed this limit on different materials (Copper, different grades of stainless steels, Zinc) at 450 GeV finding that already $10^{12} p^+$ can create serious damages to metallic structures. By simulations, this result was extrapolated to 7 TeV finding that at the nominal emittance damage would start occurring at an even lower intensity ($10^{10} p^+$). This result, while important for the design of the machine protection system, was not exhaustive of all the possible damage cases in the LHC, therefore a thorough discussion about how to measure material damage following the impact of a beam started. R. Assmann, leader of the LHC collimation project [6], proposed and pushed for the creation of a facility where candidate materials as well as full collimator assemblies could be tested in controlled conditions, as important validation test before their installation in LHC.

The facility, called HiRadMat [7], was approved by the CERN management and is presently under construction, expected to become operational by Autumn 2011. It would allow testing of materials at 440 GeV for protons, and 173.5 GeV/u for lead ions extracted from the CERN SPS.

At the same time, HiRadMat has been proposed as a trasnational access facility within the European Project EUCARD [8], to make it easily accessible to European teams wishing to perform experiments there. As all other beam facilities at CERN, HiRadMat will be open to all CERN users. Experiment proposals will be evaluated by a dedicated committee and scheduled in the available slots in the yearly planning of the CERN accelerators. Details on the application procedure and conditions can be found in [7].

THE HIRADMAT FACILITY

The HiRadMat Facility will be located in the TNC tunnel in the SPS BA7 area, used in the past by the West Area Neutrino Facility (WANF). CERN is presently dismantling the WANF components before installation of the new irradiation area, the new beam dump, and the new primary line, specially designed to shape the beam according to the user requirements and equipped with all the instrumentation necessary to measure the beam conditions.

SHOCK IMPACT OF HIGH ENERGY/INTENSITY BEAMS WITH MATTER AND HIGH ENERGY DENSITY PHYSICS

N.A. Tahir, GSI, Darmstadt, Germany

R. Schmidt, J. Blanco Sancho, CERN-AB, Geneva, Switzerland

A. Shutov, IPCP, Chernogolovka, Russia

A.R. Piriz, University of Castilla-La Mancha, Ciudad Real, Spain

Abstract

The purpose of this study is to assess the damage caused to the equipment (beamdump, collimators etc) in case of an accident involving full impact of the LHC beam. First, the FLUKA code [1] is used to calculate the proton energy loss in solid carbon and this energy loss data is used as input to a two-dimensional hydrodynamic computer code, BIG2 [2] to study the thermodynamic and hydrodynamic response of the target. The BIG2 code is run for $5\ \mu\text{s}$ and the density distribution at the end of this run time is used in FLUKA to generate new energy loss data corresponding to this density distribution. FLUKA and BIG2 are thus run iteratively with a time interval of $5\ \mu\text{s}$. Previously [3], we carried out hydrodynamic simulations using the energy loss data calculated by FLUKA using solid carbon density, but scaled according to the line density in axial direction. In the present paper, we give a comparison between the results obtained using the two models. Our simulations show that the latter model overestimates the beam penetration. Moreover, the density and the temperature distributions are quite different in the two cases.

INTRODUCTION

When the Large Hadron Collider (LHC) will achieve its full capacity, each beam will consist of a bunch train with 2808 bunches and each bunch comprising of 1.15×10^{11} protons. The bunch length will be 0.5 ns and two neighboring bunches will be separated by 25 ns while intensity distribution in the radial direction will be Gaussian with a standard deviation, $\sigma = 0.2$ mm. In the center of the physics detectors the beam will be focused to a much smaller size, down to a σ of $20\ \mu\text{m}$. The total duration of the Bunch train will be of the order of $89\ \mu\text{s}$ while the total number of protons in the beam will be 3×10^{14} which is equal to 362 MJ, sufficient to melt 500 kg of copper. When the maximum particle momentum of 7 TeV/c is reached, the two beams will be brought into collisions.

Safety of operation is a very important problem when working with such extremely powerful beams. The machine protection systems are designed to safely extract the beams from the system in case of a failure [4]. However, it is necessary to assess the damage caused to the equipment if the machine protection systems fail. In this paper, we study the scenario in which the entire beam is lost at a single point. Although, the likelihood of happening of an accident of this magnitude is extremely remote and beyond

the design of the machine protection systems, nevertheless it is important to know the consequences, if it ever happens.

Previously, we reported calculations of the full impact of the LHC beam on solid carbon [3] and solid copper [5] cylindrical targets. These calculations have been done in two steps. First, the energy loss of the LHC protons is calculated at solid density using the FLUKA code [1], which is an established particle interaction and Monte Carlo package capable of simulating all components of the particle cascades in matter, up to multi-TeV energies. Second, this energy loss data is used as input to a sophisticated two-dimensional hydrodynamic code, BIG2 [2], to calculate the beam-target interaction. The decrease in the generation of secondary particles as well as decrease in energy deposition due to the density reduction caused by the onset of hydrodynamics is modeled by using the solid density energy loss scaled with the line density in every simulation cell, at every time step (“analytic approximation”). Recently, we have carried out more advanced simulations in which the FLUKA and the BIG2 codes are run iteratively using an iteration time interval of $5\ \mu\text{s}$ in case of a solid carbon target having a length of 10 m and a radius of 2.5 cm. It has been found that the “analytic approximation” overestimates the beam penetration compared to the iterative calculations. Moreover, the density, temperature and the pressure profiles are noticeably different in the two cases.

PROTON ENERGY LOSS IN CARBON

For the study presented in this paper, the geometry for the FLUKA calculations was a cylinder of solid carbon with radius = 1 m and length = 5 m. The energy deposition is obtained using a realistic two-dimensional beam distribution, namely, a Gaussian beam (horizontal and vertical $\sigma_{rms} = 0.2$ mm) that was incident perpendicular to the front face of the cylinder.

The peak energy deposition is $30\ \text{GeV/p/cm}^3$ which is equal to a specific energy deposition of about 0.3 kJ/g per bunch as shown in Fig. 2 where we plot the specific energy deposited by a single LHC bunch along the axis.

SIMULATION RESULTS

In this section we present hydrodynamic simulation results of beam-target interaction. The data presented in Fig. 1 is converted into specific energy deposition (in kJ/g, Fig. 2) which is used as input to the BIG2 code to study heating and hydrodynamic motion of the material. The

MATERIALS UNDER IRRADIATION BY HEAVY IONS AND PERSPECTIVES FOR FRIB*

R. Ronningen[#], M. Kostin, T. Baumann, NSCL, Michigan State University, East Lansing, MI 48824, U.S.A.

Abstract

High energy heavy ion beams that are planned for the Facility for Rare Ion Beams (FRIB) will deliver power at very high densities and will produce significant radiation damage in materials with which they interact. Reliable predictions of material and component life times for FRIB are needed, yet the tools used to make the necessary predictions, for example heavy ion radiation transport codes, provide damage estimates whose levels have in the past varied significantly. In addition, there are very few appropriate data sets to validate code predictions. We will present examples of components, for example the beam dump system for FRIB, with attending predicted levels of damage obtained by radiation transport codes. We will summarize results from an experiment to produce and to quantify damage in a controlled way. Finally, we will show examples of targets used in experiments at the National Superconducting Cyclotron Laboratory (NSCL) where damage has been observed, and will present results from transport codes to quantify the damage.

INTRODUCTION

Michigan State University has prepared a conceptual design for a U.S. Department of Energy (DOE) Office of Science National User Facility for scientific research with rare isotope beams. This facility [1], the "Facility for Rare Ion Beams" (FRIB), will provide intense beams of rare isotopes to be used for cutting edge nuclear science research. The rare isotope beams will be created from intense beams of stable isotopes accelerated in a superconducting-radio-frequency linear accelerator to kinetic energies above 200 MeV/nucleon for all ions including uranium with beam power up to 400 kW. There are significant technical challenges associated with the high-power density caused by the interaction of the high-power primary heavy ion beam with matter, and with the high radiation levels associated with the nuclear interactions.

The systems most strongly affected by these challenges are the rare isotope production target, the primary beam dump, and various magnet systems. Research and development (R&D) is being performed to develop viable technical solutions. Even within previous MSU-led R&D efforts [2], it was recognized that radiation damage by high power heavy ion beams interacting with target and beam dump materials will be significant. It was also recognized that there is scant experimental information available at power and energy appropriate for FRIB. Attempts were made to use existing radiation transport

codes to predict levels of damage in the developed beam dump concept, a rotating water-filled aluminum shell. Stein et al. [3] estimated the damage using the PHITS [4] code system version available at that time, that for a 320 MeV/nucleon ²³⁸U beam having 366 kW (3e13 ions/s) passing through a 1 – 2 mm aluminum shell over a 5 cm x 220 cm area (in the case of rotation for an approximately 70 cm diameter drum) the resulting radiation damage is approximately 7e-2 dpa/day. The term "dpa" stands for displacements per atom. In metallic structures, displaced atoms result in often undesirable property changes, such as swelling and embrittlement. If the allowable dose is 5 dpa, this could be reached in about 10 weeks if the beam position on the dump is unchanged.

Currently available data suggest that the displacement damage caused by energetic heavy ions has a significant contribution from electronic stopping of the beam particles, and this contribution can be orders of magnitude larger than the damage caused by nuclear stopping. This "swift heavy-ion effect" has a strong dependence on the projectile energy. The relation of actual material damage from heavy ion radiation to dpa values calculated with commonly available transport codes is practically unknown. It is very important to FRIB design efforts to better understand heavy ion radiation damage mechanisms and to improve models and predictability.

PERSPECTIVES FOR FRIB

The preferred concept for a beam dump for FRIB at present is a water-filled rotating aluminium-shell system having approximately 70 cm diameter and approximately 1.5 mm shell thickness. This concept is shown in Figure 1. Damage predictions (in terms of dpa) were carried out for 1.5 mm aluminium using TRIM [5]. The TRIM code was chosen because it predicted higher values of dpa compared to older versions of MARS15 [6] and PHITS [4]. The representative heaviest ion beam was approximately 200 MeV/nucleon ²³⁸U. The representative "light" heavy ion was approximately 190 MeV/nucleon ⁴⁸Ca. The results are summarized in Table 1. Drum rotation and variation of beam position on the dump as a function of beam-target-rare isotope combinations that are expected during operations increase the lifetime. In addition, a mix of light and heavy ion beams is expected to be required to satisfy the science needs. Overall, the beam dump life is expected to exceed a year if our assumptions and code predictions of damage are reasonable. However, if radiation damage estimates are a factor of 10 too low, dump lifetimes of several months to several years can still be expected, depending on facility operation.

*Work supported by US Department of Energy Office of Science under financial assistance agreement DE-SC-0000661, DE-FG02-07ER41472, and by the US National Science Foundation under Grant No. PHY-0606007

[#]Ronningen@nsl.msu.edu

RADIATION HARDNESS OF INSULATING COMPONENTS FOR THE NEW HEAVY-ION ACCELERATOR FACILITY

T. Seidl, W. Ensinger, Technische Universität Darmstadt, Darmstadt, Germany

R. Lopez, D. Tommasini, CERN, Geneva, Switzerland

E. Floch, E. Mustafin, A. Plotnikov, D. Severin, C. Trautmann, GSI, Darmstadt, Germany

A. Golubev, A. Smolyakov, ITEP, Moscow, Russia

Abstract

The planned International Facility for Antiproton and Ion Research (FAIR) will consist of a superconducting double-ring synchrotron offering ion beams of intensity increased by a factor of 100-1000 compared to the existing GSI accelerators. Materials close to the beam tube will be exposed to secondary radiation of neutrons, protons, and heavier particles, limiting the lifetime and reliable function of various device components. The present study investigates the radiation hardness of insulating components with focus on polyimide as electrical insulation and thermal barrier. Dedicated irradiation experiments were performed with different projectiles. Degradation tests of irradiated materials include breakdown voltage and low temperature thermal conductivity measurements. Special attention is given to effects induced by heavy ions (e.g., Ta, Au), because they are known to create extensive damage at rather low doses.

INTRODUCTION

During long-term operation of the new FAIR facility, some parts of the superconducting magnets (sc magnets) will be exposed to high radiation levels, cryogenic temperatures, and dynamic mechanical loads (Lorentzian forces during pulsed operation). Depending on the position, different components will be hit by secondary radiation, showing a complex spectrum of gammas, neutrons, protons and heavier particles [1]. Although the number of heavy particles is small compared to the amount of neutrons or light fragments (e.g. alpha particles), their large energy deposition can induce extensive damage at rather low fluencies. Dose calculations show that depending on the angle of beam loss and position of the magnet component, the contribution of heavy ions to the total accumulated dose can reach up to 80%. In contrast to slow projectiles (keV–MeV), producing primarily elastic collisions with target atoms, the energy deposition of relativistic ions is dominated by electronic excitation and ionization processes. In the MeV to GeV energy regime, beam-induced radiation damage strongly depends on the material properties. Most metals are rather insensitive [2], whereas the irradiation of polymeric insulators results in material degradation [3-7]. The degree of damage depends on the specific sensitivity of the material and scales with the electronic stopping power.

Most of the superconducting magnets of the FAIR project will use polyimide to electrically and thermally

insulate their conductors or cables. Significant decreases of the dielectric strength of polymeric insulators are observed after irradiation with gamma, neutron and proton of high doses [8-11]. Further, the thermal conductivity of ion irradiated polymers was found to decrease with irradiation dose [12]. To the best of our knowledge not many results are shown in literature with regard to the radiation hardness of polymeric insulators under heavy ion irradiation.

In the present work, we present our results on swift heavy ion and proton induced changes in the dielectric strength of polyimide as well as heavy ion induced changes of the thermal conductivity at low temperature.

EXPERIMENTAL

Material

The polyimide (Kapton HN from Du Pont de Nemours, Apical AV from Kaneka Texas) having a thickness of 50 & 125 (+/- 2) μm were cut into 5x5 cm^2 samples from commercial rolls.

Irradiations

Polyimide samples were irradiated with various ion beams at different facilities. Table 1 lists all irradiation experiments and parameters performed. For clarification only the maximum dose applied is given. It has to be noted that in each experiment different doses were accumulated as seen in Fig. 1 to explore the trend of each irradiation.

In one explicit experiment the temperature rise of a polyimide sample was measured during irradiation with 11 MeV/u Xe beam having a flux of 10^8 ions/ cm^2 . The increase was found to be less than 2°C during 30 min of continuous ion bombardment. Effects due to a heating through the ion beam is therefore neglected under the given conditions.

Breakdown Voltage Measurements

Dielectric strength tests were performed in ambient atmosphere. Humidity and temperature was controlled during all the measurements (22-24°C and 35-45% humidity). Cylindrical stainless steel electrodes 12 mm in diameter with an edge of 1 mm were used. The voltage across each foil was ramped at 1.2 kV/s until breakdown or up to the limit of the supply (18.5 kV). The voltage was measured by means of a high voltage probe. Current measurement was performed by a voltage divider and a

HIGH POWER TARGET R&D FOR THE LBNE BEAMLINER: STATUS AND FUTURE PLANS*

P. Hurh, FNAL, Batavia, IL 60510, USA

O. Caretta, T. Davenne, C. Densham, P. Loveridge, , STFC-RAL, Didcot, OX11 0QX, UK

N. Simos, BNL, Upton, NY 11973, USA

Abstract

The Long Baseline Neutrino Experiment (LBNE) Neutrino Beam Facility at Fermilab will use a high energy proton beam on a solid target to produce a neutrino beam aimed at underground detectors at the DUSEL site in South Dakota. Initial proton beam power is planned to be 700 kW with upgrade capability to greater than 2 MW. Solid target survivability at such incident beam power is of great interest, and an R&D program has been started to study the relevant issues. Areas of study include irradiation testing of candidate target materials at the BLIP facility at BNL, multi-physics simulations of solid target/beam interactions at RAL, autopsies of used NuMI targets, and high strain rate effects in beryllium. Status and results of these studies are presented as well as a summary of planned future high power target R&D efforts.

INTRODUCTION

The LBNE Neutrino Beam Facility conceptual design for a future 2+ MW upgrade includes targeting 60-120 GeV pulsed proton beam (1.6e14 protons per pulse, 1.5-3.5 mm sigma radius, 9.8 micro-sec pulse length) on a 0.9 m long graphite target rod. Although analysis has shown the graphite can withstand the thermal shock and resulting stresses of the beam interaction, concerns over long-term survivability of the graphite in the high radiation environment have motivated research into the radiation damage limits of graphite as well as research into beryllium as an alternate candidate target material for LBNE.

To gain an understanding of the material property changes of various graphite materials under high energy proton beam irradiation, two efforts have been started. One is to autopsy failed graphite targets from the NuMI Target Hall which have shown decreased neutrino yield during operation with 120 GeV proton beam. The second is to measure key material properties of various graphite samples after exposure to 118 MeV proton beam at the BLIP facility at BNL.

To better understand the viability of using beryllium as a high power target material, the LBNE project has entered into an accord with STFC-RAL's High Power Targets Group to perform design studies and multi-physics simulations of beryllium targets under LBNE-like beam parameters. In addition, work has begun at FNAL to understand the correlation of simulation results with real-world experience of beryllium exposed to high intensity proton beam.

*Fermi Research Alliance, LLC under Contract No. DE-AC02-07CH11359 with the United States Department of Energy.

GRAPHITE R&D

Graphite has been chosen as a target material for many neutrino beam facilities (NuMI, T2K, CNGS) because of its excellent resistance to thermal shock and other advantages for neutrino production. However, graphite degrades rapidly by oxidation when heated in air environments to temperatures above 400° C [1]. This adds complexity to the target design in the form of an inerted or evacuated chamber and properly designed and cooled beam windows. In addition, and perhaps more importantly, graphite exhibits radiation damage that changes its material properties significantly at relatively low dose or Displacements Per Atom (DPA).

Figure 1 shows the significant decrease in thermal conductivity of three different graphite grades exposed to neutron irradiation. Moreover, with increased gas production associated with high energy proton irradiation (relative to neutron irradiation), the effects on graphite structure may be more severe as demonstrated by irradiation tests of graphite at BLIP (BNL) in 2006 [2]. Figure 2 shows a set of graphite samples from the 2006 BLIP test completely destroyed in the central beam spot area after irradiation to an integrated flux level of ~0.5-1e21 protons/cm². This level of structural damage at relatively low dose is obviously of great concern when considering graphite as a candidate target material.

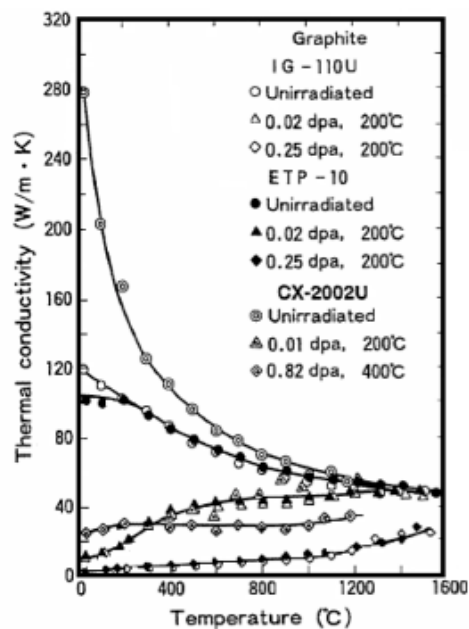


Figure 1: Effect of neutron irradiation on thermal conductivity of 3 grades of graphite [2].

NONLINEAR OPTICS AS A PATH TO HIGH-INTENSITY CIRCULAR MACHINES*

S. Nagaitsev[#], A. Valishev, FNAL, Batavia, IL 60510, U.S.A.
V. Danilov, SNS, Oak Ridge, TN 37830, U.S.A.

Abstract

What prevents us from building super-high intensity accelerators? The answer is case-specific, but it often points to one of the following phenomena: machine resonances, various tune shifts (and spreads), and instabilities. These three phenomena are interdependent in all present machines. In this paper we propose a path toward alleviating these phenomena by making accelerators nonlinear. This idea is not new: Orlov (1963) and McMillan (1967) have proposed initial ideas on nonlinear focusing systems for accelerators. However, practical implementations of such ideas previously proved elusive [1].

INTRODUCTION

All present accelerators (and storage rings) are built to have “linear” focusing optics (also called lattice). The lattice design incorporates dipole magnets to bend particle trajectory and quadrupoles to keep particles stable around the reference orbit. These are “linear” elements because the transverse force is proportional to the particle displacement, x and y . This linearity results (after the action-phase variable transformation) in a Hamiltonian of the following type:

$$H(J_1, J_2) = \nu_x J_1 + \nu_y J_2, \quad (1)$$

where ν_x and ν_y are betatron tunes and J_1 and J_2 are actions. This is an integrable Hamiltonian. The drawback of this Hamiltonian is that the betatron tunes are constant for all particles regardless of their action values. It has been known since early 1960-s that the spread of betatron tunes is extremely beneficial for beam stability due to the so-called Landau damping. However, because the Hamiltonian (1) is linear, any attempt to add non-linear elements (sextupoles, octupoles) to the accelerator generally results in a reduction of its dynamic aperture, resonant behavior and particle loss. A breakthrough in understanding of stability of Hamiltonian systems, close to integrable, was made by N. Nekhoroshev [2]. He considered a perturbed Hamiltonian system:

$$H = h(J_1, J_2) + \varepsilon q(J_1, J_2, \theta_1, \theta_2), \quad (2)$$

where h and q are analytic functions and ε is a small perturbation parameter. He proved that under certain conditions on the function h , the perturbed system (2) remains stable for an exponentially long time. Functions h satisfying such conditions are called *steep* functions

with quasi-convex and convex being the steepest. In general, the determination of steepness is quite complex. One example of a non-steep function is a linear Hamiltonian Eq. (1).

In Ref. [1] we proposed three examples of nonlinear accelerator lattices. In this paper we will concentrate on one of the lattices, which we know results in a steep (convex) Hamiltonian. We will also describe how to implement such a lattice in practice.

NON-LINEAR LATTICE

Consider an element of lattice periodicity consisting of two parts: (1) a drift space, L , with exactly equal horizontal and vertical beta-functions, followed by (2) an optics insert, T , which has the transfer matrix of a thin axially symmetric lens (Figure 1). Alternatively, the T insert can have a transfer matrix of an opposite sign with a phase advance of 180 degrees in both planes, which we use in our implementation below.

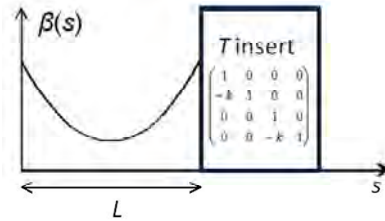


Figure 1: An element of periodicity: a drift space with equal beta-functions followed by a T insert.

Let us assume that we have equal linear focusing in the horizontal and vertical planes such that the beta-functions in the drift space are equal to

$$\beta(s) = \frac{L - sk(L - s)}{\sqrt{1 - \left(1 - \frac{Lk}{2}\right)^2}}. \quad (3)$$

The insert T can be implemented with regular elements (quadrupoles, dipoles, drifts) as described below. Let us now introduce additional transverse magnetic field along the drift space L . The potential, $V(x, y, s)$, associated with this field satisfies the Laplace equation, $\Delta V = 0$.

Now we will make a normalized-variable substitution [1] to obtain the following Hamiltonian for a particle moving in the drift space L with an additional potential V :

$$H_N = \frac{p_{xN}^2 + p_{yN}^2}{2} + \frac{x_N^2 + y_N^2}{2} + U(x_N, y_N, \psi), \quad (4)$$

where

$$U(x_N, y_N, \psi) = \beta(\psi)V(x_N\sqrt{\beta(\psi)}, y_N\sqrt{\beta(\psi)}, s(\psi)) \quad (5)$$

and ψ is the “new time” variable defined as the betatron phase,

*Work supported by UT-Battelle, LLC and by FRA, LLC for the U. S. DOE under contracts No. DE-AC05-00OR22725 and DE-AC02-07CH11359 respectively.

[#]nsergei@fnal.gov

TRANSVERSE MODE COUPLING INSTABILITY MEASUREMENTS AT TRANSITION CROSSING IN THE CERN PS

S. Aumon*, CERN and EPFL, Switzerland, H. Damerou, M. Delrieux, P. Freyermuth
S. Gilardoni, E. Metral, G. Rumolo, B. Salvant, CERN, Geneva, Switzerland

Abstract

Crossing transition energy in the CERN PS is critical for the stability of high intensity beams, even with the use of a second order gamma transition jump scheme. The intense single bunch beam used for the neutron Time-of-Flight facility (n-ToF) needs a controlled longitudinal emittance blow-up at the flat bottom to prevent a fast single-bunch vertical instability from developing near transition. This instability is believed to be of the Transverse Mode Coupling (TMCI) type. A series of measurements performed in 2009 and 2010 aims at using this TMCI observed on the ToF beam at transition as a tool for estimating the transverse global impedance of the PS. For this purpose, we compare the measurement results with the predictions of the HEADTAIL code and find the matching parameters. This will allow predicting the stability of the high brightness LHC beam near transition. The final goal is to study the feasibility of a possible cure to the fast vertical instability measured on the ToF beam by applying an improved gamma transition jump scheme instead of compromising the longitudinal density.

INTRODUCTION

The CERN Proton Synchrotron uses a second order gamma transition (γ_t) jump scheme to cross the transition energy. This optics was implemented in the past to cure the “negative mass instability” [1] and the effect of the longitudinal space charge in high intensity beams [2]. However even with the use of the gamma jump, fast losses can be observed near transition with a high intensity single bunch beam of $700 \cdot 10^{10}$ protons if the longitudinal emittance is not sufficiently large. This effect is believed to a Transverse Mode Coupling Instability (TMCI). Increasing the longitudinal emittance (1σ) from 2 eVs to 2.3 eVs is sufficient to prevent the instability to develop. A series of measurement have been performed on an intense beam with and without the gamma jump scheme in order to determine the behavior of the instability and attempt to benchmark the HEADTAIL code. We use those results as tool to estimate the transverse impedance. In the future, the results of this study could be used to predict the transverse stability of the ultimate LHC beam in the framework of the possible PS injection energy upgrade.

* sandra.aumon@cern.ch

CROSSING TRANSITION IN THE CERN PS

Transition crossing might produce unfavourable effects. Some of them can be cured by a second order γ_t -jump. This remedy was adapted in the 70's to avoid the negative mass instability which was a severe intensity limitation [1]. The method consists of crossing transition energy much faster than it would be without any special precaution. Then the instabilities for which the rise time is slower than the time spent by the beam close to the transition energy will not develop. Thanks to the γ_t -jump scheme, the intensity limitation at γ_t energy had been pushed forward during several years.

The γ_t -jump consists of an artificial increase of the transition crossing speed by dedicated fast pulsed quadrupoles placed at non-zero dispersion locations in order to adjust the momentum compaction factor η . This depends on the unperturbed and perturbed dispersion functions at the kick quadrupoles places and the amplitude of the γ_t -jump depends of the intensity. The quadrupoles are grouped in doublets and triplets (combined doublets) with two strengths $\pm K_1$ and $\pm K_2$ separated by π in betatron phase advance in order to obtain a almost zero tune shift [2]. The present situation provides a large $\Delta\gamma_t = -1.24$ performed in $500 \mu\text{s}$ as presented Fig. 1. However by doing so the dispersion and betatron functions increase and lead to a large horizontal beam size and non negligible beam loss [3]. Nowadays the γ_t -jump is used routinely. Several other tricks are applied to cross transition energy such as the change of the sign of the chromaticities when $\eta = 0$ in order to avoid head-tail instabilities [4] after transition. Despite of these measures, a fast vertical instability is observed on the high intensity single bunch beam nToF when the longitudinal density is not blown up enough [5].

TRANSVERSE INSTABILITY OBSERVATION WITHOUT γ_T -JUMP

A dedicated single bunch beam has been set up to observe the transverse instability without the γ_t -jump. the beam parameters are presented in the Table 1. In order have favorable conditions to study the transverse instability, the vertical chromaticity ξ_v is set close to zero several milliseconds around transition in such a way to obtain a 'plateau'. The values of the chromaticities cannot be measured precisely around transition due to the frozen synchrotron motion therefore there is a large uncertainty of the time at which they change sign. However, no headtail instabilities

FAST COMPRESSION OF INTENSE HEAVY-ION BUNCHES IN SIS-18

Oleksandr Chorniy, Oliver Boine-Frankenheim, Peter Hülsmann, Peter J. Spiller,
GSI, Planckstr. 1, 64291 Darmstadt, Germany

Abstract

At GSI and for the FAIR project short heavy-ion bunches are required for the production and storage of exotic fragment beams as well as for plasma physics applications. In the SIS-18 and in the projected SIS-100 synchrotron longitudinal compression via fast bunch rotation is performed directly before extraction. In order to arrive at the required bunch length the rf cycle has to be optimized for high intensities to avoid the blowup of the occupied longitudinal phase space area. We will discuss experimental and simulation results of the rf capture at injection energy, the re-bunching process at the final energy and the subsequent bunch rotation.

INTRODUCTION

Bunch compression with fast beam extraction to the experimental areas is used routinely in the SIS-18. The compression is done via 90° fast rotation of the bunch longitudinal phase space distribution. The phase space rotation is initiated by fast jump of RF voltage amplitude.

A first report describing the strategy to obtain high density beams in the SIS-18 was published in 1996 [1]. Early experiments on fast bunch compression with a parallel operation of two RF cavities were done in 1997 [2]. Two ferrite cavities with total available voltage of 32 kV at a frequency of 1 MHz were used. The resulting compressed Ar^{11+} bunch containing $1 \cdot 10^{10}$ particles at the energy 200 MeV/u had the total length of about 350 ns.

For the plasma generation using, the required compressed beams should not exceed 50 ns [3]. In order to calculate the required RF parameters at compression simulation studies were done [3]. The bunch compression should be performed at the voltage amplitude of 200 kV. The layout of the compression system consisting of several magnetic-alloy compressor cavities was described in [4]. Later, due to a restriction of the available resources it was planned to install only one cavity. In 2008 one magnetic alloy compressor cavity with 40 kV voltage amplitude was installed in the SIS-18 and the first test measurements were done at injection energy [5].

The RF system in SIS-18 consists presently of two ferrite cavities and one magnetic alloy bunch compressor cavity. In Table 1 the main parameters of the RF system in the SIS-18 are presented. The ferrite cavities are used for the RF capture and acceleration and the magnetic alloy cavity is used only for the bunch compression. The RF amplitude cycle in the SIS-18 consists of the RF capture with acceleration at $h=4$, de-bunching to coasting beam, RF recapture at $h=1$ and bunch compression (Fig. 1). The recapture pro-

cess is done by a linear ramp of the RF amplitude from 0 till final recapture amplitude.

Table 1: Parameters of SIS-18 RF System

	SIS cavity	Compressor
Inductive Load	Ferrites	Magnetic Alloy
Frequency tuning range, MHz	0.85-5.4	0.85-0.9
Peak RF-voltage, kV	16	40
Pulse duration, ms	>100	0.5
Voltage rise time, μs	150	10

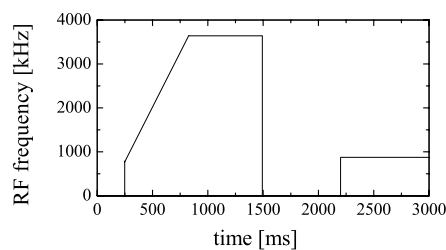
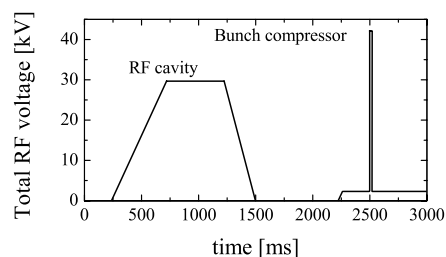


Figure 1: Scheme of the SIS-18 RF cycle with fast bunch compression.

Recently the measurements on the bunch compression at extraction energy using magnetic-alloy compressor cavity were done. Using the measurements results we try to investigate the possible issues and solutions. One of the problem considered here as well is the RF capture in the beginning of the machine cycle. Usually the RF amplitude ramp in the SIS-18 is done simultaneously with acceleration in the beginning of the acceleration ramp. In such situation the RF bucket in the beginning of RF capture should be sufficiently large in order to contain most particle inside. On the other hand the large initial RF bucket produce increase

SUMMARY OF WORKING GROUP A ON “BEAM DYNAMICS IN HIGH-INTENSITY CIRCULAR MACHINES”

G. Franchetti, GSI, Darmstadt, Germany
E. Métral, CERN, Geneva, Switzerland

Abstract

In this proceeding we summarize the presentations of the HB2010 Workshop session on “Beam Dynamics in High-Intensity Circular Machines” as well as the outcome of the discussion session.

INTRODUCTION

This working group hosted 23 presentations in total, with 22 excellent talks [1-19;21-23] and a beautiful (revolutionary?) one [20]. Eleven speakers were coming from Europe (5 CERN&EPFL, 4 GSI, 1 FZJ, 1 RAL), eight from USA (1 BNL, 5 FNAL, 1 ORNL, 1 UMD) and four from Asia (1 IHEP Beijing, 1 J-PARC, 2 KEK). We summarize below the session and the discussion.

SUMMARY OF THE WORKING GROUP ACTIVITY

Yoshihiro Shobuda [1]

A 3D (i.e. with finite longitudinal length) theory of a “short” (with respect to the beam pipe radius) resistive insert, sandwiched by perfectly conducting chambers, was presented. It has been benchmarked against ABCI, which was upgraded to handle a resistive material inside a cavity. Nature tries to minimize the beam energy loss: the entire image current runs on the thin insert (i.e. still perfect shielding) except when the skin depth is more than several orders of magnitude larger than the beam pipe thickness. If the insert length is greater than the beam pipe radius, the 2D theory (e.g. Zotter 2005, Burov-Lebedev 2002) can be used. This new theory could be applied for instance in the CERN SPS where all (~ 200) BPMs are electrically isolated by enamel flanges (one in each side). Note that another 3D study was performed by Gluckstern-Zotter 2008 (AB-Note-2008-045).

Nicolas Mounet [2]

A 2D (i.e. with infinite longitudinal length) theory for both cylindrical and flat multi-layer chambers, for both longitudinal and transverse impedances was presented, extending Zotter 2005’s formalism under the assumptions of linearity, isotropy and homogeneity, and neglecting both the anomalous skin effect and the magneto-resistance. Matrix formalism was used (already introduced by Ivanyan 2008 and Hahn 2010) where one only needs to multiply N-1 (relatively) simple 4x4 matrices and invert the final result, to get the constants. The number of layers is no longer an issue. A comparison with other formalisms is ongoing, and the codes are available, only the circular case at the moment, but the flat one should come soon. The main results for the cylindrical case are: the use of wall impedance instead of

resistive-wall impedance, and the introduction of a new quadrupolar term usually considered only for asymmetric chambers. For the flat case: the transverse quadrupolar terms are in general not opposite in sign and generalized Yokoya factors were obtained, which are material and frequency-dependent.

Alexey Burov [3]

In 1955, N.G. Van Kampen found the eigen-system of Jeans-Vlasov equation for infinite plasma. The Van Kampen modes are the numerical solutions and the spectrum consists of two parts: a continuous and a discrete one (which may not exist). A.N. Lebedev first considered eigen-modes of Jeans-Vlasov equation for bunch longitudinal motion in 1968. This method can be applied for an arbitrary impedance, RF shape, and beam distribution function. It was applied here for the case of the resistive-wall impedance, considering only the dipole azimuthal mode $m = 1$. Stability areas (intensity - emittance) were found for 3 RF modes (single RF system, BS and BL modes). Two possibilities arise for the loss of Landau damping as results of phase mixing of Van Kampen modes of the continuous spectrum: (1) the discrete mode is inside the bucket and in this case some tails can help; (2) the discrete mode is outside the bucket and there is a radical loss of Landau damping.

Elena Shaposhnikova [4]

The “peak detected Schottky” is a diagnostics tool developed by D. Boussard and T. Linnecar, which is used in the SPS since the late 1970s. The quadrupole line was always believed to represent well the particle distribution in synchrotron frequencies. A detailed analysis revealed that ideally, for the detection of the bunch peak amplitude, it would be very close to the particle distribution in synchrotron frequencies. The spectrum is similar, in revolution frequencies, to that obtained for an un-bunched beam and much closer than that given by the traditional longitudinal bunched-beam Schottky spectrum. In reality, the measured peak detected signal is proportional to an average over the bunch current around its peak value. The difference mainly depends on the phases over which the bunch current averaging is performed.

Stefan Paret [5]

Deformations of the Schottky spectra and of the BTFs were measured in SIS18 vs. intensity. An analytic model with linear space charge for a KV distribution, i.e. a homogeneous beam profile was employed to describe the deformed signals: it was pointed out that linear space

WG B – BEAM DYNAMICS IN HIGH INTENSITY LINACS

A.M. Lombardi, CERN, Geneva, Switzerland
J-M. Lagniel, Ganil, Caen, France

Abstract

Loss control, emittance preservation and the performance under the influence of machine and beam errors are just a few topics of interest to all high intensity Linacs in the world, both in operation and in planning. These topics were thoroughly discussed during the parallel sessions of Working Group B, Beam Dynamics in High Intensity Linacs. The session hosted talks on the general beam dynamics for future projects, talks on comparing simulation and measurements in operational Linacs and some more general comprehensive talks on issues related to beam quality conservation under non-optimal conditions. A total of 15 talks were presented. The details of each contribution can be found in the relevant section of these proceedings. In this paper we report the results of the discussion and some concluding remarks of general interest to all projects presented in the working group.

INTRODUCTION

The talks and discussions of the “Beam dynamics in high intensity Linacs” Working Group B can be classified in 3 main topics. A series of 6 talks dedicated to the general beam dynamics for future projects. These included the European Spallation Source in Lund; the Superconducting Proton Linac at CERN; the International Fusion Materials Irradiation Facility with its Engineering Validation and Engineering Design Activity (IFMIF-EVEDA); PROJECT X at FermiLab; the Facility for Rare Isotope Beam (FRIB) at Michigan State University; SPIRAL2 at Ganil; and the Chinese Spallation Neutron Source.

A second set of four talks was dedicated to the comparison between simulations, measurements and machine tunings for operation. This session included talks from representatives of existing facilities, like JPARC in Tokai, the Spallation Neutron Source in Oak Ridge, the

UNILAC in Darmstadt and the Soreq Applied Research Accelerator Facility (SARAF) in Yavne, Israel.

A third session (4 talks) was dedicated to more general beam dynamics themes, like instabilities, reliability and other high intensity issues.

FUTURE PROJECTS

Table 1 gives a brief description of future projects which were discussed in WG-B. As it can be seen from the table, the variety of particles accelerated and the final energy and power are quite diversified, yet all projects have in common a design based on well known and agreed standard recipes, discussed in books [1] [2] and implemented in the most widespread computer programs used for defining an optimised accelerator layout [3][4]. These projects have different specifications, and even different “Linac” shapes (of particular interest is the FRIB folded layout). The beam dynamics optimization is strongly linked to the choice of the RF cavity technology, to the choice of the frequencies and the location of the frequency jumps, the choice of the type of radial focusing period (FODO, FDO...) and the length of the focusing period.

Notwithstanding all these differences and peculiarities, the design philosophy is the same for all the projects, namely: a zero-current phase advance per period below 90° to avoid structure resonances, a smooth phase advance per unit length to avoid mismatches and, tunes chosen to avoid the radial - longitudinal coupling resonances in order to prevent emittance exchanges.

A typical behaviour of the phase advance per period, the phase advance per meter and the ratio of the longitudinal to transverse tune are illustrated in Fig. 1, taking as example the CERN SPL. Such choices guarantee a dynamics that is resonance free, a minimum emittance increase and a reduced sensitivity to errors.

Table 1: Main Parameters of the Future Project Presented in the Working Group

	ESS	SPL	IFMIF-EVEDA	PROJ-X	FRIB	SPIRAL2
Particle	p	H-	D	H-	All! Up to U	p,D, A/q=3
Power(MW)	5	4	5-1.1	3	0.4	0.2
Energy(GeV)	2.5	5	0.040-0.009	3	0.200/u	0.040 (D)
Peak current(mA)	50	64	125	1	2	1-5
Duty cycle	4%	2%	CW	CW	CW	CW
	Long pulse operation	High rep rate (50Hz)	Space charge dominated	Low current	Simultaneous acceleration of up to 5 charges	Upgrade A/q=6

SUMMARY OF THE WORKING GROUP ON ACCELERATOR SYSTEM DESIGN, INJECTION, AND EXTRACTION

D.E. Johnson*, FNAL, Batavia, IL, USA
S. Cousineau, ORNL, Oak Ridge, TN, USA

Abstract

We review the presentations and discussions of the Accelerator System Design, Injection and Extraction working group at the 46th ICFA Advanced Beam Dynamics Workshop on High-Intensity and High-Brightness Hadron Beams.

INTRODUCTION

The working group heard eight oral presentations in two sessions and saw seven posters presented. The first oral session focused on injection and extraction technologies while the second oral session focused on commissioning and accelerator facility designs. The working group had a discussion session between the two sessions. The presentations can be grouped into four major classifications: New Concepts, Technology, and Component Designs; Commissioning Efforts; New Facility Design or Upgrades; and Status of Operational Facilities. We present a brief summary of each presentation and make a few remarks on the working group perspectives.

NEW CONCEPTS, TECHNOLOGY, AND COMPONENT DESIGNS

D. Trbojevic: **Non-Scaling FFAG and their Applications**

The basic concepts of the non-scaling FFAG (NS-FFAG) were discussed. As compared to traditional FODO lattices, the non-scaling FFAG's have very strong focusing and hence small dispersion values and beam size which leads to small magnets. The application of the NS-FFAG lattice design were discussed in terms of how many turns or passes the particles traversed the lattice, from one turn (i.e. medical gantries), to a few turns (i.e. muon acceleration or pion storage rings), to many turns (i.e. accelerator for proton cancer treatment).

O. Heid: **Compact Solid State Direct Drive RF Linac: First Results**

Silicon Carbide (SiC) JFET RF transistors are a key enabling technology utilized in the design and construction of a solid-state direct drive linear induction particle accelerator concept. The presentation describes experimental results of a lower power test for prototype of a direct drive 1/4 cavity with a power rating of 1 MW at 150 Mhz. This approach could lead to a substantial decrease in RF power costs for future facilities.

Y. Liu: **Advancements in Laser Technology and Applications to Accelerators**

Yun presented a brief review of recent technology advancements in ultra-high intensity pulsed lasers, laser array beam combination, and power enhancement optical cavities. Applications to accelerators include: laser based diagnostics, photo injectors, laser assisted injection stripping, inverse Compton scattering, laser wakefield plasma acceleration and laser driven ion accelerator. Although many of these applications have been made feasible due to the rapid advancement in laser technology over the last decade, additional R&D is required to achieve the required, laser power and pulse length and repetition rate for many of these applications.

D. Fernandez-Cañoto: **Electrode Design of the Bilbao Accelerator proton Extraction System**

A design study of the extraction system for the ESS-Bilbao ion source is presented with the aim of obtaining an electrode system capable of extracting, accelerating, and delivering a high quality proton beam from the plasma chamber to the LEBT. The system must be capable of delivering beam with a 0.2 π -mm-mr emittance to the LEBT to produce acceptable matching to the RFQ. They included detailed discussion of two electrode system geometries and beam dynamics associated with each.

B. Goddard: **Considerations on a New Fast Extraction Kicker Concept for SPS**

A new 450 GeV/c extraction kicker concept for the SPS which could potentially reduce the beam coupling impedance is introduced. The scheme consists of a c-type kicker magnet with a reduced vertical aperture such that the injected beam is outside the kicker gap and only moved within the gap just prior to extraction. The kicker is excited only from the back leg. The kicker aperture and required magnet and power supply parameters are discussed. The implications on the coupling impedance have been investigated and plans for more extensive beam dynamics simulations were outlined. Additionally, the impact of the new kicker on the lattice and closed orbit control as well as other systems was presented. It was concluded that this concept looks feasible on paper and a list follow-up studies was outlined.

T. Yokoi: **Beam Extraction of PAMELA non-scaling FFAG**

One of the major design challenges for the design of a variable energy NS-FFAG medical accelerator is that of beam extraction and matching into the gantry. This paper describes a vertical extraction scheme utilizing a superconducting combined function septum. This,

*dej@fnal.gov

SUMMARY OF THE COMMISSIONING, OPERATIONS AND PERFORMANCE WORKING GROUP OF THE HB-2010 WORKSHOP

J. Galambos, SNS, Oak Ridge, TN, USA
 H. Hotchi, J-PARC, Naka, Japan
 A. Mezger, PSI, Villigen, Switzerland

Abstract

As hadron machines approach higher beam intensity and operational power levels, issues such as machine activation caused by beam loss, machine protection and machine availability become more critical concerns. The operational experience of the high power, high intensity facilities in these areas is compared.

INTRODUCTION

This working group covered commissioning and operational developments of high intensity hadron devices. On the commissioning front, the primary development was the initial operation of the Large Hadron Collider (LHC), with unprecedented beam energy and stored energy concerns. On the operational front, high power operation is a common theme, with mega-Watt beam operation at the PSI and SNS facilities, and operation at the 100's kW level at LANSCE, ISIS, J-PARC and FNAL. The high energy frontier at LHC faces unique challenges in machine protection issues, with the complex collimation schemes working well over the course of the commissioning. The high power facilities also have concerns with machine protection, as well as residual activation from uncontrolled beam loss, and machine reliability. The experience of the major facilities in these areas is summarized below. Details of each of the session contributions are presented in the individual papers. In this summary, we concentrate rather on the common themes.

COMMISSIONING

The Large Hadron Collider at CERN commissioned beam over the past year. Preparations have provided a smooth start for commissioning and initial operation. Beams were circulating within 6 hours, initial collisions within three days, and stable collisions in about two weeks. The initial commissioning was done with low intensity beam, to accommodate setup of the machine protection and collimation systems, with no beam crossing. At the time of the workshop 150 bunches (10 MJ) had been accumulated, and 400 bunches (30 MJ) are expected by year's end. This is to be compared to a design of 360 MJ stored energy. To date the protective measures are working well and no magnet quenches from beam loss have occurred. The average store time is 8 hrs. An unexpected observation is occasional unexpected fast local beam loss events, possibly caused by from beam scattering. These events are not well understood yet.

LHC Collimation

A key component of LHC operation at unprecedented stored energy levels is a complex collimation system designed to protect the beamline devices (e.g. prevent superconducting magnet system from quenching). The collimation configuration process is empirically determined for a given beam setup, with complex pre-programmed algorithms following the beam through the ramp stages. Many interlocks are required to assure the machine protection (order 10^4). The collimation setup time requires about one week, but this is not expected to hinder LHC progress. The present setup was used for about three months. Repeatability of the collimation position control is critical, with tolerances on the order of only 10 μm . Of interest is certainly the fact that the measured collimation efficiency is close to the calculated predictions.

HIGH POWER FACILITIES

In contrast to the LHC colliding stored beam facility, high power accelerator facilities have much lower instantaneous stored beam energy. However the high power facilities continuously accelerate beam and have higher peak and average beam powers. Concerns for high power facilities include protecting equipment from sudden damage caused by errant conditions in which beam hits equipment, protection against excessive build-up of residual activation, and protection of the environment (e.g. ground-water contamination). Also many high power facilities are user facilities, with high reliability expectations. Machine availability and operational aspects are discussed.

Machine Protection Systems

There are many commonalities amongst the protection systems that have evolved in the high power accelerator community. All facilities have some sort of "tune-up" machine protection system. This sort of configuration allows beam operation with higher fractional beam loss than would be permitted in full power mode, yet restricts the beam operation to a lower power mode (such as reduced current, pulse length and/or repetition rate). This mode of operation is useful for beam studies, and critical for initial beam commissioning. Also, all facilities employ redundant beam shut-off mechanisms to ensure shutting of the beam even in the case of a failure of one of the mechanisms. Another commonality of machine protection systems is some sort of by-pass control mechanism. Systems are never perfect, and sometimes

WORKING GROUP SUMMARY: COMPUTATIONAL CHALLENGES IN HIGH-INTENSITY LINACS, RINGS INCLUDING FFAGS AND CYCLOTRONS*

G. Pöplau[†], Rostock University, Rostock, Germany

Abstract

The design and operation of accelerators with high intensity and high brightness hadron beams make high demands on computational tools. The increase of the intensity of hadron beams requires a more precise investigation of the beam dynamics, the study of further phenomena and the investigation of additional design issues. Thus, more sophisticated physical models are implemented into computer codes, which often causes time-consuming numerical calculations. Hence, this process is accompanied by the development and the application of efficient numerical methods.

INTRODUCTION

What are the computational challenges in high-intensity linacs and rings? Y. Luo and W. Fischer expressed it for RHIC in their paper [1] like this: "The challenge in the lifetime and emittance calculation is to obtain meaningful physics results with limited computing resources and computing time." Certainly, this statement can be generalized to the computational effort for high-brightness high-intensity hadron beams presented within this working group.

Altogether, ten talks and two posters were contributed from working group E to the workshop. During the sessions a great variety of challenges were discussed. Although the computational challenges are often very specific for a certain machine the following list gives an overview about the topics that were addressed.

- Inclusion of more physical phenomena, improved models and appropriate models into the simulation tools for more precise calculations.
- Application and development of appropriate numerical methods.
- Utilization of new hardware.
- Efficient development of simulation software.
- Comparison of simulations and measurements.

ADDITIONAL PHYSICAL MODELS, IMPROVED MODELS

New ideas and new concepts for high-intensity, high-brightness hadron beams require a precise as possible numerical prediction of the included beam dynamics. In [2]

and [1] challenging issues for the beam-beam interaction simulations are discussed for eRHIC and RHIC, respectively. For the simulation of the effects of beam-beam collision in eRHIC the code EPIC has been developed in order to meet the special needs of the linac-ring configuration. It includes many physical effects like electron beam disruption, electron beam pinch, the kink instability of the proton bunch, the effect of fluctuating electron beam parameters on the proton beam [2]. The concept of the collision with a low energy electron beam for compensation of proton-proton beam-beam effects is investigated in [1]. The related simulations require multi-particle and million turn tracking for the calculation of the proton beam lifetime and emittance growth. Here, new approaches for the reduction of statistical errors are necessary.

The OPAL library was applied and extended for simulations of the upgrade plans of the PSI high power proton cyclotron facility [3, 4]. Here, a model for the efficient calculation of particle matter interaction is developed in order to simulate the collimator systems together with space charge [3]. Furthermore, for the study of multipacting and dark current phenomena a field emission and secondary emission model is implemented in OPAL. Since OPAL can handle complex geometric surfaces an efficient strategy for the calculation of the particle boundary collision is developed [4].

APPROPRIATE NUMERICAL METHODS

More precise simulations often require more sophisticated numerical methods such that these simulations can be performed efficiently and don't become too time consuming. Especially efficient methods for space charge calculations play an important role.

Often efficient numerical algorithms are already established in numerical mathematics but they are not yet applied or implemented for beam dynamics simulations. Thus, an algorithm of Barnes and Hut is implemented for the fast calculation of the particle - particle interaction of laser cooled ion beams [5]. A semi-analytical solver for the calculation of space charge is developed for the DYNAMION code based on the known analytical formulae for ellipsoidal bunch shapes [6]. A quite different approach that describes the space charge effect by a nonlinear transfer map is given in [7]. This development is done for the code COSY Infinity which is based on differential algebras. The advantage is that the nonlinear dynamics of an intense beam can be extracted directly from the calculations.

* Work supported by BMBF under contract number 62130009

[†] gisela.poeplau@uni-rostock.de

CLOSING PLENARY SUMMARY OF WORKING GROUP F DIAGNOSTICS AND INSTRUMENTATION FOR HIGH-INTENSITY BEAMS*

M. Wendt[#], Fermilab, Batavia, IL 60510, U.S.A.
T. Toyama, KEK, Ibaraki, Japan

Abstract

Summary of the working group F activities, presented in the closing plenary session.

OVERVIEW

Working group F was charged with presentations and discussions on diagnostics and instrumentation of high-intensity beams. We had 2 sessions spanning a total time of 3-½ hours, in which 10 talks were presented. The presentation time for each talk had to be limited to 15-20 min., in order to allow sufficient time (5-10 min.) for some discussion. This procedure went quite well, thanks to the discipline of the speakers.

A final 1 hour discussion was held as joint session with working group E (simulations).

PRESENTATIONS

Except for the last one, all presentations of working group F were focused on a specific beam instrument, most on the technology beam profile measurements:

Y. Hashimoto: Profile Monitor Using a Carbon Graphite Foil for the J-PARC

Yoshinori presented a minimum invasive beam profile SEM, based on a new graphite foil technology. The 1.6-2.0 μm thick, self supporting target material offers a low density ($Z = 6$), and was tested extensively with various proton and heavy ion beams. While the foil survived a total dose of $>5 \times 10^{20}$ protons (500 MeV) with a spot size of $45 \times 15 \text{ mm}^2$, it broke after 1 hour operation on a 3.2 MeV, 3 μA Ne^+ beam of 8 mm^2 spot size due to overheating (1400°C). Seven monitors have been build, using a laser cutting method to form a pattern of 67 foil strips, 3 mm wide at 4.5 mm pitch (also tested: 1 mm width, 2 mm pitch), epoxy glued into the $190 \times 310 \text{ mm}$ opening of a Al_2O_3 ceramic frame. A 32 channel analog integrator with $\sim 30 \mu\text{sec}$ time constant interfaces the signals of the SEM foil strips through a 10-bit ADC to a CAMAC system into the J-PARC EPICS control system. Beam halo (transverse tails) could be characterized by increasing the gain of these channels by a factor 2000.

M. Hori: Time-resolved SEM Monitor with large Dynamic Range for R&D of Linac 4

The CERN Linac 4 will operate with a chopped beam pattern, which gave the motivation for the development of

a profile monitor with high time resolution. Masaki preferred a robust, reliable “classical” technology for this important monitor: SEM in connection with gated HV grids. He presented many details on precision mechanics for the different wire and foil technologies required for various grids, i.e. SEM target and five acceleration HV grids. The avalanche diode switched HV supplies requires matched impedance RF transmission lines, a UV laser test demonstrates HV rise/fall times of $\sim 200 \text{ psec}$. Performance tests and optimization were made at the Orsay proton linac, as well as with a 700 psec Nd:YAG laser system. A spatial resolution of $\leq 2 \text{ mm}$, and a time resolution $\leq 1 \text{ nsec}$ could be demonstrated, the linear dynamic range covers 5 to 5×10^8 secondary electrons.

W. Blokland: Non-Invasive Beam Profile Measurements using an Electron-Beam Scanner

In collaboration between the Budker Institute and ORNL a novel electron-beam scanner was developed, to perform non-invasive beam profile measurements at the SNS proton accumulator ring. Wim introduced the measurement principle of a low-energy (typically 60 keV) electron beam, scanned under 45° through the proton beam, measuring the proton beam profile as reconstructed image of the deflected electrons. Layout, technical details and simulations of the system were presented, as well as many measurements with the two installed scanners (horizontal and vertical) at the SNS proton ring. Wim explained the importance of data fitting algorithms and calibration procedures to improve the measurement performance. The 20 nsec deflection sweep of the electron beam is fast compared to the $\sim 1 \mu\text{sec}$ proton bunch length and allows time-sliced profile measurements. Other topics discussed in this presentation were the influence (rejection) of external magnetic fields, as well as comparing performance and accuracy of the electron-beam scanner profile measurement to harp wire monitors.

P.-A. Duperrex: Beam Current & Transmission Measurement Challenges for High Intensity Beams

The operation of the proton accelerator complex at PSI relies on the precise monitoring of beam currents and transmission, e.g. towards the target area. Pierre-Andre discussed the development of a quarter-wave coaxial resonator, and its application as current transmission monitor, required to replace an out-of-order unit in a high radiation, difficult to access area. While the coaxial cavity resonator, here operated at the 2nd harmonic of the proton bunch frequency is a simple, rugged device, its temperature sensitivity was known. Nevertheless, the new MHC5 replacement unit had some issues due to the drift

* This work was supported by Fermi National Accelerator Laboratory, operated by Fermi Research Alliance, LLC under contract No. DE-AC02-07CH11359 with the United States Department of Energy
[#]manfred@fnal.gov

SUMMARY OF WORKING GROUP G: BEAM MATERIAL INTERACTION

D. Kiselev*, Paul Scherrer Institut, Switzerland
N.V. Mokhov, Fermi National Accelerator Laboratory, Batavia, USA
R. Schmidt, CERN, Geneva, Switzerland

Abstract

For the first time the workshop on High-Intensity and High-Brightness Hadron Beams (HB2010), held at Morschach, Switzerland and organized by the Paul Scherrer Institut, included a Working group dealing with the interaction between beam and material. Due to the high power beams of existing and future facilities, this topic is already of great relevance for such machines and is expected to become even more important in the future. While more specialized workshops related to topics of radiation damage, activation or thermo-mechanical calculations, already exist, HB2010 provided the occasion to discuss the interplay of these topics, focusing on components like targets, beam dumps and collimators, whose reliability are crucial for a user facility. In addition, a broader community of people working on a variety of issues related to the operation of accelerators could be informed and their interest sparked.

TALK AND POSTER SESSIONS

Even though organised for the first time, working group G had three sessions with 15 talks, additional two talks in a joint session with working group A "Beam Dynamics in High-Intensity Circular Machines" as well as five posters. Various topics were covered:

- Activation: nuclide inventory and dose rates
- Radiation damage: calculations and experiments
- Thermo-mechanical simulations: design tools for targets, collimators and beam dumps
- Irradiation facilities: existing and upcoming
- Future accelerator facilities: upgrades and plans

The last topic in the list, the upgrade of existing and plans of new facilities to operate with even more beam power, drives the need to seriously address the other topics. While one path for future accelerators is to increase the beam energy, the other is to increase the beam current. The product of both is an increase of the beam power which finally has to be deposited somewhere - usually on targets, collimators and beam dumps.

These components get highly activated and their nuclide inventory has to be determined, when they finally

get disposed as radioactive waste. In addition, for maintenance, dose rates have to be known in advance to plan working procedures and as design criteria in the development phase of new components (as it was done for the LHC beam dumps, S. Roesler, CERN). For these purposes, particle transport Monte Carlo codes like FLUKA (S. Roesler, CERN) and MARS15 (N. Mokhov, Fermilab) are employed. Improvements in the predictive power of the codes were made and benchmarks with experimental data were performed. Recently their capabilities were significantly extended and new features added. These activities were driven on one hand by user demands, on the other hand by applications, e.g. for the LHC. The calculation and use of H₂ and He gas production and of the quantity "Displacements Per Atom (DPA)", a measure of radiation damage, is an attempt to compare damage caused by radiation under different conditions. Regarding DPA there are still discrepancies between different codes, which have to be solved in the near future. Another issue related to the activation of components is the growing interest in choosing materials which get less activated but have the same or equivalent mechanical and physical properties needed for the application (J.H. Jang, KAERI, E. Mustafin, I. Strasik, GSI).

Due to the high power deposition which is dissipated as heat, efficient cooling systems have to be designed. Tensile stress induced by thermal expansion has to be kept within the safety margin. For this purpose thermo-mechanical simulations are performed using commercial tools like ANSYS and CFD-ACE. Thermal, mechanical and electromagnetic models can be coupled and applied to a detailed geometry. As input, the energy deposition due to the particle beam are taken from particle transport Monte Carlo codes or from a subroutine implemented into the multi-physics program as done for CFD-ACE by Y.J. Lee (PSI). Examples of components suffering from heavy power load are the T2K target at JPARC with 750 kW (J. Densham, STFC/RAL), 200 kW on a Cu collimator at PSI (Y. Lee) and the Neutrino beam factory at Fermilab, which plans to start with 700 kW power load and upgrade later to up to 2 MW (P. Hurh, Fermilab). Thermal and stress simulations for Conceptual Design Studies are underway for two target alternatives made of beryllium and graphite, respectively. At FRIB an extreme high power density of 20 to 60 MW/cm³ for the pulsed ion beam is expected (R. Ronnigen, NSCL-FRIB). To predict the behavior of components under irradiation, it would be important to include the

* Daniela.Kiselev@psi.ch